LIQUID-LIQUID EXTRACTION IN AGITATED CONTACTORS INVOLVING DROPLET COALESCENCE AND REDISPERSION

by

David Robert Arnold

A thesis submitted to the University of Aston in Birmingham for the degree of Doctor of Philosophy

Department of Chemical Engineering
The University of Aston in Birmingham

October 1974

Summary

Rotary agitated liquid-liquid extractors have been classified in terms of the rate of energy imparted to the dispersed phase, and whether contact is stagewise or differential. In the high energy contactors a droplet coalescence-redispersion mechanism predominates. The literature pertaining to these extractors has been examined and the important phenomena such as droplet break-up and coalescence, phase inversion, mass transfer and backmixing have been reviewed. The prediction of drop sizes and interfacial areas, and the extension of mathematical models from batch systems to continuous ones is discussed.

A six-inch diameter sixteen compartment Oldshue-Rushton column was designed and constructed to study hydrodynamics and mass transfer.

Cyclic phase inversion, a pseudo-steady state condition, under which stable operation is possible under high dispersed phase loading, was investigated. A design equation has been developed to predict mean drop sizes in the contactor in terms of column geometry, system properties and operating parameters. Mass transfer coefficients were computed, using previously established backmixing correlations. The mechanism of phase inversion in agitated contactors is explained.

Conclusions are drawn with respect to phase inversion, flooding, drop sizes and mass transfer coefficients in agitated contactors.

Acknowledgements

The author wishes to thank the following.

Professor G.V. Jeffreys,

for his encouragement and supervision and for providing the facilities for research

Dr. C.J. Mumford,

for his continual help and constructive criticism

The Technical Staff of the Department of Chemical Engineering

for their assistance in fabricating the equipment and in the photographic work

Mrs. Kay Davies,

for her diligence in typing the thesis

The Science Research Council,

for financial support during the first two years of this work.

Contents

List of Figures

1. Introduction

In its simplest form, liquid-liquid extraction has been used for many years as a separation process in the laboratory. It has more recently become of major importance as a chemical engineering unit operation throughout both the organic and inorganic chemical industries. Significant applications have been where the materials to be separated or purified are sensitive to heat or have a relative volatility close to unity, prohibiting distillation from the mother liquor. Examples are the large-scale production of antibiotics and close-boiling isomers. Specific solvents are available for extractions such as lubricating oils from crude oil, and aromatics from mixed hydrocarbon streams. More recently, the winning of metals from leach liquors has received much attention and is the subject of continuing university and industrial research.

1.1 Liquid-liquid extraction

When a liquid solution is contacted with a totally or partially immiscible solvent, mass transfer of the solute may take place across the interface. The driving force causing the diffusion of solute is the concentration difference between each bulk fluid and the interface, (or more specifically the chemical potential or activity). A large interfacial area between liquids is generally achieved by dispersing one liquid in the other in the form of droplets. The rate of transfer depends mainly on the physical properties of the fluids and the hydrodynamic characteristics of the system; the extent to which transfer takes place being additionally dependent on the relative solubility, or distribution coefficient, of the solute in each of the phases, and the

length of time of contact.

These interacting effects are complex, and it is therefore convenient, although simplistic, to consider the total resistance to solute transfer as a coefficient, K, which is the reciprocal resistance. The familiar equation

$$N = K . a . \Delta C \qquad (1)$$

describes the amount of transfer taking place, where

N is the mass transferred

a is the interfacial surface area

ΔC is the concentration driving force

Additionally, the overall coefficient is comprised of three fundamental resistances, which are the dispersed and continuous phase film coefficients k_d and k_c and an interfacial resistance. Usually the latter is very small and may be neglected, so that the following applies.

$$\frac{1}{K_d} = \frac{1}{mk_c} + \frac{1}{k_d} \qquad \text{or} \qquad \frac{1}{K_c} = \frac{1}{k_c} + \frac{m}{k_d} \qquad (2)$$

where m is the distribution coefficient of the solute. The choice of the use of K_d or K_c depends on the driving force chosen in equation (1), i.e. referred to the continuous or dispersed phase.

The relative magnitude of k_d depends on the hydrodynamics of the drop. The fluid inside the drop may be stagnant or circulating, or the drop may oscillate between an oblate and prolate profile. In small drops the surface drag is too small to set up internal motion, and the drop behaves

as a rigid sphere. Newmann's correlation then applies and (1)

$$k_d = \frac{d}{6t} \ln \left[\frac{6}{\pi} \sum_{n=1}^{\infty} \frac{1}{n^2} \right] \exp \left(\frac{4n\pi^2 Dt}{d_p^2} \right) . \qquad 3$$

Low values of k_d are obtained.

For larger drops, laminar internal circulation is the predominating régime, and k_d has a higher value. Kronig and Brink (2) have produced graphical data for this region.

The largest drops oscillate, and Kintner's correlation applies (3)

$$k_d = 0{\cdot}45(D\omega)^{\frac{1}{2}} \qquad 4$$

where ω is the oscillation frequency and

$$\omega = \left(\frac{\sigma b}{r^2} \right) \left[\frac{1}{3\rho_d + 2\rho_c} \right] \quad ; \quad b = \frac{d^{0{\cdot}225}}{1{\cdot}242} \qquad 5$$

These drops have the largest coefficient.

Generally drops of diameter less than 2mm are 'stagnant' and those greater than about 10mm oscillate.

The value of the continuous phase coefficient depends on the rate of renewal of the surface in contact with the drop. Highly turbulent systems therefore have higher k_d values than, for example, systems where the continuous phase is stationary i.e. where molecular diffusion applies. Many correlations for the continuous phase coefficient have

been produced. That of Garner, Foord and Tayeban appears to fit a great deal of the data, viz. (4)

$$\frac{kd}{D} = -126 + 1{\cdot}8\,Re^{\frac{1}{2}}\,Sc^{0{\cdot}42} \qquad 6$$

where the symbols have their usual meanings.

In equation (1) all the terms are interdependent. Thus the overall coefficient may vary with the interfacial area and the drop size distribution. Internal circulation or oscillation of the drop increases the coefficient over that for the stagnant or rigid drop (5). High rates of transfer may cause interfacial instabilities and turbulence which affect the coefficient. Momentum transfer caused by a surface tension driving force at the interface is known as the Marangoni Effect, investigated extensively by Sawistowski (6,7). In turn, surface tension variations are affected by rates of mass transfer and concentration driving forces. The inter-relationships between K, a, and operating conditions have been briefly summarised by Thornton (8) and are shown in a more comprehensive form in figure 1.1 The analysis of mass transfer even under ideal conditions is therefore complex, and is covered in detail in chapter 5.

1.2 Equipment

In liquid-liquid extraction equipment, the analysis is further complicated in six ways.

1. The degree of turbulence in the continuous phase affects the dispersed phase drop size and hence the internal circulation or oscillation of the drops. The effect of higher turbulence is to lower

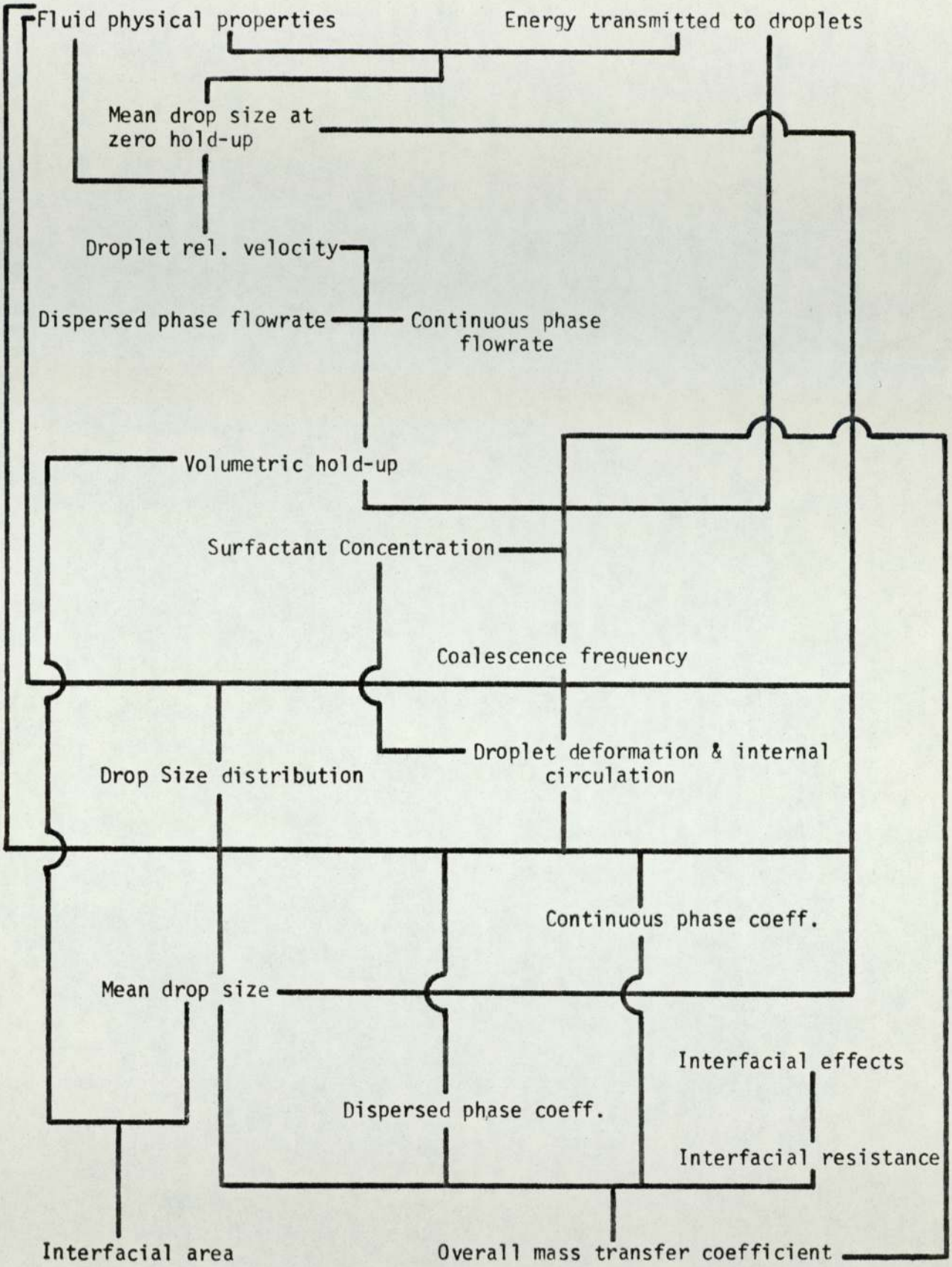

Relationships between variables in liquid extraction

Fig. 1.1

the effective diffusivity of the solute in the continuous phase and thus decrease the resistance. Conversely, the drop size affects the level of turbulence (9).

2. In an agitated system drops are continually coalescing and redispersing. This increases the amount of transfer because fresh surface is always being presented to the continuous phase.

3. Mass transfer may be arranged to take place either into or out of the drops. Coalescence is inhibited by the former and enhanced by the latter.

4. Backmixing in both dispersed and continuous phases occurs to a greater or lesser extent depending on contactor design and operating parameters. This has the effect of reducing the effective driving force.

5. Surface active agents, even if present in very low concentrations, retard drop coalescence and internal circulation.

6. Phase inversion may occur. The dispersed phase coalesces enmasse to become continuous, and the originally continuous phase becomes dispersed. The effect of this phenomenon on mass transfer has not been reported in the literature to any extent.

Many reviews on equipment selection have been published (10,11,12). Clearly, a compromise has to be made between the rate of extraction and capital and operating costs. Physical properties of process streams such as density, viscosity and interfacial tension are relevant, as well as flowrates and desired terminal solute concentrations in both raffinate and extract.

In simple spray columns a dispersion is achieved by converting pressure energy into droplet surface energy at a distributor. In agitated contactors, transmission of kinetic energy from the agitator to the continuous phase and thence by various means to the dispersed phase causes droplet distortion and subsequent break-up. The power input to the agitator is thus transferred into the kinetic, surface, potential and heat energy of the droplets. Designs of contactors may therefore be classified in terms of the rate of energy input per unit volume of continuous phase. A second classification may be made by considering whether operation is by discrete stages or by continuous countercurrent contact. The various types of unit are arranged by these two criteria in figure 1.2. As an example, a low interfacial tension system would require a low energy contactor to prevent solvent emulsification. If only a few theoretical stages were required, a continuous countercurrent device would be selected; for a large number, say in excess of ten stages, a discrete stage contactor would be best.

The most common industrial applications of the contactors listed in figure 1.2 have been mixer-settlers, various designs of spray columns, pulsed columns and the rotating disc contactor and its variations. On a small experimental scale, pulsed, packed and rotating disc contactors have received the most attention, mainly due to their relatively simple construction and ease of analysis and operation. For the continuous differential contactors, figure 1.2 shows that there is a gradation in energy, from the spray column and the packed column to the centrifugal contactor and the Oldshue-Rushton column. Considering the mechanically

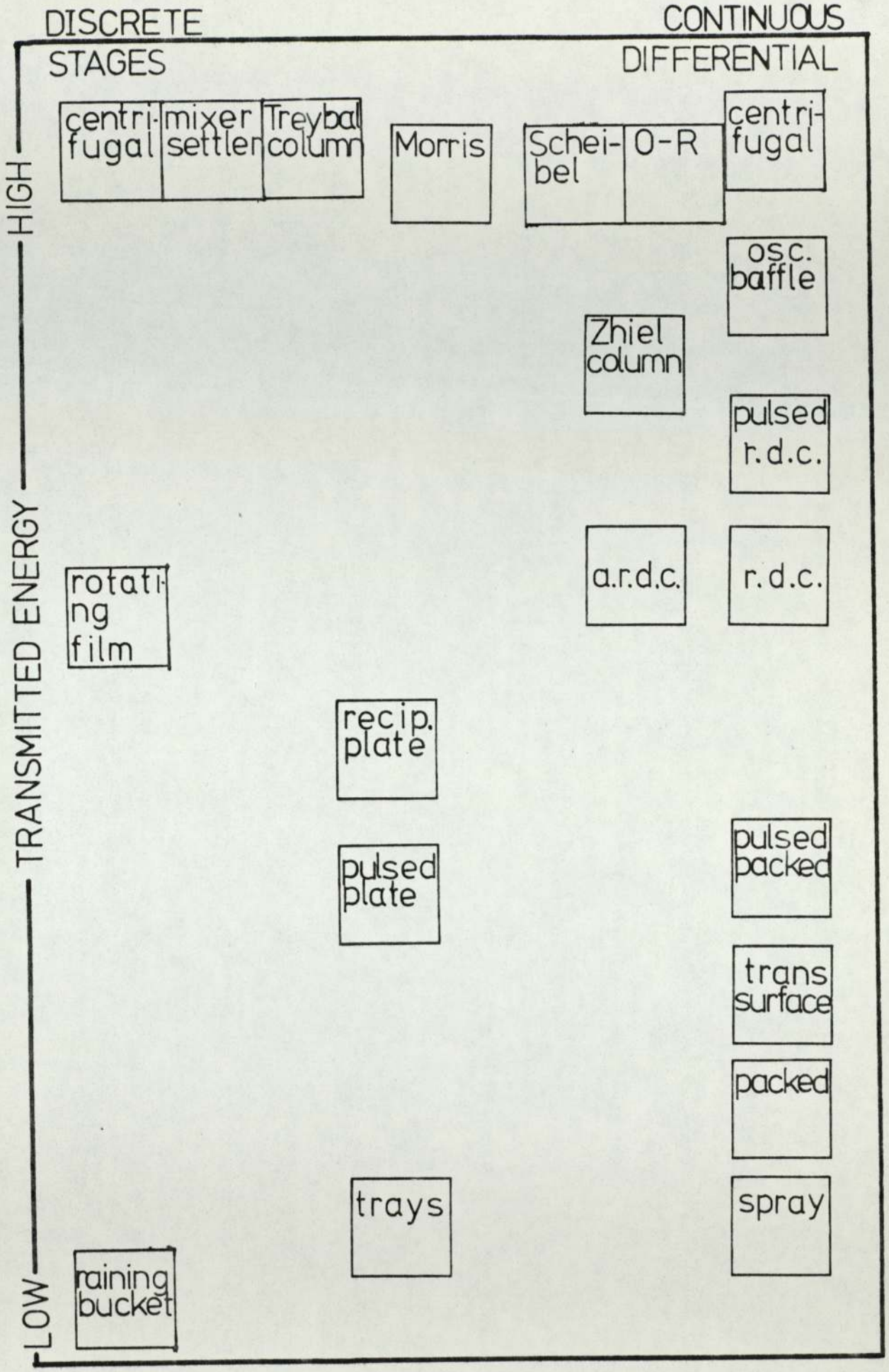

Figure 1.2 Industrial Contactors.

agitated columns, there is also a range of energy, the lowest being the R.D.C. At the same rotor speed and diameter the R.D.C. energy dissipation is only about one eightieth of the Oldshue-Rushton column. Therefore in this work the R.D.C. is considered as a low energy contactor and the Oldshue-Rushton column as a high one.

For these columns the advances in design data and mathematical analysis since the publications of Reman (13) relating to the rotating disc contactor (14,15) have not been matched for the high energy contactors. Studies of the Oldshue-Rushton column (16) have been limited to analyses of hydrodynamics based on the prediction of drop sizes as an extension to studies in stirred tanks (17) or the interpretation of mass transfer in terms of the height of a transfer unit (H.T.U.) or the height equivalent to a theoretical stage (H.E.T.S.). This approach has obvious attendant limitations, (18) as the expression of column performance in these terms is specific to the fluid physical properties and operating conditions of the test.

Therefore in this work the performance of a pilot scale Oldshue-Rushton column - a typical high energy contactor - has been investigated.

2. Rotary Agitated Contactors

Continuous rotary agitated contactors are differential countercurrent devices and fall within the upper right hand corner of figure1.2, bounded by the low energy rotating disc contactor and the high energy Oldshue-Rushton column. Centrifugal contactors have fundamentally different characteristics; for example the drops are subjected to gravitational forces in excess of two thousand times normal acceleration due to earth gravity, and the mean drop size is about 1/20th of that in columns; they are therefore not considered in this work. The remaining contactors in this group have common generic characteristics, illustrated by the following.

1. Overall columnar elevation with typical height/diameter ratios of 20/1 to 2.5/1 dependent upon scale.

2. A centrally located axially mounted agitator.

3. A variable speed control on the agitator enabling optimum operation for various flowrates.

4. Gravity operation, and are therefore dependent upon phase density difference.

5. A single interface located at one end of the unit.

Rotary agitated contactors therefore differ basically in their internal geometry, illustrated by figure 2.1, in which the columns are arranged in the same order as figure1.2.

The classification may be further sub-divided by reference to the types of agitator used, viz.

1. disc-type, similar to the R.D.C.

2. turbines, similar to the Oldshue-Rushton column.

Oldshue-
Rushton
Column

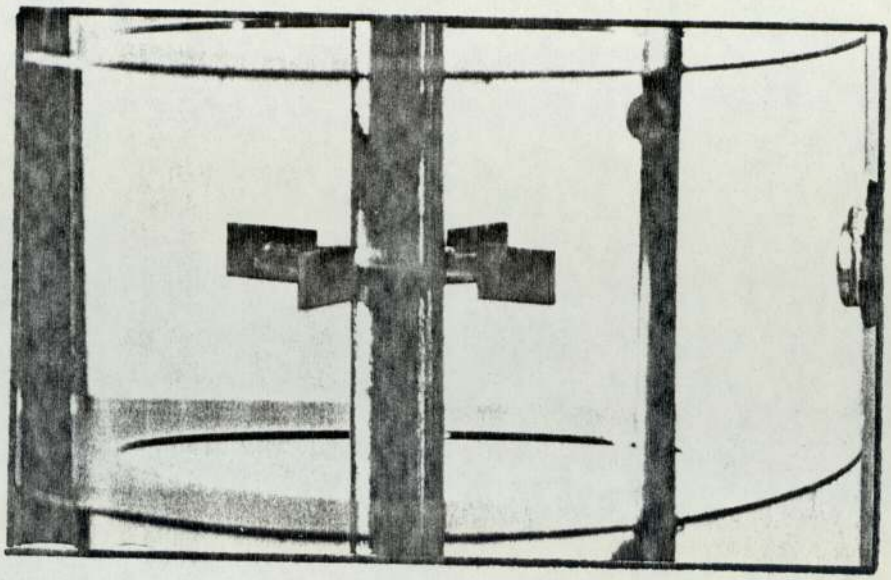

Kühni
Column

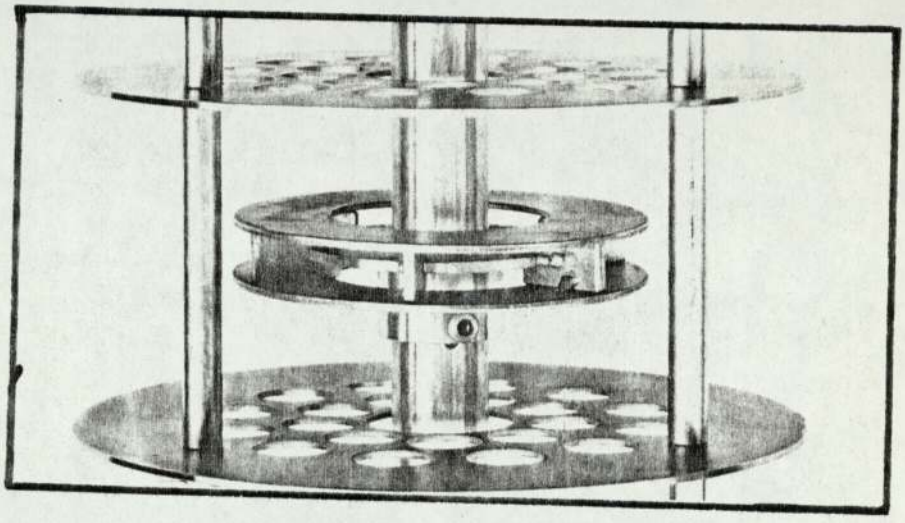

Assymetric
Rotating
Disc
Column

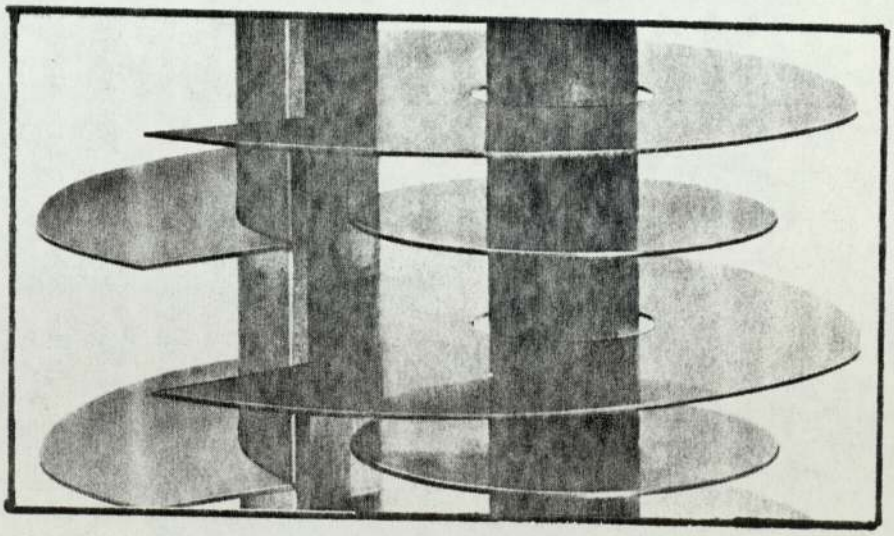

Figure 2.1 Column Internals.

Versions of the R.D.C. and other contactors have been described in the literature and in some cases used in industrial applications, where a pulsing motion of the continuous phase is superimposed on the ordinary flow. Pulsing is said to encourage oscillation of droplets, leading to better mass transfer. Pulsed columns are not considered in this work.

2.1 Rotating Disc Contactors

Reman (13) described the original type of R.D.C. in 1951, and the first application was apparently the extraction of lubricating oils from crude oil using furfural as a solvent (19). There have been many subsequent applications, especially in the petroleum industry, demonstrating the contactor's versatility.

The R.D.C. has a vertical cylindrical shell divided into a number of compartments by a series of stator rings. A rotating disc is centrally located in each compartment, each rotating on an axial shaft. Raffinate and extract streams are introduced at either end of the column. The dense phase enters at the top, and one phase may be introduced via a distributor to give a dispersion which flows countercurrently under gravity, until coalesced at the interface at the opposite end of the column. Figure 2.2 shows a typical arrangement.

Mumford (20) and Al-Hemiri (21) have summarised all aspects of the R.D.C., its operation and analysis. The R.D.C. is well established in industry, for three main factors.

1. The power transmitted to the fluids is well suited to many process stream characteristics such as density and interfacial tension.

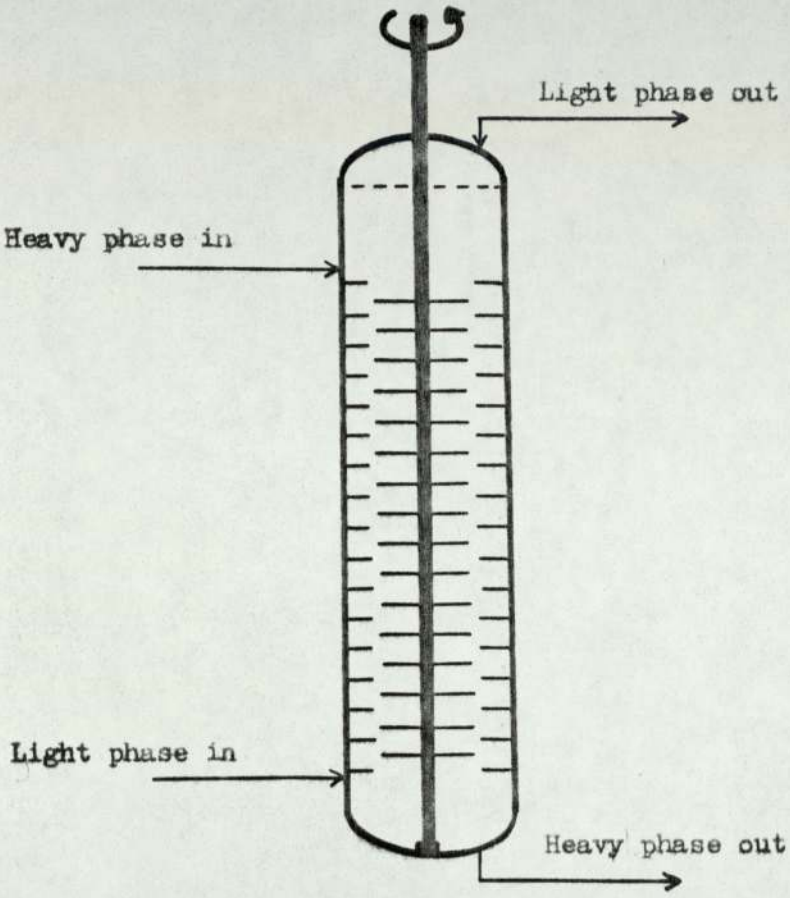

Figure 2.2 Rotating Disc Contactor.

2. The construction is fairly simple, and hence the capital cost is relatively low for a given capacity (19).

3. Flow characteristics and hydrodynamics are well defined. Therefore the results of research on a laboratory scale and on full scale units have been successful in so far as the prediction of performance is concerned, and design methods have been proposed (14,22) Consequently the large amount of published work on the R.D.C. serves as a basis for further work on other rotary agitated contactors.

2.1.1 Hydrodynamics

The interfacial area in a dispersion of spherical drops may be expressed in terms of the drop diameter and the volumetric hold-up by the equation

$$a = \frac{6x_d}{d} \qquad 7$$

When the dispersion contains a range of drop diameters, i.e. a "polydispersion", the surface mean, or "Sauter mean" diameter, d_{32}, replaces d. The concept of a droplet 'slip' velocity, V_s, is commonly employed in two phase systems (23,24,25,26,27,28) to relate volumetric flowrates and hold-up,

$$V_s = \frac{V_d}{x_d} + \frac{V_c}{1 - x_d} \qquad 8$$

for countercurrent flow. Logsdail et al (25) modified the slip velocity equation (for a three inch diameter R.D.C.) so that,

$$V_k (1 - x_d) = \frac{V_d}{x_d} + \frac{V_c}{1 - x_d} \quad , \qquad 9$$

and defined V_k as the mean vertical velocity at substantially zero flowrates and at a fixed rotor speed. An empirical equation was then fitted to experimental data to relate V_k to column and system properties,

$$\left(\frac{V_k\,\mu_c}{\sigma}\right) = 0.012\left(\frac{\Delta\rho}{\rho_c}\right)^{0.9}\left(\frac{g}{DN^2}\right)^{1.0}\left(\frac{S}{D}\right)^{2.3}\left(\frac{H}{D}\right)^{0.9}\left(\frac{D}{D_{col}}\right)^{2.7}. \qquad 10$$

Similarly, Kung and Beckman (29) found that

$$\frac{V_d}{x_d} + \frac{K_1\,V_c}{1-x_d} = V_k(1-x_d) \qquad 11$$

where K_1 was a geometric factor, and that

$$\left(\frac{V_k\,\mu_c}{\sigma}\right) = K_1\left(\frac{\Delta\rho}{\rho_c}\right)^{0.9}\left(\frac{g}{DN^2}\right)^{1.0}\left(\frac{S}{D}\right)^{2.3}\left(\frac{H}{D}\right)^{0.9}\left(\frac{D}{D_{col}}\right)^{2.6}. \qquad 12$$

The value of K_1 was between 0.012 and 0.0225.

Inter-droplet coalescence is known to occur in dispersions such as those present in the R.D.C., particularly in the presence of mass transfer, and it is surprising that this was not taken into account in equations 9 and 11. Misek (30) attempted to allow for it in a further modification of 8 ,

$$\frac{V_d}{x_d} + \frac{V_c}{1-x_d} = v_k(1-x_d)\exp(x_d(Z/m - 4{\cdot}1)) \qquad 13$$

where Z was a coalescence coefficient, dependent on hold-up and hence the number of collisions resulting in coalescence, and m was a function of droplet Reynold's number $Re = u_0\rho_c d_0/\mu_c$. Experimental data showed that equation 13 was valid for a limited number of fluid systems, but the strong dependence of Z on system properties was left to a later

study (31) where the variation of Z with a modified Reynold's number Re^* was proposed, such that

$$\ln\left(\frac{d}{d_o}\right) = 1{\cdot}59 \times 10^{-2} Re^{*0{\cdot}5} x_d = Z x_d \qquad 14$$

where $$Re^* = \left(\frac{D_{col}\,\mu_c}{\rho_c}\right)\left(\frac{\sigma}{\rho_c\, d_o}\right)^{0.5} \qquad 15$$

It was claimed that these equations were valid for a wide range of fluid physical properties and column geometries, including both the R.D.C., the A.R.D.C. and the Oldshue-Rushton column. Subsequently the use of equations of the form

$$\frac{d}{d_o} = k_1 + k_2 x_d \qquad 16$$

has become popular (32 , 33), but 16 is clearly a special case of 14 , and does not specifically apply to the R.D.C. Thus a recent study by Al-Hemiri (21) is inconclusive on the applicability of any particular design equations because of the wide range of variables affecting performance. Further, it is well established that droplet coalescence and redispersion in any two-phase liquid system is strongly dependent on fluid physical properties, system geometry, and the amount of energy employed to maintain the dispersion. Inter-droplet coalescence has been reported to occur to a significant extent even in the discharge region of an impeller turbine (34) at low values of hold-up. Therefore the use of the Z factor is greatly oversimplified. In low energy contactors the variation of continuous phase turbulence

in the axial direction is considerable (35) and hence coalescence of droplets is strongly dependent on position.

2.1.2 Mass Transfer

Fundamentally, mass transfer is expressed by equations 1 and 2 . Unfortunately the procedure is complicated since the determination of interfacial area depends on the somewhat unreliable correlations of hold-up and drop sizes with fluid physical properties and operating parameters. Furthermore the driving force for mass transfer is reduced by backmixing.

A less rigorous procedure relies on the evaluation of

1. The number of transfer units required,
2. The height of a transfer unit,
3. The column capacity.

Although the number of transfer units may be accurately found from the desired terminal concentrations, the height of a transfer unit must either be calculated from empirical correlations (13,36,37,38), or predicted from experience. Similarly the column capacity is an arbitrary fraction of the 'flooding' capacity, also determined from experimental tests. Alternatively, the number of theoretical stages is calculated, and the size of column required determined using stage efficiences. Again, this procedure relies to a great extent on experience and empiricisms.

Significant work on the sizes of drops in the R.D.C. has been done by Misek (14,31) and Jeffreys and Mumford (39). The work is fundamental to the understanding of operation and to the prediction of

performance, and is discussed in detail in chapter 4, together with the reported work on drop sizes in agitated tanks.

It is important to note the proposed correlations for backmixing in the R.D.C., the first of which appears to have been that of Strand et al (40) for a range of column diameters from six to eighty-five inches

$$\frac{(1-x_d)E_c'}{V_c H} = 0{\cdot}5 + 0{\cdot}9(1-x_d)\frac{RN}{V_c}\left(\frac{R}{D}\right)^2\left[\left(\frac{S}{D}\right)^2 - \left(\frac{R}{D}\right)^2\right] \qquad 17$$

for the continuous phase, and

$$\frac{xE_D'}{V_d H} = 0{\cdot}5 + 0{\cdot}09x_d\frac{RN}{V_d}\left(\frac{R}{D}\right)^2\left[\left(\frac{S}{D}\right)^2 - \left(\frac{R}{D}\right)^2\right] \qquad 18$$

for the dispersed phase.

Later, Stemerding (41) proposed, for the continuous phase,

$$E_c' = 0{\cdot}5\,H.V_c + 0{\cdot}012.R.N.H.\left(\frac{S}{D}\right)^2 \qquad 19$$

which gave only a fair agreement in a six inch column. Westerterp and Landsman (42) studied the phenomenon in two units up to five inches diameter and suggested

$$\frac{E_c L}{E_a} = \frac{2n}{\left[1+13\times10^{3}.\frac{NR}{F_c}\right]} \qquad 20$$

Stainthorp and Sudall (43) found that the continuous phase coefficient E_c was about 15% higher than the values of Strand, and values of E_d about

double. Conversely, Misek and Rozkos (44) found Strand's values to be between 27% to 55% too high. Misek's correlation,

$$F_B = N.R.(0{\cdot}00434\left(\frac{S}{D}\right)^2 + 0{\cdot}0264\left(\frac{R}{D}\right)^2 - 0{\cdot}00212) \qquad 21$$

is little better however, especially for large columns diameters.

Finally, Miyauchi et al (45) found the following equations agreed well with much of the previous experimental work.

$$\frac{f}{NR} = 4{\cdot}3\times10^{-3}\left(\frac{D}{H}\right)^{\frac{1}{2}}\left(\frac{D}{S}\right)^{\frac{1}{4}} \quad \text{for} \quad \frac{NR^2\rho_m}{\mu_m} > 1{\cdot}2\times10^5 \qquad 22$$

$$\frac{f}{NR} = 4{\cdot}5\times10^{-2}\left(\frac{D}{H}\right)^{\frac{1}{2}}\left(\frac{D}{S}\right)^{\frac{1}{4}} \quad \text{for} \quad \frac{NR^2\rho_m}{\mu_m} < 1{\cdot}2\times10^5 \qquad 23$$

They also claimed applicability of 22 and 23 to both the R.D.C. and the Oldshue-Rushton column.

Mass transfer, expressed as an efficiency, increases when (36)

1. The stator opening is decreased
2. The compartment height is decreased
3. The ratio of dispersed to continuous phase is increased
4. The agitator speed increases
5. The specific load increases.

However under certain conditions backmixing is increased at higher agitator speeds and specific loadings (36,46). The method of correlation proposed by Reman and Olney, viz. plotting efficiency against

energy input per unit volume, is spurious since no account is taken of fluid physical properties, backmixing, and the variation of turbulence with column diameter and hold-up.

Logsdail et al (25) express performance in terms of H.T.U.'s in the form

$$\left[\frac{(HTU)_{OC}}{V_C}\left(\frac{g^2\rho_C}{\mu_C}\right)^{1/3}\right] x_d = \frac{x_d}{K_{OC}\,a}\left(\frac{g^2\rho_C}{\mu_C}\right)^{1/3} = K\left(\frac{\mu_C g}{V_K^3 (1-x_d)^3 \rho_C}\right)^{\frac{2m}{3}}\left(\frac{\Delta\rho}{\rho_C}\right)^{\frac{2(m-1)}{3}} \qquad 24$$

where evaluation of the constant K, the exponent m and the velocity V_K is by experiment. Where coalescence is not great, V_K may be determined from equation 8 . An accuracy of 15% to 20% was claimed, depending whether the direction of mass transfer was into or out of the dispersed phase.

Bruin et al (47) have calculated 'true' H.T.U. values for cobalt extraction in a 6 cm diameter unit by modifying the values for plug flow by using the Peclet number equations of Stemerding and Zuiderweg, viz:

$$\frac{1}{(Pe)_1} = \frac{\varepsilon}{(Pe)_d} + \frac{1}{(Pe)_c} \quad , \quad \frac{1}{(Pe)_2} = \frac{1}{(Pe)_d} + \frac{\varepsilon}{Pe} \qquad 25$$

$$(Pe)_o = (Pe)_1 \frac{0.1\ H_T/(H.T.U.)_{true} + 1}{0.1\ H_T/(H.T.U.)_{true} + (Pe)_1/(Pe)_2} \qquad 26$$

$$H.D.U. = \frac{1}{\frac{(Pe)_0}{h} + \frac{0.8}{H_T}\,\frac{\ln\varepsilon}{\varepsilon - 1}} \qquad 27$$

$$(H.T.U.)_{true} = \frac{H_T}{N_{or}} - H.D.U. \qquad 28$$

where H.D.U. is the height of a dispersion unit and the Peclet numbers are defined in the normal way by

$$Pe_c = \frac{V_c H_t}{(1-x_d)E_c} \quad , \quad Pe_d = \frac{V_d H_t}{x_d E_d} \quad . \qquad 29$$

Recently, Borrel et al (48) have measured values of Pe_c and Pe_d in a 50mm diameter R.D.C. by a trace injection technique. They found that as the rotor speed increased the Peclet number for the continuous phase increased, as expected, and that in two phase operation, backmixing in the continuous phase is accentuated by the droplets present. The actual values of Pe_c varied between 40 and 20, dependent on rotor speed and flowrates.

2.2 Other Rotary Agitated Contactors

A limited amount of hydrodynamic and mass transfer data for other columns have been reported in the literature, and are reviewed below.

2.2.1 Assymetric Rotating Disc Contactor

The A.R.D.C. is a minor variation of the R.D.C. proposed by Misek (49,50). The rotor is offset from the column axis, and separation of the phases is said to take place in a shielded transfer section, as shown in figure 2.1 . It is claimed that the presence of separate mixing and separating zones reduces backmixing (51), but this is at the expense of reduced capacity and a larger column diameter. Design equations similar to those for the R.D.C. have been published (50,51,52). There are several known applications (50), such as the extraction of caprolactam. The A.R.D.C. appears to offer no improvement over the R.D.C. in terms of performance.

2.2.2 Other Variations of the R.D.C.

Many varying designs have been proposed, concerned mainly with variations in the way energy is transmitted to the fluids. One example is a design by Reman (53), having two rotors in the shell. Another has perforated discs (54,55), and another 4 arcs, each 60° (56). Yet another has no stator ring, but discs of two diameters with the larger ones perforated (57), and one design utilises merely a rotating shaft with no discs at all (58). The Zheil extractor (59) has rotating star-shaped impellers combined with vertical oscillations, and has found commercial application for phenol extraction. Rotating polypropylene cones have been proposed by Al-Hemiri to utilise a wetting-redispersion phenomenon, but in tests these proved to have no advantage over equal sized discs. (21)

2.2.3 The Oldshue-Rushton Column

Just as the R.D.C. is the basic contactor in the class of lower energy rotary units, so the Oldshue-Rushton column occupies a similar position in the higher energy class. It is in this class of units that the coalescence-redispersion phenomenon is predominant. The Oldshue-Rushton column is therefore fundamental to this work, and is discussed at length in chapter 3. Some related high energy contactors are discussed below.

2.2.4 The Scheibel Column

Alternate fully-baffled mixing sections and packed sections are the characteristic design features of this unit, as shown in figure 2.3 . The droplet coalescence-redispersion phenomenon predominates in the

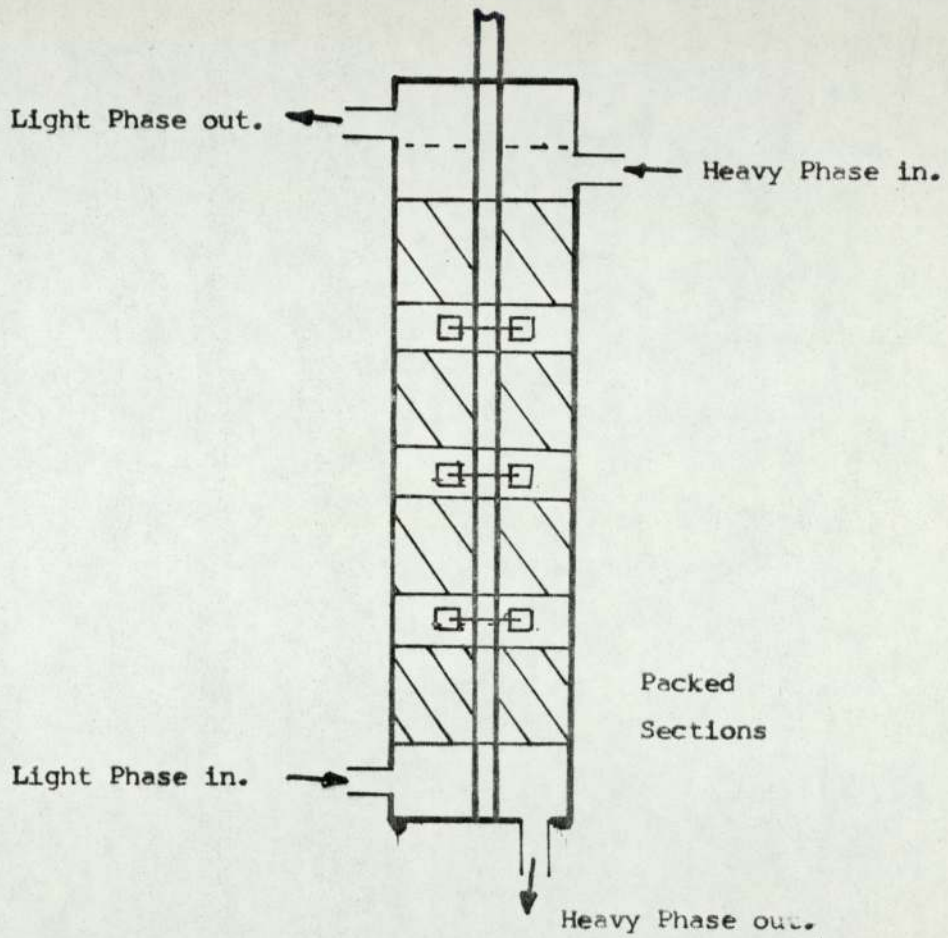

Figure 2.3 Original Scheibel Column.

mixing sections, and therefore the column is reviewed in some detail. The unit was patented by Scheibel (60) in 1950. Design equations for the column were presented by Karr and Scheibel (61) for the mixing sections only, where the dependence of the overall mass transfer coefficient Ka was found to be dependent on the physical properties of the system, and related by

$$Ka = C\left(\frac{\Delta\rho}{\sigma}\right)^{1.5} . \qquad 30$$

By applying the concept of a critical flowrate, which was dependent on system properties, it was found that, for several systems, the mass transfer coefficient was proportional to the dispersed phase flowrate raised to an exponent which was zero below the critical flowrate and unity above it. However, no correlation for the critical flowrate was proposed.

Coefficients were also found to be dependent on agitator speed and diameter, i.e. power input, and are summarised in table 2.1. Drop sizes were not measured, but the dependence of mass transfer coefficients on drop size was established by the power input relationship. Enhanced coalescence due to mass transfer from the dispersed phase and increased wetting effects when water was dispersed are reflected in the varying exponents of the power group ND and the different values of the constants. Unfortunately the correlations presented in the table are oversimplified, and no account was taken of the following, which have an influence on mass transfer in this situation

1. Drop-drop coalescence

Table 2.1 Correlations for mass transfer in a Scheibel column (61)

	3" diameter column[1]	12" diameter column[2]
Organic dispersed †	$\frac{Ka.D}{V_d \left(\frac{\Delta\rho}{\sigma i}\right)^{1.5}} = 1.09 \times 10^{-7} (ND)^{4.0}$	$\frac{Ka}{V_d \left(\frac{\Delta\rho}{\sigma i}\right)^{1.5}} = 7.0 \times 10^{-6} N^{4.0}$
Organic dispersed *	$\frac{Ka.D}{\left(\frac{\Delta\rho}{\sigma i}\right)^{1.5}} = 3.36 \times 10^{-7} (ND)^{4.0}$	$\frac{Ka}{\left(\frac{\Delta\rho}{\sigma i}\right)^{1.5}} = 21.5 \times 10^{-6} N^{4.0}$
Water dispersed *†	$\frac{Ka.D^{0.3}}{\left(\frac{\Delta\rho}{\sigma_i}\right)^{1.5}} = 7.9 \times 10^{-6} (ND)^{3.0}$	$\frac{Ka}{V_d \left(\frac{\Delta\rho}{\sigma i}\right)^{1.5}} = 3.34 \times 10^{-4} N^{3.0}$

* Raffinate phase

† Extract phase

1 System : Methylisobutylketone/acetic acid/water

2 Systems: Methylisobutylketone/acetic acid/water
O - xylene/acetic acid/water
O - xylene/acetone/water.

2. Backmixing in the mixing sections

3. Mass transfer in the packed sections

4. Backmixing in the packed sections.

The equations are of limited use because they are specific to the systems studied. Subsequently, Honekamp and Burkhart (62) confirmed that the mean drop size in the extractor is determined by the drop size generated in the mixing sections, and that little drop size change takes place in the packing. In a three inch diameter unit using the system MIBK/acetic acid/water they found that between 25% and 50% of the mass transfer occurs in the packed sections. Clearly, therefore, the usefulness of the packing is debatable, since a smaller overall column height would be needed for a given duty if the packed sections were replaced by mixers. Indeed, this is reinforced from the hydrodynamics. Since drop sizes change very little in the packing (62), the presence of the packed sections serves only to lower the flooding capacity.

In an attempt to overcome these difficulties for systems of low viscosity and interfacial tension, a modified design was proposed (63) whereby ring-shaped baffles were installed between compartments. Tudose (64) replaced the packed sections with baffled calming zones, and used discs with orifices and blades. Greater efficiency was claimed for this column over all others. A design by Leisibach (65) uses a complex arrangement of transfer ports for each phase together with an annulus of packing around the blade agitator acting as a separating medium.

2.2.5 Other High Energy Rotary Contactors

The Khüni column (figure 2.1) has found applications in extraction with and without mass transfer (66). Capacity and scale-up are expressed by

$$\frac{d}{D} = C \cdot Re^{0.61} \cdot We^{0.6} \cdot Fr^{0.05} \qquad 31$$

The claim that with increasing rate of rotation of the impeller the droplet size decreases and hence the interfacial area and mass transfer coefficient increases is an oversimplification, since droplets below a certain size will have no internal circulation or oscillation, and then mass transfer from a 'rigid' drop becomes the limiting resistance. Flooding in the column has been related to the velocity of droplets through the perforated plate baffles. Axial mixing is said to be related to circulation time of the continuous phase in each compartment and overall dispersed phase flow (67). Published mass transfer data is limited, and the usual claim to increased efficiency (albeit at the expense of throughput) is made.

Other modified designs make similar claims, but have found very limited application and are therefore not discussed here in any detail.

2.3 Conclusions

There are two basic designs of rotary agitated extraction column, the lower energy R.D.C. and the higher energy Oldshue-Rushton column. An indeterminate number of modifications have been proposed, but experiments give no conclusive evidence of the better performance of any

one in particular. It is unfortunate that similar systems have not been studied so as to allow a more equable comparison. The extensive studies on the R.D.C. have not been paralleled by investigations into the Oldshue-Rushton column, and therefore the latter is studied in detail in this work.

3. The Oldshue-Rushton Column

The Oldshue-Rushton contactor was conceived by Oldshue and Rushton (16) in 1952, as a natural extension to the use of mixer settlers for liquid-liquid mass transfer operations. The basic design is illustrated in figure 3.1, and consists of a series of fully baffled mixing vessels sequenced vertically to form a column. The mixing zones are separated by stator rings having a single central hole through which the phases flow. The preferred arrangement of four baffles in each mixer and a centrally located four blade turbine agitator gives good agitation and minimises the volume of interstage flow, which contributes to backmixing. Normally, for consistency in scale-up of power requirements, the preferred dimensions are as shown in table 3.1.

Table 3.1. Dimension ratios for Oldshue-Rushton Column

(Nomenclature is given in figure 3.1)

D	D_{col}	B_h	B_w	D_d	b	A_s	H
20	60	4	5	15	5	20 to 30	30

The column has been used industrially (68) for the extraction of organics, such as phenol or aniline and for the extraction of uranium (69, 70), the number of stages varying from about four to about forty.

3.1 Column Hydrodynamics

In any application it has been common practice to choose to disperse the process stream having the lower volumetric throughput, so that the overall phase ratio in the contactor (i.e. dispersed phase

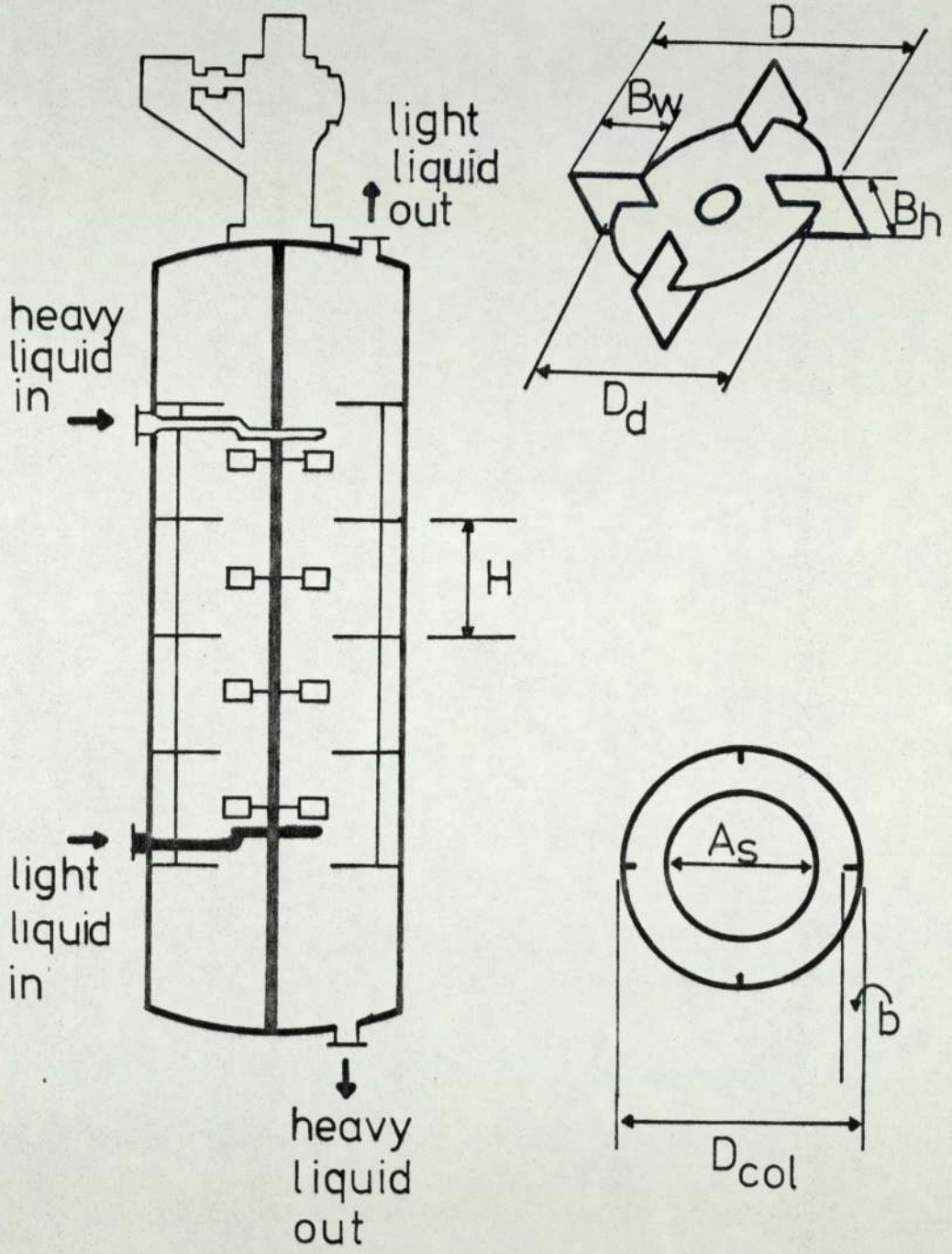

FIGURE 3.1 OLDSHUE-RUSHTON COLUMN

volume/continuous phase volume) is such that excessive coalescence of the dispersed phase does not occur, which might give rise to the phenomenon of phase inversion. This has previously been regarded as an unfavourable event, and is dealt with in detail in chapter 4. The droplets may be heavier or lighter than the continuous phase. Commonly, organic liquids have the lower throughput due to economic considerations. They also, generally, have a specific gravity less than unity, and therefore it is common to disperse the organic into the aqueous continuous phase, at the lower end of the column so that it rises by buoyancy countercurrent to the aqueous phase. The description of overall column flow will assume these conditions, but it is recognised that aqueous dispersions in organic liquids may have a specific gravity greater than unity, in which case the dispersed phase would enter the top of the column. Nevertheless, a similar description of column operation would still apply.

Dispersed phase droplets enter the base of the column via either an open pipe, as is the case in commercial columns, (68) or via a distributor, as used by Mumford (20). The provision of a distributor, of the perforated plate type, appears to offer some advantage in small scale research units in that the dispersion entering the first compartment is of a fairly uniform and known size distribution. The section of the column between the distributor and the first compartment would then act as a spray column, which would not be advantageous from the point of view of the extra column height required and that it may act as a region where premature flooding may take place. Additionally, any particular distributor will give only satisfactory performance for a limited range of flowrate.

The contactor is neither a truly compartmental or truly continuously differential device, but has some properties of both. It is reported (16) that, in an experiment using acetic acid as solute and an acid-base indicator in the continuous phase, there is a distinct and uniform concentration in each stage, and that the column operates as a series of distinct stages. This is misleading because even a truly continuously differential contactor such as a spray or packed column would have a constant concentration at any point when operating under steady state conditions. The fact that each compartment is well mixed does not of itself mean that the contactor is operating in a truly stagewise fashion.

Not withstanding these arguments, the vertical component of velocity relative to the continuous phase of any droplet within each stator opening determines whether or not it moves to the next compartment, since compartments are physically separated by the stator rings. For the purpose of analysis of droplet sizes, each compartment may be regarded as a stirred tank in its own right. The motion of droplets between compartments is fundamental in determining the operating characteristics of the column, and is dependent upon droplet sizes, the physical properties of the phases, the overall phase flowrates and the agitator speed for a fixed geometry system. The correlation of these variables therefore involves an examination of fluid flow patterns within each compartment, and between adjacent compartments.

The sizes of the droplets within each compartment depends upon similar variables, and, since the drop size distribution of the

dispersion passing through the stator opening is determined by conditions within the previous compartment, it is droplet behaviour within the circulating flow of each compartment that determines column operating characteristics.

A decrease in mean drop sizes was observed (18) as drops progress up the column, but no measurements of drop sizes have been reported. Volumetric hold-up is also an important parameter, and indeed, because the mechanisms of coalescence and redispersion are balanced in the column, any measurements of drop sizes must be quoted with the corresponding hold-ups. This is vital where interfacial areas are to be calculated.

3.1.1 Compartmental Flow

Flow patterns in fully baffled stirred tanks have been the subject of extensive study. The similarity of compartmental flow to that of a stirred tank was noted by Oldshue and Rushton, and is illustrated in figure 3.2. The comparison is utilised further in discussing drop sizes in chapter 4.

The overall flow from the impeller is radial, and is similar to a high velocity jet which broadens and due to entrainment slows down as it progresses towards the wall. At or near the wall the radial component of the fluid velocity decreases rapidly to zero, with a corresponding increase in the tangential and axial components. There is a stagnation point at the wall where the centreline of the impeller intersects it, and here the flow splits into two equal parts which then circulate through the rest of the tank, returning along a toroidal path

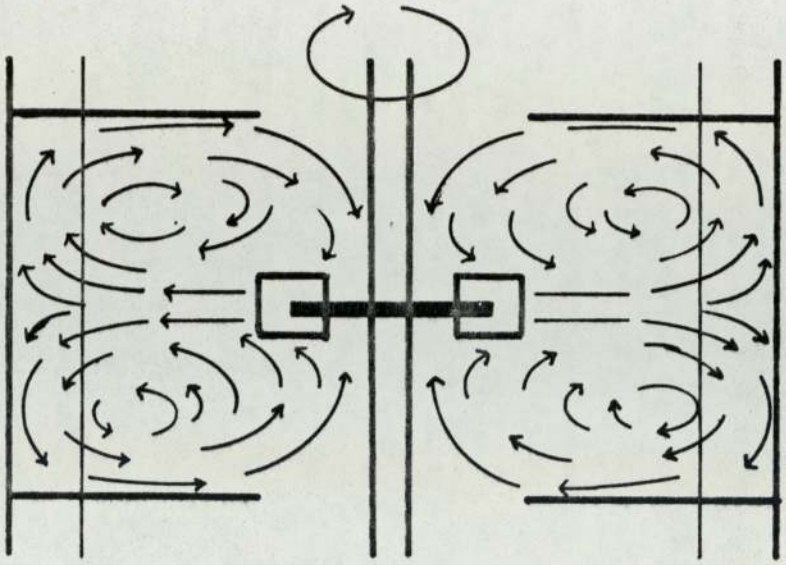

FIGURE 3.2 Compartmental flow

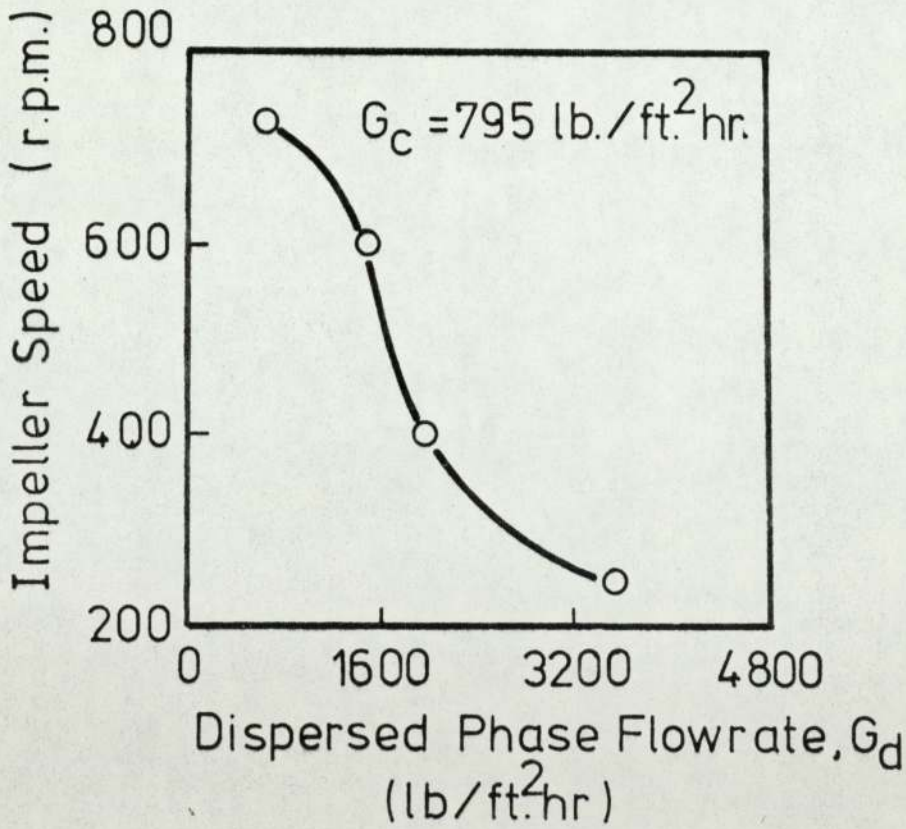

FIGURE 3.3 Flooding in the O/R column.

to the impeller region. Some fluid may be entrained in the flow of the next compartment, by flow through the stator hole. This effect is more pronounced at higher rotor speeds, (18) and contributes to the continuous phase backmixing discussed later.

Droplets follow very closely the flow patterns of the continuous phase within each compartment. It has been shown (71) even with relatively dense particles of iron or aluminium that this occurs. Where the axial velocity of the compartmental flow is very low, in the region around the stator ring orifice, droplet terminal velocities predominate over the continuous phase velocity, and some intercompartmental flow of dispersed phase occurs. By this mechanism droplets progress up the column through consecutive compartments, later to coalesce with the interface at the top of the column. The claim (16) that there is little intermixing between compartments must therefore be viewed with some doubt, especially at the higher operating speeds.

3.1.2 Column Capacity

The maximum column throughput occurs just before flooding takes place. Flooding in agitated contactors is usually defined as the point at which the continuous phase outlet becomes contaminated with droplets of dispersed phase. It may also be defined as that point when the interface leaves the end of the column, and the continuous phase leaves via the dispersed phase outlet.

The flooding point depends primarily on two factors for any given process fluids and system geometry, viz. fluid flowrates and impeller speed. For a particular flowrate, there is a definite impeller speed

which produces flooding, as illustrated by figure 3.3, (16). With the flowrate of continuous phase as parameter, a family of curves would be obtained. Generally, for any particular flowrate, columns operate at agitator speeds about 90 per cent of the flooding speed.

3.2 Mass Transfer

Oldshue and Rushton measured terminal stream concentrations in the transfer of acetic acid between water and methylisobutyl ketone in a six inch diameter column. Results were analysed in terms of height of column equivalent to a theoretical stage (H.E.T.S.) and efficiency, defined as the ratio of the number of equivalent contacts, computed from results, to the actual number of stages in the column. Values of the number of theoretical stages were plotted against the turbine speed for various flowrates, all other conditions remaining constant. Figure 3.4 shows a typical plot, showing the expected decrease in efficiency when the flowrate is decreased. The optimum flowrate was taken as the highest point of curve 3, flooding occurring before the maximum efficiency was reached in curve 4.

It is impossible to extrapolate from the results obtained from any specific experiments when attempting to predict the mass transfer performance of a column. Oldshue and Rushton investigated seven variables, viz.

Liquid Flowrate	Compartment Height
Impeller Speed	Diameter of Stator Opening
Impeller diameter	Direction of Mass Transfer
Impeller position	

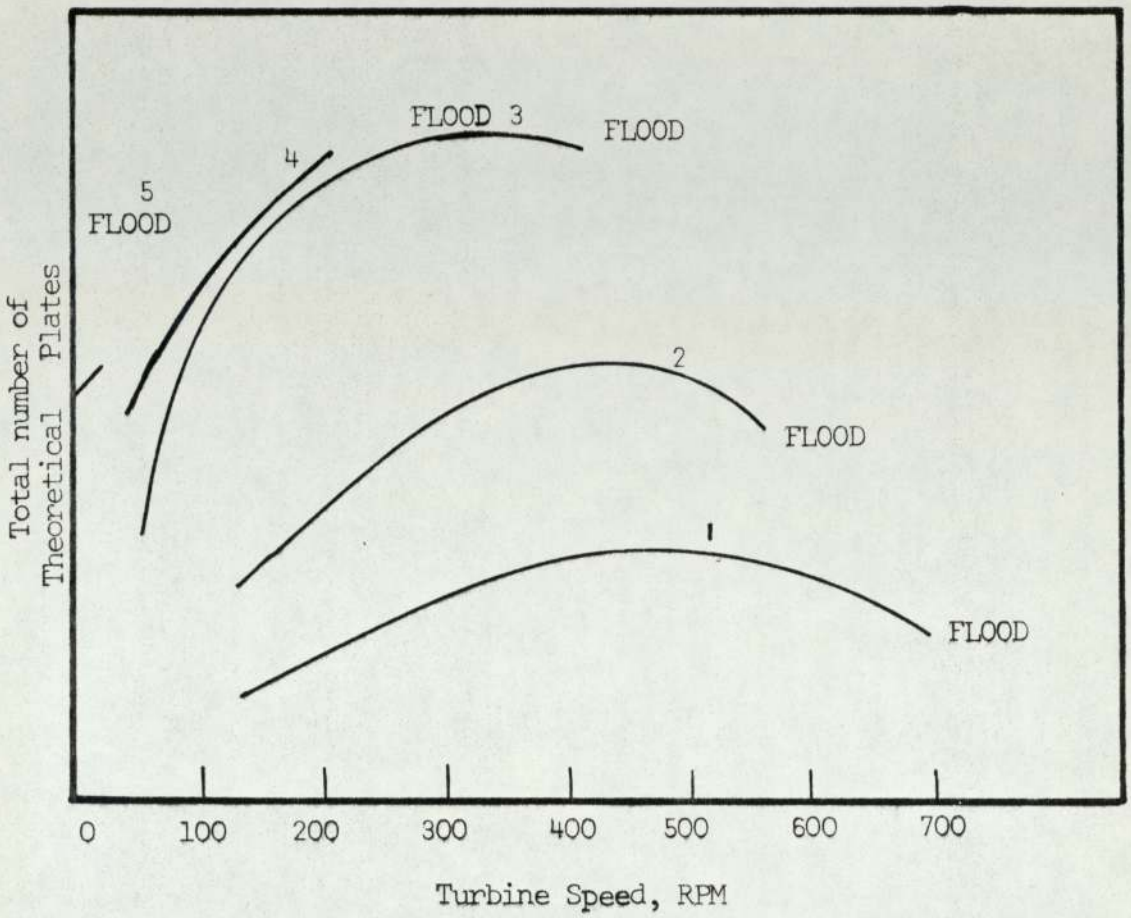

Flow rate increases from Run 1 to Run 5. Ratio of individual stream rates constant. All other conditions constant.

Runs 1,2 - Low flow rates. Maximum efficiency present
Run 3 - Optimum flow rate
Run 4 - Floods before maximum point is reached
Run 5 - Floods at no agitation

Figure 3.4 Typical schematic diagram for effect of flow rate on stage efficiency (16)

These were regarded as independent variables. The dependent variables, not considered, are drop sizes, coalescence and break-up rates of droplets, and variations in the physical properties of fluids. However, as discussed in chapter 1, mass transfer coefficients, interfacial areas and drop size distributions etc., are interdependent, and evaluation of column performance in the absence of such vital data is impossible.

In the only other published work on mass transfer in the column, Bibaud and Treybal (16), calculated values of the mass transfer coefficient K consequent to measuring axial mixing. It was necessary to use estimates for the interfacial area a, from drop sizes computed from Thornton's correlations (28), the use of which is open to criticism, and is discussed in chapter 4. Nevertheless, the values obtained for K compared favourably with those postulated for rigid spheres, as shown in figure 3.5. Again, no measurements of drop sizes were made, and therefore the values of K obtained experimentally are suspect.

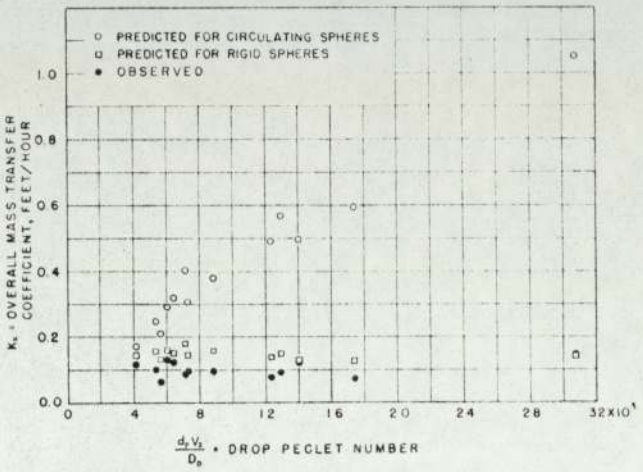

Figure 3.5 Overall Coefficients (18).

4. Droplet Phenomena

Hydrodynamic and mass transfer behaviour in liquid extraction columns depends on the properties of the dispersion of one phase in the other. Of particular interest in this work are those contactors which utilise a coalescence-redispersion mechanism. Therefore an understanding of droplet break-up and coalescence is presented.

4.1 Fundamental Theory

The deformation of drops by external forces has been summarised by Hinze (72). Three basic types were identified,

1. 'Lenticular' deformation. The drop is flattened into an oblate ellipsoid.

2. 'Cigar' shaped deformation. The drop extends to a prolate ellipsoid, then a long cylindrical thread.

3. 'Bulgy' deformation, where the drop surface is deformed in certain places and protuberances created.

Subsequently break-up of the drops occurs if the extent of deformation is sufficient and persists for long enough.

For a single drop, Hinze (72) suggested that the force per unit area τ causing deformation could be a viscous stress or a dynamic pressure. These would correspond to essentially laminar or turbulent flow in the continuous phase. The surface force within the droplet, resisting deformation arising from the interfacial tension σ is σ/d. If the dynamic pressure creates velocities of $(\tau/\rho_d)^{\frac{1}{2}}$, the viscous stress will be $\frac{\mu_d}{d}(\tau/\rho_d)^{\frac{1}{2}}$.

Therefore the three forces controlling break-up are

$$\tau \quad , \quad \frac{\sigma}{d} \quad \text{and} \quad \frac{\mu_d}{d}\left(\tau/\rho_d\right)^{\frac{1}{2}} .$$

Two dimensionless groups arise from these,

$$N_{Vi} = \mu_d / \sqrt{\rho_d \sigma d} \quad , \text{ a viscosity group,}$$

and $N_{We} = \frac{\tau d}{\sigma}$, a modified Weber number.

At critical values of N_{We} break-up occurs.

4.1.1 Break-up in Turbulent Flow

It has been postulated by Kolmogorov (73) that in turbulent flow a whole range of eddy sizes exist. In a stirred tank the largest eddies will have the same order of magnitude as the impeller blade, and the smallest will be on a molecular scale. The largest eddies are the means by which energy is transferred from the impeller blade to the fluid, and contains the bulk of the kinetic energy of the fluid. These interact with the surrounding fluid to produce smaller eddies of a higher frequency and the process is repeated until the energy is dissipated in the form of viscous shear and converted to heat.

Kolmogorov's theory is that at high values of a modified Reynold's number Re_m, the smaller eddies are independent of the bulk motion, and are isotropic. The characteristic velocities, dissipation time and other properties of these eddies are a function of the energy

distribution throughout the fluid. The kinematic viscosity, ν, ultimately governs the energy dissipation.

Two parameters were defined in order to characterise length and velocity.

The length scale $$\eta = \left(\frac{\nu^3}{\varepsilon}\right)^{\frac{1}{4}} \qquad 32$$

and the velocity scale $$v = \left(\nu\varepsilon\right)^{\frac{1}{4}} \qquad 33$$

where ε is the energy dissipation per unit mass.

For isotropic turbulence a relation exists between these such that

$$\frac{u_r}{v} = \beta\left(\frac{d}{\eta}\right) \qquad 34$$

where u_r is the root mean square relative velocity between two points a distance d apart, and β is a specific function.

Kolmogorov argued that if the Reynold's number of the main stream is high enough an "inertial subrange" should exist, outside the region where viscous dissipation is taking place.

For this region,

$$u_r = \left(\varepsilon d\right)^{\frac{1}{3}} \qquad \text{where} \quad \eta \ll d \ll L \qquad 35$$

$$\therefore \beta\left(\frac{d}{\eta}\right) = \left(\frac{d}{\eta}\right)^{\frac{1}{3}} \qquad 36$$

In any volume of characteristic dimension d ($\ll L$) all velocity correlations are functions of d and η (or ε and ν) only. Thus the mean square relative velocity $u_r^2(d)$ between any two points a distance d apart is a function of v and η for all regions where the theory holds. Also, if $L \gg d \gg \eta$ then $u_r^2(d)$ is a function of ε only, and not ν.

However, it is possible that at high impeller speeds, drop sizes could be smaller than the microscale of turbulence, η,

$$\text{i.e.} \quad L \gg \eta \gg d \qquad 37$$

In this case the velocity gradient function becomes, according to Kolmogorov,

$$\beta\left(\frac{d}{\eta}\right) = \left(\frac{d}{\eta}\right) , \qquad 38$$

a linear relationship. This function $\beta = 1$ allows us to realise the boundary condition $u_r = 0$ when $d = 0$

$$u_r = d\left(\frac{\varepsilon}{\nu}\right)^{\frac{1}{2}} \qquad 39$$

It is essential, therefore, to know the magnitude of η in order to predict the velocity relationship.

Values of η for a standard fully baffled mixing vessel of identical geometry to a single compartment of a six inch diameter Oldshue-Rushton column containing water have been calculated using equation (32) and are given in table 4.1 below.

Values for the energy per unit mass ε for different regions of the vessel are proportional to the mean value given by (16)

$$\bar{\varepsilon} = \frac{C\, N^3 D^5 \rho_c}{M} \qquad 40$$

where C = 4.4 for this geometry,

N = impeller speed (r.p.m)

M = mass of fluid in vessel (g)

ρ_c = density of fluid (g/cm^3)

D = agitator diameter (cm)

Cutter (35) has shown that for the impeller stream $\varepsilon/\bar{\varepsilon} \simeq 7.7$ and for the lower energy recirculation regions $\varepsilon/\bar{\varepsilon} \simeq 0.26$.

Table 4.1 Microscales of Turbulence for Water

N (r.p.m.)	Re_I	$\bar{\varepsilon}$ ($cm^2 s^{-3}$)	η (mm)	
			Impeller region	Circulation Zone
200	0.86×10^4	39.6	0.075	0.176
300	1.30×10^4	134	0.056	0.130
400	1.71×10^4	317	0.045	0.105
500	2.15×10^4	620	0.038	0.089
600	2.58×10^4	1070	0.033	0.077

The magnitude of the calculated microscales is of the same order as the droplet diameter commonly encountered in mixer-settlers and the Oldshue-Rushton and other high energy contactors. The use of either equation (35) or equation (39) therefore requires caution.

Furthermore, Stuart and Townsend (74) have estimated that

$$Re_\lambda = \frac{u\lambda_g}{\nu} > 1500 \qquad 41$$

For the inertial subrange to exist, where λ_g is Taylor's microscale of lateral turbulence. Values of λ_g are similar to those of η in most systems. Taylor (75) gave an expression for λ_g,

$$\lambda_g = u.\sqrt{\frac{15\,\nu}{\varepsilon}} \quad . \qquad 42$$

Combining (41) with (42),

$$Re_\lambda = u^2.\sqrt{\frac{15\,\nu}{\varepsilon}} \quad . \qquad 43$$

Jandrell (76) gives typical maximum values for u in a tank geometrically identical to the Oldshue-Rushton column as 0.25 m/s at $Re_I = \frac{ND^2\rho_c}{\mu_c} = 1.29 \times 10^4$, which leads to a value of Re_λ of 270, clearly much less than the required 1500. This is confirmed by Levins and Glastonbury (71) who calculated a value of 144 for the circulation region of a similar fully baffled vessel.

Therefore the use of Kolmogorov's laws to predict relative velocities requires caution. Nevertheless, many authors have reported good agreement between equations derived on this basis and experimental results. The paper by Kuboi et al (77) gives added confirmation of equation (35).

Based on equations (35) and (39), the corresponding equations for the prediction of drop sizes are

$$r_{s.d.} = K_1 \left(\frac{\sigma}{\rho_c}\right)^{0.6} \left(\frac{1}{\varepsilon}\right)^{0.4} \qquad L \gg r \gg \eta \qquad 44$$

and

$$r_{s.d.} = K_2 \left(\frac{\sigma \mu_c}{\rho_c^2}\right)^{\frac{1}{3}} \left(\frac{1}{\varepsilon}\right)^{\frac{1}{3}} \qquad L \gg \eta \gg r \,, \qquad 45$$

where r is the drop radius and $r_{s.d.}$ is the maximum stable drop size. The detailed derivation is given in Appendix 1.

For fully turbulent flow the power number is constant and equation (40) applies.

Therefore

$$\varepsilon \sim N^3 \qquad 46$$

and hence

$$r_{s.d.} \sim N^{-1.2} \qquad L \gg r \gg \eta \qquad 47$$

and

$$r_{s.d.} \sim N^{-1.0} \qquad L \gg \eta \gg r \,. \qquad 48$$

These relationships (47) and (48) were verified experimentally (78) for the nitration of toluene. For that system it was argued that which of equations (44) and (45) was applicable was dependent only on the value of the volumetric hold-up. No attempt was made to estimate the microscale of turbulence.

An alternative approach was suggested by Hinze (72) and Shinnar and Church (79), where an expression for sauter mean drop size d_{32} was derived in terms of a droplet Weber number, We. Hinze considered that droplet break-up by viscous shear did not take place because observed drop sizes were much greater than the expected values of the microscale

of turbulence that determines maximum drop sizes. Thus

$$We_{crit.} = \frac{\rho \bar{u}_r^2 d_{max}}{\sigma} \qquad 49$$

This applied to a dilute dispersion where no interdroplet coalescence occurred, and has been confirmed experimentally (72).

Shinnar and Church (79) assumed that for a drop with essentially equal density and viscosity to the continuous phase, the drop oscillates with the surrounding fluid. If the kinetic energy E_d supplied to the drop is equal to or greater than the difference in total energy of the parent drop and the daughter droplets, then if two droplets are formed upon rupture

$$\frac{E_d}{\sigma d^2} \simeq 0{\cdot}26 \; . \qquad 50$$

For local isotropic turbulence

$$E_d \sim \rho_c u_r^2 d^3 \qquad 51$$

Therefore from (51) and (52)

$$\frac{\rho_c u_r^2 d}{\sigma} = We = 0{\cdot}26 \qquad 52$$

Evaluation of u_r^2 is difficult in a practical dispersion, but it can be related to the energy supplied to maintain the dispersion.

Thus, in a fully baffled vessel, (80)

$$\bar{\varepsilon} \sim N^3 D^2 \qquad 53$$

Substitution into (35) gives

$$u_r = K_3 N D^{2/3} d^{1/3} \qquad L \gg d \gg \eta \qquad 54$$

and into (38) gives

$$u_r = K_4 N^{3/2} D d^{1/2} \qquad L \gg \eta \gg d \qquad 55$$

$$\therefore \quad We = \frac{K_5 N^2 D^{4/3} d^{5/3} \rho_c}{\sigma} \qquad L \gg d \gg \eta \qquad 56$$

and

$$We = \frac{K_6 N^{3/2} D d^{3/2} \rho_c}{\sigma} \qquad L \gg \eta \gg d \qquad 57$$

In a study of the break-up of drops in a rotating disc contactor, Misek (81) derived a relationship for drop size based on the work of Hinze. The following assumptions were made.

1. Vertical rise of droplets is negligible in its effect on drop splitting,

2. the highest dynamic pressure is exerted near the column wall and is proportional to the continuous phase velocity,

and 3. the continuous phase velocity u is proportional to the rotor tip speed, and diminishes exponentially towards the wall.

Thus

$$u = u_o / \exp(K_7 \Delta D) \qquad 58$$

Substitution into (49) gives

$$We = \frac{\rho_c u_o^2 d}{\sigma \exp(K_8 \Delta D)} = \frac{\rho_c N^2 D^2 d}{\sigma \exp(K_8 \Delta D)} \quad . \qquad 59$$

Misek then assumed that the variation with compartment height in an R.D.C. was a power function

i.e. $$We = K_9 \left(\frac{H}{D}\right)^{a'} \qquad 60$$

Equating (59) and (60) would then give a correlation for drop size in the contactor, with undetermined constants K_8 and K_9.

Additionally, for less intense mixing when the Reynold's number is below a critical value of 6×10^4

i.e.

$$10^4 < Re_{crit} = \left[\frac{D N \rho_c}{\mu^2}\right]_{crit} < 6 \times 10^4 \qquad 61$$

in the 'transition' region,

$$\frac{d N^2 D^2 \rho_c}{\sigma \exp(K_8' \Delta D)} = K_9' \left[\frac{D^2 N \rho_c}{\mu_c}\right]^{1.42} \qquad 62$$

In the 'laminar' region, when $Re_{crit} < 10^4$, the vertical velocity of the drops becomes significant and break-up by impact on internals predominates.

Thus

$$d = K_{10} \left(\frac{\sigma}{\Delta \rho g}\right)^{0.5} \qquad 63$$

In this region agitation speed has no effect on drop size.

4.2 Coalescence Fundamentals

The coalescence of drops in an extractor affects the performance significantly, by three separate mechanisms.

1. Drop - interface coalescence
2. Drop - solid surface coalescence
3. Drop - drop coalescence.

4.2.1 The Drop-interface mechanism

Unless a coalescing aid, such as wire or plastic packing, is present at the outlet of an extractor, drops must come together and form a continuum by coalescence with an interface of coalesced dispersed phase. If this does not occur, flooding takes place. Although essential to the satisfactory operation of an extractor, a detailed study of the coalescence of drops in packing is beyond the scope of this work. Experimental work in this area is particularly tedious because the presence of impurities, especially surface active substances, can increase or decrease coalescence times significantly. Several studies have been made (82, 83, 84).

4.2.2 Drop - Solid Surface Mechanism

The coalescence of drops onto a solid surface otherwise known as 'wetting' is also not dealt with in detail here. It s importance lies in the fact that if the internals of an extractor are wetted by the dispersed phase, they will be constantly covered with a film of that phase. Although this may seem at first sight to be significant in modifying the operating characteristics, a study by Al-Hemiri (21) has

shown that replacing non-wetted internals by wetted ones in a four inch diameter R.D.C. had no measurable effect on the overall mass transfer. This type of coalescence may be a special case of (1) above.

4.2.3 Drop-drop Coalescence

In high energy contactors of the Oldshue-Rushton type, operating at steady state, a dynamic equilibrium between interdroplet coalescence and subsequent break-up maintains a constant mean drop size. The rate of formation of drops by rupture therefore equals the rate of agglomeration by coalescence. It is likely that drop-drop coalescence occurs mainly between pairs of drops, and that the simultaneous coalescence of three or more drops is a rare event. Thus in the analysis of coalescence processes, only binary collisions are considered.

During the process, four steps may be identified.

1. A binary collision
2. Drainage of the continuous phase film between the drops to some critical thickness
3. Rupture of the film
4. Consolidation of the new drop.

In a turbulent flow field, drops which are in stage 2 and 3 above may become separated again, but the force of collision may be greater than in quiescent coalescence.

In simplifying the complex process taking place, Howarth (85) made the following assumptions.

1. All drops are spherical and of uniform size.

2. The flow field is a homogeneous isotropic one of infinite extent.

3. The drops are in random motion.

4. Most collisions result in cohesion or immediate coalescence.

5. The drops are small compared to the smallest wave-length in the turbulence i.e. $L \gg \eta \gg r$.

6. The drop relative terminal velocities are described by Stokes' law.

7. The only force acting on the drops is potential.

8. The nature of the turbulence is not affected by the presence of the drops.

9. The density difference between phases is small.

The number of collisions per unit time per drop is

$$N' = 4\pi n' r \mathcal{D}_d' \qquad 64$$

where $\mathcal{D}_d'$ is the diffusion coefficient for drops which where when their centres are a distance r apart.

The time dependence of the diffusion coefficient, applying Taylor's theory, is

$$\mathcal{E}_p = \mathcal{E}_f = \overline{u}_r^2 \theta \qquad 65$$

If the time interval for collision is the diffusion time,

$$N' = (4\pi n' r \overline{u}_r^2)^{\frac{1}{2}} \qquad 66$$

The number of drops per unit volume is

$$n' = \frac{6 x_d}{\pi d^3} \qquad 67$$

$$N' = \left[\frac{24 x_d \nu \overline{u}_r^2}{d^3} \right]^{\frac{1}{2}} \qquad 68$$

By further assuming that an analogy with drop-interface coalescence is applicable in that there is a critical approach velocity above which coalescence is immediate and below which coherence occurs but rarely results in coalescence, the fraction of collisions resulting in coalescence is

$$f = \exp \left(-3 w^{*2} / 4 \overline{u}_r^2 \right) \qquad 69$$

Combination of (68) and (69) gives the collision frequency

$$\psi = \left[\frac{24 x_d \nu \overline{u}_r^2}{d^3} \right] \cdot \exp \left[-3 w^{*2} / 4 \overline{u}_r^2 \right] \qquad 70$$

The applicability of this equation is seriously limited by the restrictive assumptions necessary for the derivation. In a real situation,

1. Drops are rarely spherical and have a wide distribution of sizes

2. There is some doubt as to the existence of an isotropic field

3. The drops do not have a true random motion

4. Shinnar (86) has previously argued that since the cohesive force holding any two drops together is dependent on drop diameter, there should exist a minimum size of separable drops at a given turbulence level , and that drops below this size should coalesce rapidly. This is supported by the fact, argues Shinnar, that there exists a critical agitator speed below which coalescence does not occur. However, compared to turbulence force, the interfacial tension cohesive force is small, and a significant function of collisions result in immediate coalescence.

5. There is some doubt as to the relative magnitude of drops i.e. is $L \gg \eta \gg r$ or is $L \gg r \gg \eta$?

6. Some modification of Stokes' law is necessary to describe terminal velocities in turbulent flow,

7. There are other forces acting on the drops, e.g. rotational, translational, etc.

8. Drops will be expected to affect the level of turbulence, by absorbing high frequency eddies and returning only part of this to the continuous phase as a lower frequency eddy, another part being lost by viscous dissipation both inside and outside the drop. Further turbulent energy is absorbed by surface deformation.

Misek (31) has derived an expression for drop-drop coalescence

based on the work of Levich (87), assuming that

1. Each collision results in combination

2. Drops follow the turbulent fluctuations of the continuous phase

3. The dispersion is characterised by a hydraulic mean diameter.

Levich derived the frequency of collision in the bulk of the fluid as

$$N' = \frac{K_{11}\, n'^2\, d^3\, u_r^{3/2}}{\sqrt{\vartheta D}} \qquad 71$$

and at the wall of a column

$$N'_w = \frac{K_{12}\, n'^2\, d^3\, u_r^2}{\vartheta} \qquad 72$$

Because the sizes of any two drops immediately prior to collision will be governed by the result of the last combination, the diameter ratio of combined to original drops is

$$\frac{d}{d_o} = \exp\left[\frac{K_{13}\, N'\theta}{n'}\right] \qquad 73$$

Equating dynamic pressure causing break-up to surface force preventing it gives

$$u_r = K_{14}\sqrt{\frac{\sigma}{d_o \rho_c}} \qquad 74$$

By further assuming that the time during which coalescence occurs is proportional to the ratio of the column characteristic dimensions D to u_r, combination of (72), (73) and (74) yields

$$\ln\left[\frac{d}{d_o}\right] = K_{15}\left[n'd^3\right]u_r\left[\frac{D}{\nu}\right] = K_{16}\,x_d\left[\frac{\sigma}{d_o\rho_c}\right]^{\frac{1}{2}}\left[\frac{D}{\nu}\right] = Z_1 x_d \qquad 75$$

for coalescence at the wall.

Coalescence in the bulk is described similarly by

$$\ln\left[\frac{d}{d_o}\right] = K_{17}\left[n'd^3\right]u_r^{\frac{1}{2}}\left[\frac{D}{\nu}\right]^{\frac{1}{2}} = K_{18}\,x_d\left[\frac{\sigma}{d_o\rho_c}\right]^{\frac{1}{4}}\left[\frac{D}{\nu}\right]^{\frac{1}{2}} = Z_2 x_d \qquad 76$$

where the value of Z_1 and Z_2 is determined from equation (13) and u_r is calculated from the terminal velocities of falling spheres (88).

4.3 Empirical Models and Verified Correlations

Hinze (72) has fitted the data of Clay (89) obtained for two phase flow between rotating cylinders to equation (49),

$$We_{crit} = \frac{\rho_c\,\bar{u}_r^2\,d_{max}}{\sigma} \qquad 49$$

utilising Kolmogorov's relationship

$$u_r = K_{19}\,(\varepsilon d)^{1/3} \qquad 35$$

Thus

$$d_{max}\left(\frac{\rho_c}{\sigma}\right)^{\frac{3}{5}}.(\varepsilon)^{\frac{3}{5}} = K_{20} \quad . \qquad 77$$

This is reproduced in figure 4.1, from which the constant K_{20} was found to be equal to 0.725. However, Sleicher has pointed out that the presentation of Clay's data in the form

$$\left[\frac{\rho_c \sigma d_{max}}{\mu_c^2}\right] = 0.725 \left[\frac{\mu_c^5 \varepsilon}{\rho_c \sigma^4}\right]^{-\frac{2}{5}} \qquad 78$$

by Hinze is invalid because most of the variation in the dimensionless groups is caused by variation of fluid properties, and has shown conclusively that Clay's data does not fit equation (77).

Misek (81) has evaluated the constants K_8, a' and K_9 in equations (59) and (60) in an R.D.C.

Thus

$$\frac{\rho_c N^2 D^2 d}{\sigma \exp(0.0887 \Delta D)} = 16.3 \left(\frac{H}{D}\right)^{0.46} \qquad 79$$

and similarly for equation (62),

$$\frac{d N^2 D^2 \rho_c}{\sigma \exp(0.0887 \Delta D)} = 1.345 \times 10^{-6} \left(\frac{D^2 N \rho_c}{\mu_c}\right)^{1.42} \qquad 80$$

and for equation (63),

$$d = 0.38 \left(\frac{\sigma}{\Delta \rho g}\right)^{0.5} \qquad 81$$

These equations do not account for the coalescence of drops, and are therefore limited in application to very dilute dispersions. However,

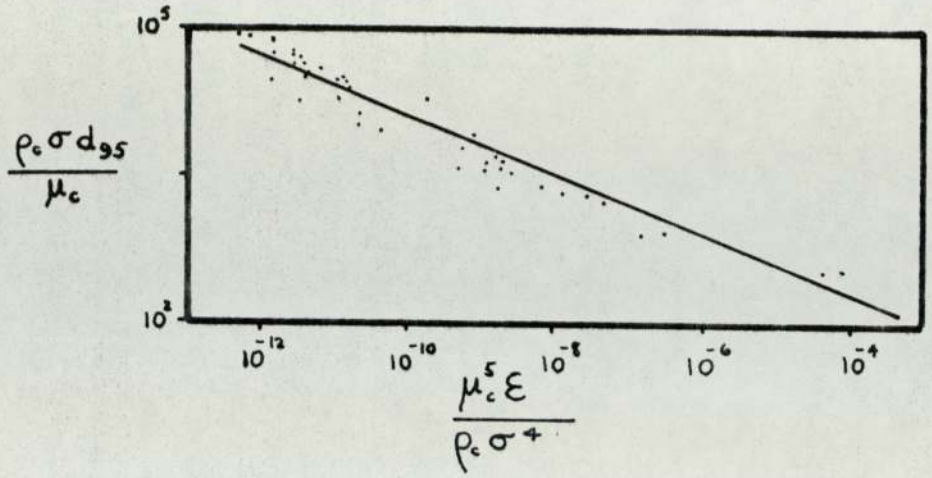

Figure 4.1 Maximum drop size as a function of the energy input according to experimental data by Clay. (89)

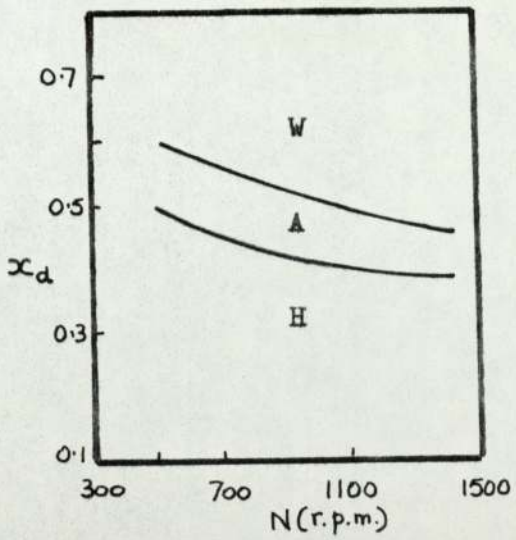

Figure 4.2 Inversion characteristics for the hexane-water system (100)

W Water dispersed

A Ambivalent region

H Hexane dispersed

Misek evaluated the constants in his coalescence equations (75) and (76) by experiment, and obtained $K_{18} = 1{\cdot}59 \times 10^{-2}$. It was claimed that this value of K_{18} was independent of the type of mixer used, but because of the difference in energy levels in the R.D.C. and the Oldshue-Rushton column, it is doubtful whether a single equation can be used for all types. Impact velocities of discrete drops are greater in the Oldshue-Rushton column, whereas coalescence in the R.D.C. can be quite quiescent. The variation of the probability of coalescence with drop size has been established (90) and Misek's equations do not take account of this.

Vermeulen et al (32) studied drop sizes in agitated tanks, and correlated their results by

$$\frac{N^2 D^{4/3} d^{5/3} \rho_c}{\sigma} = 0{\cdot}016 (f_x)^{5/3}, \qquad 82$$

in confirmation of equation (56) developed by Shinnar and Church (79). The function f_x is an empirically determined function of dispersed phase hold-up to allow for coalescence.

Many studies of drop sizes in stirred tanks have been made, with hold-up of dispersed phase ranging from zero to 30 per cent. Generally, these studies have been empirical, and numerous correlations have been produced, many supporting Kolmogorov's theory. One of the first was that of Thornton and Bouyatiotis (28) who studied several systems in a single stirred tank at various hold-up values and impeller speeds. Both batch and continuous operation was used. Their results were correlated

by three equations. The effect of hold-up on mean drop size was found to be linear,

i.e. $$d_{32} = d_{32}^{\circ} + m x_d \quad , \qquad 83$$

where d_{32}° is the mean drop size at zero hold-up and d_{32}° is correlated by

$$\left[\frac{d_{32}^{\circ}\,\rho_c^2\,g}{\mu_c^2}\right] = 29.0\left[\frac{\frac{\varepsilon}{M}^3\,g_c^3}{\rho_c^2\,\mu_c\,g^4}\right]^{-0.32}\left[\frac{\rho_c^3\,\sigma}{\mu_c^4\,g}\right]^{0.14} \qquad 84$$

and

$$m = 1.18\left[\frac{\sigma^2}{\mu_c^2\,g}\right]\left[\frac{\Delta\rho\,\sigma^3}{\mu^4}\right]^{-0.62}\left[\frac{\Delta\rho}{\rho_c}\right]^{0.05} \qquad 85$$

Other studies are summarised in table 4.2 where the dependence of d_{32} on impeller speed N and impeller diameter D has been expressed in the form

$$d_{32} \sim N^{a} D^{b} \qquad 86$$

Significantly, the exponent of the impeller speed N varies between -1.5 and -0.72 and the exponent of the impeller between -2.45 and -0.70. For experimental studies these wide variations may be explained by the use of different systems, which cannot be characterised solely in terms of density, viscosity and surface tension. For example, difficulty has often been experienced in the purification and standardisation of systems (91). It is not clear in some cases whether the systems were in thermodynamic equilibrium. Additionally, the expression of drop sizes in terms of a limited number of variables may be invalid. A notable exception in the table is the correlation of Rodger et al (80) which gives $d \sim N^{-0.72}$. The dimensional analysis of their results contains a group to account for the degree of contamination of the drops by surfactants, expressed as the ratio of the settling time of the dispersion to that of the pure liquid. However, in addition to surfactant concentration, settling time must be dependent on drop size, and therefore the precise relationship between d and N is difficult to determine from the correlation. Equations (47) and (48) predict the value of a in table 4.2 to be -1.2 or -1.0 depending on the relative sizes of drops to the microscale of turbulence.

Table 4.2 Exponents for Single Tanks

	Authors	a	b	Reference
*	Kolmogorov	-1.2	-2.0	73
*	Obukhov	-1.2	-2.0	92
+	Vermeulen et al	-1.2	-0.8	32
+	Rea et al	-1.0	-1.5	93
+	Kafarov and Babanov	-1.1	-0.7	94
+	Pavlushenko et al	-1.0	-1.65	95
+	Rodger et al	-0.72	-0.75	80
+	Yamoguchi et al	-1.5	-2.45	96
+	Pebalk and Mishev	-0.912	-1.624	97
+	Calderbank	-1.1	-0.7	98
*	Shinnar	-1.2	-0.8	86
*	Shinnar and Church	-1.2	-0.8	79
+	Brown and Pitt	-1.2	-0.8	33
*	Hinze	-1.2	-2.0	72
*	Taylor	-1.5	-1.0	75
+	Mylneck and Resnick	-1.2	-0.8	99
+	Giles et al	-1.2		78
+	Giles et al	-1.0		78
+	Luhning and Sawistowski	-1.2		100

+ Experimental Data * Theoretical

4.4 Applicability to the Oldshue-Rushton Column

All the models published to date to predict drop sizes in stirred tanks are restricted to batch operations or continuous operations with either one or both of the fluids flowing in a single tank. Fluids enter and leave the tank via many diverse geometric arrangements, which may or may not affect the hydrodynamics of operation. For example, the geometry used by Thornton (28) resulted in the drop size being independent of flowrate, i.e. the mean residence time of the dispersed phase was large compared with the flowrate, and thus the dynamic equilibrium between droplet break-up and coalescence remained unaffected. Operation was therefore effectively batchwise.

In rotary agitated columns, entrance and exit mechanisms are very important. Larger drops have a greater vertical velocity than smaller ones and are less affected by small scale disturbances in other directions. Classification therefore occurs between compartments resulting in a tendency for the smaller drops to remain in a compartment and larger ones to pass to the next.

Oldshue-Rushton column designs based upon a mean drop size throughout the length of the column in which the drop size correlations are themselves based on data from single stirred tanks are therefore open to criticism.

4.5 Drop Size Distribution

In any practical dispersion there exists a wide range of drop diameters. In high energy systems the range of diameters is large,

and submicroscopic-size droplets may be formed as a 'secondary haze' either by impact with stators, etc., or as residual drops from a coalescence. Large drops are formed by repeated coalescence.

Bouyatiotis and Thornton (28) found that for both batch and continuous operation with four different systems in a stirred tank the measured distribution approximated to a normal one. Similar results for other systems have been reported by Chen and Middleman (101), Sprow (102) and Brown and Pitt (33). Pebalk and Mishev, however, reported that for a variety of liquid-liquid systems, including kerosine/water used by Brown and Pitt, the drop size distribution in a stirred tank was log-normal. Giles et al (78) reported a log-normal distribution during the nitration of toluene.

Whether the drop size distribution is normal or log-normal is of practical significance in an extraction column. For a fixed volumetric throughput, a comparison of the two types of dispersion is illustrated in table 4.2.

Table 4.2

Property of dispersion	Normal	Log-normal
Proportion of smaller droplets	Lower	Higher
mean m.t. coeffs.	Higher because more drops are circulating	Lower - more stagnant drops
Interfacial area	Lower	Higher
Settling rate	Higher	Lower
Tendency to flood column	Higher	Lower

From the point of view of predicting hydrodynamic and mass transfer performance the preferred distribution is a mono-dispersion with a consequent standard deviation of zero. Although this is impracticable in an extractor, a distribution where the mode is equal to the mean results in more drops being nearer the mean size than with a log-normal distribution. Droplet characteristics are thus more predictable in a normal distribution. Therefore it is desirable to obtain a normal distribution around a certain mean drop diameter rather than a log-normal one.

The normal distribution of drop sizes where variations either side of the mean are equally likely, may be expressed in the usual way,

$$Y = \frac{1}{s\sqrt{2\pi}} \exp\left[-\frac{(d - \bar{d})^2}{2s^2}\right] \qquad 87$$

where Y = probability density function

d = drop diameter

$\bar{d}$ = mean arithmetic mean diameter

s = standard deviation

$$s^2 = \sum_{o}^{\infty}\left(\frac{d - \bar{d}^2}{T - 1}\right) \qquad 88$$

T = total number of drops measured.

A normal drop size distribution is characterised by two parameters, the mean and the standard deviation, and a plot of diameter against cumulative per cent frequency gives a straight line.

When ratios of equal amounts in excess of or in deficiency from the mean are equally likely, the distribution is said to be log-normal. Thus

$$Y = \frac{1}{\log s \sqrt{2\pi}} \exp\left(\frac{-(\log d - \log \bar{d})^2}{2(\log s)^2} \right) \quad 89$$

and a plot of log d versus cumulative per cent frequency gives a straight line.

For a normal distribution the mean, d_{32}, equals the mode, d_m but for the log-normal case it can be shown that $d_{32} = 1.08\, d_m$.

4.6 Phase Inversion

When the dynamic balance between droplet break-up and coalescence is upset by an increase in the latter, phase inversion may occur under favourable conditions. Inversion is said to take place when the dispersed phase droplets coalesce to form a homophase, and the previously continuous phase becomes dispersed. The phenomenon was first reported by Ostwald (103); the phase ratio at which it occurred was 3 : 1 and became known as "Ostwald's Ratio". During the course of this work it became clear that phase inversion occurred in the column, and the topic is therefore discussed in some detail.

Phase inversion studies were conducted in a stirred tank by Luhning and Sawistowski (100). Their experiments were conducted by adding discrete quantities of the dispersed phase to the system by a preliminary estimation of phase ratio at inversion and adjusting the starting volumes accordingly. Phase inversion was recorded by measuring changes in

electrical conductivity and this was supplemented by visual observations. Two conductivity sensors were positioned at the top and bottom parts of the tank respectively. In drop size determination they used the direct method of submerged photography and the indirect method of light transmittance.

Drop coalescence rate was measured by the droplet growth method. This required a step change reduction in the stirring speed while following the changes in the mean size using the light transmittance method. The required step change was obtained by sharply grasping the stirrer shaft with a gloved hand and simultaneously changing the speed setting. The drop size increased with increasing concentration of the dispersed phase, probably as the result of more frequent drop collision, the increase being more pronounced at lower speeds. According to Luhning and Sawistowski, close to the inversion point drops of the continuous phase were noticed contained within drops of the dispersed phase. It appears that at high dispersion concentrations the continuous process of drop coalescence and break-up results in the entrainment of the continuous phase by the dispersed phase. This was also noted by Quinn and Sigloh (104) who stated that in concentrated dispersions which appeared to be water continuous, photographs taken through the side of the tank actually revealed droplets of the organic fluid dispersed within larger droplets of water which in turn were surrounded by the organic phase. The first step in developing a means of predicting which phase would be the continuous one was to determine the upper limit of hold-up of each compartment under a given set of

conditions. According to Selker and Sleicher (105), there is always a range of volume fractions throughout which either component would remain stably dispersed. This range was termed the ambivalent range. The limits of this range may be influenced by the size and shape and material of the vessel, the stirring speed, and the physical properties of the liquid. It is also to be expected that the viscosity ratio would influence the limit of ambivalence. If fluid volumes are within the ambivalent range, the phase that remains continuous will depend on the immediate history of the dispersion.

Luhning and Sawistowski represented phase inversion graphically by plotting the volume fraction of one phase at inversion against stirring speed. From this it was deduced that a hysteresis effect existed, represented graphically by two curves defining a metastable or ambivalent region, reproduced in figure 4.2 . Thus if at a constant speed the organic liquid is added to the system, inversion takes place on reaching the upper curve. Conversely, on adding water, inversion is indicated by the lower line. The presence of propionic acid in phase equilibrium, changes the inversion characteristics of the system by widening the ambivalent region considerably. This is an indication of interfacial tension being one of the principal factors affecting the width of the ambivalent region. At phase inversion from toluene/water to water/toluene the mean drop size decreased: the reverse was found to be true for inversion in the opposite direction. The interfacial area increases with increasing volume fraction of the dispersed phase and with increasing speed (100). Rodger, Trice and Rushton (80) noted

that at low rates of energy input the stable dispersion was oil/water and the rate of energy input was increased the dispersion would invert to water/oil. Also they observed that phase inversion occurred most readily in systems in which the ratio of the difference in densities to continuous phase density was large. Quinn and Sigloh (104) carried out experiments in baffled tanks having a height-to-diameter ratio of approximately one. The impeller entered through a mercury seal, and the tanks were suspended in a 30°C constant temperature bath. They indicated that all the inversion curves are similar in that the concentration of the organic phase at phase inversion decreases with increasing rotor speed and the volume concentration becomes independent of stirring speed at two to three times the minimum stirring speed necessary for complete suspension.

Phase inversion is a process accompanied by a decrease in the total energy of the system. Since the measured power input of the impeller remained constant at phase inversion, the energy changes must come from within the system itself. Also, phase inversion can be accompanied either by an increase or decrease in interfacial energy. Minimization of interfacial energy cannot therefore be used as an inversion criterion. Instead, the total energy of the system should be considered. At a fixed volume concentration the dispersed and continuous phase can be inverted by changing the impeller geometry and by changing the rate of energy input (104).

Phase inversion will occur in a batch system only when the rate of coalescence of drops is greater than the rate of break-up. In a

continuous system additional factors have to be taken into account. In a continuous single stirred tank both phases are in flow and as mentioned earlier the geometric arrangement for the entrance and exit of each phase will affect the dynamics of operation. The volumetric hold-up of dispersed phase reaches a steady state value in each compartment when the column is operating normally. This is achieved only when the input of each phase is equal to the output, and this is particularly important with reference to the dispersed phase.

A complex situation exists between consecutive compartments, because the droplets exist in a distribution of diameters, not as a monodispersion. Thus a polydispersion of droplets is flowing by buoyancy through the stator opening against the flow of continuous phase. Superimposed on the varying terminal velocities of the droplets in the dispersion is the turbulent flow mainly across the opening generated by the impellers at the centre of each compartment. When hold-up in the Oldshue-Rushton contactor is large, (about 0.6 - 0.8) phase inversion would be expected to occur, and will have the effect of relieving the imminent flooding situation. Phase inversion would then occur in preference to flooding.

In any two phase counter current operation therefore there is a limit above which normal operation is not possible as either flowrate is increased incrementally. Under certain operating conditions flooding in the usual sense of the word takes place.

5. Mass Transfer

The extent of mass transfer, occurring in practical equipment may be expressed in two ways,

1. The Transfer unit, or theoretical stage concepts. There are three similar definitions of a transfer unit (106)

(a) The true number of transfer units

$$(N.T.U.)_t = \int_{x_o}^{x_1} \frac{Ka\ dx}{G_c} \qquad 90$$

where K is the overall mass transfer coefficient

a is the interfacial area for mass transfer

dx is the solute concentration

and G is the superficial phase velocity.

This is the familiar Chilton-Colburn expression.

(b) The apparent number of transfer units

$$(N.T.U.)_a = \int_{x_o}^{x_1} \frac{dx}{(x^1 - x^*)} \qquad 91$$

where $y = mx^*$

(c) The measured number of transfer units

$$(N.T.U.)_m = \int_{x_o}^{x_1} \frac{dx}{x - x^*} \qquad 92$$

Figure 5.1 illustrates the limiting concentrations in the three equations on a distribution diagram. The concepts of heights of transfer units is discussed further with respect to axial mixing in section 5.5.

The theoretical stage concept uses the fact that the amount of mass transfer taking place may be expressed as a number (not necessarily an integer) of discrete equilibrium contacts, analogous to the height equivalent to a theoretical plate utilised in distillation column analysis. Of course, if the extraction factor is unity, the height equivalent to a theoretical stage becomes equal to the measured transfer unit.

An efficiency may be used to express equipment performance, defined as the H.E.T.S., divided by the height of a practical stage.

It is a limitation of any of the above approaches that equipment performance, expressed in terms of the terminal concentrations, will include any deviations from ideal behaviour. Thus, the $(N.T.U.)_a$ and $(N.T.U.)_m$ are only valid for the conditions prevailing at the time of measurement, and the equipment used. These points are discussed further in section 5.5.

2. <u>The mass transfer coefficient</u>. As mentioned in chapter 1, the mass transfer coefficient is a proportionality constant between the amount of transfer taking place and the driving force promoting it. Overall coefficients in agitated contactors depend upon the individual coefficients relating to the dispersed and continuous phases, together

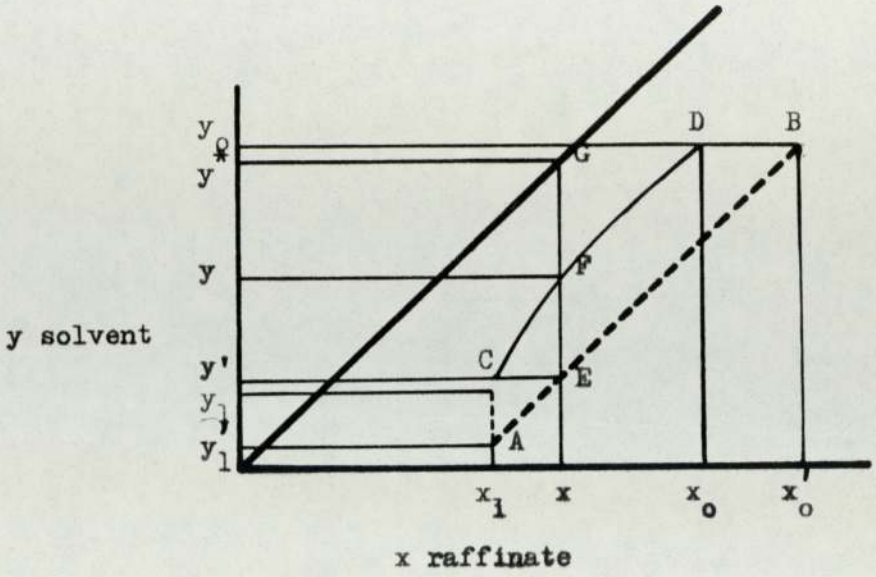

Figure 5.1 Schematic representation of concentration profiles in a differential contactor.

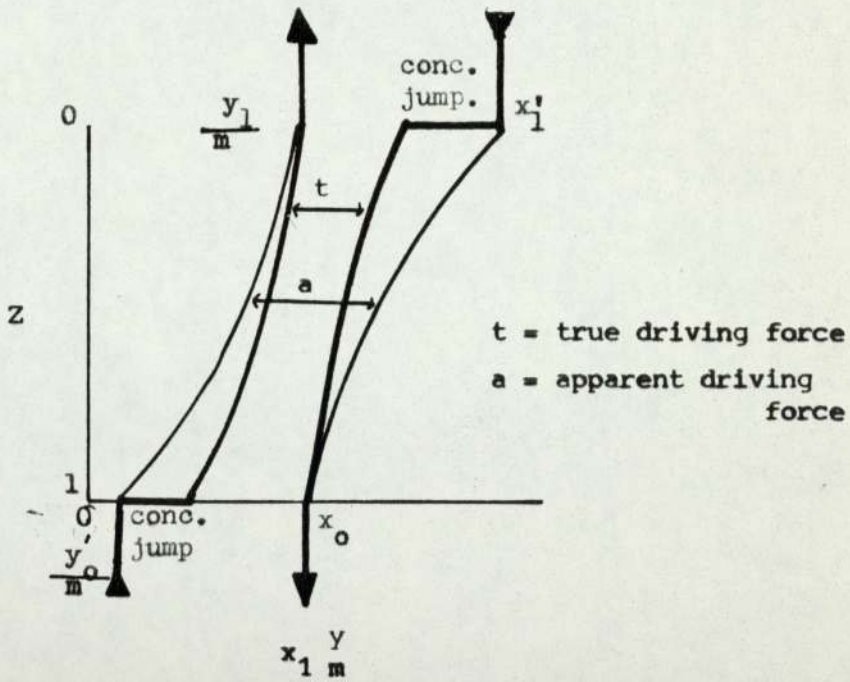

Figure 5.2 Concentration Profiles in the Column.

with any interfacial resistance. For all practical purposes the interfacial resistance may be neglected except, for example, when solute transfer is accompanied by slow chemical reaction. The equation 1 and 2 then apply.

An indication has been given in figure 1.1 of the complex interactions present when extraction occurs. Myriads of small drops are present in a column and the evaluation of interfacial area, which is a function of drop size and hold-up, is difficult. The distribution of drop sizes results in differences in the modes of mass transfer between the size fractions. The presence of a polydispersion further aggravates the non-ideal behaviour of any monodispersion produced in an apparatus which gives the dispersed phase a spread of residence times. The larger-drop fractions have a lower mean residence time in the column than the smaller drops. The calculation of residence times is therefore complicated. The complexity is exacerbated by the changes in drop size distribution which occur axially in the column. Similarly, by design, concentration driving forces vary axially, and with varying residence times. Additionally, turbulence intensities in the continuous phase affect the drop hydrodynamics, causing increased mixing within the drop. Hence it has been necessary to study mass transfer to and from single drops to gain insight into the practical situation.

5.1 Single Drops

Data on mass transfer to and from single drops have been interpreted in terms of the three hydrodynamic regimes mentioned in

chapter 2, viz 'stagnant', or rigid, drops, 'circulating' drops and 'oscillating' drops. These are described by the three equations of Newmann (1), Kronig and Brink (2) and Rose and Kintner (3). To these must be added the correlation of Angelo et al (107) based on the 'surface stretch' concept, where

$$k_d = k' \left[\frac{\mathcal{D}}{\pi\theta}\right]^{0.5} \quad , \qquad 93$$

k' being a dimensionless mass transfer coefficient dependent on the degree and type of surface stretching.

The application of single drop correlations to extraction columns requires caution for the following reasons.

1. The evaluation of the driving force is subject to the difficulties discussed, coupled with the additional disturbances due to the mixing action of the rotors or impellers, and the wake entrainment of the continuous phase by the drops. This contributes to the backmixing, and is discussed in section 5.5.

2. Drop-drop coalescence has a significant effect in reducing surface area and increasing internal mixing. Drop-interface coalescence on column internals can also occur, resulting in unpredictable effects.

3. Drop break-up may lead to higher coefficients due to an enhanced surface renewal effect (107), which may counteract lower ones caused by non-circulation in smaller drops

4. Turbulence in the continuous phase is transmitted to the droplet, increasing internal mixing.

5.2 Interfacial Effects

Interfacial resistance contributes to the overall resistance to transfer (coefficient) in accordance with the additive law. It may be attributed to the presence of surface-active agents, which form a barrier to solute diffusion. A secondary, but perhaps more common, surfactant effect is the prevention of circulation within the drop. Molecules adhering to the surface increase the drag arising from the velocity difference between the drop and the continuous phase. 'Crowding' of surfactant molecules at the rear of the spherical drop surface prevents internal flow patterns developing, (108) and the rate of mass transfer to the drop approximates to that for solid spheres.

Alternatively, mass transfer may be enhanced at the interface by two different effects. The first, reported by Marangoni (109) and named accordingly, is due to momentum transfer caused by a surface tension driving force. The effect is manifested in several ways, by local disruptions, "roll calls", and random disturbances (7). Dependent on the systems employed, these may range in intensity from negligible to being sufficiently large to affect the dispersed (or continuous) phase coefficient. Secondly, very high mass transfer rates may cause gross interfacial stability. Both of these effects are described quantitatively and qualitatively by Sawistowski (7).

5.3 Continuous Phase Coefficients

Existing empirical correlations for mass transfer outside the drop are summarised in table 5.1 (110).

Table 5.1 Empirical Correlations for Mass Transfer in the Continuous Phase

Reference	Equation	Hydrodynamic regime of drop	
(112)	$Sh = 0.582(Re)^{1/2}(Sc)^{1/3}$	solid sphere	96
(113)	$Sh = 2 + 0.76(Re)^{1/2}(Sc)^{1/3}$	solid sphere	97
(114)	$Sh = 2 + (Sh)_n + 0.45(Re)^{1/2}(Sc)^{1/3} + 0.048(Re)(Sc)^{1/3}$	solid sphere	98
(110)	$Sh = 1.13(Re)^{1/2}(Sc)^{1/2}$	non-rigid drop	99
(4)	$Sh = 0.6(Re)^{1/2}(Sc)^{1/2}$	non-rigid drop	100
(4)	$Sh = 50 + 0.0085(Re)(Sc)^{0.7}$	oscillating drop	102
(116)	$Sh = 2 + 0.084(Re)^{0.484}(Sc)^{0.0339}(d\,g^{1/3}/D^{2/3})^{0.072}$ $3/2$	oscillating drop	102

The usual form of the equation is

94

$$Sh = A.Re^{b} Sc^{c}$$

where Sh is the Sherwood number $\frac{kd}{\mathcal{D}}$

Re is a Reynold's number $\frac{vd\rho}{\mu}$

and Sc is the Schmidt number $\frac{\mu}{\rho\mathcal{D}}$

Sawistowski (7) has pointed out that these equations should only apply to conditions away from the interface when instabilities occur, or, by implication, for all regions up to the interface when there are no interfacial disturbances.

Kinard's equation was developed to account for the modification of the driving force due to the entrainment of a wake behind the drop. Although significant for quiescent flow, wakes may become less important in turbulent flow because the continuous phase is continually renewed and the wake is not allowed to develop. The contribution of the wake continues to be a source of debate, but has been shown to be significant only in some types of equipment eg. spray towers (111).

For non-rigid drops the value of the coefficient A in equation (94) varies between 1.13 (110) and 0.6 (4). Thorsen (117) gives a correlation for the coefficient,

$$A = 1.13 \left[1 - \frac{4(3\sqrt{3} - 2)}{5\sqrt{\pi}} \cdot \frac{1}{Re^{1/2}} \cdot \frac{1 + 4\,\mu_d/\mu_c}{1 + (\rho_d/\rho_c \cdot \mu_d/\mu_c)^{1/2}} \right]^{1/2} \quad . \quad 95$$

For oscillating drops, Garner's equation (6) has been recommended. Hughmark has suggested the use of equation (102).

Of special significance is the equation proposed by Treybal et al (118), for mass transfer from the dispersed to continuous phase in an agitated vessel. Under conditions of coalescence and redispersion it was shown that

$$k_c = k_s + 3.9 \left[\frac{D_A}{\theta_c}\right]^{1/2} \qquad 103$$

where k_s = estimated steady state coefficient for solid particles identical in size to the drops (119)

θ_c = time between coalescence and redispersion, estimated from the change in mean drop size between the impeller discharge region and the top and bottom of the vessel.

This correlation gave a fit of $\pm$20% for hold-up values between 0.5 and 10%.

5.4 The Overall Coefficient

The additive property of resistances is used to calculate the overall coefficient, as given in equation (2). Usually, as previously mentioned, the interfacial resistance may be neglected if there are no surface active agents, etc, present. Also, the resistance of one of the phases may predominate, so that the other may be neglected for practical purposes. This situation may depend however upon concentration.

5.5 Axial Mixing

In practical extraction equipment, axial mixing reduces the concentration driving force along the column by depressing the concentration profile. This has been shown to be caused by three effects,

1. A droplet of the dispersed phase may carry through the extractor a 'wake', which entrains the continuous phase. This effect is predominant at low agitator speeds, and decreases rapidly as speed is increased (120).

2. Eddies of continuous phase are displaced between compartments by the agitation of the impellers. This effect is reported to become less significant at high values of hold-up due to the impedance of eddy movement caused by the presence of the droplets (120).

3. The so-called 'forward mixing' effect due to drop size distribution described by Rod (121).

The combined result of these causes is illustrated in figures 2.1 & 2.2, the schematic representation of concentration profiles for a differential contactor. The three different expressions for (N.T.U.) then arise as given earlier. Naturally, for the case of true 'plug' or 'piston' flow, $(N.T.U.)_t = (N.T.U.)_a$ for dilute solutions.

Calculation of true mass transfer coefficients requires the evaluation of $(N.T.U.)_t$. However, direct measurement of concentrations in the exit and inlet streams of a column can only give the $(N.T.U)_m$. Therefore to obtain true mass transfer coefficients via equation (90) a relationship between $(N.T.U.)_m$ and $(N.T.U.)_t$ is necessary. Furthermore, this relationship will be dependent on the operating characteristics of the column (rotor speed, phase ratio, flowrates, temperature, etc.), the column geometry (compartment height, diameter, impeller design and size, etc.), the physical properties of the process streams (interfacial

tension, density and viscosity, surfactant concentration), the feed stream concentrations and the direction of mass transfer (into or out of the dispersed phase). Values of $(N.T.U.)_m$ are specific to the experimental conditions under which they were measured.

5.5.1 Theoretical Considerations

Four models for backmixing have been described by Misek (122)

5.5.1.1 Stage Model

For cases where the influence of backmixing on mass transfer is not high, such as a mixer settler chain in which entrainment is the main cause, the simple stage model can be used (123). It is assumed that each stage is perfectly mixed and that the distribution coefficient m is constant. Distinction between the contribution of each phase to the overall effect is not possible, and the concentration profile is only described approximately. Misek recommends this model for use only where backmixing in each phase is about equal. Miyauchi and Vermeulen(124) suggest that the following conditions must also apply for the stage model to be used,

1. Interdroplet coalescence is a frequent event
2. Interdroplet coalescence is not frequent, but the drop size distribution is narrow, and m, x_d and K are constant.

The model derivation results in two finite difference equations which may be solved by trial and error. The main advantages of the stage model lie in its simplicity for design calculations and the ease of evaluation of design data. The model is of limited applicability

due to the assumption of equal mixing in both phases.

A cascade of ideal mixers for each 'stage' has been used by Kerkhof and Thijssen (125) in a theoretical description of axial mixing.

The stage model leads to the following expressions relating $(N.T.U.)_m$ to $(N.T.U.)_t$,

$$(N.T.U.)_m = \frac{H_T}{h_m} \frac{\ln \lambda}{\epsilon - 1} \qquad 104$$

and

$$\lambda = \frac{\frac{H_T}{(N.T.U.)_t} + \epsilon\, h_m}{\frac{H_T}{(N.T.U.)_t} + h_m} \qquad 105$$

where H_T is the total column height

ϵ is the extraction factor

and h_m is a 'height of a stage'.

In order to fit the model to extraction equipment, an appropriate value of h_m must be determined. Misek recommends equating the respective variances of residence time distribution of the model to those of the equipment, yielding the relationship

$$h_m = H_T s^2 \qquad 106$$

Alternatively, Miyauchi (124) suggests

$$h_m = 2\frac{e}{U}\left[1 - \frac{h_m}{H_T}\right]f_T$$

where e is the phase dispersion coefficient

U is the phase superficial velocity

and f_T is a correction factor

Values of f_T are given as a function of the extraction factor $\mathcal{E}$ and the backflow ratios α_x and α_y by Miyauchi (124), reproduced in figure 5.3.

5.5.1.2 Backflow Model

When a two phase system can be described by a series of stages in which the axial mixing may be represented by a counter-flow of material, the backflow model is applicable. The theoretical interpretation is due to several authors (106,126,127,128,129). It is assumed that an extractor acts as a series of perfectly mixed stages in which material is also transferred upstream counter to the main flow by backmixing. Misek (122) suggests that the backflow model represents a very good description of a number of real extraction units, especially those operating under conditions where intensive coalescence and redispersion takes place.

The analytical solution of the complex finite difference equations arising in this case has been performed by Hartland and Mecklenburg (127). The resulting equations for special cases are shown in table 5.2, in

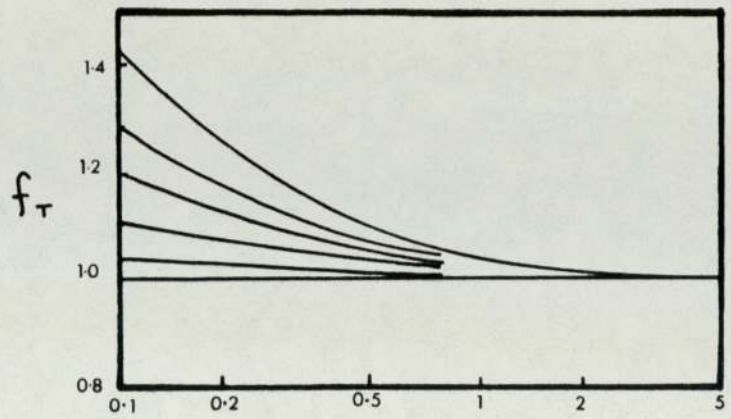

$\varepsilon\alpha_x + \alpha_y$ for $\varepsilon < 1$

$\frac{\alpha_x + \alpha_y}{\varepsilon}$ for $\varepsilon > 1$

Figure 5·3 (124)

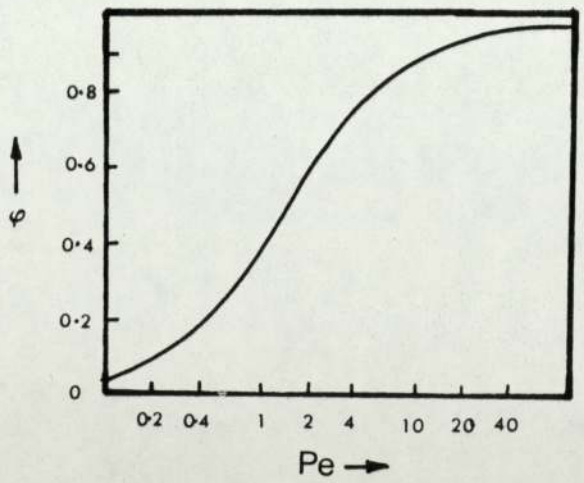

Figure 5·4 Correction factor

Table 5.2

Special Cases of the Backflow Model Solution

$h_m/(HTU)_t$	α_x	α_y	ε	
∞	0	0	1	$\xi_i = 1 - \frac{i}{1+n}$
∞	0	0		$\xi_i = 1 - \frac{\varepsilon^i - 1}{\varepsilon^{n+1} - 1}$
	∞	∞		$\xi_i = 1 - \frac{n \frac{h_m}{(HTU)_t}}{1 + n \frac{h_m}{(HTU)_t} + n \frac{h_m}{(HTU)_t}}$
	0	0	1	$\xi_i = 1 - \frac{\frac{h_m}{(HTU)_t} i}{1 - \frac{h_m}{(HTU)_t} + n \frac{h_m}{(HTU)_t}}$
	0	0		$\xi_i = 1 - \frac{\lambda^i - 1}{\varepsilon \lambda^n - 1}$; $= \frac{1 + \varepsilon \frac{h_m}{(HTU)_t}}{1 + \frac{h_m}{(HTU)_t}}$
∞		=	1	$\xi_i = 1 - \frac{\alpha_x + \alpha_y + i}{2(\alpha_x + \alpha_y) + 1 + n}$
∞				$\xi_i = 1 - \frac{\varepsilon \lambda^i - \lambda}{\varepsilon^2 \lambda^n - \lambda}$; $\lambda = \frac{\varepsilon + \alpha_x + \alpha_y}{1 + \alpha_x \varepsilon + \alpha_y}$
	0			$\xi_i = 1 - \frac{(1-a_1^i)/(a_1-1)g_1 - (1-a_2^i)/(a_2-1)g_2}{(1-\varepsilon a_1^n)/(a_1-1)g_1 - (1-\varepsilon a_2^n)/(a_2-1)g_2}$ $g_i = \frac{1}{1+(1+\alpha_y)(a_i-1)}$ $a_{1,2}$ are the roots of $a_j^2(1+\alpha_y)\left(1+\frac{h_m}{(HTU)_t}\right) - a_j\left(1+2\alpha_y + \frac{h_m}{(HTU)_t}\left[\varepsilon+\alpha_y\right]\right) + \alpha_y = 0$
		0		$\xi_i = 1 - \frac{(h_1 - a_1^i)/(a_1-1)a_1^n - (h_2-a_2^i)/(a_2-1)a_2^n}{h_1(1-\varepsilon a_1^n)/(a_1-1)a_1^n - h_2(1-\varepsilon a_2^n)/(a_2-1)a_2^n}$ $h_j = 1 - \alpha_x(a_j - 1)$.

terms of the dimensionless concentration ξ, defined by

$$\xi = \frac{x - x^*}{x_o - x^*} \qquad 108$$

Landau and Prochazka (129) have described a graphico-numerical procedure, reviewed by Misek (122).

Rod (121) has expressed the backflow model as

$$\frac{h_m}{(H.T.U.)_t} = \frac{x_o - x_1}{\sum_1^n (x_i - x_i^*)} \qquad 109$$

Again there is the problem of relating h_m to operating variables, etc., in a column.

Simplified approximate solutions have been given (130,131), where equations (104) is used together with a new expression for λ, viz:,

$$\lambda = \frac{(H.T.U.)_t + h_m (\varepsilon \alpha_x + \alpha_y + \varepsilon)}{(H.T.U.)_t + h_m (\varepsilon \alpha_x + \alpha_y + 1)} \qquad 110$$

when $\varepsilon = 1$ this reduces to

$$(H.T.U.)_m = (H.T.U.)_t + h_m (1 + \alpha_x + \alpha_y) \qquad 111$$

where α_x and α_y are the backflows in the respective phases. A table of special solutions is given in table 5.2.

Tolic and Miyanchi (132) have devised a complete but complex graphical solution procedure for this model.

5.5.1.3 Diffusion Model

For extraction columns where the solute concentration changes continuously along the axis, an analogy to Fick's law of diffusion can be used to describe backmixing. Solute transfer in a single phase is assumed to take place from high to lower concentrations, and the mass flux is assumed proportional to the concentration gradient. The theoretical development was due to many authors (106,133,134,135,130,136,124). Misek (122) reports that the physical situation at the ends of any column, where the mathematical boundary conditions exist, is complex and therefore the conditions are only a rough approximation.

Sleicher (106) produced solutions for this model, tabulated as

$$1 - \xi = f\,(\varepsilon, Pe_x, Pe_y, (N.T.U.)_t) \qquad 112$$

Miyauchi's analytical solution is very complex and inconvenient for calculations, but by the use of a digital computer, tables of concentration profiles have been produced (137). Hartland and Mecklenburg's analytical solution (127) is again complex. Solutions for special cases analogous to those for the backflow model are given in table 5.3. Wilburn (138) has also produced an analytical solution. Other solutions have been reviewed by Misek (122).

For $\varepsilon = 1$, Beek (139) derived the following expression:

$$(H.T.U.)_m = (H.T.U.)_t + \frac{e_x}{U_x} + \frac{e_y}{U_y} \qquad 113$$

where e_x and e_y are the phase dispersion coefficients

and U_x and U_y are the superficial phase velocities.

Table 5.2

Special Cases of the Diffusion Model

$H_T/(HTU)_t$	Pe_x	Pe_y		Solution
	0	0		$\xi_i = \dfrac{1+\dfrac{H_T}{(HTU)_t}}{1+(1+\varepsilon)\dfrac{H_T}{(HTU)_t}}$
	∞	∞	1	$\xi_i = \dfrac{1+\dfrac{H_T}{(HTU)_t}\left(1-\dfrac{H}{H_T}\right)}{1+\dfrac{H_T}{(HTU)_t}}$
	∞	∞		$\xi_i = \dfrac{\exp(-\lambda z)-\varepsilon\exp(-\lambda)}{1-\varepsilon\exp(-\lambda)}$; $\lambda = (1-\varepsilon)\dfrac{H_T}{(HTU)_t}$
∞			1	$\xi_i = 1-\dfrac{Pe_x+Pe_y+Pe_xPe_yH/H_T}{2(Pe_x+Pe_y)+Pe_x+Pe_y}$
∞				$\xi_i = 1-\dfrac{1-\varepsilon\exp(\lambda H/H_T)}{1-\varepsilon^2\exp(\lambda)}$; $\lambda = \dfrac{Pe_xPe_y(\varepsilon-1)}{Pe_x+\varepsilon Pe_y}$
	∞			$\xi_i = 1-\dfrac{\left[1-\exp(q_1H/H_T)\right]/q_1g_1-\left[1-\exp(q_2H/H_T)\right]/q_2g_2}{\left[1-\varepsilon\exp(q_1)\right]/q_1g_1-\left[1-\varepsilon\exp(q_2)\right]/q_2g_2}$ $g_j = \dfrac{1}{1+q_j/Pe_y}$ $q_{1,2}$ are the roots of $q_j^2+\left(\dfrac{H_T}{(HTU)_t}+Pe_y\right)q_j-\dfrac{H_T}{(HTU)_t}Pe_y(\varepsilon-1)=0$
		∞		$\xi_i = 1-\dfrac{\dfrac{h_1-\exp(q_1(H/H_T))}{q_1\exp(q_1)}-\dfrac{h_2-\exp(q_2(H/H_T))}{q_2\exp(q_2)}}{\dfrac{h_1\left[1-\varepsilon\exp(q_1)\right]}{q_1\exp(q_1)}-\dfrac{h_2\left[1-\varepsilon\exp(q_2)\right]}{q_2\exp(q_2)}}$ $h_j = 1-q_j/Pe_x$ $q_{1,2}$ are the roots of $q_j^2+\left(Pe_x+\dfrac{\varepsilon(HTU)_t}{H_x}\right)q_j+\dfrac{H_T}{H_x}Pe_x(\varepsilon-1)=0$

Rod (140) has proposed a modification to allow for the end effects of reduced longitudinal solute transport at the phase outlets. Thus

$$\Phi_j = 1 - \frac{1}{Pe_j}\left(1 - \exp\left(-Pe_j\right)\right); \quad j = x,y. \qquad 114$$

Combining the original equations with equation (114) gives the following explicit relationships.

$$(H.T.U.)_m = (H.T.U.)_t + \frac{1}{f_x}\frac{e_x}{U_x} + \frac{1}{f_y}\frac{e_y}{U_y} \qquad 115$$

where

$$f_x = \frac{1}{\Phi_x} + (1 - \varepsilon)\frac{e_x}{U_x(H.T.U.)_m} \qquad 116$$

and

$$f_y = \frac{1}{\Phi_y} + (1 - \varepsilon)\frac{e_y}{U_y(H.T.U.)_m} \qquad 117$$

Misek (122) has produced a graph for the simple determination of Φ_j, reproduced in figure 5.4.

Mecklenburg and Hartland's solution (141) is more complex,

$$(H.T.U.)_m = (H.T.U.)_t + \frac{\varepsilon e_x}{U_x} + \frac{e_y}{U_y} + h^* \qquad 118$$

where

$$h^* = \frac{1}{(N.T.U.)_m}\left[\frac{\frac{e_x}{U_x(H.T.U.)_t} - \frac{e_y}{U_y(H.T.U.)_t}}{1 + \varepsilon\frac{e_x}{U_x(H.T.U.)_t} + \frac{e_y}{U_y(H.T.U.)_t}}\right.$$

$$\left. + \frac{(H.T.U.)_t + \varepsilon\frac{e_x}{U_x} + \frac{e_y}{U_y}}{1 - \varepsilon}\cdot\ln\left\{\frac{(H.T.U.)_t + \varepsilon\frac{e_x}{U_x} + \zeta\frac{e_y}{U_y}}{(H.T.U.)_t + \frac{e_x}{U_x} + \frac{e_y}{U_y}}\right\}\right] \qquad 119$$

Both Miyauchi and Vermeulen (124)and Stemerding (142) have solved the equations for the limiting case of infinite mass transfer ($(N.T.U.)_t \to \infty$). Empirically determined correction factors ensure a correct value of $(H.T.U.)_m$.

$$\text{Thus} \qquad (H.T.U.)_m = (H.T.U.)_t + \frac{h^*}{1 + \frac{h^*}{H_T} \cdot \frac{\beta \ln \varepsilon}{\varepsilon - 1}} \qquad 120$$

$$\text{where} \qquad h^* = \frac{\varepsilon}{f_x} \frac{e_x}{U_x} + \frac{e_y}{f_y U_y} \qquad 121$$

Table 5.4 gives values of f_x, f_y and β.

Misek (122) suggests that although all these methods give satisfactory accuracy, equation(120)is to be preferred on account of its simplicity. Stemerding and Zuiderweg (142) have produced a convenient method of solution, which has already been mentioned in section 2.1.2 in connection with the R.D.C. The method is equally applicable to the Oldshue-Rushton column.

5.5.1.4 Forward Mixing Model

Where coalescence and redispersion do not take place, and the droplets have a wide size distribution, Misek and Rod (143) have shown that the diffusion and backflow models do not describe the backmixing effect adequately. Both the polydispersity of droplet sizes and the consequent velocity distribution cause a decrease in the effective driving force for mass transfer compared with that for piston flow. Olney (144) has developed the theory of the combined model, and Misek (122)

Table 5.4

	Miyauchi (146)	Stemerding (147)
f_x	$\frac{N_x + 6.8\varepsilon^{-0.5}}{N_x + 6.8\varepsilon^{-1.5}}$	$\frac{0.1\,N_x + 1}{0.1\,N_x + 1/\varepsilon}$
f_y	$\frac{N_x + 6.8\varepsilon^{0.5}}{N_x + 6.8\varepsilon^{1.5}}$	$\frac{0.1\,N_x + 1}{0.1\,N_x + \varepsilon}$
β	1	0.8

has presented approximate solutions for certain simplified circumstances. Thus for no end effects,

$$(H.T.U.)_m = \sum \frac{\varphi_i}{\partial_i} (H.T.U.)_{ti} + \frac{e_i}{\gamma_i U_i} + \frac{\mathcal{E}}{f_y} \frac{e_y}{U_y} \qquad 122$$

where

$$f_y = 1 - \frac{e_y}{U_y (H.T.U.)_m} (1 - \mathcal{E}) \qquad 123$$

$$\gamma_i = 1 + \frac{e_i}{U_i (H.T.U.)_m} (1 - \mathcal{E}) \qquad 124$$

$$\partial_i = \frac{f_y}{\mathcal{E}} \frac{1}{\gamma_i} - (1 - \mathcal{E}) . \frac{(H.T.U.)_t}{(H.T.U.)_m} \qquad 125$$

where i refers to the ith fraction of the dispersed phase distribution. For $i = 1$, $\varphi_i = 1$, $\partial_i = 1$ equation (122) reduces to a form equivalent to the dispersion model.

For $\mathcal{E} = 1$, equation (122) becomes

$$(H.T.U.)_m = \sum \varphi_i (H.T.U.)_{ti} + \sum \varphi_i \frac{e_i}{U_i} + \frac{e_y}{U_y} \qquad 126$$

which can be used to evaluate the effect of forward mixing in contactors where coalescence of droplets does not occur to a great extent.

5.5.2 Application to the Oldshue-Rushton Column

From a consideration of the assumptions made in each case, the diffusion model will be more applicable to continuous differential contactors, such as the spray column, and the backflow model to contactors having discrete stages, such as the mixer-settler. The

Oldshue-Rushton column falls between these two extremes, and Ingham (120) reports that both models are equally successful.

Gutoff (145), as a result of studying backmixing in a four inch diameter column, confirmed the intuitive supposition that, for single phase operation, backmixing was minimal at low rotor speeds, but increased linearly as N increased. The effect of geometrical modifications was reported.

Subsequently, Bibaud and Treybal (18) utilised a six inch diameter column with water as the continuous phase and kerosene or toluene as the dispersed phase. Single phase backmixing was expressed by

$$\frac{e_x}{G_c H/\rho_c} = 0.449 + 0.01118 \frac{DN}{G_c/\rho_c} \qquad 127$$

where the symbols have meanings given in the Nomenclature. For continuous phase mixing in a two phase system

$$\frac{(1 - x_d)e_x}{G_c H/\rho_c} = -0.1400 + 0.0268 \frac{DN(1 - x_d)}{G_c/\rho_c} \qquad 128$$

for constant compartment height and impeller diameter.

For backmixing in the dispersed phase,

$$\frac{D^2N}{e_y} = 3.39 \times 10^{-3} \left(\frac{D^3N^2\rho_c}{\sigma}\right)^{1.54} \left(\frac{\rho_c}{\Delta\rho}\right)^{4.18} \left(\frac{D^2N\rho_c}{\mu_c}\right)^{0.61} . \qquad 129$$

In equation (129) no account is taken of variation of e_y with flowrate, and, perhaps more surprisingly, $e_y \sim \frac{1}{N}2.69$. The reasons, for the decrease of backmixing with increased impeller speed in this case were said to be the elimination of stagnant pockets of fluid under the stator

rings, and the creation of a more uniform drop size. The latter would decrease the forward mixing effect.

In the same study, the ratio $(N.T.U.)_t/(N.T.U.)_m$ was found to vary between 1.14 and 3.70. Unfortunately, drop sizes were not measured directly, but predicted from Thornton's correlation (28), for stirred tanks, which would be expected to be inapplicable to the column because of the entrance and exit effects discussed in chapter 4.

In a two-stage column section, Miyauchi et al (146) correlated backmixing by

$$\frac{f}{ND} = 2.7 \times 10^{-2} \left(\frac{D_{col}}{H}\right)^{1/2} \qquad 130$$

For a 15 cm diameter full column,

$$\frac{f}{ND} = 1.0 \times 10^{-2} \left(\frac{D_{col}}{H}\right)^{1/2} \qquad 131$$

From a consideration of Kolmogorov's theory of local isotropy, the fundamental equation

$$\frac{f}{ND} = b\,(N_p)^{1/3} \left(\frac{D_{col}}{H}\right)^{1/2} \qquad 132$$

was derived, where b is a coefficient dependent on the impeller Reynolds number. Thus, because the value of b is constant over a wide range of Re, a unified correlation for both the Oldshue-Rushton column and the R.D.C. was given as

$$\frac{f}{ND} = 0.017\,(N_p)^{1/3} \left(\frac{D_{col}}{H}\right)^{1/2} \qquad 133$$

The unified correlation is presented as figure 5.5, and incorporates the data of Westerterp and Landsman (148), Strand et al (40), and Stemerding et al (147).

Haug (149) has correlated previous data together with experimental results from several columns of varying dimensions. For the continuous phase in single and two phase flow,

$$\frac{f}{G_c A/\rho_c} = 0.0098 \left[k_1 \left(\frac{ND}{G_c} \right) \left(\frac{4D^2 A_s}{\pi_H D^3_{col}} \right)^{0.5} \right]^{1.24} \qquad 134$$

where k_1 is an impeller correction factor. The correlation is also said to apply to the dispersed phase, for both co-current and countercurrent flow.

Ingham (120), in an attempt to reduce backmixing in a six inch column by adding a draught-tube to the stator opening, correlated the single phase backmixing with the relationship

$$\frac{e_x}{G_c H/\rho_c} = 0.0375 \left[\frac{ND}{G_c} \right] \left[\frac{A_s}{D_{col}} \right]^2 . \qquad 135$$

This is in good agreement with the correlation of Bibaud and Treybal (18). For two phase flow, the commonly used factor $(1 - x_d)$ was used to modify equation 35 to give

$$\frac{e_x}{G_c H/\rho_c} = 0.0375 \, (1 - x_d) \left[\frac{ND}{G_c/\rho_c} \right] \left[\frac{A_s}{D_{col}} \right]^2 \qquad 136$$

Lelli et al (150) have developed a theoretical model similar to that of Thijssen (125) and express the backmixing in the column as a function

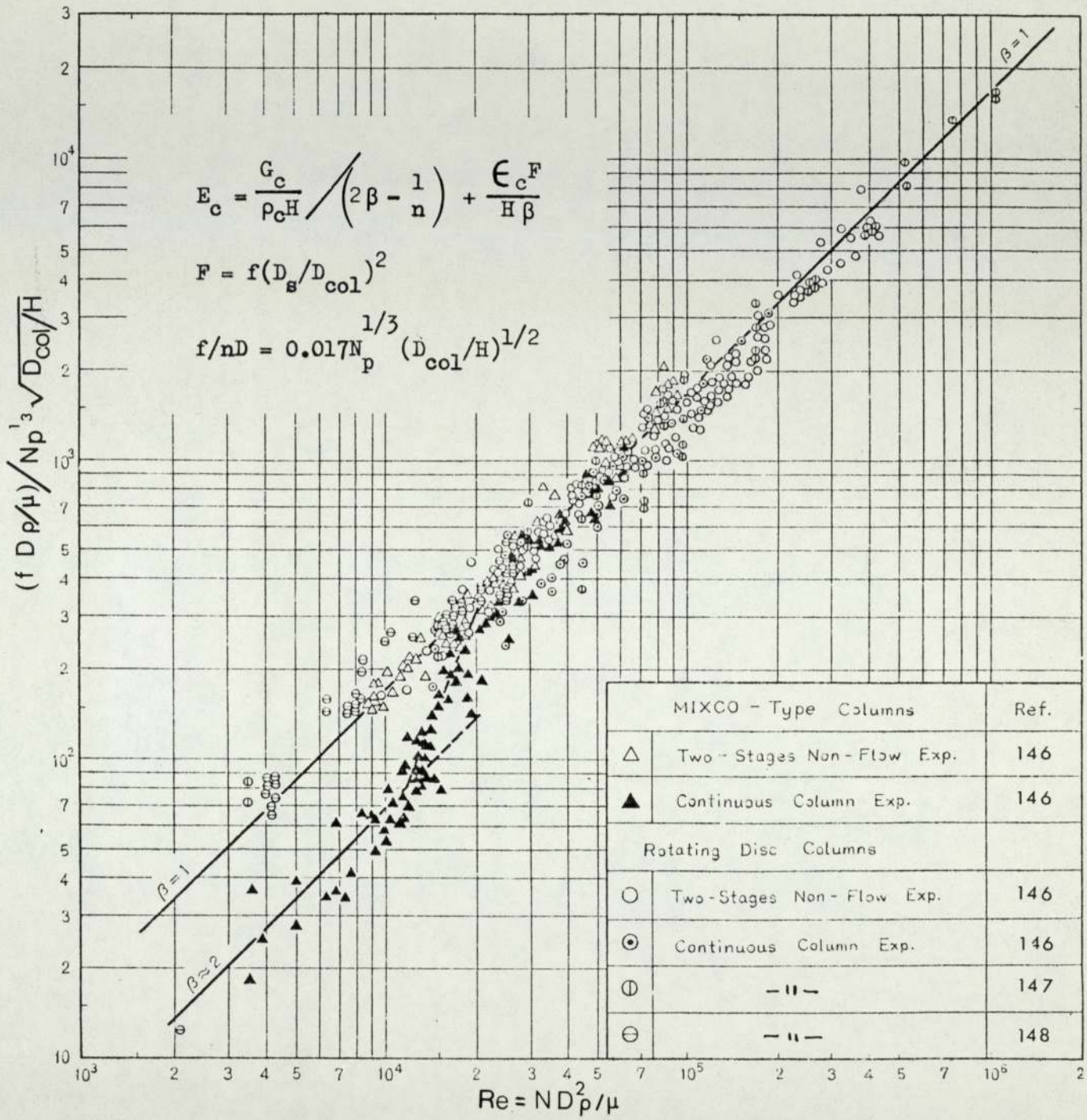

Figure 5·5 Unified correlation for both of RDC and Mixco columns.

of an interstage flow and an intrastage flow. The intrastage flow accounts for the backmixing within the ideal stages of the model. For $10^3 \leq Re_I \leq 2 \times 10^5$ the data was correlated by

$$\frac{g}{ND^3} = \frac{0.038}{1 + 19.5 \frac{q}{ND^3}} \qquad 137$$

where g is the intrastage flowrate and q is the net volumetric flowrate. The agreement of equation (137) with Miyauchi's correlation is reported to be within seven per cent.

From the foregoing it is clear that although the elegant theoretical models describing backmixing generally have been developed to a high degree, the experimental data necessary for their application is lacking. The use of mean values for hold-up in the column is usually invalid. It has been shown (120,121) that hold-up profiles in the Oldshue-Rushton contactor are significant, and that a variation of volumetric hold-up of up to four times is obtained between the top and bottom of the column under normal operating conditions.

Similarly, drop sizes may vary by a like amount, and drop size distributions also change along the length of the column. The non-idealities are compounded by the variation of these effects with flowrate, impeller speed, and fluid physical properties. None of these effects are accounted for in the empirical correlations, necessitating pilot plant trials under actual operating conditions to obtain backmixing data.

Furthermore, there have been no reported backmixing studies performed when mass transfer is occurring. Obviously, since the departure of solute concentrations from their plug flow values are the prime manifestations of backmixing, this is a serious omission. Additionally, mass transfer has a secondary effect on backmixing via increased or hindered interdroplet coalescence, possible coalescence on column intervals, and thus a change in hold-up. None of these factors can be accounted for analytically at present.

Finally, the use of correlations for the single phase only is of doubtful validity, since it is well established that the effects of the dispersed phase on the continuous phase backmixing behaviour is significant.

6. Apparatus and Measurement Techniques

6.1 Objectives

It is clear from the previous chapters that there is a lack of co-ordinated reliable data regarding the design and performance of high energy rotary agitated columns. In particular information is lacking on:

1. The prediction of drop sizes and hold-up, and hence interfacial areas.
2. The nature of the drop size distribution.
3. The nature and effect of phase inversion.
4. Mass transfer performance.

The present investigation was therefore undertaken to elucidate the effects of operating variables upon 1 to 4 above, using a typical high energy column under carefully controlled conditions.

6.2 Description of Equipment

A flow diagram of the equipment is shown in figure 6.1. This was arranged so that the column was accessible from all sides and all valves were within easy reach. The instrumentation and the main flow control valves were located conveniently on the control panel, as shown in figure 6.2.

All the fluid reservoirs could be used as feed tanks or receivers. A recycle line for each fluid gave fine control of flowrates. Drain points were incorporated at the lowest points in the system.

6.2.1 The Column

It is commonly accepted that a diameter of 15 cm is sufficient to eliminate wall effects as a major influence in the operation of

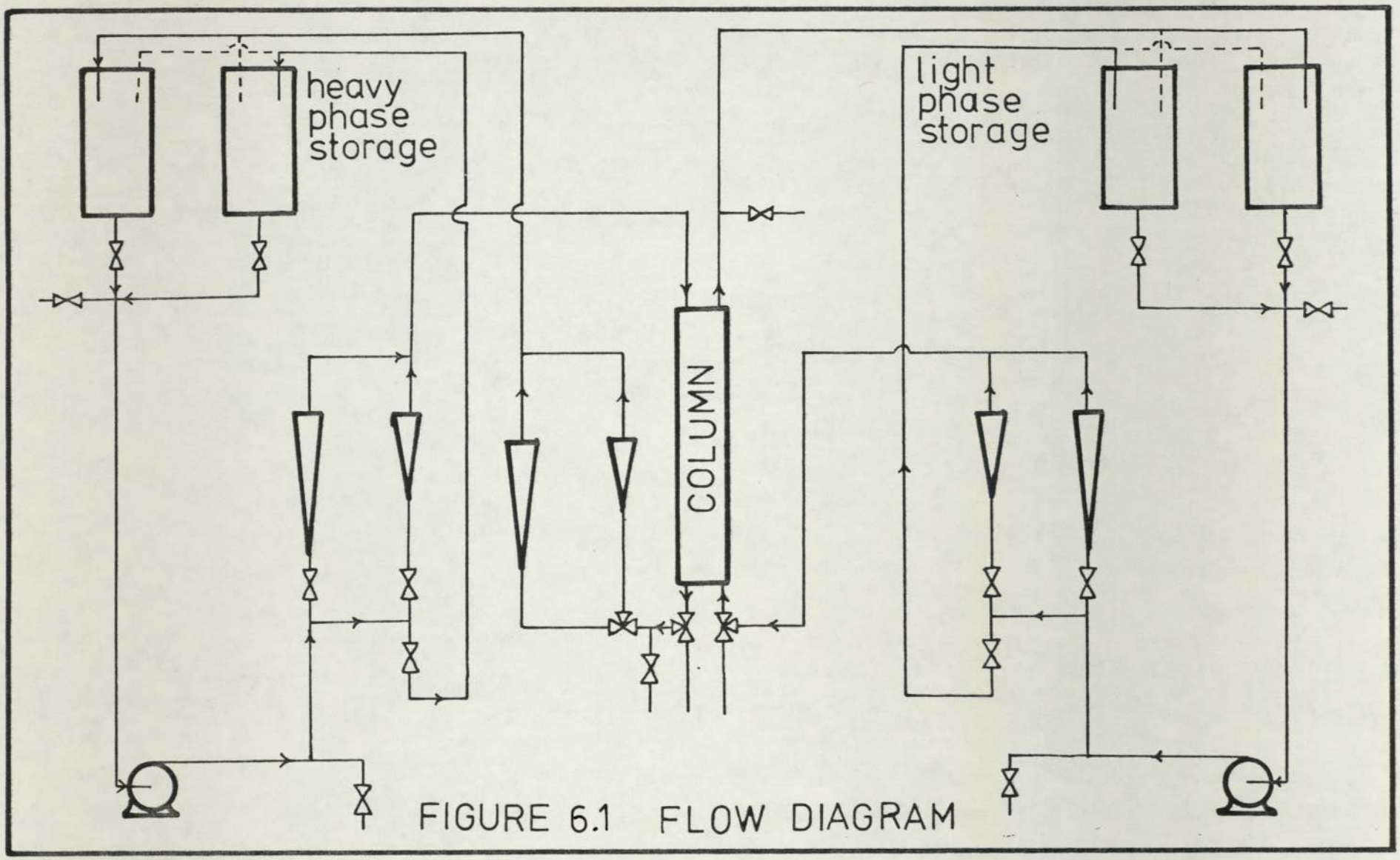

FIGURE 6.1 FLOW DIAGRAM

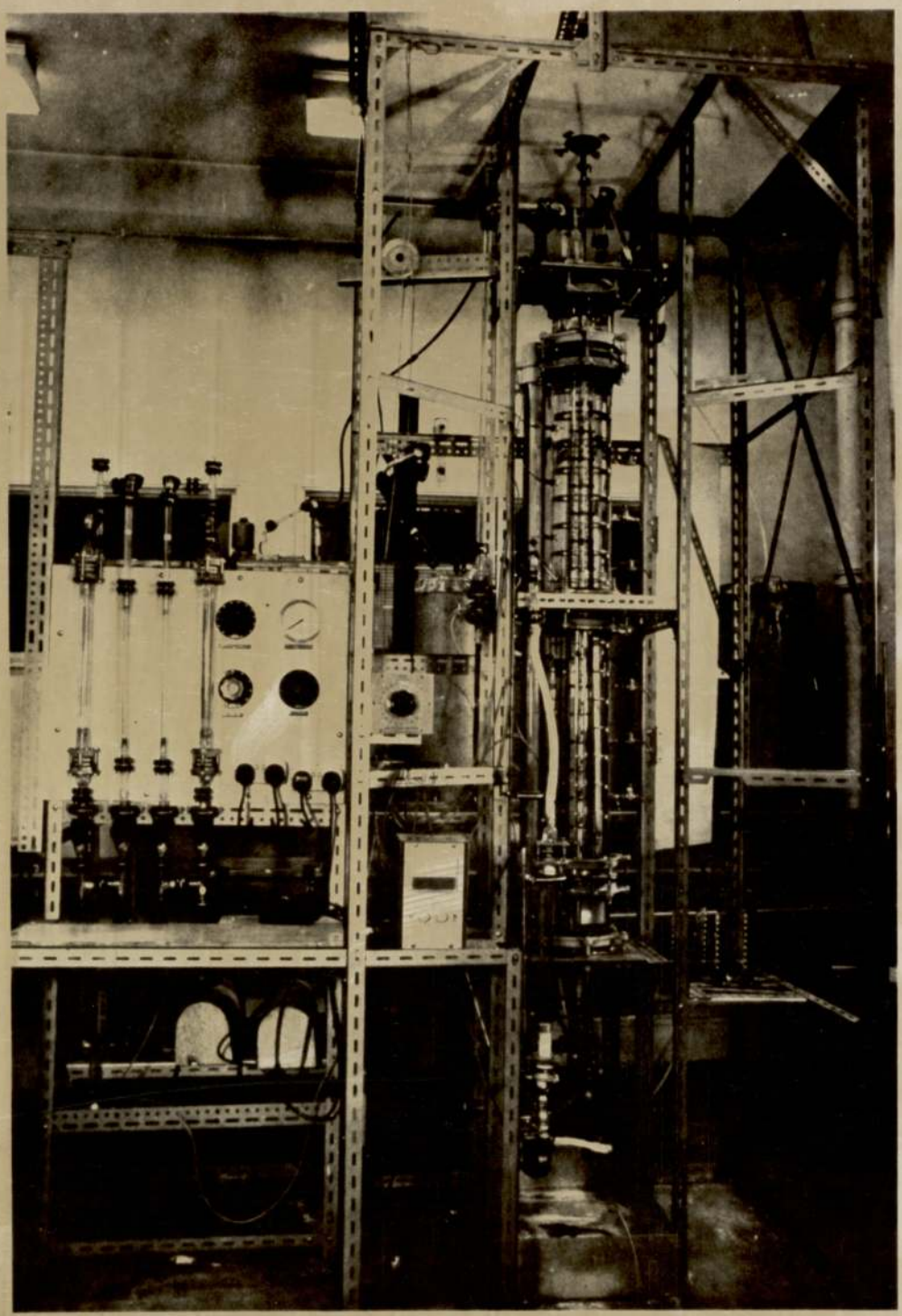

Figure 6.2 Oldshue-Rushton Column

liquid-liquid extraction columns. Oldshue and Rushton (16) and Ingham (120) have used six inch diameter columns, and this size was selected for this investigation, to facilitate comparison of results.

The design of the column was based upon that devised by Oldshue and Rushton in their original paper (16). The column consisted of two Q.V.F. nominal six inch diameter borosilicate glass pipe sections each 0.75 m long, as shown in figure 6.2. Six pairs of 10 mm diameter holes were drilled in the column to act as sampling ports, locators for conductivity probes or for injection of tracer material. Details of the arrangement of these fittings are given in sections 6.4.2 and 6.4.3.

Two end plates and a centre bearing plate were fabricated from 8 mm thick 18/8 stainless steel plate. The end plate at the dispersed phase entry end of the column supported the distributor, described in section 6.2.2, and a P.T.F.E. end step bearing, (figure 6.3). The other, upper, end plate housed a P.T.F.E. bearing and a stuffing box filled with "T-seal" P.T.F.E. granules. A phosphor-bronze bearing suppressed whipping of the rotor shaft in the centre of the column. Each end plate was fitted with the necessary inlet and outlet pipes and a drain pipe sealed by a P.T.F.E. tube and a screw clip.

Column internals were fabricated entirely from 18/8 stainless steel (figure 6.4). In their column Oldshue and Rushton (16) sealed the inevitable gap between stator rings with "Saran" tubing. However, use of such materials greatly restricts the solvent systems that can be used, due to effects of swelling, degradation, and leaching out of

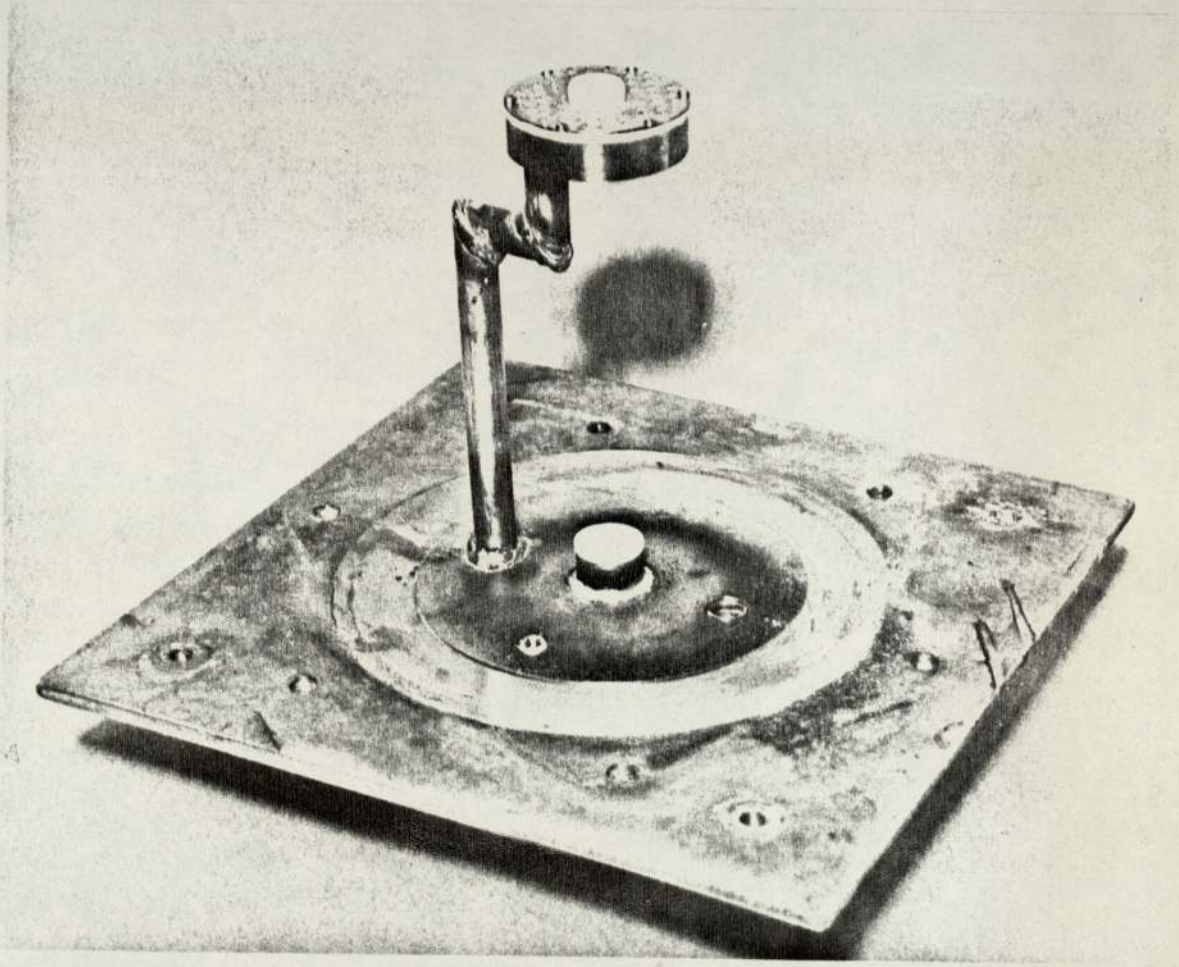

Figure 6.3 Stainless Steel end plate with Distributor and p.t.f.e. step bearing.

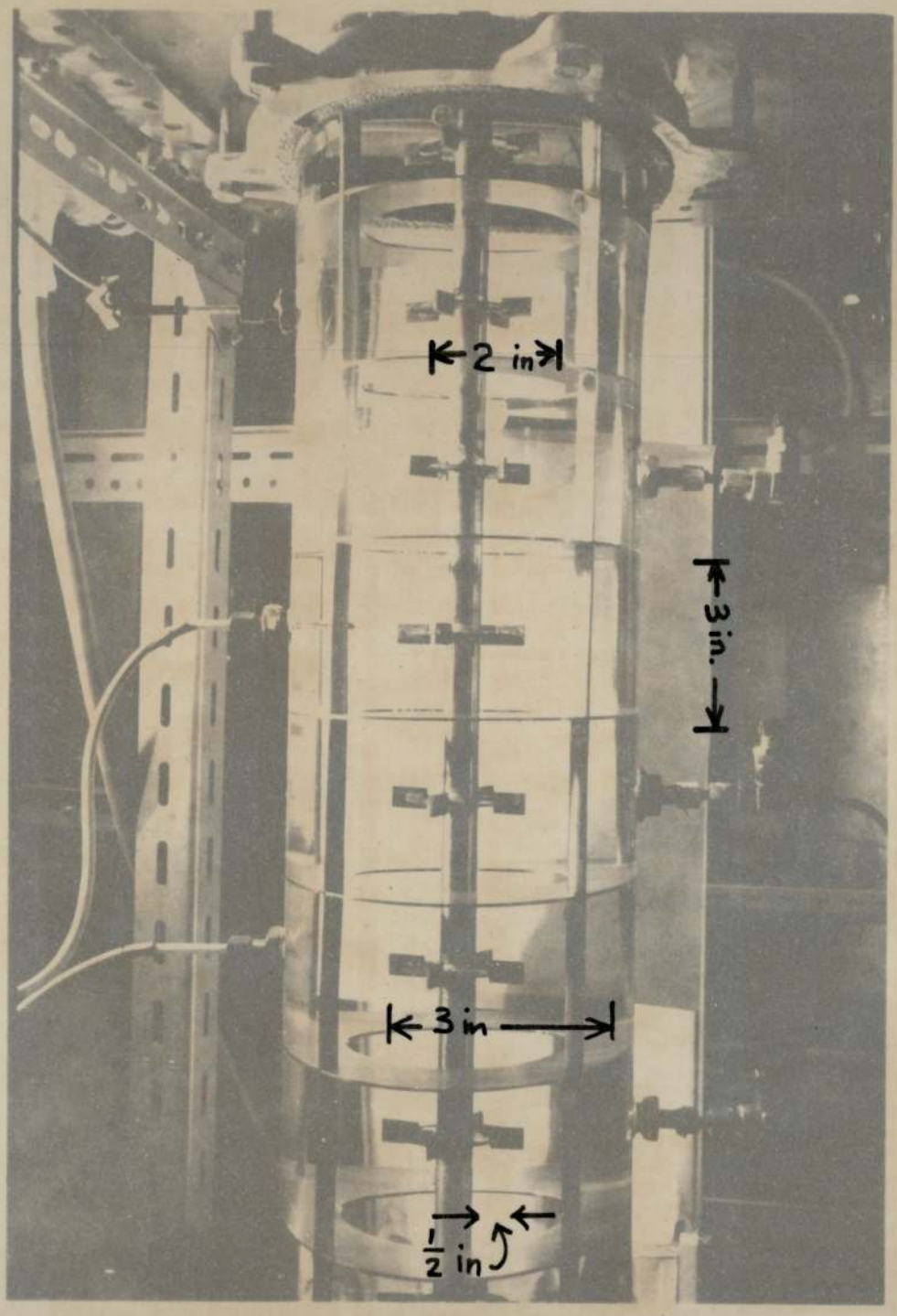

Figure 6.4 Column Internals and Sample Ports

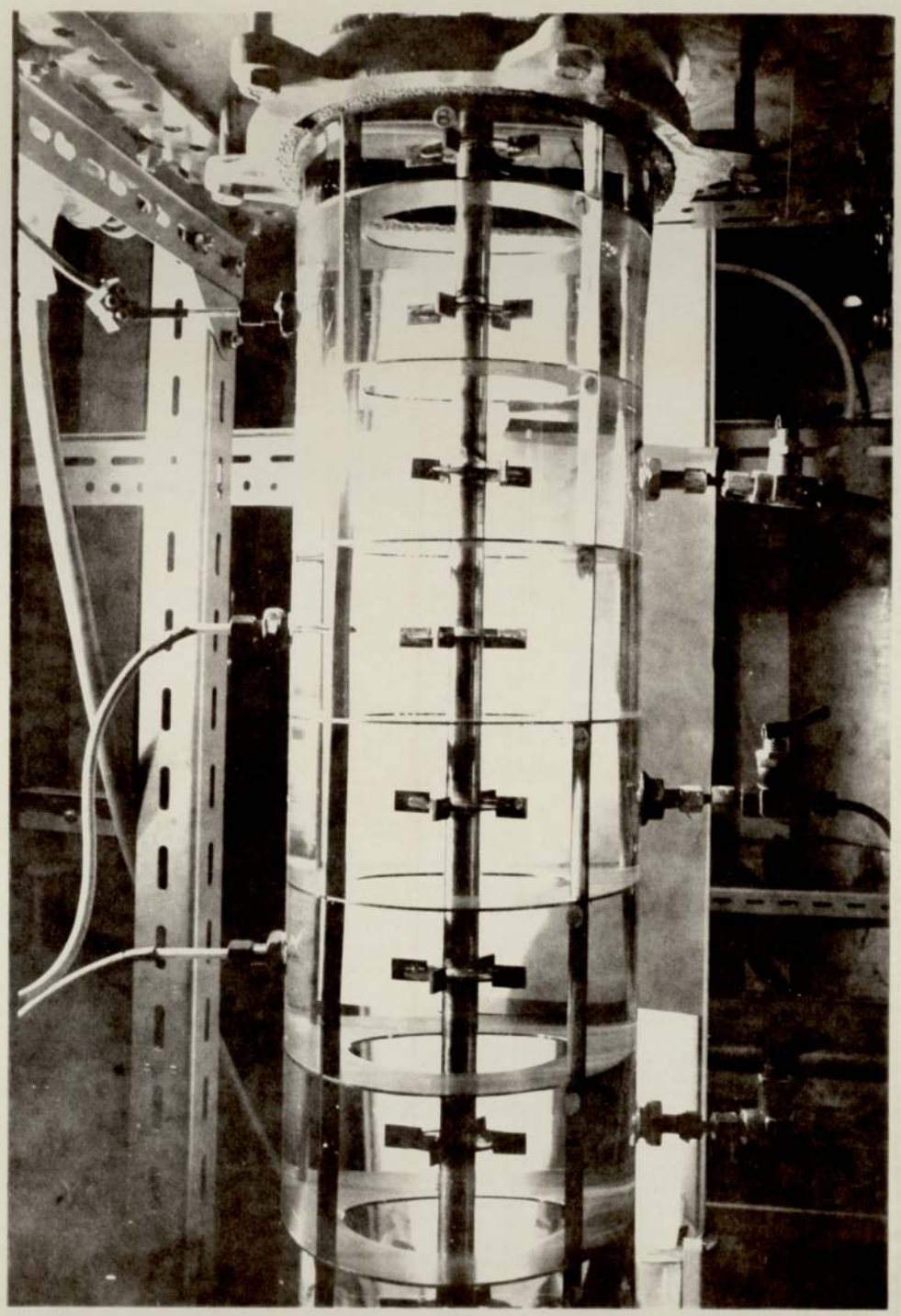

Figure 6.4 Column Internals and Sample Ports

plasticisers. Therefore in the present column extremely low tolerances of less than 0.1 mm were allowed between the stator rings and the glass, each ring being machined individually to fit axial variations in column internal diameter. Thus almost an exact fit was achieved between stator ring and column wall. Vertical baffles were slotted into the stator rings before assembly of the column and bolted to brackets on the centre bearing plate to prevent rotation.

The agitator shaft was 1/2" diameter stainless steel rod made in two sections screwed together at the centre to facilitate construction. Careful straightening with a mandrel ensured that whipping of the shaft on rotation was eliminated. Each disc turbine was made from 1/16" thick stainless steel elements which were welded together and welded or brazed to the shaft as shown in figure 6.5. Dimensions of the turbines were as recommended by Oldshue and Rushton (16) as were the essential dimensions of the compartment inter als. This made it possible to accurately compute energy requirements and to identify flow patterns as discussed in chapter 3.

The phase entering the bottom of the column was dispersed as droplets of substantially equal size by a distributor designed according to the method of Treybal (151). Since such a punched plate distributor can only be designed for a narrow range of flowrates, i.e. for linear velocities below 'jetting', a mean value of expected flowrates was used as a basis. The distributor contained 46 holes each 1.5 mm diameter on a 1/4 inch square pitch as shown in figure 6.6.

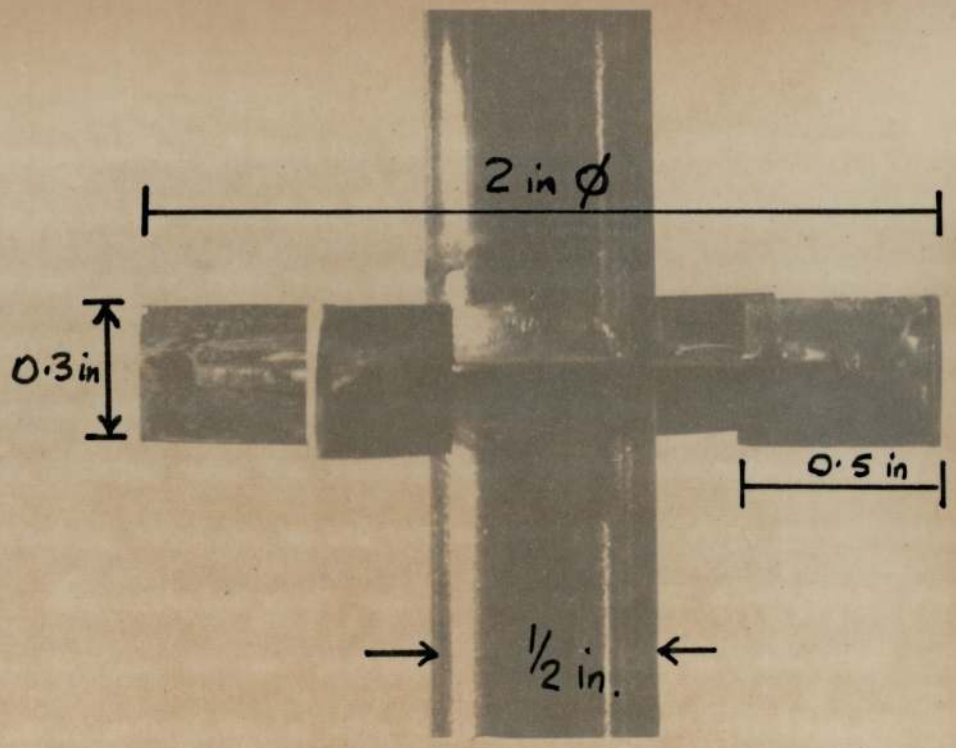

Figure 6.5 Impeller

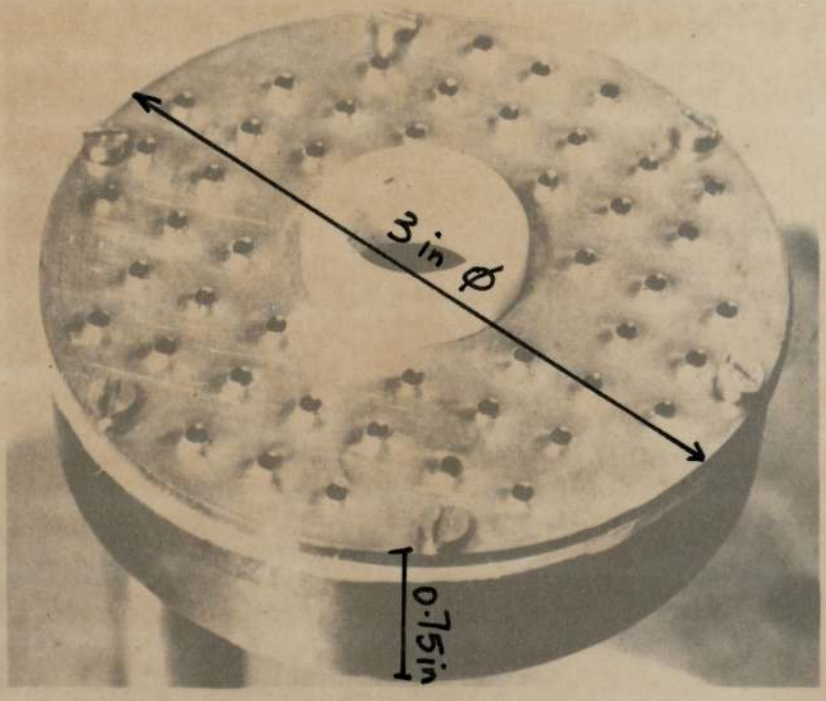

Figure 6.6 Punched Plate Distributor

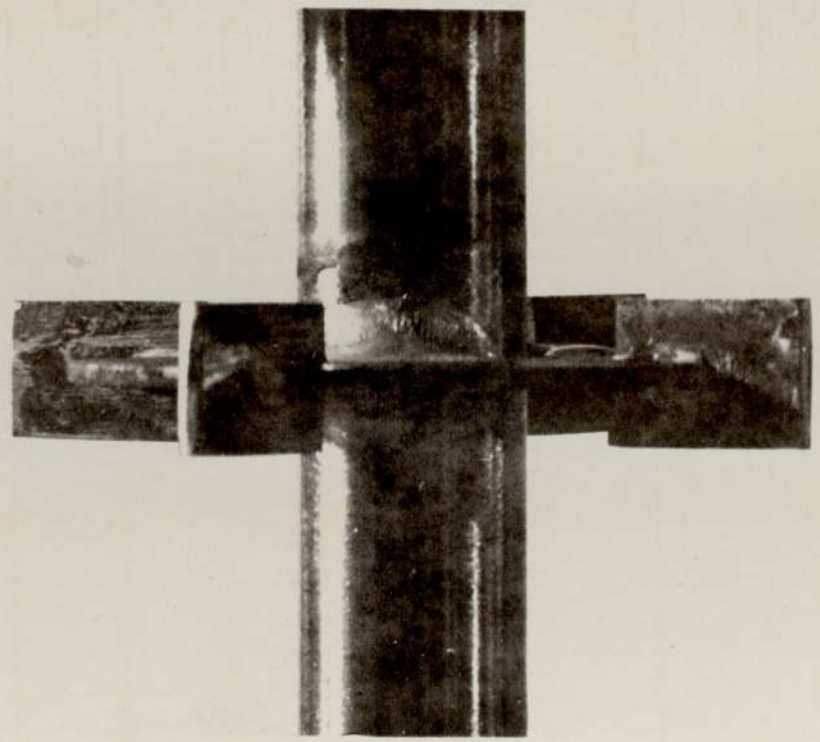

Figure 6.5 Impeller

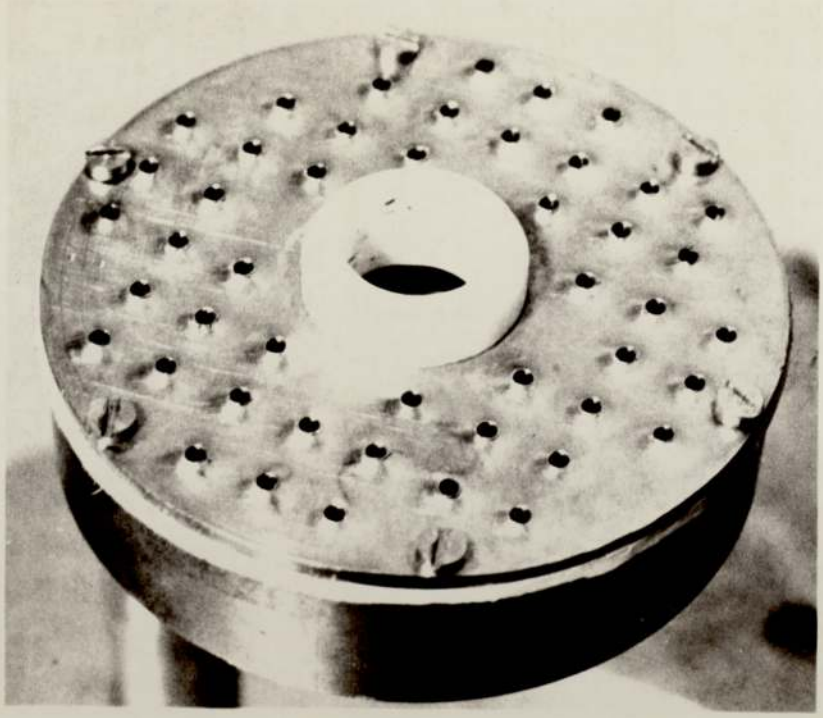

Figure 6.6 Punched Plate Distributor

6.2.2 Other Equipment

Power to the agitator shaft was supplied by an A.E.I. 1/4 h.p. electric motor, controlled by a 'torovolt' variable voltage mains transformer. The rotation speed of the shaft was monitored by a Smiths Industries "Venture" magnetic tachometer reading 0 - 1000 rpm.

Process fluids were stored in stainless steel cylindrical tanks. These were designed to be of 150 dm^3 nominal capacity, or five times the column volume, and were arranged as shown in figure 6.7. Two of these served as reservoirs and two as receivers. Pipework was mainly of 16 mm i.d. borosilicate glass but where flexible lines were unavoidable, 12 mm diameter inert P.T.F.E. tubing was used.

Flow control valves were made of glass with a P.T.F.E. stem and seat, supplied by Q.V.F. Ltd. All other valves were of the all-glass stopcock type, lubricated by silicone grease (for water) or mannitol grease (a mixture of glycerol, mannitol and dextrin) for organic solvent lines. Flowrates were measured by size 18 and size 10 rotameters with Korranite ceramic floats. These were used in combination to provide a wide range of flowrate measurement. Each rotameter was individually calibrated at $20^{\circ}C \pm 1^{\circ}C$. Suitable drainpoints were incorporated in the pipework to allow complete draining of the system.

Fluids were pumped by two Stuart Turner No. 12 centrifugal pumps designed to give flowrates of 1.25/0.45 $m^3 s^{-1}$ at hydrostatic heads of 2.0/10.0 m. Stainless steel casings and impellers were incorporated in these pumps together with graphite and "Viton A" seals. Immersion

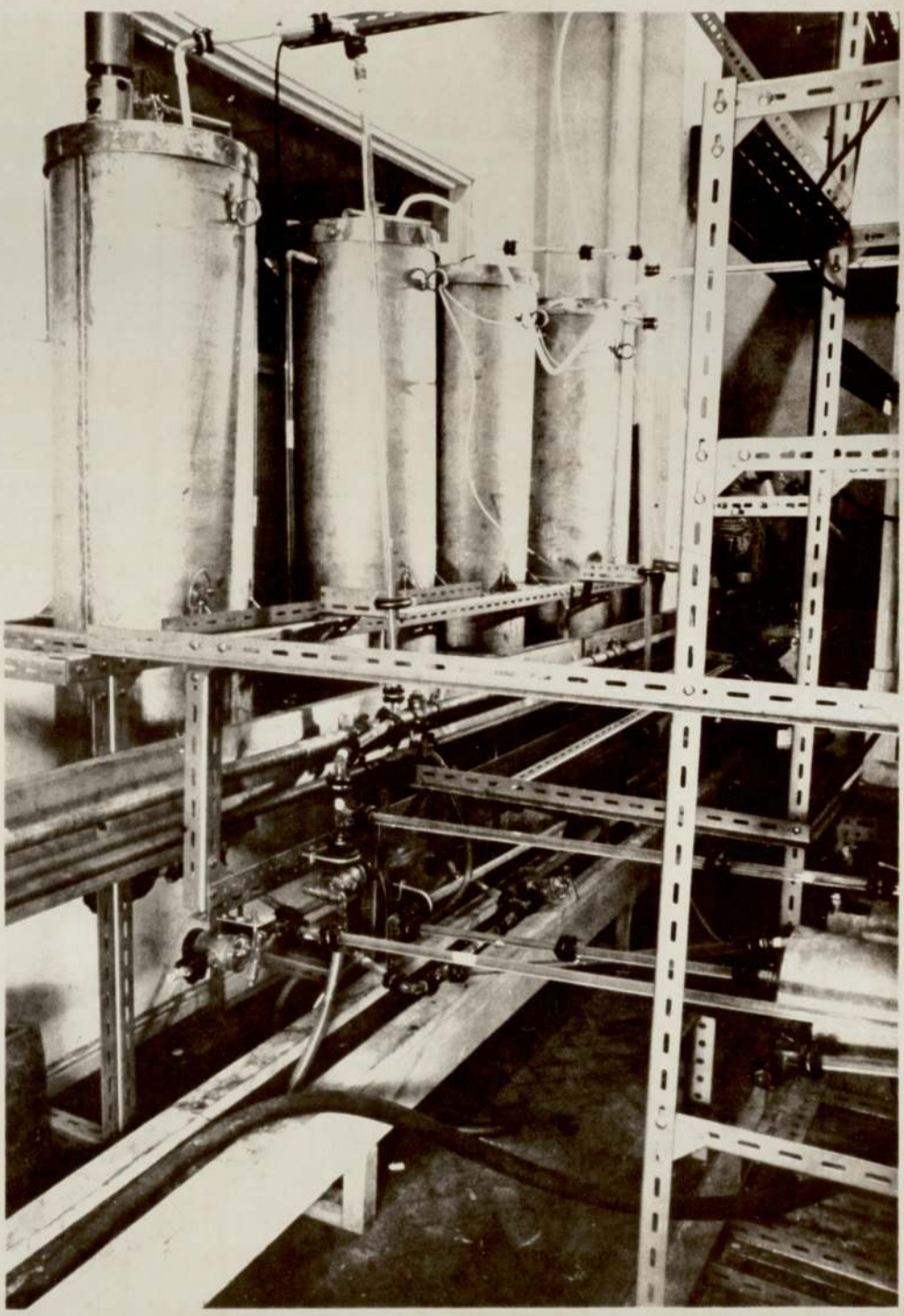

Figure 6.7 Storage Vessels

tests confirmed that "Viton A" was unaffected chemically by the process fluids chosen. A very slight but quite acceptable swelling was noticed; this did not give rise to any leaks. The speed of each pump was controlled by a 'torovolt' variable voltage unit to give fine control.

6.3 Selection of Liquid-Liquid Systems

High energy levels are created in the Oldshue-Rushton Contactor due to the high degree of turbulence generated by the impellers. It is well established that the stable size of a drop in a turbulent environment is roughly proportional to $(\sigma/\rho_c)^{0.6}$. Thus ideally a high interfacial tension system would be preferred for study since the resulting drop sizes would be larger and thus easier to record and measure. Furthermore their residence times in the column would be lower so that steady state could be achieved more quickly. For studies of the hydrodynamic properties of the contactor, the continuous phase was distilled water, and the dispersed phase toluene. The advantages of this system from the points of view of availability, cost, stability and low toxicity have been described (20). Subsequently communications of the European Federation of Chemical Engineering Working Party on Distillation, Absorption and Extraction have indicated that a system of standardisation of test solvents for liquid extraction research is imminent, and the system toluene/distilled water combined with various solutes will be favoured. The object is to facilitate comparison of results from different sources.

For mass transfer studies acetyl acetone (2 : 4 pentandione) was initially selected as solute for the following reasons:-

(a) Solubility in toluene and distilled water.

(b) Distribution coefficient m = 5.98. Therefore the greatest resistance to mass transfer lay in the continuous water phase, conditions for which this contactor was considered most suitable due to the high degree of agitation.

(c) A high specific conductivity in the aqueous phase which allowed conductivity probes to be used for concentration measurement.

(d) Its ease of detection by colorimetric means.

(e) The linear relationship between refractive index and concentration for solutions in toluene and water.

Additionally, butyric acid was used as a solute when certain difficulties, mentioned in section 6.4.3 were encountered in the use of acetyl acetone, and was preferred eventually because of its stability over a long period of time.

Distilled water was used as the continuous phase in all runs because of the constraints of economics and safety.

6.4 Measurement and Calibration Techniques

6.4.1 Drop Sizes

Mumford (20) has reviewed the techniques available for drop size measurement. From a discussion of photoelectric techniques, (80,32,98,152) use of radioisotopes (scintillation) (62), capacitance

measurements (102), chemical encapsulation (153) and photography (62,40,154), he concluded that the measurement of drop size distributions in primary dispersions was best made by the latter method. Conversely for the measurement of mean drop sizes where the actual distribution of drop sizes is not required the photoelectric technique would be the most convenient. A sonic probe has recently shown some promise in the measurement of both drop sizes and hold-up (155). Recent work (83) has shown that it is possible to analyse photographs of a polydispersion automatically even when the drops are not spherical. Unfortunately no means of allowing for spurious results due to overlapping drops has yet been developed.

Thus semi-automatic counting of drops was performed using the Zeiss TG3 Particle Counter. Photographs of the dispersion at the wall of the column were taken on Kodak Plus-X panchromatic 35 mm film, 120 ASA, using an Asahi Pentax Spotmatic still camera with a No.1 single extension ring at a shutter speed of 1×10^{-3} s to 'freeze' the movement of the drops. A constant distance, established by trial and error, between the column wall and the film was maintained using the simple spacing adaptor shown in figure 6.8.

Illumination of the compartment under study was provided by a twin Kobold SR2 cine light. The two quartz-iodine bulbs gave an output of 1250 w at 125 v. Light was directed into the compartment under study at an angle of 90° to the camera axis. A pulley and counterweight system allowed the lights to be moved along the column.

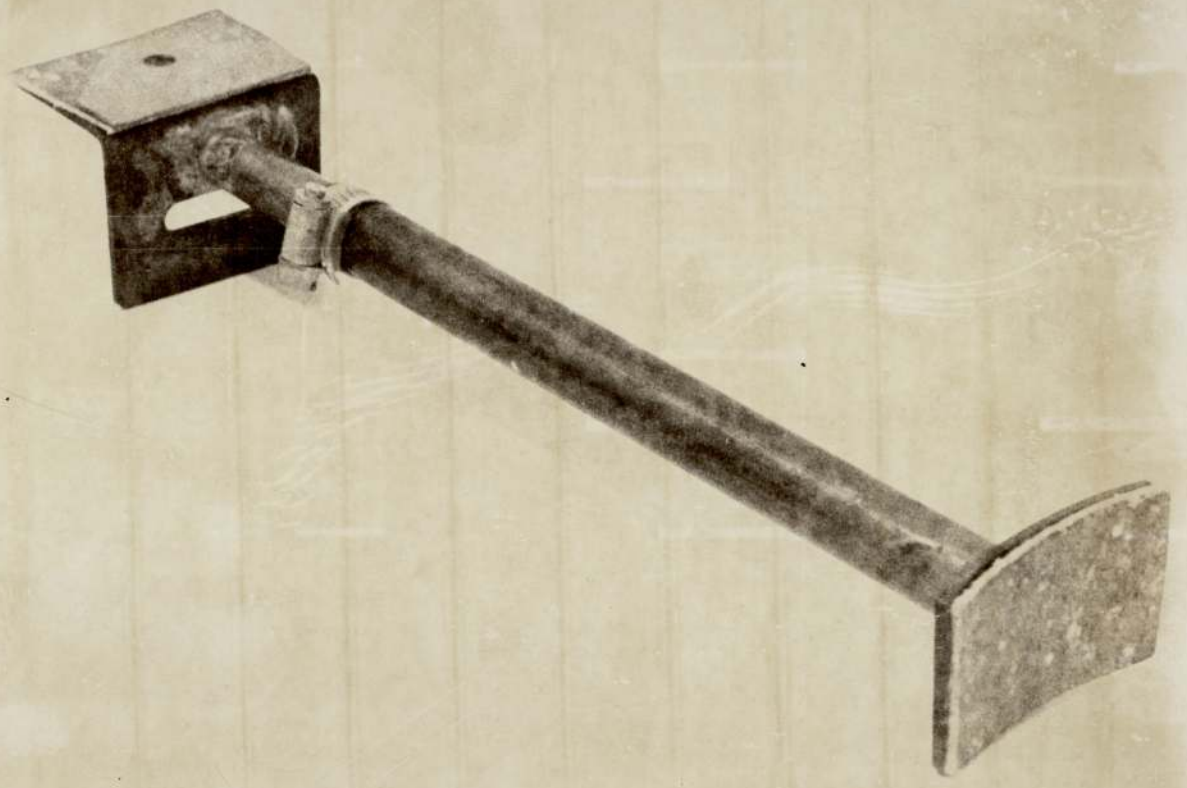

Figure 6.8 Spacing Adaptor

Enlargement of the negative to give an overall magnification of four times the true drop size, and printing Kodak grade 4 "Bromesko" paper, gave sufficient magnification and contrast for counting. A Honeywell 316 digital computer was used to process the measurements to produce a comprehensive statistical analysis of the distribution. The programme is described in Appendix (2). At least 300 drops were counted for each distribution measurement obtained from three separate negatives for each compartment. This gave a statistical accuracy of better than 3% (157).

Calibration of the counting procedure was performed by photographing a graduated millimetre scale inside the wall of the column, where it was intended to record the drop size distribution, at the standard distance using the spacing adaptor. The resulting enlarged photographic print of the scale was then compared with the readings on the drop size counter.

Distortion and magnification caused by the circular column wall was found to be negligible. The actual area of the column wall which was used to sample the distribution was centred on the area where the radial jet from the impeller met the wall. Although the field of view of the camera was almost the whole of one compartment, consideration of possible distortion resulted in a print of A5 DIN size. Therefore the actual sampling area was about 2 cm x 1 cm centred on the particular compartment under study. The method of photography is illustrated in figure 6.9.

Figure 6.9 Photography of Drop Sizes

Additional cine films were used to qualitatively analyse droplet behaviour in the column. Kodak 16 mm Tri-X Reversal roll film, type 7278, was used in two cameras. For normal speeds, up to 64 frames per second, a Beaulieu R16 was used with a P3 type, f 0.75 lens. At high speeds up to 500 f.p.s. a Milliken DBM3 fitted with the same lens was used. Lighting for cine films was provided by two 500 w photoflood lamps in addition to the Kobold lamp.

6.4.2 Hold-up

Hold-up of the dispersed phase was measured by sampling in several compartments via the 'Simplifix' toggle valves shown in figure 6.4. The rubber sealing discs were replaced by P.T.F.E. to eliminate solvent attack, and the bore was increased from 1/16" to 1/8" to increase the sampling flowrate. Thus 100 ml samples could be taken in about five seconds.

It is important to note that the parts of the sample ports in contact with the dispersion inside the column were made from 18/8 stainless steel. A metal both resistant to attack by solvents and solutes is essential. Low surface energy materials such as plastics (including P.T.F.E.) are preferentially wetted by organic liquids, and therefore any of such surfaces in the proximity of the sampling valve would lead to increased coalescence of the dispersion. Consequently higher point values of hold-up would occur, and lead to sampling errors.

The accuracy of this technique was checked by comparison with overall hold-up determinations in which the agitator was stopped and

the column isolated. Three samples for each compartment were taken, and these were generally internally consistent within $\pm$5%. Samples were collected directly in 100 ml glass measuring cylinders and the volumes of each phase read directly after separation.

6.4.3 Chemical Concentrations

A method of measuring concentrations of ionised solutes in the aqueous phase was developed, using the variation of conductivity with concentration. Doyle (158) developed a conductivity probe with a response independent of both the flowrate and the direction of flow around the electrodes. It consisted of a central rod electrode surrounded by a second spiral electrode, as shown in figure 6.10. The electrical resistance of the fluid was monitored by a special amplifier circuit, also developed by Doyle, giving an output voltage in the range 0-10 mV proportional to the conductance of the solution. The amplifier is shown in figure 6.11. The output from the amplifier was fed to one channel of a servoscribe twin pen recorder. Variable zero and range controls on both the amplifier and the recorder enabled the zero to be adjusted to the conductivity of the aqueous solutions entering or leaving the column so establishing a measurement datum. Probes were located in six compartments in the column. The radial position of each probe could be adjusted simply by sliding it through the flexible 'O' ring seal in the respective sample port. Probes were also located at the aqueous phase inlet and outlet of the column.

Organic phase solute concentrations were not determinable by the

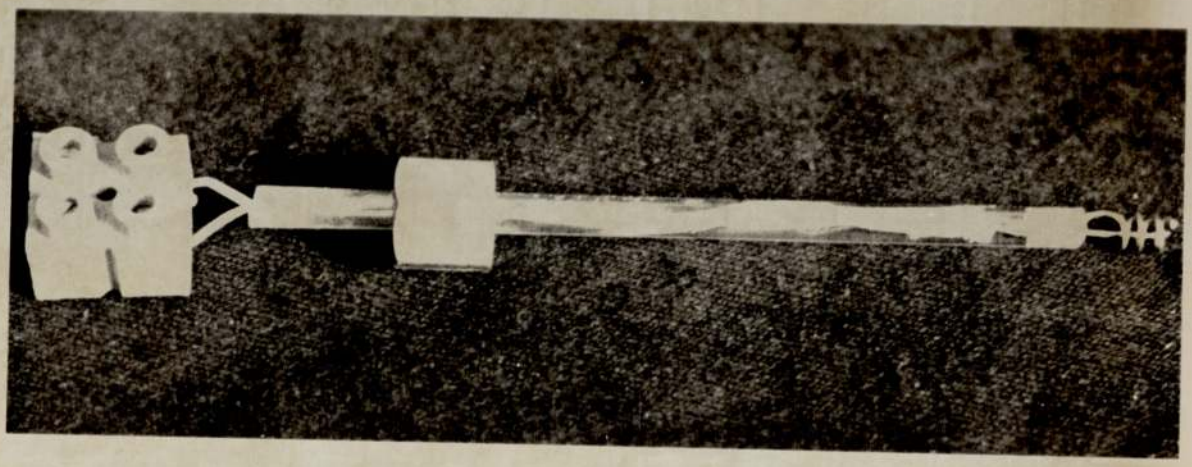

Figure 6.10
Conductivity Probes

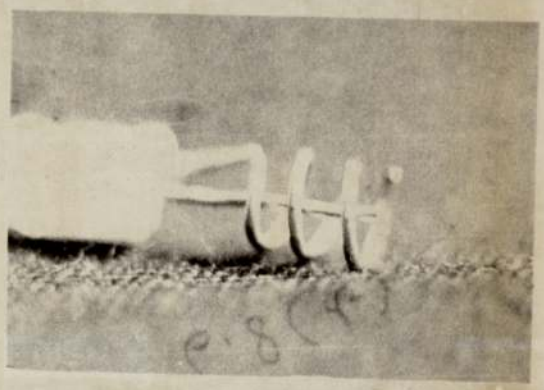

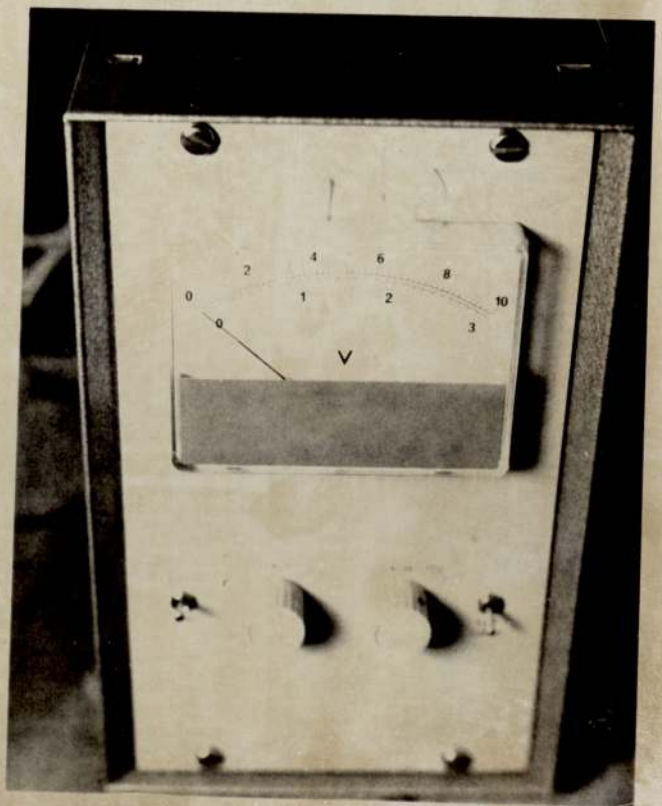

Figure 6.11
Amplifier

same technique because organic solvents are, in general, non-polar. Therefore a technique was derived for this by means of a mass balance on samples taken from the column. If the aqueous phase concentration was known before the sample was taken, i.e. in the column, then when the sample came to equilibrium it was measured again, the amount of solute transferred to the organic phase during the sample-taking procedure could be found. From a knowledge of the equilibrium distribution coefficient at the temperature of the sample, and the sample volume, the original concentration of the organic phase could be estimated without a direct measurement. Concentration profiles and driving forces in the column could then be used for mass transfer calculations.

A second electronic circuit was constructed to feed a second recorder channel to indicate on a chart which compartment was being measured at any instant. This consisted of a simple set of parallel 10K resistances and a multipoint switch.

Concentrations measured by conductivity were checked by chemical analysis. For acetyl acetone, a colorimetric method using the ferric chloride complex and a Spekker colorimeter was developed. Some difficulties were encountered with respect to the satisfactory performance of the colorimeter. Also, it was found that the extract phase from the column became contaminated with metal ions, mostly iron, which rendered accurate analytical work most difficult.

For butyric acid as solute, a simple titration with 0.01 M and 0.1 M

sodium hydroxide in Analar methyl alcohol was found to be most satisfactory for both aqueous and organic solutions. An accuracy of 0.01 % $^{w}/_{w}$ butyric acid was easily obtained. The sodium hydroxide solution was made up periodically from pellets, and standardised using approximately 0.01 M sulphuric acid in distilled water, in turn standardised with Analar grade anhydrous sodium carbonate.

The use of standard 5 ml aliquot samples from the column simplified the technique, allowing a graph of volume of sodium hydroxide needed versus concentration of butyric acid to be used. Thymol blue was used as indicator.

6.4.4 Physical Properties

(a) Specific gravity

The standard pyknometer technique was employed for all solutions. Measurements were made at 20°C $\pm$ 0.1°C.

(b) Viscosity

The method of timing the passage of the fluid through a capilliary immersed in a constant temperature bath (20°C $\pm$ 0.1°C) was used.

(c) Interfacial Tension

The standard Wilhelmy Plate method was used on a "Cambridge" torsion balance. The table of measured physical properties is given in Appendix (3).

6.4.5 Flowrates

One each of sizes number 10 and number 18 rotameter with appropriate 'korranite' ceramic floats were used to measure the flowrate of each feed

stream. Each pair was mounted in parallel, only one of each pair being used at a time. Thus a wide range of flows could be measured accurately. Calibration was performed by weighing samples over a limited time period for toluene and distilled water at 20°C $\pm$ 1°C, giving an accuracy better than 1% of maximum reading. For solutions of butyric acid in water and toluene, it was assumed that density and viscosity variations at the low concentrations used were small enough to allow calibrations for the pure fluids to be used.

6.4.6 Agitator Speed

A Smiths Industries 'Venture' magnetic tachometer reading 0-1000 rpm x 50 rpm, was mechanically coupled via a 10 ft flexible drive to the agitator motor spindle. The accuracy was confirmed using a stroboscope in turn standardised by comparison with the mains frequency of 50 Hz. It was found to be correct over the full scale range, and could be read within $\pm$ 10 rpm.

7. Experimental Procedures and Results

7.1 Non-Mass-transfer Runs

7.1.1 Cleaning Procedure

The column, transfer lines and storage vessels were carefully and thoroughly cleaned with a 2% v/v solution of Decon 75 decontaminant in tap water. The apparatus was then flushed once through with clean tap water and finally rinsed with distilled water. Care was taken to ensure that all sample points and drainage points were well flushed and free of traces of detergent. Checks were made by measuring the surface tension of the distilled water.

7.1.2 Preparation of fluid systems

Toluene was employed as the dispersed phase throughout. Before use it was purified to the specification given in Appendix 3 in an Oldershaw distillation column with minimum reflux.

The continuous phase throughout was once-distilled water produced from an all-glass still.

Before use the phases were mutally saturated by recycling them through the column for at least two hours. About 75 dm^3 of each phase was needed for most of the runs.

7.1.3 Flooding

The flooding characteristics of the column were investigated to assess the maximum flowrates to be used in subsequent experiments, and to compare the capacity of the column with published data. For this work flooding was defined as discussed in section 3.1.2.

The operating procedure was as follows.

The column was filled with the aqueous continuous phase up to the position to be occupied by the interface. A convenient position for the interface was found to be 10 cm from the top of the column. With the agitator stationary and with no continuous phase flow, dispersed toluene phase was admitted to the column at a rate just below that expected to bring about flooding. Large drops, of the order of 0.5 to 2.0 cm diameter, rose rapidly through the column to the interface. Many drops were trapped beneath the stator rings and coalesced to form pools.

When the build-up of coalesced dispersed phase above the interface was sufficiently high, it flowed out of the column and back to the reservoir. At this point the agitator was started and adjusted to the desired speed.

The dispersed phase hold-up steadily increased, and the continuous phase was allowed to flow slowly out of the column via the outlet rotameter.

The continuous phase was then admitted to the top of the column at the desired rate.

Careful control of the outlet flowrate of the continuous phase was necessary to maintain the interface at a constant level at the top of the column throughout this start-up period during which the hold-up was increasing. Steady state was achieved when the interface level remained steady and the continuous phase inlet and outlet flowrates were equal.

The dispersed phase flowrate was then increased incrementally until flooding occurred. Sufficient time was allowed for steady state conditions to be re-established following each increase. Occasionally temporary incremental increases in the continuous phase outlet flow were used to maintain a constant interface position during re-establishment.

Steady state was achieved when about three column volumes (3×33 dm^3) total flow had passed through the contactor. This is in agreement with previous experience (16).

The flowrate of dispersed phase at the flooding point was recorded. As a check, it was then decreased by about ten per cent to allow the column to revert to normal operation, and then increased again.

At low impeller speeds, less than 250 r.p.m., droplets were rejected from the dispersed phase inlet end of the column when the flooding point was approached. Droplets were unable to proceed into the first compartment due to the high counter flow of continuous phase, and a build-up of droplets occurred below the lowest stator ring.

Flooding also occurred at high impeller speeds, greater than 700 r.p.m., and at high continuous phase flowrates, greater than 4.0 kg/m^2s. Drops entering the first compartment ruptured instantly into very small droplets due to the very high level of turbulence. The sizes were estimated to be less than 0.05 mm diameter. Since the terminal velocities of these droplets was very much less than the downward velocity of the continuous phase they were carried out of the

column with that phase.

In between these two extremes, that is, before the flooding point was reached, phase inversion was observed. Consequently, no flooding data could be recorded within the normal operating range of the unit.

7.1.4 Phase Inversion

The flowrates of each phase which were sufficient to promote phase inversion were determined in the following way.

The start-up procedure described under flooding (section 7.1.3) was carried out.

At steady state, the dispersed phase flowrate was increased incrementally by between 2 - 5% in the same manner as for the flooding determinations. Time was allowed for steady state to be re-established at each new flowrate. This was usually about ten minutes, dependent on the total flowrate. It was noted that inversion occurred on a cyclic basis. When one particular compartment became inverted, the inversion passed to the next compartment after a certain time, and proceeded up the column, ultimately coalescing with the bulk interface. After the 'slug' of inverted phases had left that compartment, normal operating conditions pertained. Subsequently the hold-up built up to a value sufficient to give inversion, and the process was repeated.

As soon as phase inversion began to occur in this cyclic way and a pseudo-steady-state was established, the dispersed phase flowrate was decreased by intervals of about 1% until the cycling ceased and phase inversion did not appear for at least ten minutes. A slight increase in the dispersed phase flowrate then caused the column to invert.

Phase inversion always occurred in one particular compartment or group of compartments for any specific set of operating conditions.

Hold-up values immediately prior to, and immediately after inversion were measured via the sample valves described in section 6.4.2. Three samples were taken during a run, consistent within $\pm$ 5%, and the mean was recorded. The results are plotted in figure 7.1.

All the phase inversion results are given in Appendix 4 . Phase inversion curves are plotted in figure 7.2 for impeller speeds of 225 to 700 r.p.m. Outside this range, flooding took place in preference to phase inversion as discussed in section 7.1.3. The value at N = 225 is of doubtful significance since stratification of droplets occurred at such a low rotor speed, and inversion was difficult to detect.

A cine film of the phenomenon was taken using the Beaulieu camera and this has been deposited in the Departmental Film Library. Selected prints from one sequence are shown as figure 7.3. A description of the whole film is given in Appendix 5 .

In figure 7.3, the 'slug' of inverted phases can be seen as lighter parts of each print. This is due to better light transmittance of the inverted toluene phase over the transmittance under normal operation. The hold-up of toluene is of the order of 70 to 80 per cent, and therefore under inversion conditions there are less drops present in each compartment. The slug moved up the column, from compartments 1 and 2 in print number 1 to 3 and 4 in print 9. The time taken to do this is about one minute.

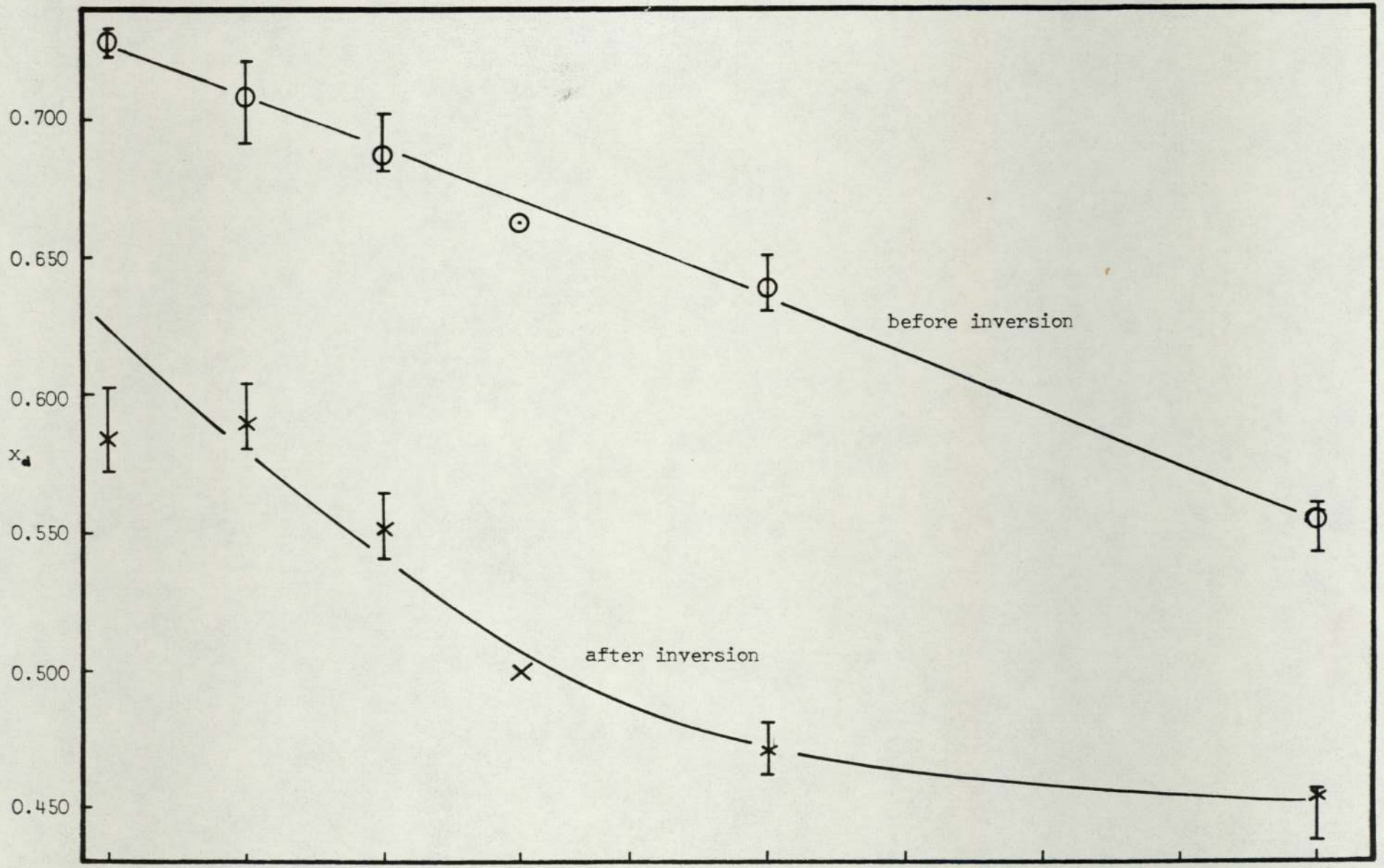

Figure 7.1 Variation of phase inversion hold-up with impeller speed

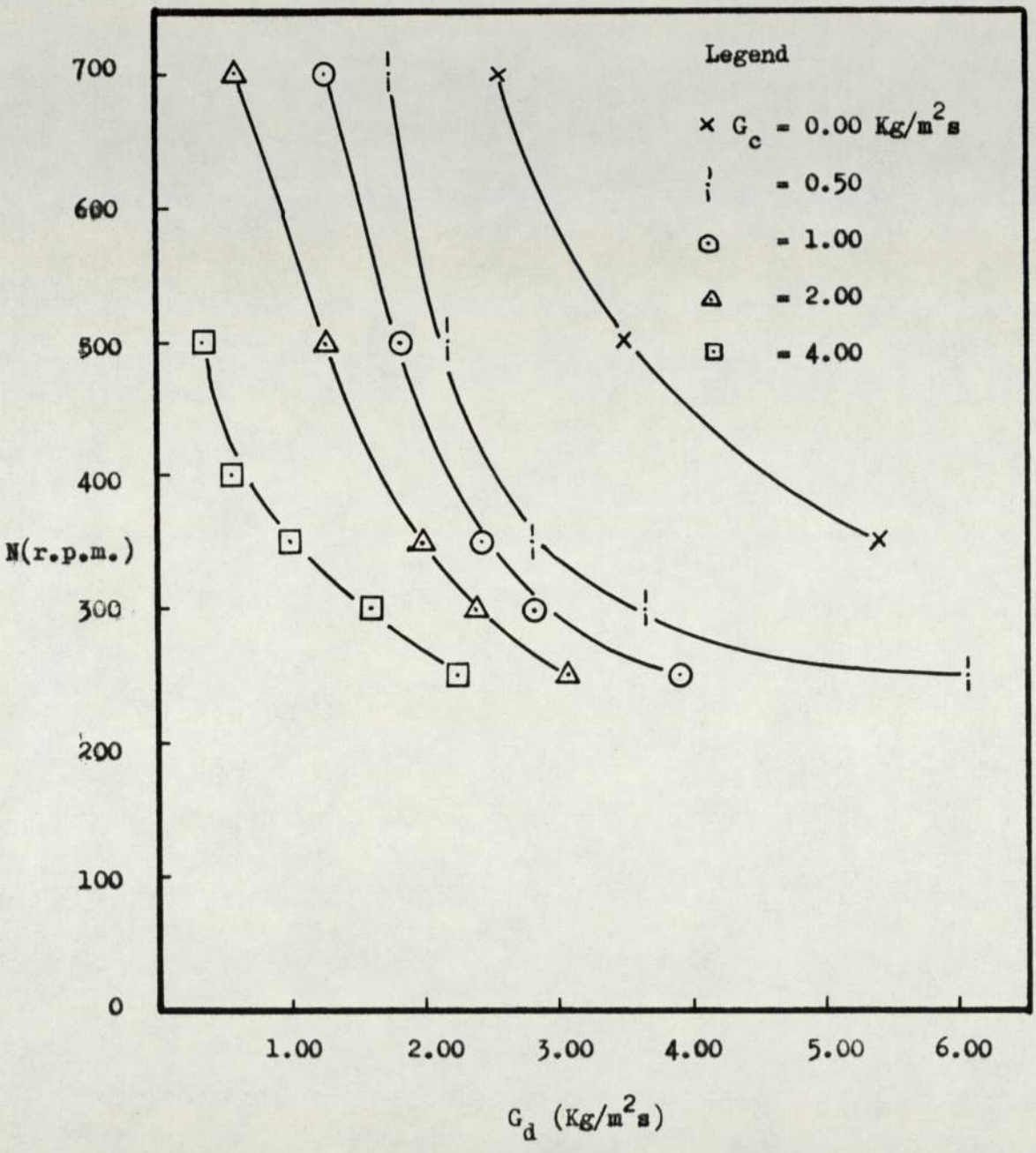

Figure 7.2 Variation of Dispersed Phase with Impeller Speed at Phase Inversion.

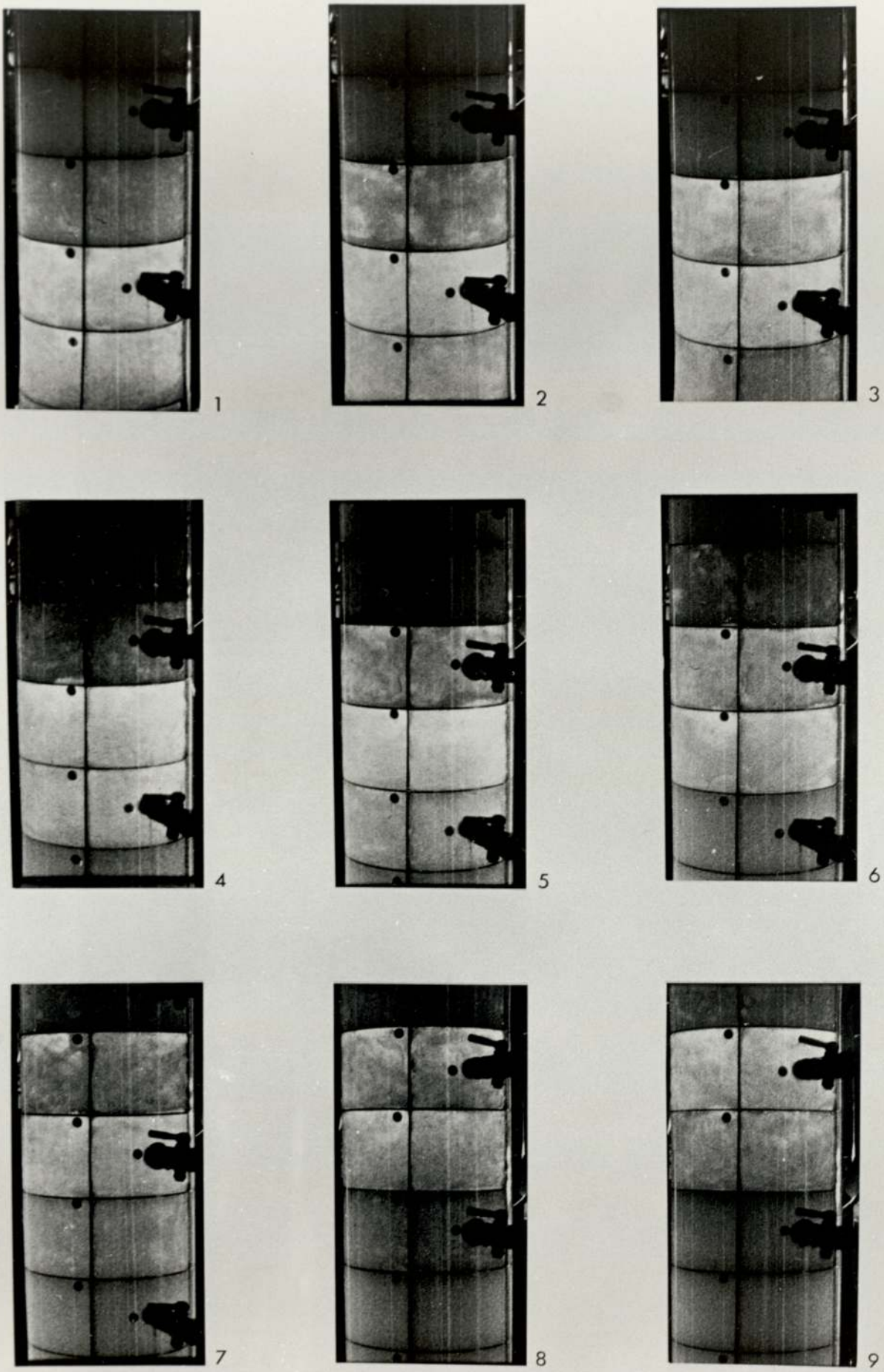

Figure 7.3 Phase Inversion.

7.1.5 Drop Sizes

Drop sizes were measured at various column heights within compartment numbers 2, 4, 6, 10, 12, 14. The construction of the column made the measurement of drop sizes in compartment 8 impracticable, due to the proximity of the central bearers. The column was started at selected flowrates and impeller speeds as described in section 7.1.3. At steady state, the drops at the wall of the column were then photographed as described in section 6.4.1. Duplicate and triplicate photographs were subsequently taken after intervals of five and ten minutes, giving a total of eighteen prints for each run. Drop size distributions were computed for each compartment, and plotted as a number distribution graph by computer. A total of 300 or more drops were counted from the three prints for each compartment, giving a statistical accuracy of better than 3% (156). A total of 21 runs were performed, covering a range of impeller speeds from 200 to 600 r.p.m., and flowrates from 0.25 to 1.00 kg/m^2s and mean drop sizes are given in Appendix 6 . The results are plotted on figures 7.4 to 7.10.

The distribution of drop sizes within each individual compartment was found to be consistently log-normal. A typical set of ogives is shown as figure 7.11. A cumulative per cent undersize plot is shown as figure 7.12. Typical photographs of dispersions are shown as figure 7.13.

7.1.6 Hold-up

Hold-up measurements were taken of the dispersed phase immediately after the drop size photograph was taken. Samples were withdrawn from

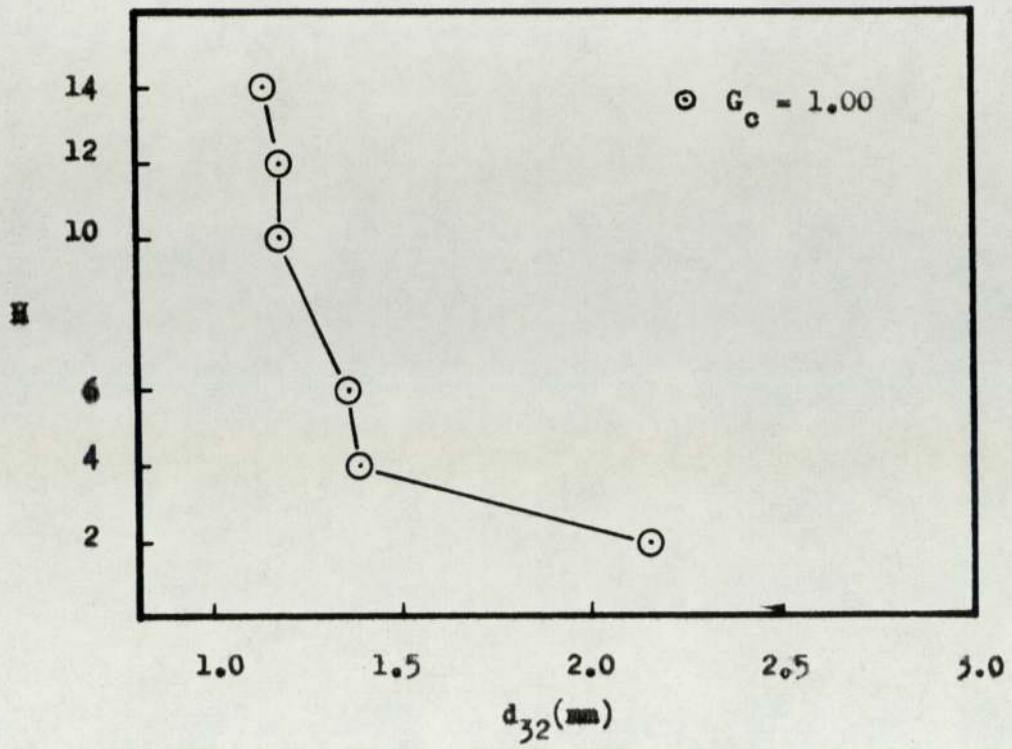

Figure 7.4 Variation of Mean Drop Size with Height, N= 200.

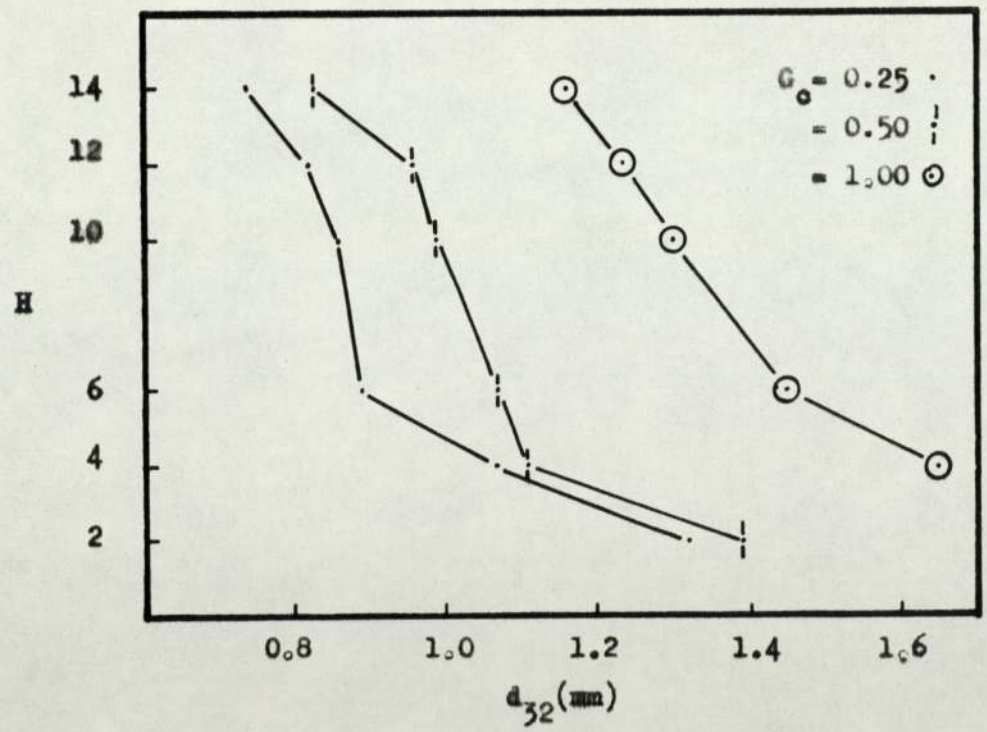

Figure 7.5 Variation of Mean Drop Size with Height, N = 250.

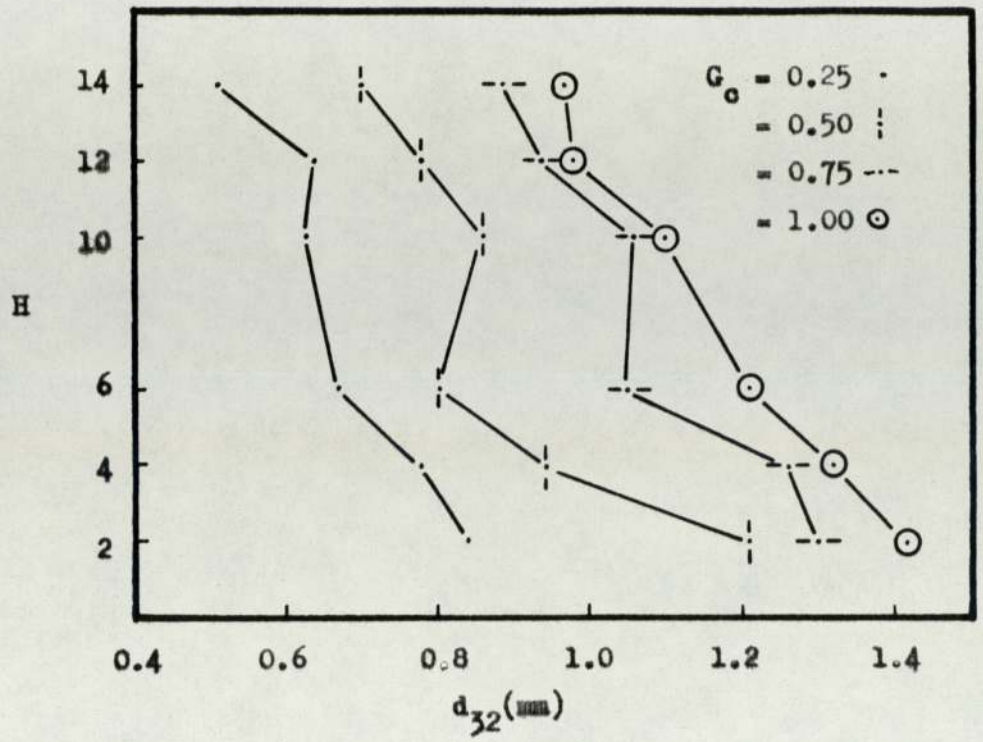

Figure 7.6 Variation of Mean Drop Size with Height, N = 300.

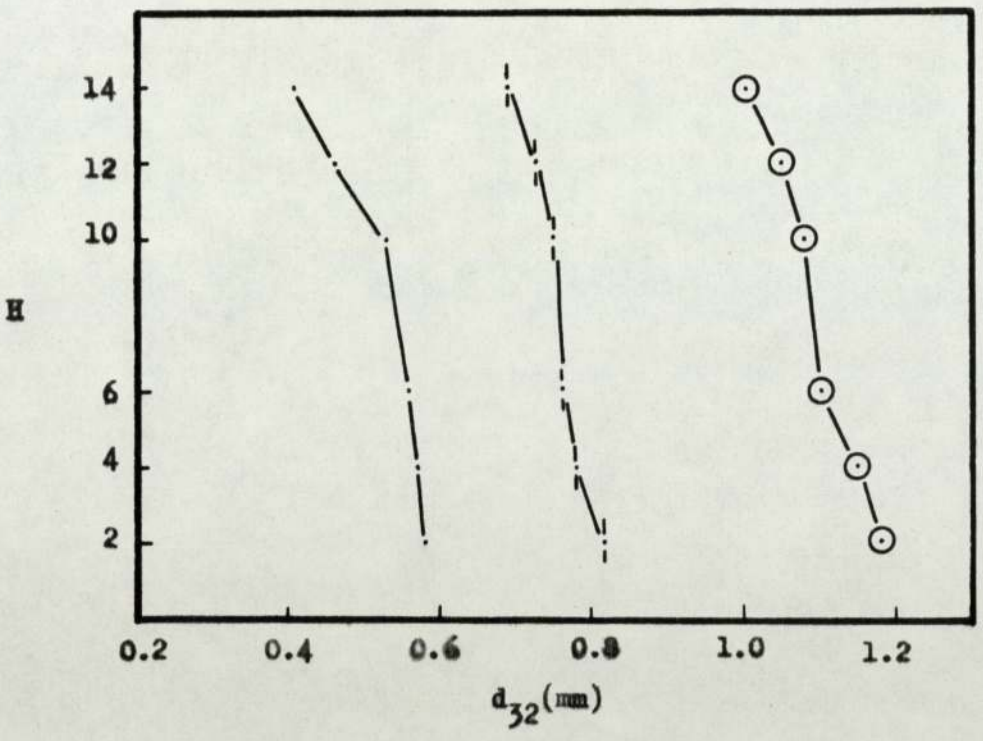

Figure 7.7 Variation of Mean Drop Size with Height, N = 360.

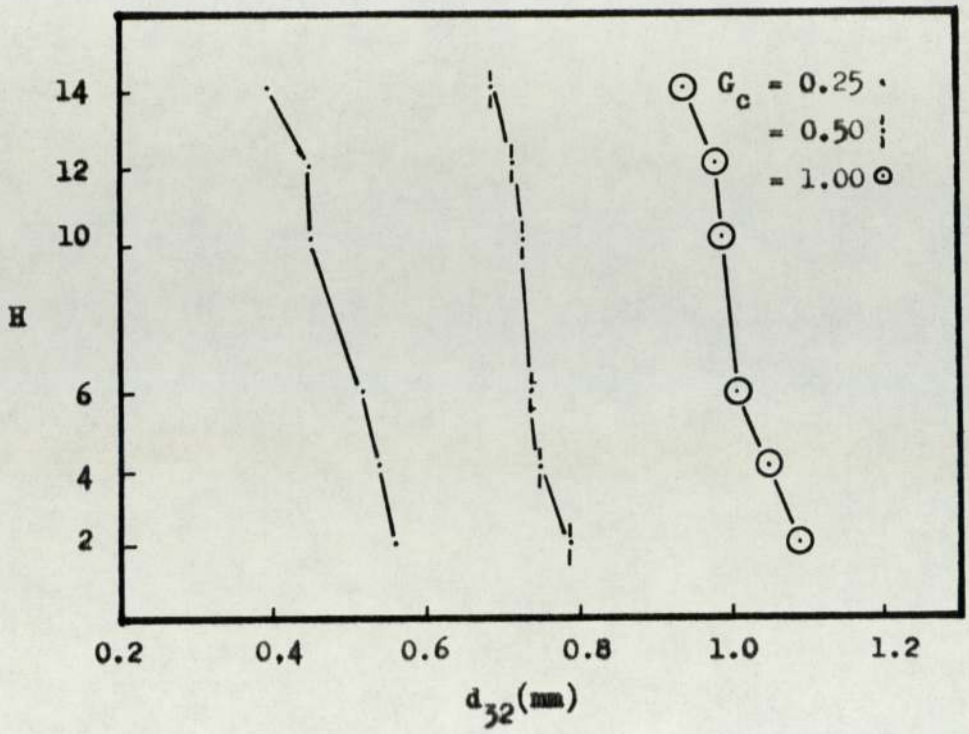

Figure 7.8 Variation of Mean Drop Size with Height, N = 400.

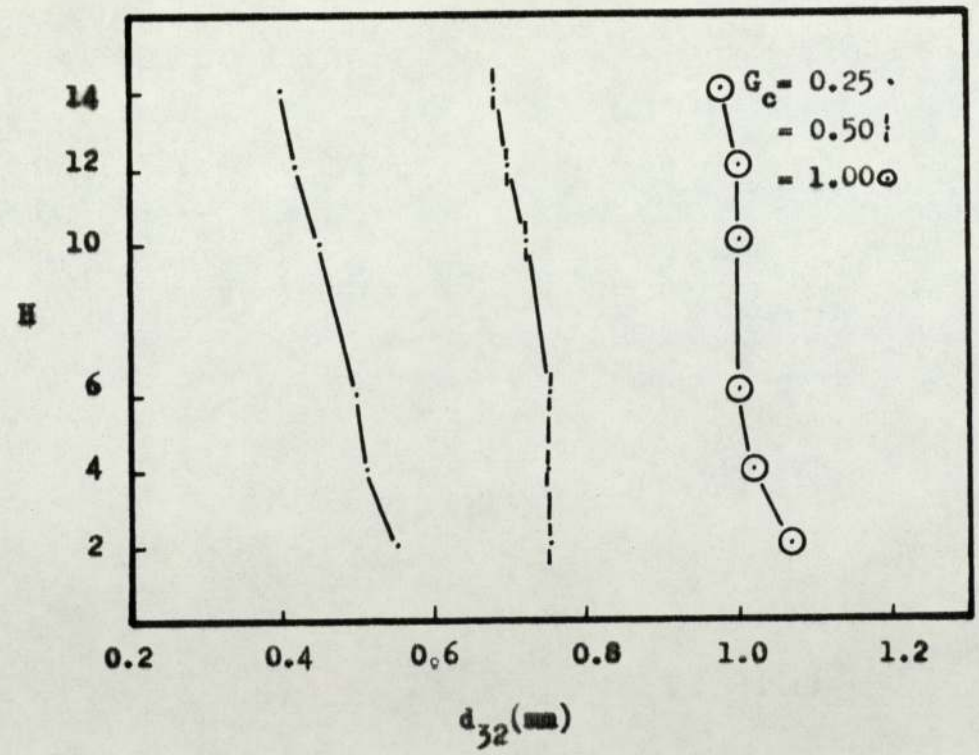

Figure 7.9 Variation of Mean Drop Size with Height, N = 500.

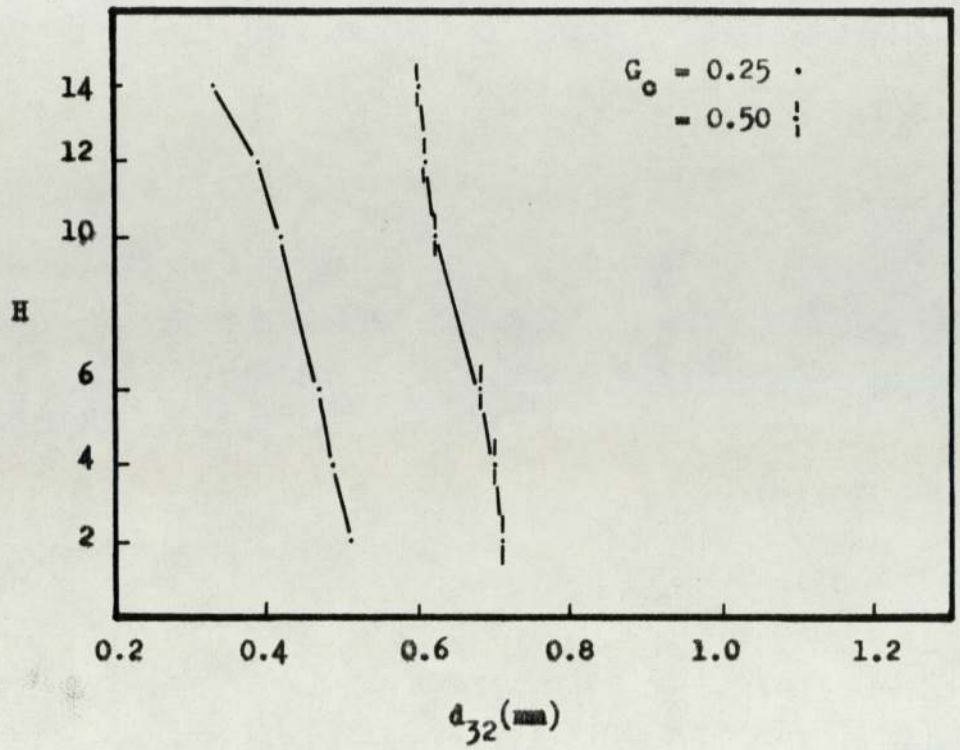

Figure 7.10 Variation of Mean Drop Size with Height, N = 600.

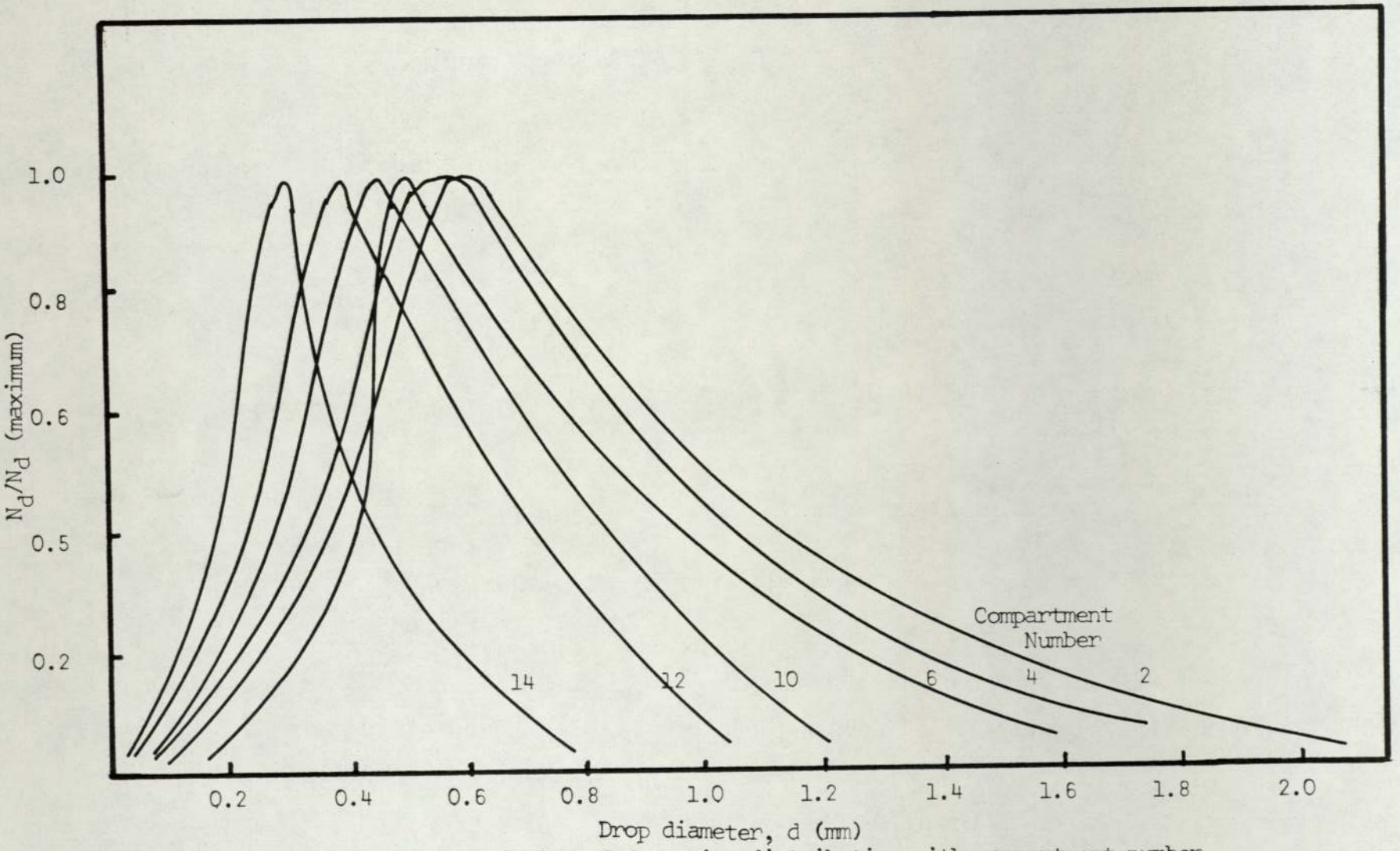

Figure 7.11 Variation of drop size distribution with compartment number

N = 400 r.p.m. $G_c = G_d = 0.5$ K_g/m^2s system: toluene/water

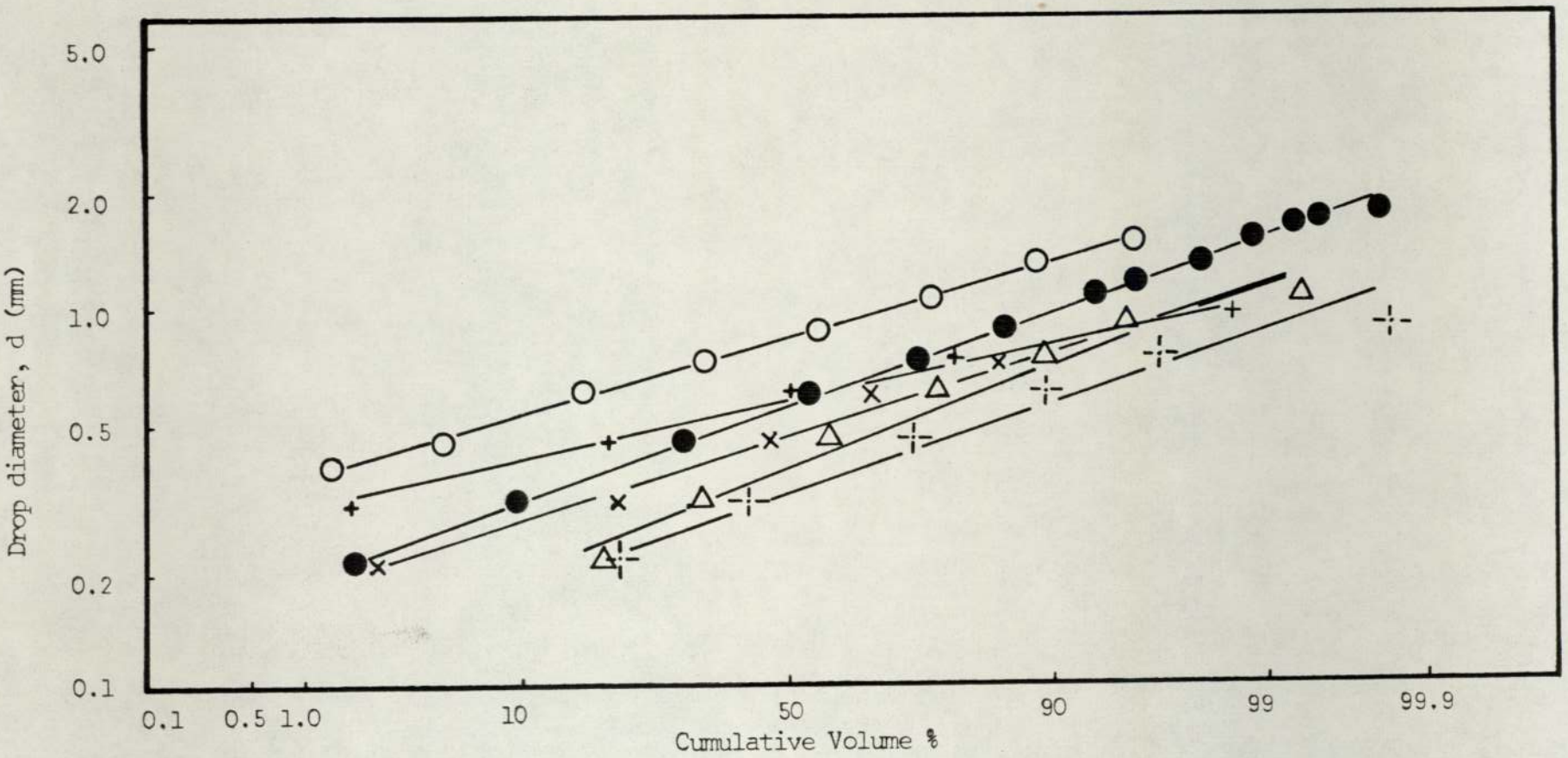

Figure 7.12 Log-normal drop size distribution in the column

N = 400 r.p.m. $G_c = G_d = 0.5$ K_g/m^2 system; toluene/water

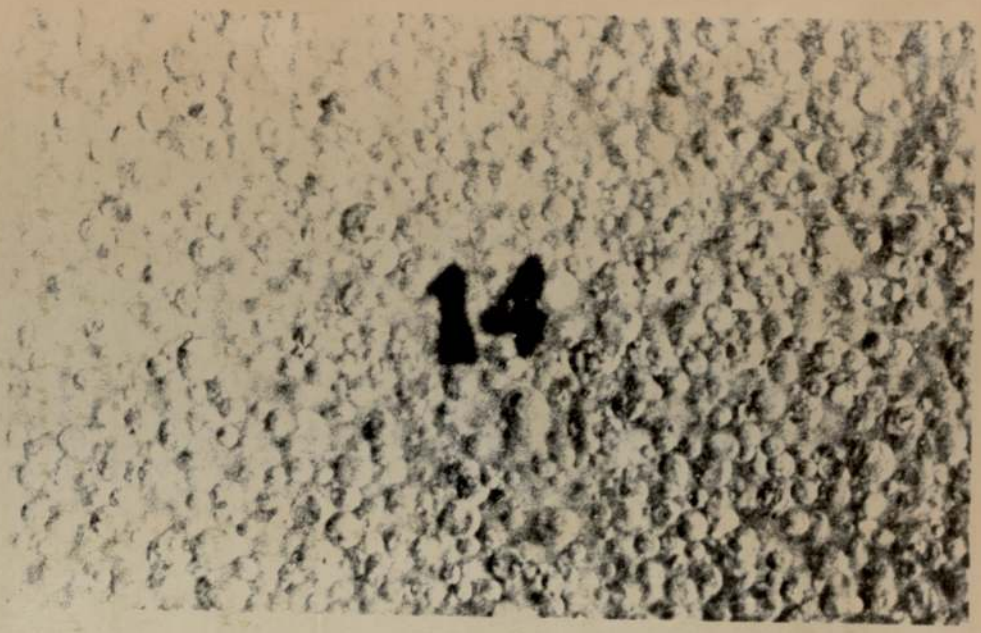

(a)

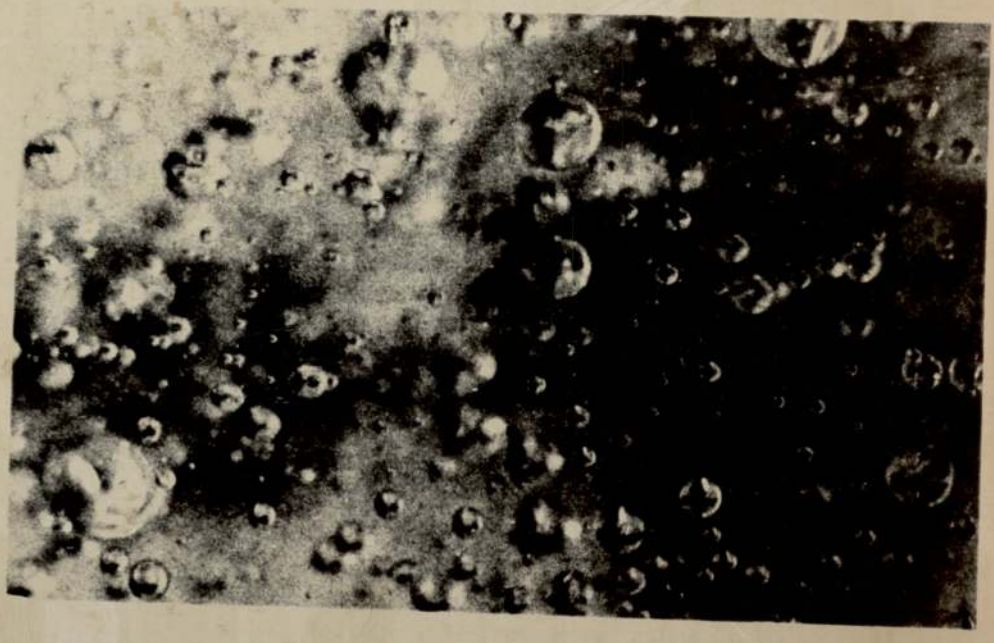

(b)

Figure 7.13. Typical Photographs of Dispersions
(a) Compartment 14 (top)
(b) Compartment 2 (bottom)

compartments 2, 4, 6, 10, 12 and 14 via the sampling valves described in section 6.4.2. Three samples were taken from each of the compartments, and the mean recorded. Samples were consistent within $\pm$ 5%. Hold-up results for a range of impeller speeds between 200 and 600 r.p.m., and flowrates of 0.25 kg/m^{2}s to 1.00 kg/m^{2}s are given in Appendix 7 . Results are plotted in figures 7.14 to 7.19.

The hold-up values recorded were representative of the overall value in each compartment sampled. The large sampling orifice to drop size ratio of about 50 : 1 ensured that drops did not block the entrance to the port. This would have caused a higher proportion of continuous phase in the sample. Additionally, the sample volume of 100 ml was removed in about five seconds so that there was a high flowrate through the orifice. The hold-up values obtained at steady state were verified for certain runs by quickly closing the inlet and outlet valves. After stopping the agitator, drops coalesced at the interface. The average hold-up in the column was calculated from the change in interface level, and compared with the hold-up obtained by summation of the samples.

7.2 Mass Transfer Runs

7.2.1 Experimental Design

It was established in chapter 1 and chapter 5 that many variables affect the rate of mass transfer in the column. Those independent variables which are capable of control, are listed below.

1. Impeller speed
2. Continuous Phase flowrate

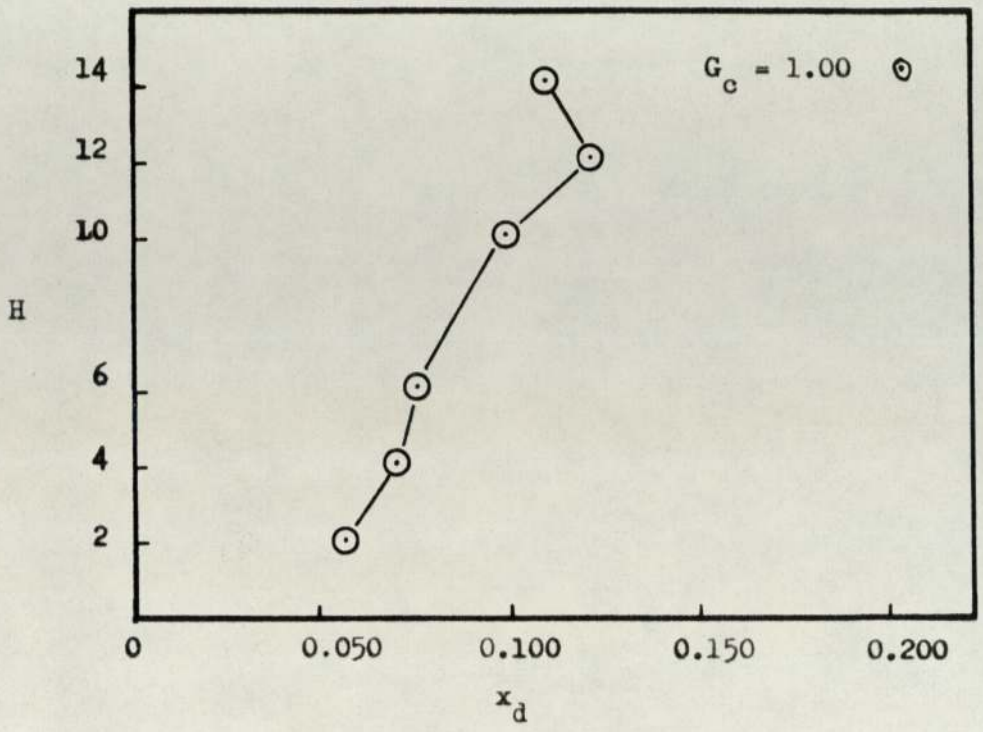

Figure 7.14 Variation of hold-up with height, N = 200

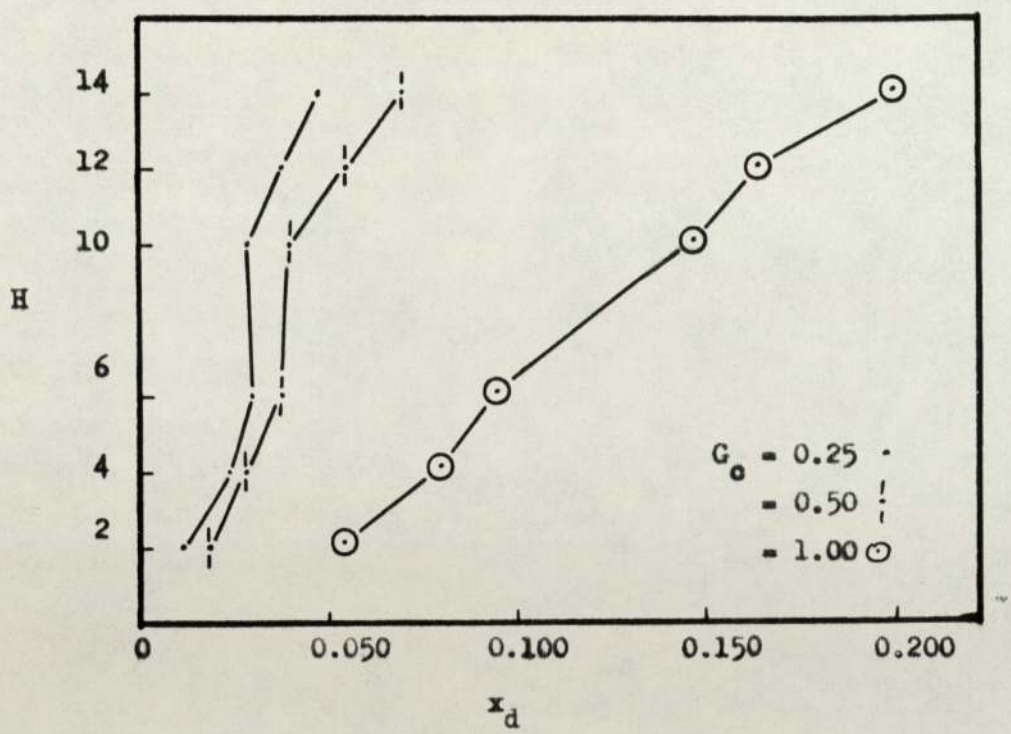

Figure 7.15 Variation of hold-up with height, N = 250

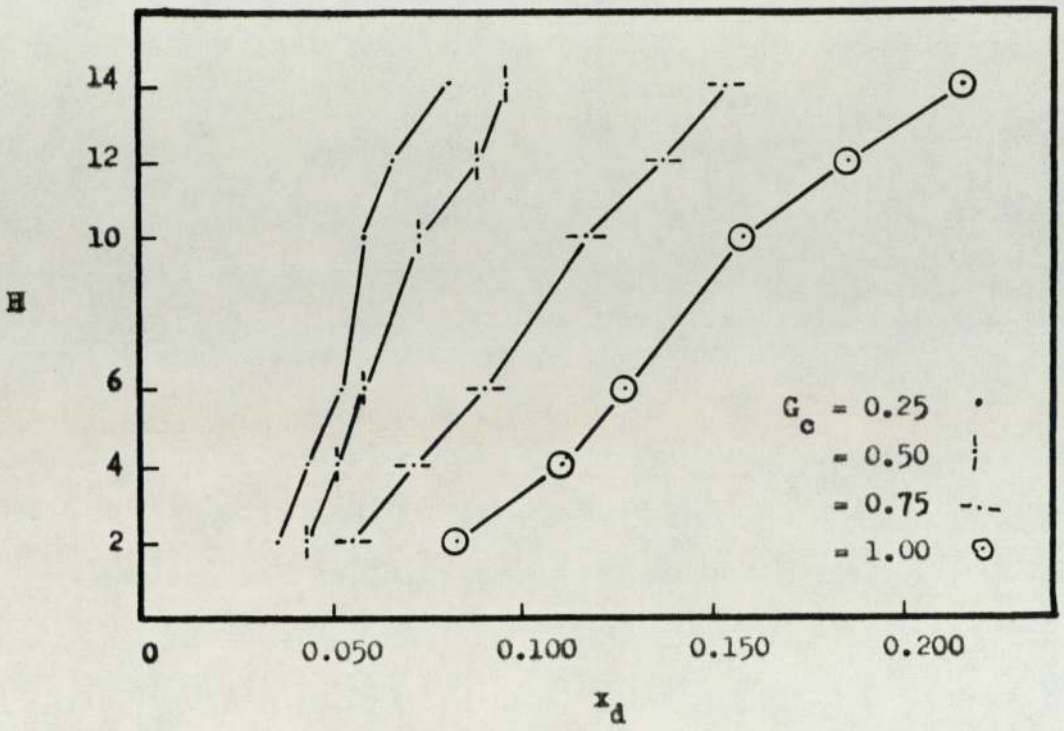

Figure 7.16 Variation of hold-up with height, N = 300

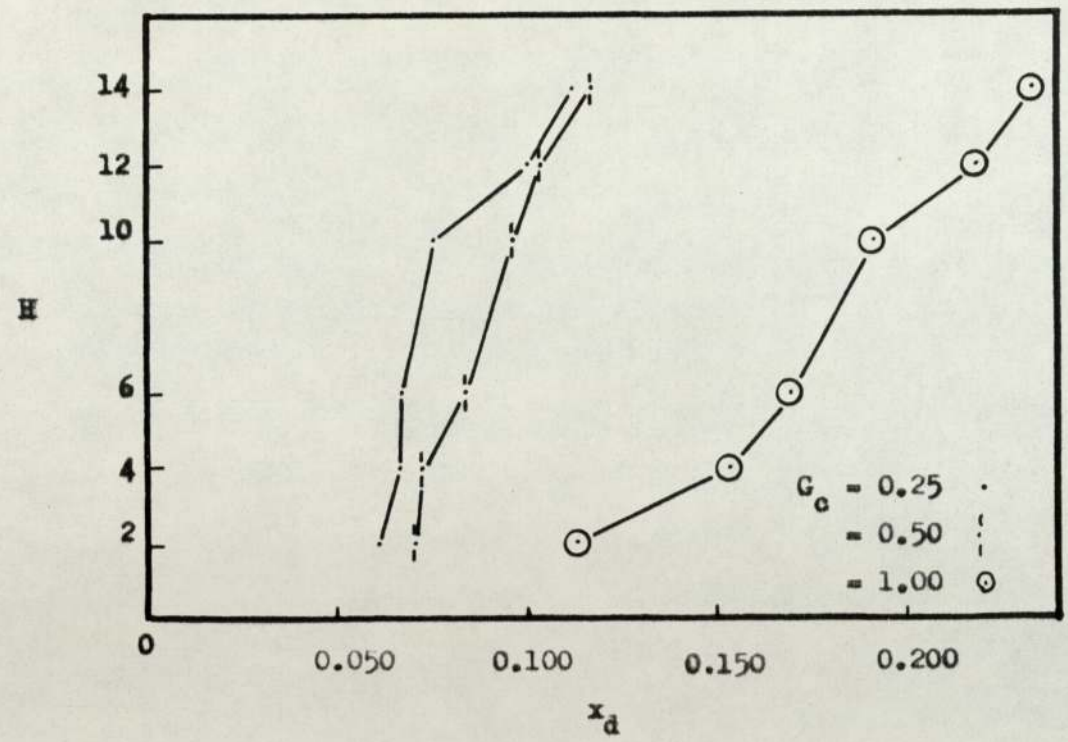

Figure 7.17 Variation of hold-up with height, N = 350

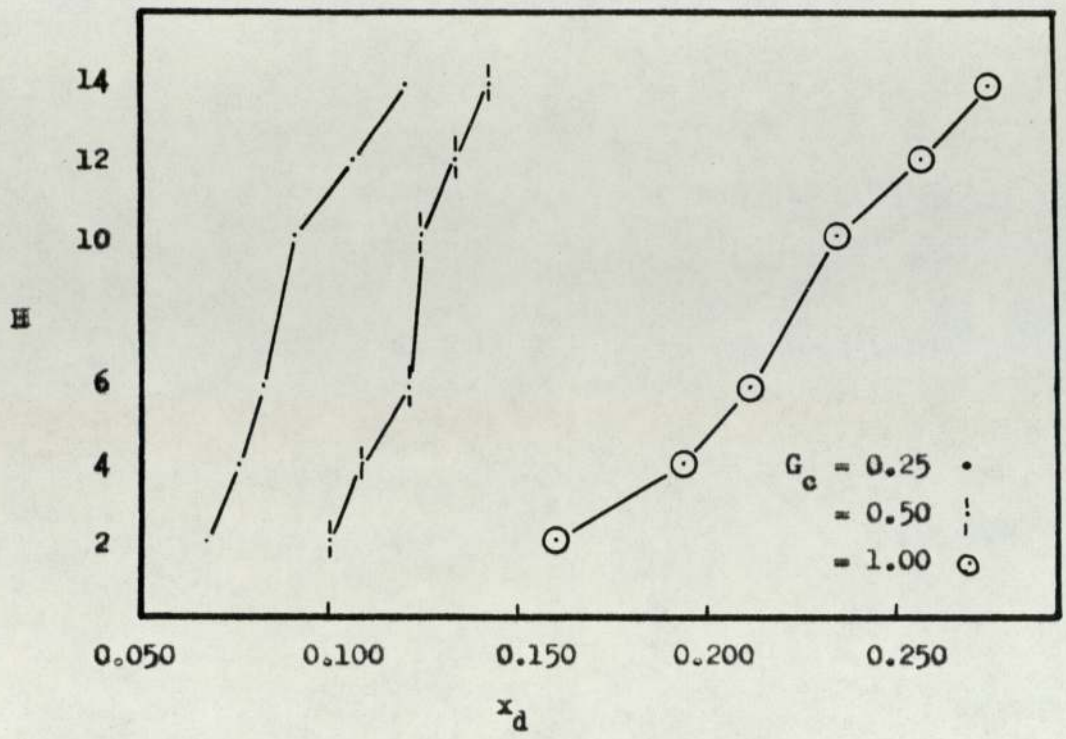

Figure 7.18 Variation of hold-up with height, N = 400

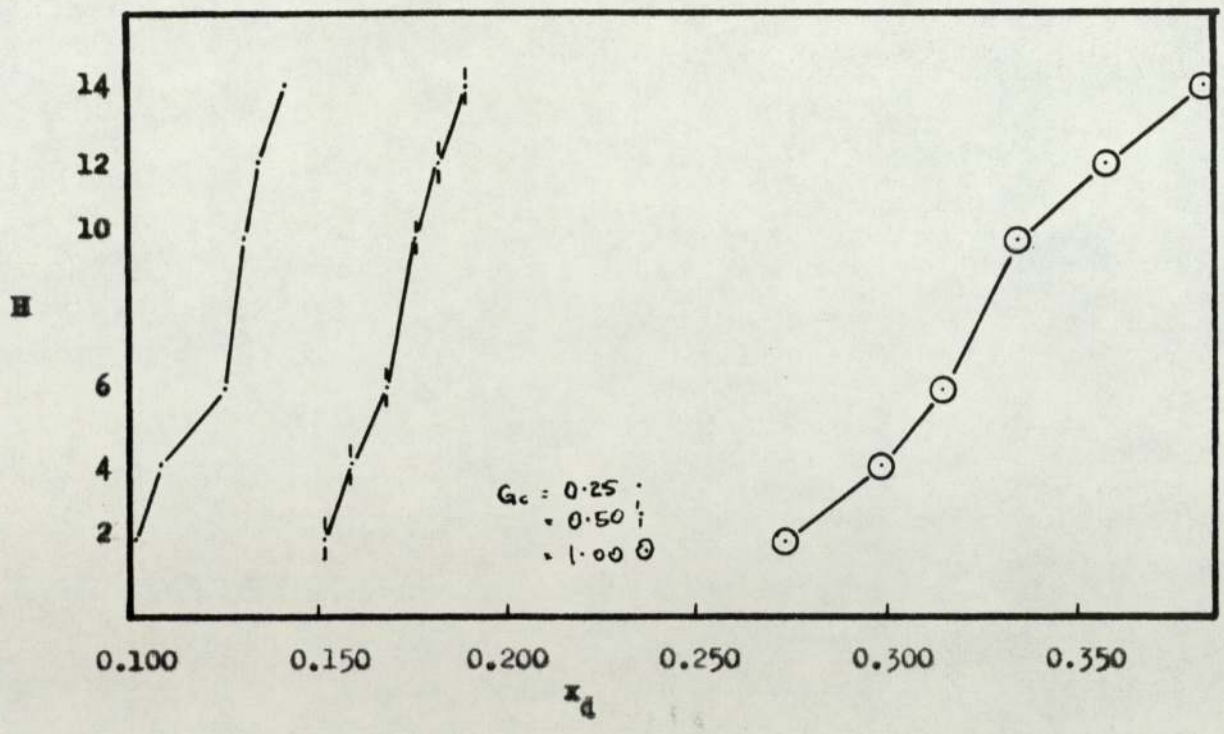

Figure 7.19 Variation of hold-up with height, N = 500

3. Direction of mass transfer

4. Dispersed Phase flowrate

5. Extraction Factor

6. Initial concentration of solute in feed

7. Initial concentration of solute in extract.

Initially it was considered desirable to investigate the effect of all of these variables on the overall mass transfer coefficient. Mass transfer experiments were performed at room temperature, $18^{\circ}C \pm 3^{\circ}C$

The seven variables were treated in a Graeco-Latin Square arrangement. A summary of the design is shown in figure 7.20.

7.2.1.1 Impeller Speeds

Impeller speeds of 250, 300 and 350 r.p.m. were chosen as representative of the range of normal operating speeds for this diameter of column. Speeds below 250 r.p.m., did not give sufficient agitation for the dispersion to be fully circulated in each compartment, and at speeds of 400 r.p.m, and above drop sizes were very small. At speeds of 700 r.p.m., camera shutter speeds greater than the available 1×10^{-3}s were necessary to 'freeze' the motion of the drops.

7.2.1.2 Interfacial Tension

Measurement of the interfacial tension of equilibrium mixtures of n-butyric acid in water and toluene indicated that drop sizes in the column with this system could be expected to be smaller than those for toluene/water only by a factor of up to 0.6, using the relationship $d_1/d_2 = (\sigma_1/\sigma_2)^{0.6}$. The interfacial tension between toluene and water at various equilibrium concentrations of n-butyric acid was

Figure 7.20 Experimental Design

Variable	Levels →	1	2	3
Impeller Speed, N	r.p.m.	250	300	350
Concentration, C	%	1.0	2.0	3.0
Extraction Factor, ε	-	1.0	1.5	2.0
Continuous Phase, Flowrate G_c	kg/m^2s	0.5	1.0	1.5
Direction of mass transfer	-	D → C	C → D	

Direction of Mass Transfer

D → C

ΔC	ε		
	1.0	1.5	2.0
1.0	N = 250	300	350
	G_C = 0.5	1.5	1.0
	Run No. 1/1	1/2	1/3
2.0	300	350	250
	1.0	0.5	1.5
	1/4	1/5	1/6
3.0	350	250	300
	1.5	1.0	0.5
	1/7	1/8	1/9

C → D

ΔC	ε		
	1.0	1.5	2.0
1.0	N = 250	300	350
	G_C = 0.5	1.5	1.0
	Run No. 2/1	2/2	2/3
2.0	300	350	250
	1.0	0.5	1.5
	2/4	2/5	2/6
3.0	350	250	300
	1.5	1.0	0.5
	2/7	2/8	2/9

C = continuous phase

D = disperse phase

measured and is shown as a function of concentration in both phases in Appendix 8 . The method used was described in section 6.4.4.

7.2.1.3 Distribution Coefficient

Samples of the toluene/n-butyric acid/water system were brought to equilibrium for the interfacial tension measurements and the distribution coefficient measurements as follows. Equal volumes of toluene and water, which had been redistilled according to the procedure described, were measured into a 250 ml conical flask via an appropriate pipette, and a measured volume of acid added. The mixture was shaken by hand for a few minutes and then placed on a shaking machine for 24 hours to ensure that equilibrium was reached. The mixtures were kept at room temperature, $18^{o}C \pm 1^{o}C$. Acid concentrations were measured by titration by the method described in section 6.4.3. The results are plotted in figure 7.21. The distribution curve can be divided into two sections. Below concentrations of 2.00%^{w}/w in toluene and 1.30%^{w}/w in water, m is a function of acid concentration. Above these values, m is a constant and $y = mx$, with $m = 4.00$.

7.2.1.4 Concentrations

The analysis of mass transfer in the column, involving the integration of equation (92), is considerably simplified when m is independent of concentration. Therefore concentrations below the straight line portion of the graph were avoided. In practice, this meant that aqueous inlet concentrations when water was the extracting solvent had a minimum concentration of 1.30%^{w}/w, and organic inlet concentrations when toluene was the extract were not less than 2.00%^{w}/w.

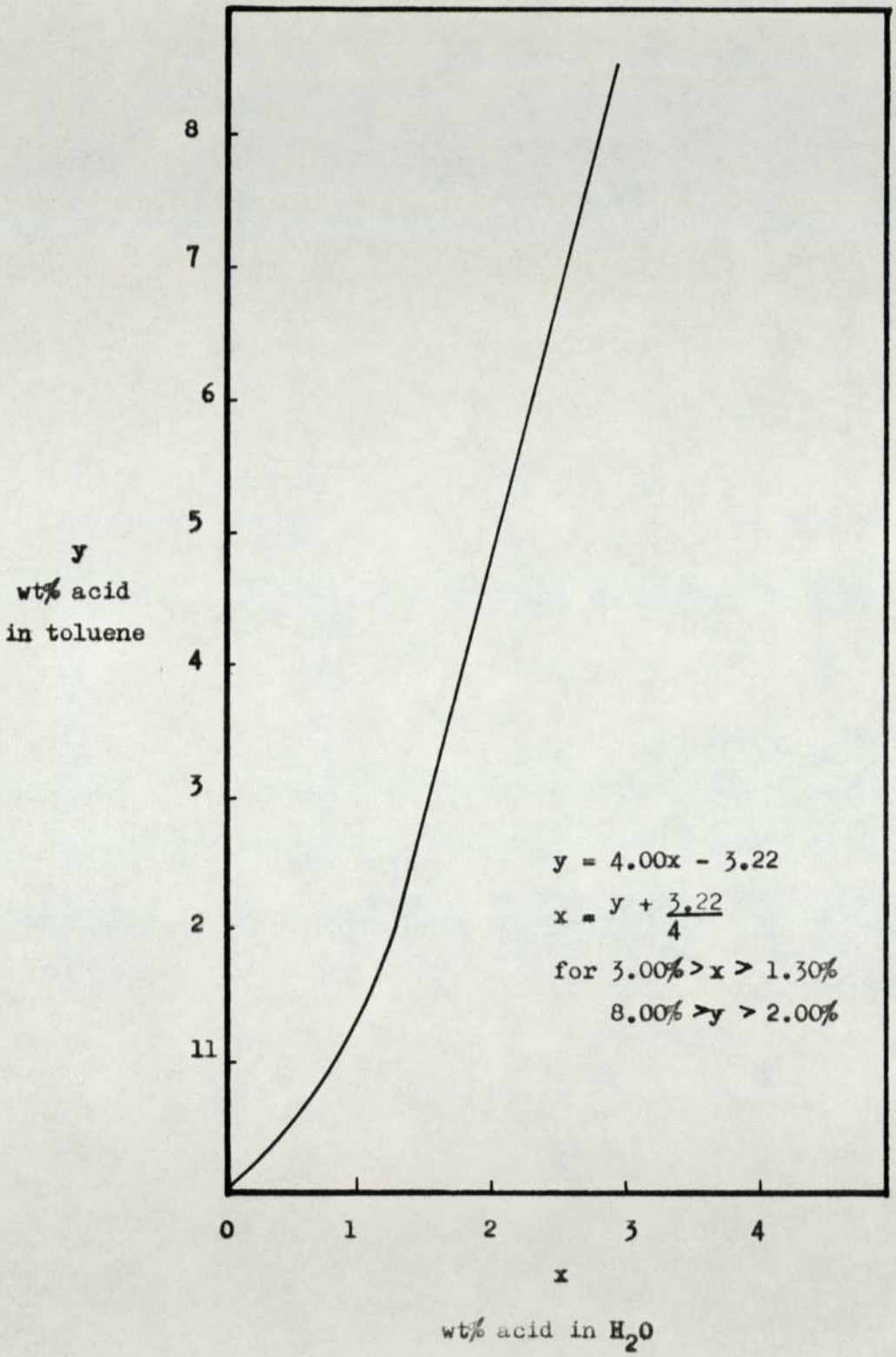

Figure 7.21 Distribution diagram at 18°C.

System: toluene/n-butyric acid/distilled water.

Linear regression on the linear part of the graph gave the equations,

$$y = 4.00\,x - 3.22 \quad \text{and} \quad x = \frac{y + 3.22}{4.00} \qquad 138$$

where y is the weight fraction of solute in toluene, and x in water. The correlation coefficient was 0.999. For the purposes of experimentation, inlet concentration differences between extract and raffinate were calculated from

$$\Delta C = C_{RI} - \frac{C_{EI}}{m} \qquad 139$$

where C_R and C_E refer to the raffinate and extract concentrations, and I denotes inlet values. A subsidiary table was prepared for convenience.

Table 7.1 Experimental Inlet Concentrations

Run Number	Mass transfer Direction R E	ΔC $\%^{w}/_{w}$	x_I $\%^{w}/_{w}$	y_I $\%^{w}/_{w}$
1/1,1/2,1/3	T → W	1	1.30	3.00
1/4,1/5,1/6	T → W	2	1.30	4.00
1/7,1/8,1/9	T → W	3	1.30	5.00
2/1,2/2,2/3	W → T	1	2.30	2.00
2/4,2/5,2/6	W → T	2	3.30	2.00
2/7,2/8,2/9	W → T	3	4.30	2.00

7.2.1.5 Extraction Factor and Flowrates

The extraction factor (151) is

$$\varepsilon = \frac{mG_E}{G_R} \qquad 140$$

Variations of ε directly affect the amount of mass transfer taking place. ε is represented on an equilibrium diagram as the ratio of the slope of the equilibrium line to that of the operating line. Therefore values of ε were specified in the experimental design. Consequently, values of G_E or G_R are related through ε via equation (140). For any run, the flowrate of the continuous phase G_C was fixed by the design. For the first set of experiments, transfer was from dispersed to continuous phase, so that $G_C = G_E$, and values of G_d ($= G_R$) were obtained from equation (140). Similarly, for the second set, $G_C = G_R$ and values of G_d ($= G_E$) were calculated. As the distribution coefficient is also defined in terms of extract and raffinate,

$$m = \frac{C_E^*}{C_R^*} \qquad 141$$

then m had a value of 0.25 for the first set (T → W) and 4.00 for the second (W → T).

A subsidiary table was prepared for the flowrates:

Table 7.2 Flowrates for Mass Transfer Experiments

Run Number	G_C kg/m^{2}s	G_D kg/m^{2}s	Run Number	G_C kg/m^{2}s	G_D kg/m^{2}s
1/1	0.50	0.125	2/1	0.50	0.125
2	1.50	0.250	2	1.50	0.502
3	1.00	0.125	3	1.00	0.500
4	1.00	0.250	4	1.00	0.250
5	0.50	0.083	5	0.50	0.182
6	1.50	0.187	6	1.50	0.750
7	1.50	0.375	7	1.50	0.375
8	1.00	0.133	8	1.00	0.375
9	0.50	0.062	9	0.50	0.250

7.2.2 Cleaning Procedure

This was identical to that used in the non-mass-transfer runs, as described in section 7.1.1.

7.2.3 Preparation of Fluid Systems

The toluene dispersed phase was prepared in the same manner as described in section 7.1.2, as was the distilled water. Solutions were made up to the required strength by the addition of G.P.R. grade n-butyric acid. Suitable precautions were taken against spillage of concentrated acid. Protective gloves and clothing were worn.

For the runs in which transfer was from toluene to water, solute concentrations were high in the toluene and low in the water before the run and vice-versa at the end. Solute levels were restored by simply adding the required amount of concentrated acid to the toluene phase in storage. About half of the used water phase was utilised for flushing out the column after a run. The washings were discarded. Fresh distilled water was then added to the water to obtain the correct concentration of 1.30%$^{w}/_{w}$.

When transfer was from water to toluene, residual concentrations in the toluene phase were high, and low in the water phase. Consequently, it was convenient to transfer the solute back from the toluene to fresh distilled water using the column. By careful control of flowrates, and in some cases multiple extraction of the toluene, it was possible to reduce the solute level in the toluene and increase it in the water to return the organic phase concentration to below the desired level for the next run. Make-up concentrated acid was then used to obtain the required solute level. The aqueous phase concentration was similarly adjusted by the addition of either solute or fresh distilled water.

7.2.4 Drop Sizes and Hold-up

An identical procedure to that described for non-mass-transfer runs was followed. Steady state operation was deemed to have been achieved when successive samples taken at five minute intervals from the continuous phase outlet sample port gave consistent solute concentrations. The results are tabulated in Appendix 9 .

7.2.5 Solute Concentrations

At steady state 10 ml samples of the entry and exit streams were removed via the sampling valves. Duplicate samples were taken. In all cases the duplicates were found to have the same concentration as the originals. The analytical method has been described in section 6.4.3 and a table of results is given in Appendix 10.

It was intended to measure the continuous phase concentration profile in the column using the conductivity probes designed for this purpose. However, although batch tests in a one litre beaker demonstrated the method to be feasible even when two phases were present, difficulty was encountered when the technique was applied to the column. At impeller speeds below about 200 r.p.m., the technique worked well. Unfortunately at higher agitation intensities, large discrepancies occurred, and indicated concentrations were very low. After careful investigation it was found that a large number of small droplets, probably about 10 microns diameter and just visible to the naked eye were present in the column. These were not apparent in the beaker tests, and the failure of the conductivity probes to record the right values was attributed to these very small droplets.

7.2.6 Phase Inversion

Phase inversion occurred during several runs. These are marked with an asterisk in the table in Appendix 10. The flowrates and impeller speeds chosen in the experimental design were well below those expected to give rise to inversion, based on the inversion curves obtained for the non-mass-transfer results.

8. Discussion of Results

8.1 Flooding

At the flooding point operation became impracticable because of entrainment of dispersed phase in the continuous phase outlet and vice-versa. At continuous phase flowrates well above that required for flooding, the column ceases to operate because all the drops are rejected. Flooding occurred at impeller speeds below 200 r.p.m. and above 700 r.p.m., corresponding to Reynold's numbers $Re_I = \frac{DN^2 \rho c}{\mu c}$ of 0.858×10^4 and 3.01×10^4 respectively. These were outside the normal operating range of the column, between 250 and 500 r.p.m. ($Re_I = 1.075 \times 10^4$ and 2.15×10^4).

At the lower speed, flooding is caused by relatively large drops of the order of 1 to 5 mm diameter being swept downwards from the distributor by the high flowrate of the continuous phase. At the higher impeller speed, flooding was caused by droplets being broken down into small drops of the order of 0.1 mm diameter. The terminal velocities of these drops were smaller than even the relatively low continuous phase flowrates of about 0.1 kg/m^2s, causing them to be swept out with the continuous phase.

This is contrary to the flooding data recorded by other workers (16), where flooding was found to occur over a wide range of impeller speeds. Since both flooding and phase inversion are loading points, there are visual similarities between the onset of each. It is possible that the two were confused in the previous study. Different fluid systems and

varying column geometry were used in (16) so that a direct comparison of flowrates is not meaningful.

8.2 Phase Inversion

Phase inversion in single stirred tanks has been discussed in section 4.6. No previous work was found describing inversion in liquid-liquid extraction columns. Compartments or groups of compartments were observed to invert individually or in small groups of two or three. For any particular rotor speed, inversion first appeared in one or two specific compartments irrespective of flowrate. The results are given below.

Table 8.1 Compartments in which inversion first appeared

N(r.p.m.)	Compartment Number
250	12,13,14
300	12,13
350	10,11,12
500	3,4,5,6
700	1
	[Bottom of Column] [Top of Column]

Total number of compartments was 16.

No matter in which compartment the inversion began, it always proceeded sequentially through the column. A 'slug' of inverted phase, usually comprising two or at most three compartments, was observed to

make its way up the column occupying successive compartments. The rate of advance of the 'slug' was about one compartment every 10 - 20 s. At low impeller speeds the rate was higher than at high impeller speeds. When the slug had left a compartment, the phases reverted. This is best illustrated by the cine film which has been deposited in the Departmental Film Library. A description is given in Appendix 5 . Selected stills from this film are shown as figure 7.3.

Inversion is also cyclic. As soon as the inverted 'slug' had left the compartment in which it was first generated, the dispersed phase hold-up began to increase again up to the inversion point, and a new 'slug' was formed. Mean compartment hold-up values have been measured in the column at inversion and also immediately after the slug had left the compartment. The results are given in Appendix 4, and plotted graphically in figure 7.1 as a function of impeller speed. Hold-up at phase inversion is independent of flowrates. Valid comparisons may therefore be made with stirred tanks, operated batchwise. The results are in very good agreement with those of Sawistowski (100) in batch vessels and with the value of 0.75 given by Ostwald (103) for spherical drops in any system. Phase inversion hold-up would be expected to be dependent on system properties, particularly the interfacial tension, as this governs interdroplet coalescence to a large extent. Under mass transfer conditions inversion occurred at lower flowrates and impeller speeds irrespective of the direction of transfer. For the toluene/n-butyric acid/water system, the

interfacial tension was significantly lower than for simply toluene/water.

For any particular set of operating conditions there was a hold-up profile along the column. Normally, hold-up values were higher at the top of the column than at the bottom. This trend was maintained throughout the whole range of flowrates and impeller speeds investigated for non-mass-transfer runs, as shown in figures 7.14 to 7.19. For a fixed impeller speed, the hold-up in each compartment increases as the flowrate of either phase is increased. When the hold-up value in any compartment reaches that necessary for inversion, that compartment inverts.

The mechanism resulting in phase inversion in continuous flow columns is believed to be as follows.

In countercurrent operation, there is a continuous input of both dispersed and continuous phase into any given compartments by virtue of their buoyancy. The volumetric hold-up of dispersed phase reaches a steady-state value in each compartment, and this is acheived only when the input rate of each phase is equal to the output. This is particularly important with respect to the dispersed phase, since for any continuous phase flowrate the amount of interstage dispersed phase flow depends on drop sizes. Thus a polydispersion of droplets flows by buoyancy through the opening in the stator ring against the flow of continuous phase. There will be a limit, set by hydrodynamics, to the volume of dispersed phase that can pass through the stator opening, but in general the larger the drop size the greater the throughput.

The self-balancing phenomenon by which larger drop sizes with increased buoyancy are produced due to increased coalescence at higher hold-up will only operate up to a certain hold-up value. Above this value, the droplet coalescence effect becomes very much greater than the break-up effect, almost all of the dispersed phase droplets coalesce, and phase inversion occurs.

There is a region of very high shear in the vicinity of the agitator within each compartment, where the break-up of drops takes place. The continual break-up of drops in this high energy area is counterbalanced in a normal dispersion by coalescence in the lower energy recirculation region. At high overall hold-up in the compartment, the hold-up in the agitator discharge region is higher than the overall value because large drops from the previous compartment are entering this region. It is here that the hold-up first reaches the inversion value. When inversion occurs, the agitator discharge region is no longer able to keep the 'slug' of coalesced dispersed phase and it passes on to the next compartment through the stator gap. The phases are then observed to revert to the normal mode, and the process begins again.

At low agitator speeds of 250 to 350 r.p.m., the energy in the discharge region was not sufficient to cause inversion until the hold-up reached a value of between 0.68 and 71 as shown by figure 7.1. This value was first reached towards the top of the column and therefore inversion occurred in compartments 10 to 13, as shown in table 8.1.

(The escape of droplets from the last compartment caused an 'end effect', by which hold-up values in compartments 15 and 16 were lower than would be expected, so that inversion did not occur at the very top of the column).

At the higher impeller speeds, hold-up occurred at about 0.55. This value was reached at the lower end of the column first, because the dispersed phase entered at the bottom. Therefore inversion occurred here first. Again, this is shown in table 8.1.

As a result of observations made in this study, Al Hemiri (21) and Jillood (158) have generated phase inversion in an R.D.C. when they operated the column at flowrates and impeller speeds outside the normal range. It was found that inversion occurred before flooding over a narrow range of flowrates. In contrast with the compartmental cyclic inversion of the Oldshue-Rushton column - in an R.D.C., the column inverts first at the centre. The inversion spreads immediately to the whole column, which remains inverted as long as the operating conditions are maintained. This is conducive with the hold-up profile in an R.D.C. observed by Rod (140), which had a maximum in the central region of the column.

In the R.D.C. energy levels are much lower, of the order of one eightieth of those in the Oldshue-Rushton column for the same rotor speed. Consequently drops are generally much larger, and cannot be held in the immediate agitator discharge region of the disc. Therefore in the R.D.C. inversion cannot occur on a cyclic basis, and the spread

through the column is rapid.

In conclusion, phase inversion is a pseudo-steady-state condition in the Oldshue-Rushton column in which continuous operation is quite feasible, and no cross-contamination of phases occurs. This is in contrast to flooding, when operation of the column is not possible. A characteristic feature of operation under inverted conditions is that the process is cyclic. Indeed, because of the intense mixing of the phases during inversion, it is possible that better mass transfer may prevail under these conditions.

8.3 Drop Sizes and Hold-up

8.3.1 Drop Size Distribution

Drop size distributions were measured in six compartments of the column for varying rotor speeds and flowrates. Figure 7.11 is typical of the distributions obtained, which were too numerous to include. All the distributions were similar in shape for both mass transfer and non-transfer conditions.

There has been considerable argument over the shape of drop size distributions in agitated systems, as discussed in section 4.5. Some investigations reported normal and some log-normal distributions. For mass transfer studies the use of the Sauter mean diameter is preferred, since the transfer across the interface is an area-dependent process. Conversely, for reaction studies, the volume mean is more applicable.

In this study Sauter mean diameters were found to be consistently

log-normally distributed, and volume mean diameters of the same dispersions normally distributed. This is consistent with previous reports.

8.3.2 Mean Drop Size and Hold-up

Sauter mean drop size, subsequently termed 'drop size', was found to vary with column height, as shown in figures 7.5 to 7.10. At low rotor speeds the variation was greater than at the higher speeds. Since there is a distribution of residence times for drops in each compartment, only a proportion of the drops will spend a sufficient time in the discharge region of the impeller to cause break-up. Levich (87) has shown that there is a finite time required for a drop to break-up. Calculations show that for the conditions in the Oldshue-Rushton column for the system toluene/water, this time of break-up is of the order of 10^{-2}s. At higher rotor speeds the residence time of the drops in the discharge region is smaller than at lower speeds, but the number of drops passing through the region is much larger and the energy available to rupture drops is also greater. Conversely, the hold-up of drops is larger at higher rotor speeds, and hold-up increases with column height. The effect of a higher hold-up is to increase drop-drop collisions and drop-drop coalescence.

Additionally, flowrates clearly affect the magnitudes of both drop size and hold-up. Higher flowrates lead to larger drop sizes. Since each compartment might be considered as an individual stirred tank, the equation of Thornton and Bouyatiotis (28), described in section 4.3.

might be applicable to quantify the effect of hold-up on drop size. However, in figures 8.1 to 8.5 drop size is plotted against hold-up for fixed impeller speeds. Clearly if Thornton's equation applied,

$$\text{i.e.} \quad d_{32} = d_{32}^{o} + mx_d$$

straight lines of slope m would be expected. Furthermore, since m depended solely on the physical properties of the system, the lines should be parallel. Thornton's equation was used by Bibaud and Treybal (18) to obtain drop sizes in an Oldshue-Rushton column. Figures 8.1 to 8.5 clearly demonstrate that this approach is only approximate, and that in fact straight lines of constant slope are not obtained. For very high rotor speeds the equation would be feasible for design purposes if hold-up values could be predicted with sufficient accuracy. No correlations for hold-up or drop sizes in an Oldshue-Rushton column are available in the literature.

As would be expected there are many more variables which affect drop sizes in the column than hold-up, column height and agitator speed. These are listed in table 8.2, in which there are 15 independent variables in addition to the drop size which is considered as the dependent variable. The coalescence factor γ_1 and the break-up factor γ_2 represent the proportion of the total drops present which coalesce and break-up per unit time. The drop size is expressed as a function of column height, impeller speed and flowrates. The inclusion of impeller diameter and fluid physical properties was

Table 8.2 Variables Considered in the Dimensional Analysis

Quantity	Symbol		Dimensional Formula
Drop Size	d_{32}		L
Impeller Tip Speed	V_I		$L\ T^{-1}$
Column Height	H		L
*Mean Viscosity	μ_m		$M\ L^{-1}T^{-1}$
Mean Density	ρ_m		$M\ L^{-3}$
Drop Characteristic Velocity	G_K		$L\ T^{-1}$
*Interfacial Tension	σ		$M\ T^{-2}$
*Compartment Height	H	Combined as a geometric factor Fg, dimensionless	-
*Column Diameter	D_T		
*Baffle Width	B		
*Blade height	b_h		
*Blade width	b_w		
*Impeller diameter	D		L
*Coalescence factor	γ_1		-
*Break-up factor	γ_2		-
*Buoyancy	$\Delta\rho/\rho_c$		-

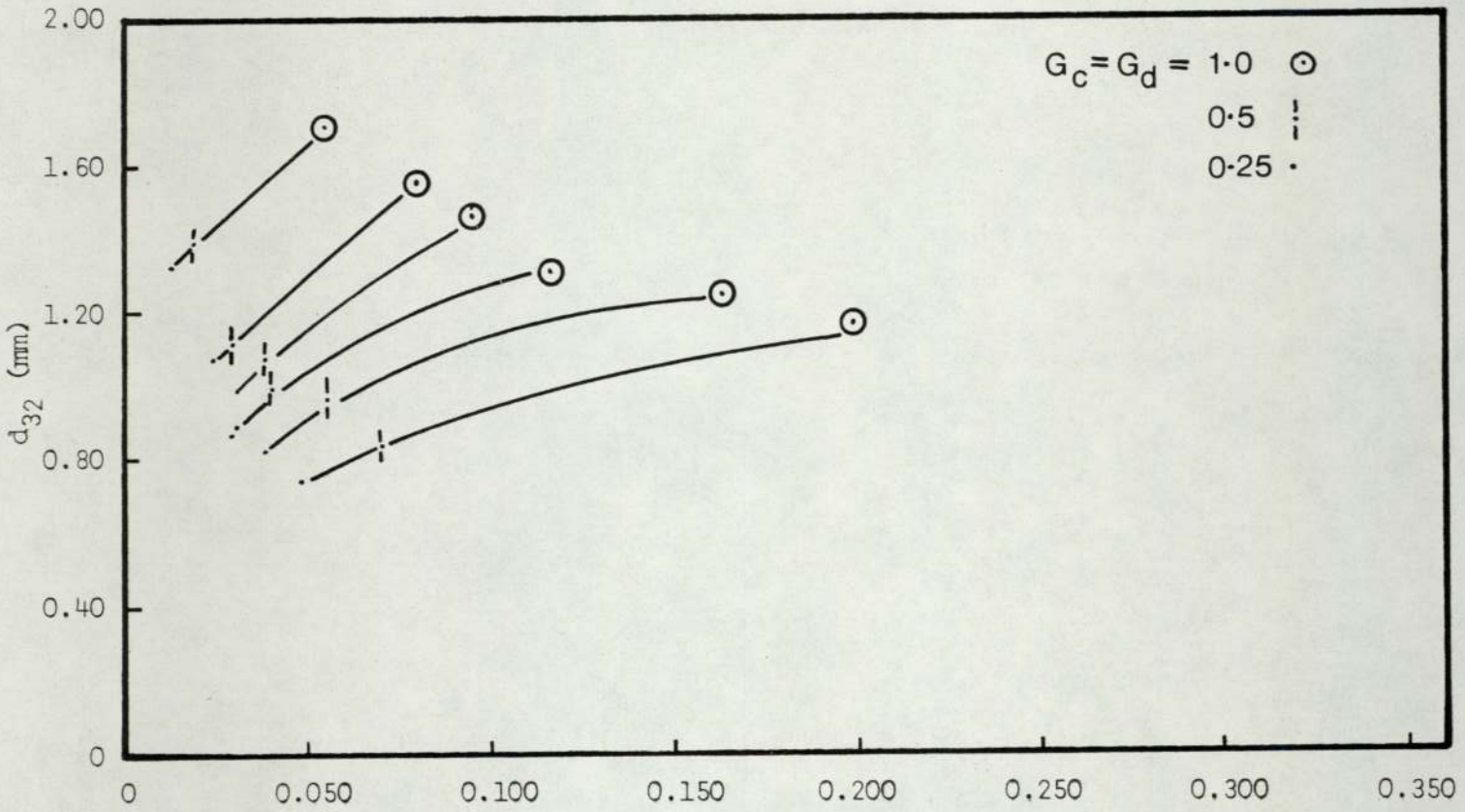

Figure 8.1 Variation of drop size with hold-up N = 250

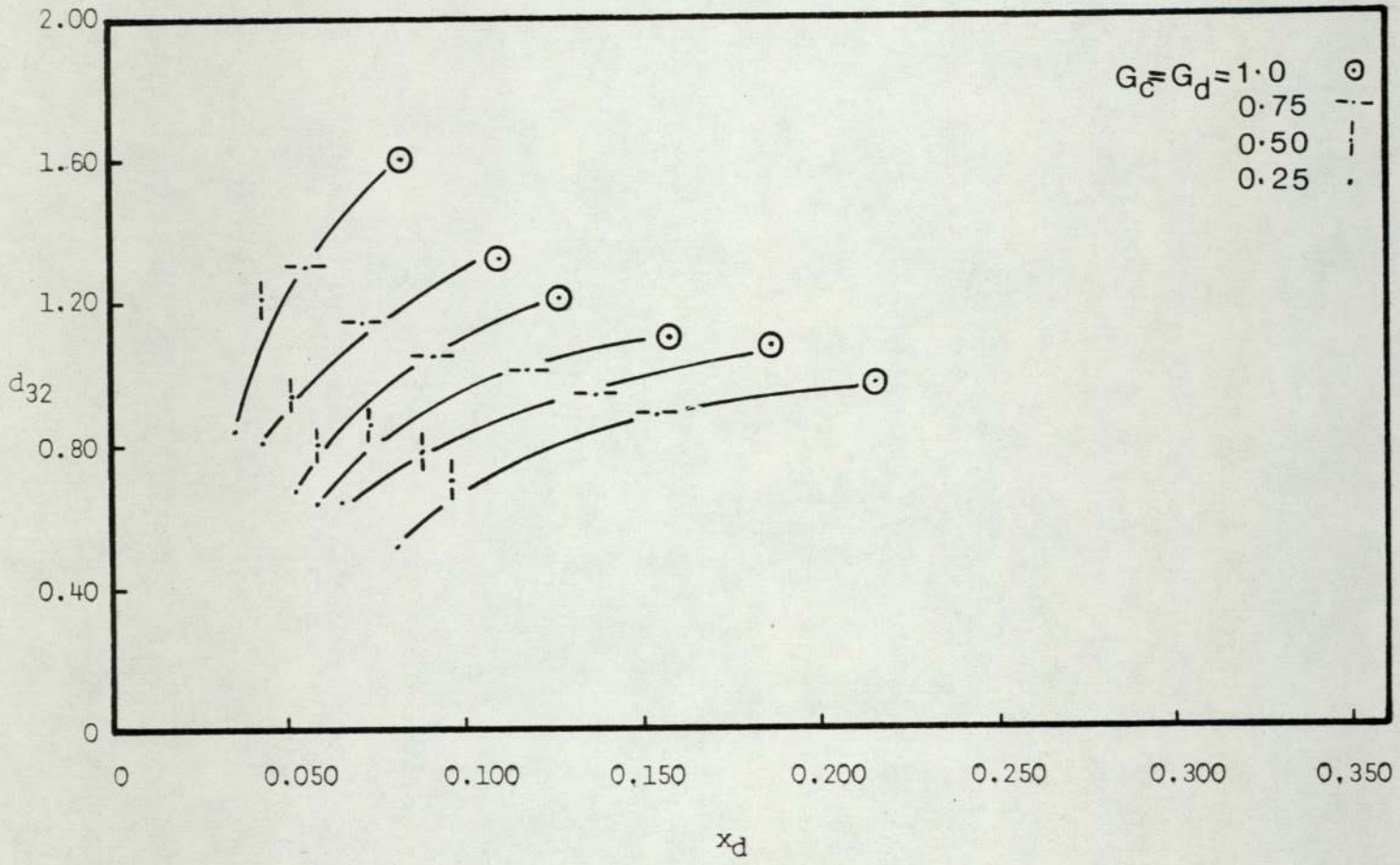

Figure 8.2 Variation of drop size with hold-up N = 300

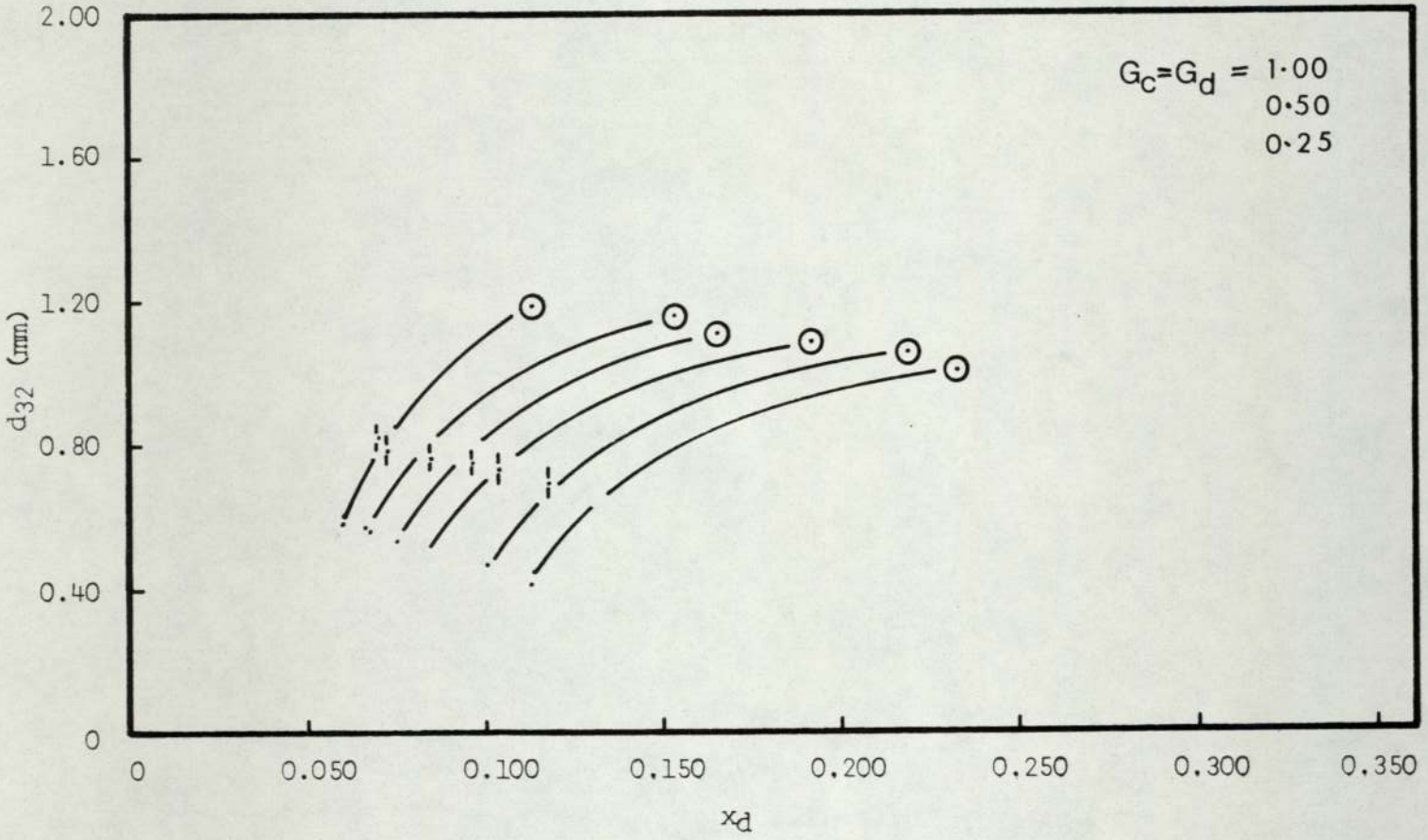

Figure 8.3 Variation of drop size with hold-up N = 350

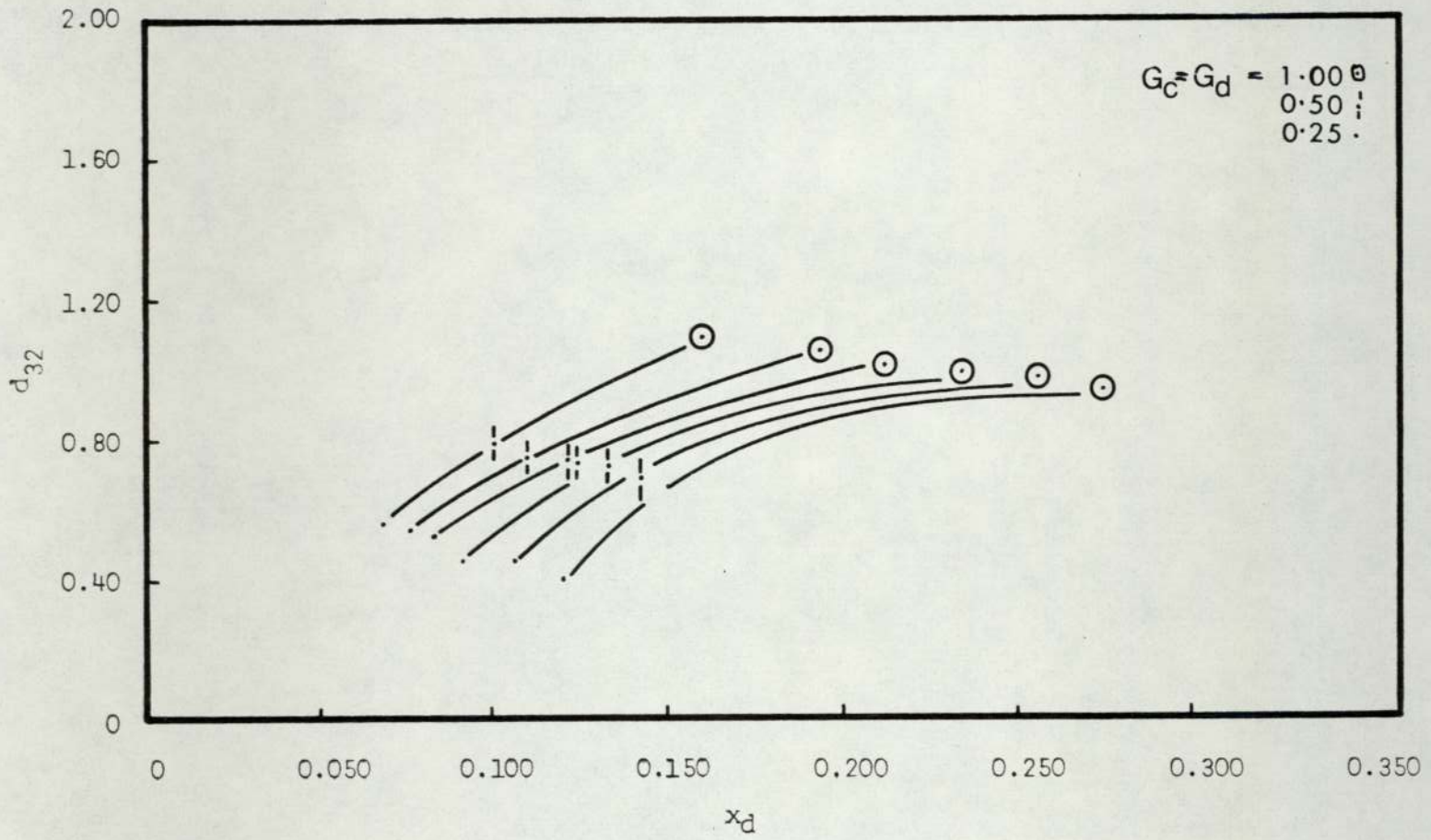

Figure 8.4 Variation of Drop size with hold-up N = 400

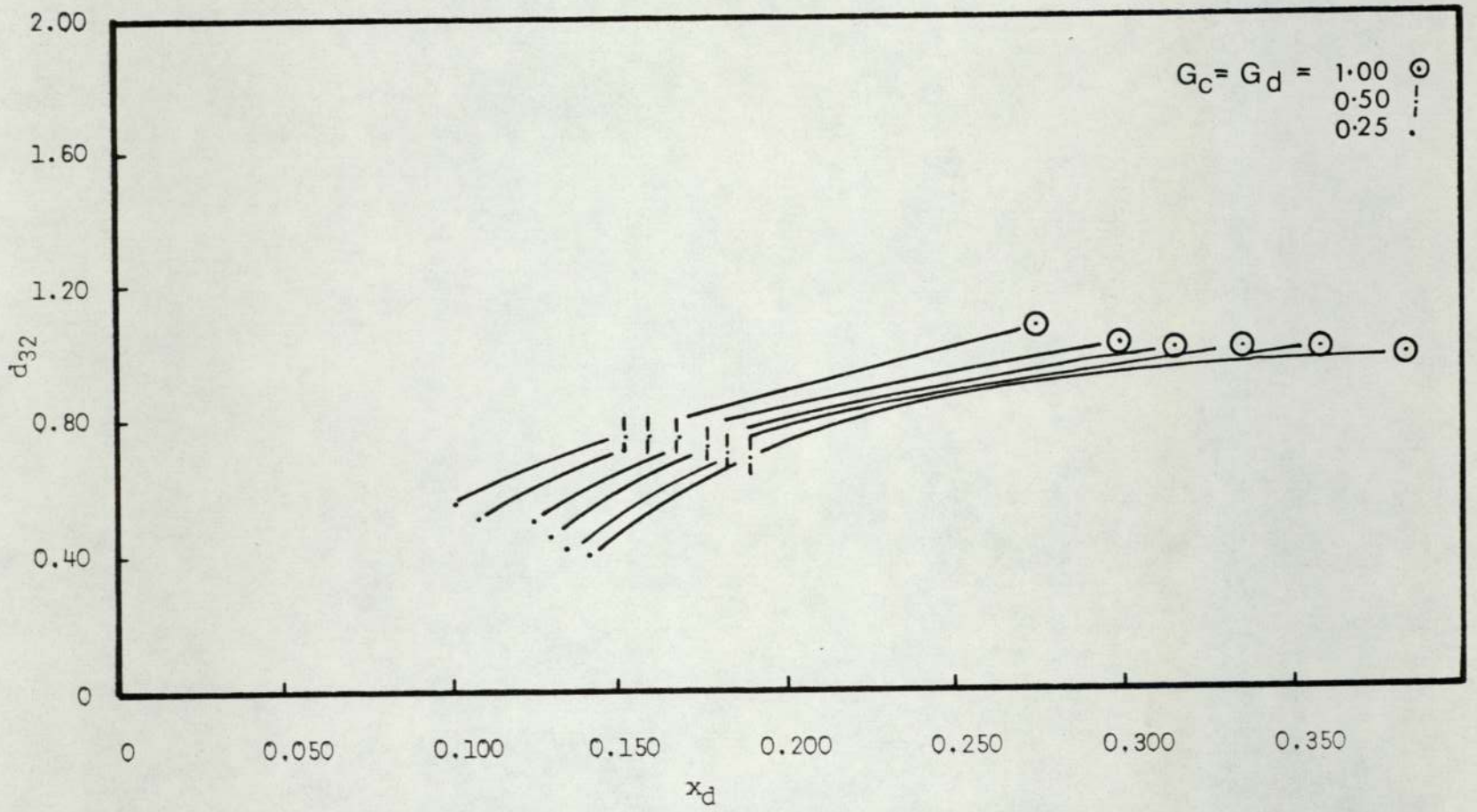

Figure 8.5 Variation of drop size with hold-up N = 500

necessary to obtain suitable dimensionless groups.

Column height is expressed as a fraction of the total height, as opposed to H/D which would be strictly required by a formal analysis.

The flowrates are contrived as a single quantity V_K, the common expression of characteristic velocity for two phase flow. A re-arrangement of equation 9 leads to

$$V_K = \frac{V_d(1 - x_d)}{x_d} + V_C$$

For a countercurrent system V_c is a negative quantity if V_d is regarded as positive.

Mean viscosity can be regarded as constant because the two correlations of Vermeulen (32) and Rodger (80) give only a weak dependence of μ_m on x_d.

Fluid densities are expressed by ρ_m

$$\rho_m = (1 - x_d)\rho_c + x_d\rho_d \qquad 142$$

which has been shown in this for m to be a realistic measure of mean density (159).

Impeller speed is expressed as a tip velocity V_I,

$$V_I = \pi N D \qquad 143$$

In the experiments many of the variables were kept constant. These are marked with an asterisk in table 8.2. The factors γ_1 and γ_2 cannot be evaluated. For a single system it would be reasonable to assume they would be dependent on agitator speed and hold-up. Since

these two variables appear in the analysis, it is permissible to exclude γ_1 and γ_2 from the final equation in this case. A prior computer cross-correlation matrix gave a correlation between the Froude number V_I^2/D_g and the Weber number $V_I^2 D/\sigma$ of 0.9998. The Froude number was therefore omitted from the analysis since it represents the ratio of kinetic to surface forces. The Weber number has been shown in chapter 4 to be a significant parameter in two phase systems.

Dimensional analysis by the pi-theorem method led to

$$\frac{d_{32}}{D} = C\left(\frac{H}{H_T}\right)^{p1}\left(\frac{V_K}{V_I}\right)^{p2}\left(\frac{V_I^2 D\rho_m}{\sigma}\right)^{p3} \qquad 144$$

where $\frac{V_K}{V_I}$ is a dimensionless flow term,

and $\frac{V_I^2 D \rho_m}{\sigma}$ is the Weber number.

The exponents C, p1, p2 and p3 were evaluated from the experimental results using the I.C.L. "statspackage" yielding the equation

$$\frac{d_{32}}{D} = 2.44\left(\frac{H}{H_T}\right)^{-0.06}\left(\frac{V_I^2 D\rho_m}{\sigma}\right)^{-0.63}\left(\frac{V_K}{V_I}\right)^{0.18} \qquad 145$$

The data gave an error sum of squares of 0.383 and a residual error of 0.095, leading to a correlation coefficient of 0.900.

In equation (145),

$$d_{32} \sim D^{-1.07}$$
$$\sim N^{-1.42}$$
$$\sim We^{-0.63}$$

The exponents of N and D are within the range of experimental correlations and theoretical equations listed in table 4.1. Drop sizes in the contactor cannot be determined from Thornton's correlation (28) as previously discussed. As discussed in chapter 4 Kolmogorov's law of isotropic turbulence gives a dependence of d_{32} on $N^{-1.2}$ or $N^{-1.0}$ and $D^{-2.0}$ or $D^{-1.5}$, and therefore does not apply specifically to the column. However, the variation of d_{32} with $We^{-0.63}$ in this work is in excellent agreement with all previous studies, where the exponent of the Weber number has consistently been given as -0.6.

The evaluation of drop size data and hold-up values when mass transfer took place is more difficult. In most runs, mean drop size decreased up the column as it did under non-mass-transfer conditions. For mass transfer in either direction drop sizes were smaller than for non-mass-transfer by up to a factor of two. This is partially, but not totally, due to the lower interfacial tension when the solute was present. If the drop size is proportional to $We^{-0.6}$, the lowering of σ from 34.2 dynes/cm to 15.4 dynes/cm would lead to reduced drop

sizes under mass transfer conditions by a factor of about 1.6. For transfer from the continuous to the dispersed phase this is the case. When solute passed from dispersed to continuous, drop sizes are smaller by a factor of about 2. This is contrary to previous reports, where the effect of transfer from dispersed to continuous phase is an enlargement of drop sizes over those in the opposite direction.

Classic coalescence models apply under carefully controlled conditions, and mass transfer from dispersed phase to continuous usually produces an increased possibility of interdroplet coalescence. The highly turbulent environment of the Oldshue-Rushton column is a separate case, however. There is a polydispersion of drops, variation in concentrations around drops, and backmixing effects. Additionally, very low concentrations were used in this work to reduce interfacial effects (160). The effect of solute concentrations may therefore have been more to lower the interfacial tension than to create increased coalescence.

Hold-up values for mass transfer are also anomalous. In some runs, hold-up decreased with column height, whereas in others it increased. There would appear to be no consistency in this effect with respect to the variables studied, except that there were more cases where hold-up increased with column height when transfer was from dispersed to continuous. Duplication of about 25% of the runs confirmed the results. Notwithstanding these inconsistencies, the drop sizes were of the same order of magnitude as those for non-mass-transfer runs, and it is

concluded that, for transfer in the direction continuous to dispersed phase at least, drop sizes may be estimated from the regression equation for the purpose of evaluating interfacial areas.

8.4 Mass Transfer

The analysis of the rate of mass transfer in the column from the measured terminal concentrations involved the following steps for each set of experimental conditions.

1. The measured number of transfer units was calculated assuming

(a) Equilibrium concentrations were described by $y = mx^{*} + y_o$, where y and x denote weight fractions of solute in the toluene and water phases respectively and m was the distribution coefficient. Since concentrations were chosen so that only the straight line part of the distribution diagram was used, m was constant (see figure 7.21). The asterisk denotes equilibrium conditions, and y_o is the intercept of the equilibrium line on the y-axis.

(b) The column could be described as a countercurrent differential contactor for the purposes of mass transfer.

(c) Fluids pass through the column by 'plug' flow. The derivation of $(N.T.U.)_m$ is given in Appendix 11.

2. The mean interfacial area for each compartment was computed from the mean drop size and the hold-up. The mean interfacial area a was then calculated for the whole column.

3. The apparent mass transfer coefficient K_e' or K_R', for the continuous phase was calculated. For transfer in the direction continuous

to dispersed, K_R' was found, and K_E' for dispersed to continuous phase.

4. The amount of backmixing in both phases was evaluated to account for the deviation from plug flow using the correlation of Bibaud and Treybal (18) together with the analytical solution of the diffusion model of Hartland and Mecklenburgh (127). The correlation of Inham (120) gave very similar results. A computer program was written for these calculations, and is given as Appendix 12.

5. The $(H.T.U.)_t$ was found, and hence the $(N.T.U.)_t$.

6. The 'true' area-free overall mass transfer coefficients were found from

$$K_R = \frac{(N.T.U.)_{tR} G_R}{H_T \cdot \rho_R \cdot a} \quad \text{and} \quad K_E = \frac{(N.T.U.)_{tE} G_E}{H_T \cdot \rho_E \cdot a} \qquad 146$$

The number of transfer units is comparable to values given for a similar column, but using difference fluid systems, by Bibaud and Treybal (18) and Oldshue and Rushton.

The transfer units measured from terminal concentrations were higher when transfer was from the continuous phase to the dispersed phase. These are shown in table 8.3. However, analysis of mass transfer is more meaningful in terms of area-free mass transfer coefficients, since as discussed earlier, the H.T.U. concept is specific to the conditions prevailing during measurement. Coefficients are also specific to local conditions around the drops such as the degree of turbulence, but are free from the effects of flowrate, terminal column concentration driving forces and interfacial areas.

Table 8.3 Heights of Transfer Units

Values of $(N.T.U.)_m$, $(H.T.U.)_m$ and $(H.T.U.)_t$

Run Number	$(N.T.U.)_m$ -	$(H.T.U.)_m$ (m)	$(H.T.U.)_t$ (m)
1/1	0.77	1.58	0.97
1/2	0.69	1.77	1.05
1/3	0.49	2.49	1.69
1/4	1.15	1.06	0.46
1/5	1.01	1.20	0.40
1/6	1.28	0.95	0.35
1/7	2.04	0.60	0.21
1/8	1.56	0.78	0.46
1/9	1.06	1.15	0.45
2/1	2.60	0.59	0.19
2/2	2.81	0.43	0.24
2/3	3.74	0.33	0.13
2/4	2.02	0.60	0.27
2/5	1.42	0.86	0.36
2/6	3.70	0.33	0.26
2/7	2.10	0.58	0.16
2/8	5.21	0.23	0.17
2/9	4.31	0.28	0.19

Runs 1/1 to 1/9 are with reference to the extract
Runs 2/1 to 2/9 are with reference to the raffinate

Apparent and true mass tranfer coefficients are tabulated in table 8.4. It is significant that true area-free coefficients are not appreciably greater for either direction of transfer. The highest coefficients were obtained for both directions of transfer when the concentration driving forces were highest. However, it cannot be concluded specifically that coefficients vary with driving force. The number of experiments performed was not sufficient to gain a proper insight into the variation of the coefficient, since so many variables affect performance.

The gross variations in hold-up between mass transfer runs did not have any measurable effect on the coefficients. Nor did they appear to vary significantly over the range of drop sizes encountered.

It is concluded therefore that the variables affecting the mass transfer coefficient were not all covered by the experimental variables. Because of this no correlations have been produced for mass transfer.

Mass transfer data and equations are to be found throughout the literature for many different types of equipment. The difficulty encountered in this work in producing a reliable correlation for a single system for one particular design of column suggests that all correlations must be used with caution. Recently, Oldshue (161) has confirmed that there is no reliable data available for the prediction of mass transfer in the Oldshue-Rushton column and that without exception pilot-plant data for specific systems must be obtained. Furthermore, a variable speed agitator is a pre-requisite in column design to obtain the flexibility required to overcome the shortcomings of design data.

Table 8.4 Mass Transfer Coefficients

Values of K'_Ea, K'_Ra, K'_E, K'_R, K_E, K_R

Run Number	K'_Ea (s^{-1}) x 10^{-3}	K'_Ra (s^{-1}) x 10^{-3}	K'_E (m/s) x 10^{-6}	K'_R (m/s) x 10^{-6}	K_E (m/s) x 10^{-6}	K_R (m/s) x 10^{-6}
1/1	0.31		0.88		1.43	
1/2	0.85		0.20		0.34	
1/3	0.40		0.06		0.09	
1/4	0.94		0.24		0.55	
1/5	0.41		0.17		0.51	
1/6	1.57		1.34		3.64	
1/7	2.51		0.72		2.06	
1/8	1.28		2.28		3.87	
1/9	0.43		0.47		1.20	
2/1		1.05		0.53		1.64
2/2		3.45		0.77		1.38
2/3		3.06		0.74		1.88
2/4		1.63		0.44		0.98
2/5		0.30		0.06		0.14
2/6		3.70		1.32		1.67
2/7		2.10		2.87		2.32
2/8		4.20		2.02		2.73
2/9		1.76		0.40		0.65

9. Conclusions

This work is an attempt to develop the parameters for the systematic design of Oldshue-Rushton columns and it has been shown that the correllation of mass transfer coefficients with operating conditions, column geometry and physical properties is extremely difficult.

The main conclusions may be summarised as follows.

1. Phase inversion is a stable mode of operation. At high ratios of dispersed phase to continuous phase 'slugs' of coalesced dispersed phase travel through the column periodically. The height up the column where the 'slugs' first appear is predictable.

2. Flooding in the normally accepted sense only occurs when the agitator Reynold's number is outside the range 0.9×10^4 to 5.0×10^4. In between these extremes, that is within the normal operating range, phase inversion occurs instead.

3. Drop size distributions are log-normal with and without mass transfer, and are highly skewed towards small drop sizes. The shape of the distributions changes little with height up the column.

4. Sauter mean drop sizes under non-mass transfer conditions can best be estimated by equation (145). Some modification is neccessary in the presence of mass transfer.

5. Backmixing accounts for up to half of the installed column height for a six inch diameter Oldshue-Rushton contactor. The number of transfer units is not a good guide to column performance. Mass transfer coefficients are marginally higher when transfer is from the continuous phase to the dispersed phase.

10. Recommendations for further work

1. The onset of phase inversion has been shown to be governed by the number of drops able to pass through the stator-gap against the flow of continuous phase. Studies were initated to measure velocities around this region, for a single phase in a perspex column section. A technique has been developed using intermittent light flashes in a single flat plane to illuminate small perspex particles suspended in the continuous phase. The interval between flashes was varied in a set pattern, enabling both the velocity and direction of each particle to be recorded on a ciné film. Further work should elucidate the flow patterns and scales of turbulence in this region and could lead to the modelling of both the capacity and inversion phenomena in the column.

2. Work is also in hand to investigate further phase inversion in a three compartment column section. The investigation will be concerned with the verification of the inversion results obtained in this work with particular reference to the effect of variations in fluid properties, especially interfacial tension.

3. The Oldshue-Rushton column is eminently suitable for heterogeneous mass transfer with chemical reaction and work has commenced in a four inch diameter unit to study operating variables, column geometry and fluid physical properties.

4. It has been shown in this study that, contrary to claims made in the literature, continuous countercurrent extraction operations in agitated columns are extremely difficult to scale-up with realistic systems undergoing mass transfer. Therefore reliable data are required relating the turbulent drop break-up/coalescence and mass transfer mechanisms in practical columns with those on a smaller scale.

Appendix 1

Stable Drop Size from Kolmogorov's Theory of Homogeneous Isotropic Turbulence

Kolmogorov defined two parameters in order to characterise length and velocity. They are the length scale

$$z_\gamma = \left(\frac{\nu}{\varepsilon}\right)^{1/4} \qquad \text{A1}$$

and the velocity scale

$$v = (\nu\varepsilon)^{1/4} \qquad \text{A2}$$

If isotropic turbulence exists

$$u = (\varepsilon d)^{1/3}$$

for $z_\gamma \ll d \ll L$ and in any volume of characteristic dimension r ($\ll L$) all velocity correlations are functions of r and z (or ε and ν) only. Thus the mean square relative velocity u(r) between any two points a distance r apart is a function of v and z for all regions where the theory holds. Also, if $L \gg r \gg z$ then $u^2(r)$ is a function of ε only, and not ν.

Shinnar (86) states that for very small values of r and when $L \gg r \gg z$, the form of this function can be obtained from dimensional analysis.

$$\overline{u^2(r)} = C_1 \varepsilon^{2/3} r^{2/3} \quad \text{for } L \gg r \gg z \; . \qquad \text{A3}$$

When $L \gg z \gg r$, the relationship becomes

$$\overline{u^2(r)} = C_2 \frac{\varepsilon r^2}{\nu} \qquad \text{for } L \gg z \gg r \qquad \text{A4}$$

where C_1 and C_2 are constants.

Levich (87) has postulated that the difference in "dynamic pressure" between two points in a fluid is

$$\Delta P_d = \frac{k_f \rho_c (\bar{u}_1^2(r) - \bar{u}_2^2(r))}{2} \qquad A5$$

where ΔP_d = difference in dynamic pressure between two points,

k_f = factor

ρ_c = fluid density

$\bar{u}^2$ = mean square velocity

For a drop of diameter d this becomes

$$\Delta P_d = \frac{k_f \rho_c (\bar{u}^2(d))}{2} \qquad A6$$

assuming $\bar{u}_1^2 - \bar{u}_2^2 = \bar{u}^2$ A7

Substituting equation 3 into 6 for $L \gg r \gg z$ we have

$$\Delta P_d = \frac{k_f \rho_c \varepsilon^{2/3} d^{2/3}}{2} \qquad A8$$

Now ΔP_d is the force imparted by the continuous phase on the drop causing break-up, and it will be balanced by the interfacial tension force which tends to hold the drop together, equal to $\frac{2\sigma}{r}$

$$\therefore \quad \frac{2\sigma}{r_{sd}} = \frac{k_f}{2} \rho \varepsilon^{2/3} d_{sd}^{2/3} \qquad A9$$

where sd refers to the stable drop size.

Re-arrangement gives

$$r_{sd} = K_1 \left(\frac{\sigma}{\rho}\right)^{0.6} \left(\frac{1}{\varepsilon}\right)^{0.4} \qquad A10$$

For the case of $L \gg z \gg r$,

$$\frac{2\sigma}{r_{sd}} = \frac{k_f \rho_c \varepsilon r_{sd}^2 \rho_c}{2 \mu} \qquad A11$$

$$\therefore \quad r_{sd} = K_2 \left(\frac{\sigma \mu}{\rho_c^2}\right)^{1/3} \left(\frac{1}{\varepsilon}\right)^{1/3} \qquad A12$$

Appendix 2 (a)

Drop Size Analysis Program

```
10  REM          "DROP SIZE ANALYSIS, D.R .ARNOLD."
20  DIM D(48),N(48),B(48)
25  DIM M(6),S(6),C(6),V(6)
27  FOR C=1,6
30  B(1)=1.49:B(2)=2.04:B(3)=2.59:B(4)=3.14:B(5)=3.7
40  B(6)=4.25:B(7)=4.8:B(8)=5.35:B(9)=5.9:B(10)=6.46
50  B(11)=7.01:B(12)=7.56:B(13)=8.11:B(14)=8.66:B(15)=9.22
60  B(16)=9.77:B(17)=10.32:B(18)=10.87:B(19)=11.42:B(20)=11.98
70  B(21)=12.53:B(22)=13.08:B(23)=13.63:B(24)=14.18:B(25)=14.74
80  B(26)=15.29:B(27)=15.84:B(28)=16.39:B(29)=16.94:B(30)=17.5
90  B(31)=18.05:B(32)=18.6:B(33)=19.15:B(34)=19.7:B(35)=20.26
100  B(36)=20.81:B(37)=21.36:B(38)=21.91:B(39)=22.46:B(40)=23.02
110  B(41)=23.57:B(42)=24.12:B(43)=24.67:B(44)=25.22:B(45)=25.78
120  B(46)=26.33:B(47)=26.88:B(48)=27.43
130  N1=0:N2=0:N3=0:N4=0
140  T=0
150  PRINT "R ? "
160  INPUT R
162  IF C<=3 THEN C1=2*C
163  IF C>=4 THEN C1=2*C+2
170  PRINT "MAG. FACTOR, 0 IF RED., 1 IF STD. COMPARIMENT ";C1;"?"
180  INPUT A
182  IF A=0 THEN 188
186  F=.2435
187  GOTO 190
188  F=.2435/3
190  PRINT "TYPE IN N VALUES "
610  FOR J=1 TO 48 STEP 1
620  INPUT N(J)
625  IF N(J)<0 THEN 990
630  T=N(J)+T
640  D(J)=F*B(J)
660  N1=N1+N(J)*D(J)
680  N2=N2+N(J)*(D(J))↑2
690  N3=N3+N(J)*(D(J))↑3
700  N4=N4+N(J)*(D(J))↑4
725  NEXT J
727  V(C)=48
730  M(1)=N1/T
740  M(2)=SQR(N2/T)
750  M(3)=(N3/T)↑.33333
760  M(4)=N2/N1
770  M(5)=N3/N2
780  M(6)=N4/N3
785  FOR K=1 TO 6 STEP 1
787  S(K)=0
790  FOR J=1 TO V(C) STEP 1
800  S(K)=S(K)+(D(J)-M(K))↑2
810  NEXT J
820  S(K)=S(K)/T
830  NEXT K
840  GOTO 9000
```

```
990  J(C)=J-1
1000  FOR I=J TO 48 STEP 1
1010  N(I)=0
1020  N(J)=N(I)
1030  NEXT I
1040  GOTO 730
9000  PRINT "PRESS SS4 & TYPE ZERO, RELEASE SS4 WHEN PUNCH STOPS"
9001  PRINT "AND TYPE IN RUN NO."
9002  INPUT P6
9005  PRINT "RUN NUMBER",R,"COMPARTMENT",C1
9010  PRINT "MAGNIFICATION FACTOR",F
9020  FOR J=1,J(C)
9030  PRINT D(J),N(J)
9040  NEXT J
9045  DIM P(48,6),W(48,6)
9070  PRINT "TOTAL NUMBER OF DROPLETS IS",T
9080  PRINT "MEAN",TAB(18),"VALUE","STD.  DEV."
9090  PRINT "MLD",M(1),S(1)
9100  PRINT "MSD",M(2),S(2)
9110  PRINT "MVD",M(3),S(3)
9130  PRINT "LMD",M(4),S(4)
9140  PRINT "SMD",M(5),S(5)
9150  PRINT "VMD",M(6),S(6)
9160  PRINT "**************************************"
9161  FOR J=1,48
9162  W(J,C)=N(J)
9164  P(J,C)=D(J)
9165  NEXT J
9180  NEXT C
9182  INPUT P6
9185  PRINT "RUN OUT FROM PUNCH, THEN S.S.4"
9187  INPUT P6
9190  A=0
9200  FOR I=1,48
9210  FOR C=1,6
9220  L1=6500+A
9230  PRINT L1;"DATA  ";P(I,C);",";W(I,C)
9235  A=A+1
9240  NEXT C
9250  NEXT I
9260  PRINT "6999  DATA  ";R
```

Appendix 2 (b)

Graphplotter Subroutine for Drop Size Distributions

```
1500  REM                GRPHPLTTR SBRTN
1505  DIM F(6)
1510  DIM X(7),E(6),D(48,6),N(48,6)
1520  FOR I=1,48
1530  FOR C=1,6
1540  READ D(I,C),N(I,C)
1549  NEXT C
1550  NEXT I
1560  READ R
1570  GOSUB 4000
1595  Y=0
1600  PRINT : PRINT : PRINT : PRINT : PRINT
1610  PRINT TAB(10);"RUN NUMBER ";R,"N. MAX. =";U
1614  PRINT
1615  PRINT TAB(10);"* COMP. 2          + COMP. 4          . COMP. 6"
1620  PRINT TAB(10);"X COMP. 10         0 COMP. 12         # COMP. 14"
1630  PRINT : PRINT : PRINT : PRINT : PRINT
1640  PRINT TAB(30);"N/N.MAX  >> "
1645  IF Y>.5 THEN 2140
1650  PRINT TAB(9);"0.0";TAB(19);"0.2";TAB(29);"0.4";TAB(39);"0.6";
1651  PRINT TAB(49);"0.8";TAB(59);"1.0"
1655  IF Y>.5 THEN 1640
1660  PRINT TAB(10);"+----+----+----+----+----+----+----+----+----+---
1665  IF Y>.5 THEN 1650
1666  GOSUB 1701
1670  FOR J=1,48
1680  GOSUB 6000
1685  Y=0
1690  Q=INT(J+.5)
1699  GOTO 1710
1700  REM                AXIS LABELS 1700-1840
1701  FOR L=1,48
1702  FOR M=1,6
1703  D(L,M)=INT(100*(D(L,M)+.5E-02))/100
1704  NEXT M
1705  NEXT L
1706  RETURN
1710  IF Q=1 THEN 1760
1720  IF Q=12 THEN 1780
1730  IF Q=24 THEN 1800
1740  IF Q=36 THEN 1820
1750  IF Q=48 THEN 1840
1755  GOTO 1850
1760  PRINT D(1,1);
1770  GOTO 1850
1780  PRINT D(12,1);
1790  GOTO 1850
1800  PRINT D(24,1);
1810  GOTO 1850
1820  PRINT D(36,1);
1830  GOTO 1850
1840  PRINT D(48,1);
1850  IF Y>.5 THEN 2120
1855  PRINT TAB(10);"1";
```

```
1860  FOR K=1,6
1865  K=INT(K+.5)
1867  IF X(K)=0 THEN 2089
1868  IF E(K)=0 THEN 2089
1869  X(K)=(X(K)/J)*50+10
1870  IF F(K)=1 THEN 1930
1880  IF F(K)=2 THEN 1950
1890  IF F(K)=3 THEN 2010
1900  IF F(K)=4 THEN 2030
1910  IF F(K)=5 THEN 2050
1920  IF F(K)=6 THEN 2070
1930  PRINT TAB(X(K));"*";
1935  IF E(K)>1 THEN 2085
1940  GOTO 2089
1950  PRINT TAB(X(K));"+";
1955  IF E(K)>1 THEN 2085
1960  GOTO 2089
2010  PRINT TAB(X(K));".";
2015  IF E(K)>1 THEN 2085
2020  GOTO 2089
2030  PRINT TAB(X(K));"X";
2035  IF E(K)>1 THEN 2085
2040  GOTO 2089
2050  PRINT TAB(X(K));"O";
2055  IF E(K)>1 THEN 2085
2060  GOTO 2089
2070  PRINT TAB(X(K));"#";
2080  IF E(K)<=1 THEN 2089
2085  GOTO 2089
2089  NEXT K
2090  PRINT TAB(X(K))
2100  Y=1
2120  NEXT J
2130  GOTO 1660
2135  GOTO 7000
2140  GOTO 7000
3000  REM              MLTPNT SBRTN
3020  G=1
3030  FOR I=1,6
3040  IF X(I)=X(I+1) THEN 3080
3045  IF G=1 THEN 3050
3047  E(I)=0
3049  GOTO 3060
3050  E(I)=1
3060  G=1
3070  GOTO 3500
3080  IF G=1 THEN 3120
3090  G=G+1
3100  E(H)=G
3110  GOTO 3500
3120  H=I
3130  G=G+1
3140  E(H)=G
```

```
3500  NEXT I
3510  RETURN
4000  REM           N MAG SBRTN
4010  N=0
4020  FOR C=1,6
4030  FOR J=1,48
4040  IF N(J,C)>=N THEN 4060
4050  GOTO 4070
4060  N=N(J,C)
4070  NEXT J
4080  NEXT C
4090  U=N
4100  RETURN
6000  REM           MAG. SBRTN
6010  DIM X(6)
6020  K=6
6030  N=0
6040  FOR I=1,6
6050  N(J,I)=INT(N(J,I)+.5)
6055  IF N(J,I)>=N THEN 6070
6060  GOTO 6090
6070  N=N(J,I)
6080  Z=I
6090  NEXT I
6100  X(K)=N(J,Z)
6105  F(K)=Z
6110  K=K-1
6120  N(J,Z)=0
6130  IF K=0 THEN 6150
6140  GOTO 6030
6150  GOSUB 3000
6160  RETURN
7000  PRINT : PRINT : PRINT : PRINT : PRINT
7010  END
```

RUN NUMBER 4.7 COMPARTMENT 2

MAGNIFICATION FACTOR .811667E-01

.120938	2
.16558	13
.210222	29
.254863	51
.300317	61
.344958	42
.3896	29
.434242	31
.478883	14
.524337	19
.568978	19
.61362	9
.658262	13
.702903	11
.748357	10
.792998	6
.83764	3
.882282	6
.926923	3
.972377	2
1.01702	5
1.06166	1
1.1063	1
1.15094	1
1.1964	0
1.24104	0
1.28568	0
1.33032	1
1.37496	1
1.42042	0
1.46506	1
1.5097	0
1.55434	0
1.59898	1
1.64444	1
1.68908	0
1.73372	0
1.77836	0
1.823	0
1.86846	0
1.9131	0
1.95774	0
2.00238	0
2.04702	0
2.09248	0
2.13712	0
2.18176	0
2.2264	1

TOTAL NUMBER OF DROPLETS IS 387

MEAN	VALUE	STD. DEV.
MLD	.442283	.251893
MSD	.508984	.260575
MVD	.592485	.293276
LMD	.585744	.289882
SMD	.802818	.439814
VMD	1.09256	.697357

****

R

```
   ?
!
RUN NUMBER          4.7          COMPARTMENT          4
MAGNIFICATION FACTOR              .811667E-01
      .120938        3
      .16558        14
      .210222       38
      .254863       44
      .300317       66
      .344958       47
      .3896         37
      .434242       31
      .478883       27
      .524337       29
      .568978       47
      .61362        19
      .658262       13
      .702903       17
      .748357       13
      .792998       21
      .83764         5
      .882282        4
      .926923        3
      .972377        4
     1.01702         6
     1.06166         2
     1.1063          0
     1.15094         1
     1.1964          0
     1.24104         1
     1.28568         0
     1.33032         1
     1.37496         1
     1.42042         0
     1.46506         1
     1.5097          0
     1.55434         1
TOTAL NUMBER OF DROPLETS IS    496
MEAN                VALUE       STD.  DEV.
MLD                  .463606          .224277
MSD                  .515005          .230092
MVD                  .568365          .247538
LMD                  .572104          .249143
SMD                  .692231          .320265
VMD                  .818579          .419889
**************************************
R
```

```
   ?
!
RUN NUMBER          4.7          COMPARTMENT          6
MAGNIFICATION FACTOR              .811667E-01
      .120938        4
      .16558        19
      .210222       46
      .254863       42
      .300317       48
      .344958       39
      .3896         30
      .434242       32
      .478883       24
      .524337       14
      .568978       13
      .61362         8
      .658262       11
      .702903       12
      .748357       11
      .792998        8
      .83764         7
      .882282        4
      .926923        2
      .972377        1
     1.01702         1
     1.06166         2
     1.1063          3
     1.15094         4
     1.1964          1
     1.24104         1
     1.28568         0
     1.33032         1
     1.37496         0
     1.42042         0
     1.46506         0
     1.5097          1
TOTAL NUMBER OF DROPLETS IS    389
MEAN                VALUE       STD.  DEV.
MLD                  .430352          .233905
MSD                  .489811          .241344
MVD                  .552797          .264016
LMD                  .557484          .266222
SMD                  .704095          .360065
VMD                  .845988          .476932
**************************************
R
```

```
   ?
!
RUN NUMBER          4.7          COMPARTMENT        10
MAGNIFICATION FACTOR              .811667E-01
      .120938        0
      .16558         3
      .210222       26
      .254863       35
      .300317       35
      .344958       21
      .3896         27
      .434242       17
      .478883       14
      .524337       13
      .568978       10
      .61362         8
      .658262        8
      .702903        7
      .748357        6
      .792998        7
      .83764         7
      .882282        3
      .926923        4
      .972377        1
     1.01702         1
     1.06166         0
     1.1063          2
     1.15094         0
     1.1964          0
     1.24104         1
     1.28568         0
     1.33032         0
     1.37496         0
     1.42042         0
     1.46506         0
     1.5097          0
     1.55434         1
TOTAL NUMBER OF DROPLETS IS    257
MEAN                VALUE       STD.  DEV.
MLD                  .443976          .221373
MSD                  .496105          .227428
MVD                  .551717          .2462
LMD                  .554355          .247366
SMD                  .682331          .325299
VMD                  .814579          .431687
**************************************
```

RUN NUMBER 4.7 COMPARTMENT 12
MAGNIFICATION FACTOR .811667E-01

.120938	10
.16558	24
.210222	30
.254863	22
.300317	28
.344958	23
.3896	16
.434242	9
.478883	23
.524337	9
.568978	6
.61362	9
.658262	8
.702903	3
.748357	7
.792998	6
.83764	2
.882282	0
.926923	0
.972377	3

TOTAL NUMBER OF DROPLETS IS 238

MEAN	VALUE	STD. DEV.
MLD	.379055	.19133
MSD	.424606	.196677
MVD	.467687	.210862
LMD	.47563	.214321
SMD	.567393	.268474
VMD	.64394	.326758

****

RUN NUMBER 4.7 COMPARTMENT 14
MAGNIFICATION FACTOR .811667E-01

.120938	29
.16558	47
.210222	49
.254863	31
.300317	21
.344958	14
.3896	8
.434242	11
.478883	3
.524337	4
.568978	3
.61362	4
.658262	5
.702903	5
.748357	4
.792998	5
.83764	0
.882282	2

TOTAL NUMBER OF DROPLETS IS 245

MEAN	VALUE	STD. DEV.
MLD	.292836	.175824
MSD	.341566	.182452
MVD	.392722	.202216
LMD	.398404	.205083
SMD	.519153	.28659
VMD	.617094	.368859

****

!

RUN NUMBER 4.7 N. MAX. = 66

* COMP. 2 + COMP. 4 . COMP. 6
X COMP. 10 0 COMP. 12 # COMP. 14

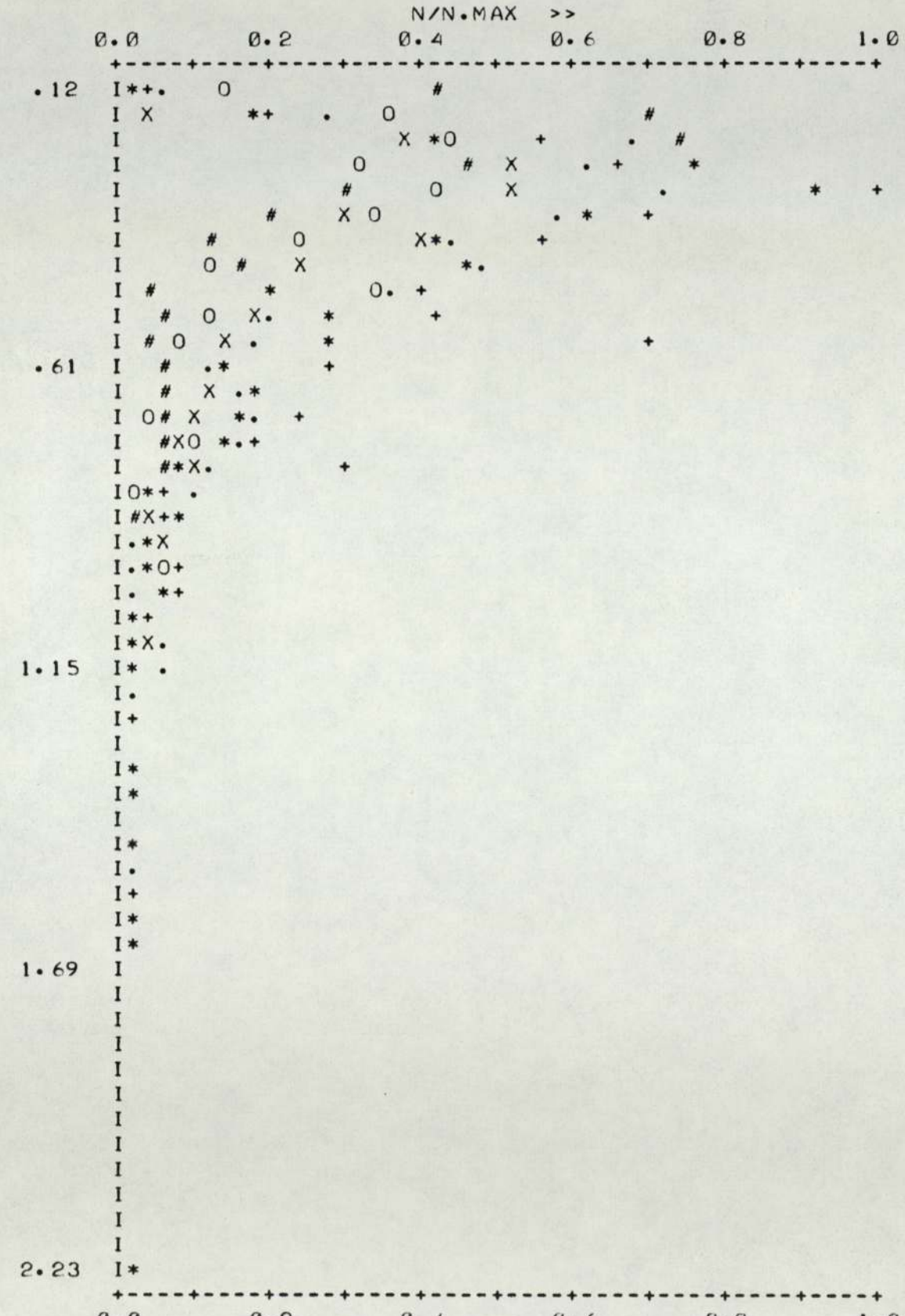

Appendix 3

Measured physical properties of fluid systems at 18°C

(a) Toluene

Interfacial tension with distilled water	34.1 ± 1	dynes/cm
Density	0.865 ± 0.002	g/cm^3
Viscosity	0.58 ± 0.01	cP
Boiling range	108 to 111°C	

(b) Distilled Water

Interfacial tension with toluene	34.1 ± 1	dynes/cm
Density	1.000 ± 0.002	g/cm^3
Viscosity	1.01 ± 0.01	cP

(c) System toluene/n-butyric acid/distilled water

Interfacial tension, see figure .

Distribution coefficient, see figure .

Appendix 4

Flowrates and hold-up at Phase Inversion as a function of Impeller Speed

N	G_c	G_d	x_d	
			at inversion point	after inversion
(r.p.m.)	(kg/m^2s)	(kg/m^2s)		
225	2.00	6.10		
250	0.50	6.05	0.730	0.601
	1.00	3.90	0.722	0.572
	2.00	3.07	0.732	0.575
	4.00	2.25	0.729	0.580
			mean 0.728	0.582
300	0.50	3.65	0.716	0.591
	1.00	2.84	0.704	0.580
	2.00	2.39	0.691	0.582
	4.00	1.63	0.721	0.604
			mean 0.708	0.589
350	0.00	5.40	0.702	0.558
	0.50	2.80	0.681	0.537
	1.00	2.43	0.683	0.564
	2.00	2.00	0.684	0.540
	4.00	1.00	mean 0.687	0.550
400	4.00	0.60	0.662	0.498
			mean 0.662	0.498
500	0.00	3.50	0.642	0.462
	0.50	2.20	0.631	0.480
	1.00	1.84	0.650	0.461
	2.00	1.29	0.629	0.478
	4.00	0.35	0.636	0.470
			mean 0.638	0.470
700	0.00	2.58	0.560	0.455
	0.50	1.76	0.542	0.455
	1.00	1.27	0.560	0.437
	2.00	0.60	0.555	0.460
			mean 0.554	0.452

Appendix 5

Description of Cine Film

1st sequence

Drops are shown breaking up in the region of the agitator. The hold-up is about 1% and the impellor speed is 200 r.p.m. Drops are broken by stretching in the vortices behind the blades. When break-up occurs, drops have a shape similar to rods, or jets, with length to diameter ratios of the order of 10 to 1. At these low values of hold-up, it might be expected that each drop would be uninfluenced by its neighbour, but a close inspection reveals that coalescences between drops occur in the high shear region of the agitator.

2nd sequence

At 300 r.p.m. hold-up is greater at about 5%. Many more coalescences occur, but the mechanism of break-up is essentially the same.

3rd sequence

Phase inversion is taking place at high flowrates and at N = 400 r.p.m. The sequential inversion of consecutive compartments can be seen as the 'slug' moves up the column.

Appendix 6

Mean Drop Size as a function of Impeller Speed, Phase Flowrate and Column Height

N	G_c	G_d	Compartment Number					
(r.p.m.)	(kg/m^2s)	(kg/m^2s)	2	4	6	10	12	14
200	0.25	0.25	1.42	-	-	-	-	-
	0.75	0.75	1.97	-	-	-	-	-
	1.00	1.00	2.16	1.39	1.38	1.18	1.18	1.14
250	0.25	0.25	1.32	1.07	0.89	0.86	0.82	0.74
	0.50	0.50	1.39	1.11	1.07	0.99	0.96	0.83
	1.00	1.00	1.70	1.55	1.45	1.30	1.24	1.16
300	0.25	0.25	0.84	0.81	0.67	0.63	0.64	0.51
	0.50	0.50	1.21	0.94	0.80	0.86	0.78	0.70
	0.75	0.75	1.30	1.14	1.05	1.01	0.94	0.89
	1.00	1.00	1.60	1.32	1.21	1.10	1.07	0.97
350	0.25	0.25	0.58	0.57	0.56	0.53	0.46	0.41
	0.50	0.50	0.82	0.78	0.76	0.75	0.73	0.69
	1.00	1.00	1.18	1.15	1.10	1.08	1.05	1.00
400	0.25	0.25	0.56	0.54	0.52	0.45	0.45	0.40
	0.50	0.50	0.79	0.75	0.74	0.73	0.72	0.69
	1.00	1.00	1.09	1.05	1.01	0.99	0.98	0.94
500	0.25	0.25	0.55	0.51	0.50	0.45	0.42	0.40
	0.50	0.50	0.75	0.75	0.75	0.72	0.70	0.68
	1.00	1.00	1.07	1.02	1.00	1.00	1.00	0.98
600	0.25	0.25	0.51	0.49	0.47	0.42	0.39	0.33
	0.50	0.50	0.71	0.70	0.68	0.63	0.61	0.60

Appendix 7

Volumetric Hold-up as a function of Impeller Speed, Phase Flowrate and Column Height

N	G_c	G_d	Compartment Number					
(r.p.m.)	(kg/m^2s)	(kg/m^2s)	2	4	6	10	12	14
200	0.25	0.25	-	-	-	-	-	-
	0.75	0.75	-	-	-	-	-	-
	1.00	1.00	0.055	0.069	0.076	0.098	0.120	0.108
250	0.25	0.25	0.012	0.024	0.030	0.029	0.038	0.048
	0.50	0.50	0.019	0.029	0.038	0.040	0.055	0.070
	1.00	1.00	0.055	0.080	0.095	0.146	0.163	0.199
300	0.25	0.25	0.035	0.043	0.052	0.058	0.066	0.081
	0.50	0.50	0.043	0.051	0.058	0.073	0.088	0.096
	0.75	0.75	0.055	0.071	0.090	0.117	0.137	0.154
	1.00	1.00	0.082	0.110	0.127	0.158	0.186	0.216
350	0.25	0.25	0.060	0.066	0.067	0.075	0.100	0.112
	0.50	0.50	0.070	0.072	0.084	0.096	0.103	0.117
	1.00	1.00	0.113	0.153	0.169	0.191	0.218	0.232
400	0.25	0.25	0.068	0.076	0.083	0.091	0.106	0.120
	0.50	0.50	0.100	0.109	0.121	0.124	0.133	0.142
	1.00	1.00	0.160	0.194	0.212	0.234	0.256	0.274
500	0.25	0.25	0.101	0.108	0.125	0.130	0.134	0.141
	0.50	0.50	0.152	0.159	0.168	0.176	0.182	0.189
	1.00	1.00	0.274	0.299	0.315	0.335	0.358	0.383
600	0.25	0.25	0.121	0.126	0.133	0.138	0.141	0.145
	0.50	0.50	0.199	0.169	0.204	0.213	0.224	0.235

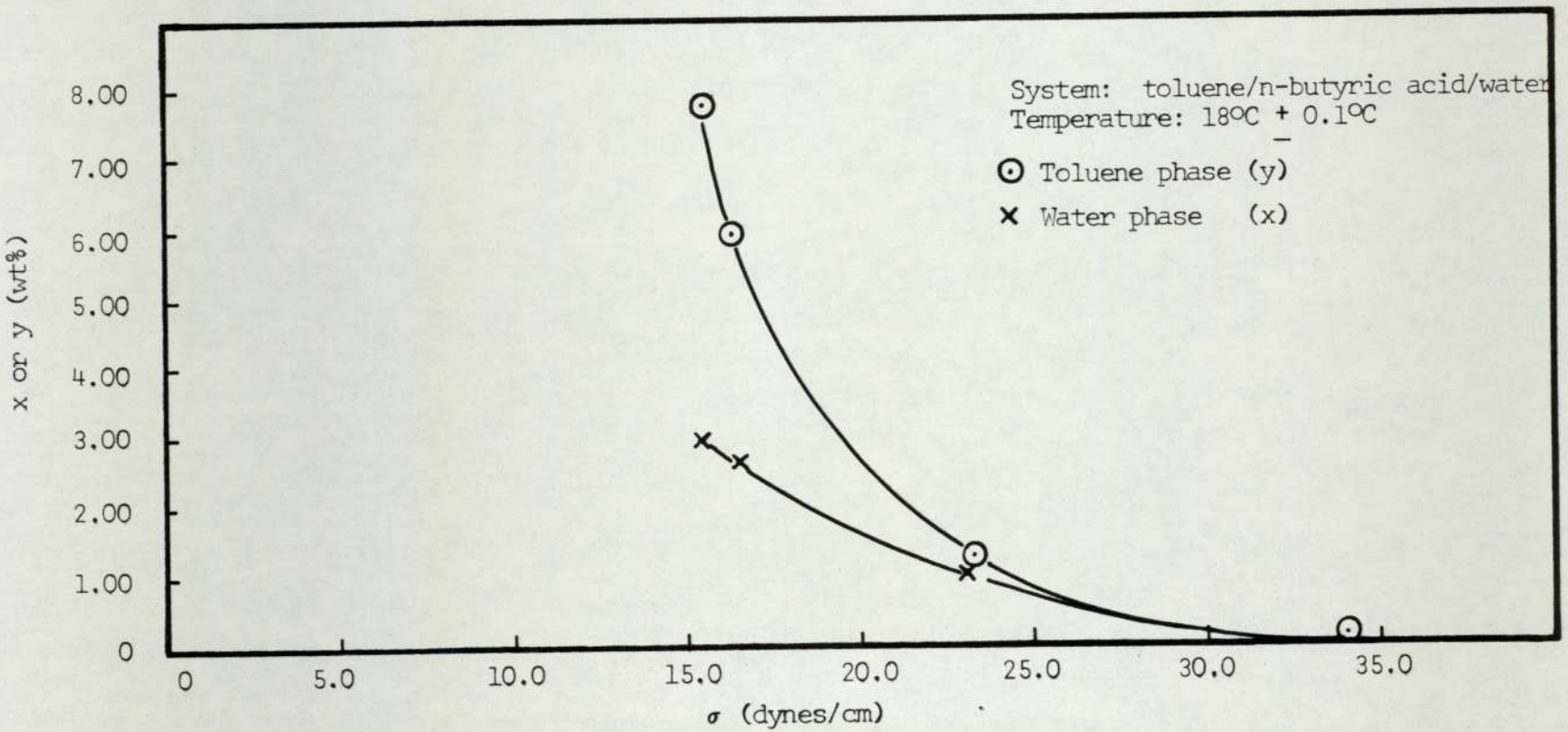

Appendix 8. Variation of Interfacial Tension with concentration.

Appendix 9 A

Mean drop sizes as a function of column height during mass transfer

Run Number	d_{32} (mm)					
	Compartment number					
	2	4	6	10	12	14
1/1	1.16	0.82	0.64	0.50	0.39	0.36
1/2	1.00	0.92	0.85	0.50	0.40	0.35
1/3	0.43	0.34	0.31	0.21	0.20	0.18
1/4	0.90	0.72	0.68	0.48	0.31	0.27
1/5	0.84	0.32	0.25	0.20	0.18	0.17
1/6	1.03	1.00	0.79	0.69	0.41	0.34
1/7	0.72	0.72	0.72	0.51	0.30	0.27
1/8	1.25	0.96	0.71	0.54	0.55	0.50
1/9	0.85	0.50	0.49	0.32	0.28	0.22
2/1	0.65	0.48	0.43	0.34	0.27	0.23
2/2	1.06	0.97	0.86	0.57	0.39	0.39
2/3	0.50	0.56	0.50	0.51	0.49	0.29
2/4	0.94	0.76	0.72	0.61	0.49	0.35
2/5	0.93	0.55	0.43	0.38	0.30	0.29
2/6	0.95	1.07	1.00	0.91	0.99	1.15
2/7	0.96	0.62	0.84	0.61	0.49	0.40
2/8	1.32	1.22	1.17	1.05	0.84	0.80
2/9	0.90	0.70	0.61	0.52	0.41	0.32

Appendix 9 B

Hold-up as a function of column height during mass transfer

Run Number	x_d						
	Compartment number						
	2	4	6	10	12	14	Mean
1/1	.020	.020	.020	.010	.051	.048	0.028
1/2	.888	.928	.596	.357	.229	.124	0.520
1/3	.921	.550	.290	.168	.112	.062	0.350
1/4	.440	.479	.479	.495	.323	.172	0.398
1/5	.099	.122	.119	.113	.092	.071	0.102
1/6	.021	.066	.082	.180	.163	.111	0.103
1/7	.862	.618	.312	.204	.173	.051	0.370
1/8	.010	.021	.031	.092	.091	.082	0.054
1/9	.109	.021	.095	.065	.067	.043	0.050
2/1	.041	.072	.130	.150	.129	.121	0.028
2/2	.949	.871	.642	.400	.291	.191	0.557
2/3	.472	.471	.384	.276	.206	.175	0.331
2/4	.602	.484	.467	.401	.290	.189	0.405
2/5	.630	.501	.434	.386	.287	.202	0.407
2/6	.489	.484	.342	.487	.491	.561	0.477
2/7	.821	.764	.682	.553	.416	.303	0.590
2/8	.453	.387	.301	.422	.344	.296	0.366
2/9	.401	.390	.216	.349	.352	.487	0.366

Appendix 10

Terminal steady-state concentrations during mass transfer

Run Number	Concentration of acid (wt%)			
	x_1 (top)	x_2 (bottom)	y_1 (top)	y_2 (bottom)
1/1	1.30	1.58	1.93	3.05
* 1/2	1.30	1.61	2.12	3.05
1/3	1.30	1.39	2.34	3.05
* 1/4	1.26	1.78	2.26	4.27
1/5	1.27	1.54	2.46	4.00
* 1/6	1.27	1.45	2.54	4.00
* 1/7	1.28	2.02	2.06	5.20
1/8	1.39	1.71	2.74	5.10
1/9	1.39	1.60	3.30	5.10
2/1	2.44	1.70	5.20	2.46
* 2/2	3.36	1.63	7.03	2.41
* 2/3	4.29	1.51	9.67	2.41
2/4	3.32	2.05	8.35	2.46
2/5	3.32	1.74	7.20	2.46
* 2/6	2.60	1.42	6.60	2.06
* 2/7	4.15	1.48	8.10	2.10
2/8	4.34	1.54	8.65	2.16
2/9	4.34	1.24	8.31	2.16

* denotes phase inversion

Appendix 11

Derivation of $(N.T.U.)_m$

Consider the contactor overall, and a small element δH

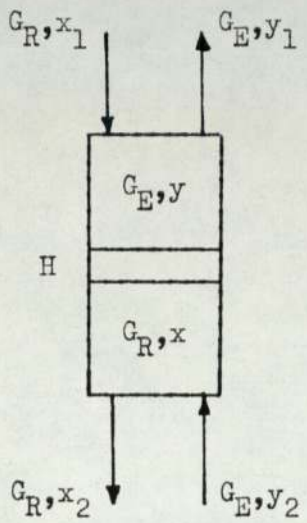

Assume : 1. Equilibrium is described by $y = mx^* + y_o$

2. m is constant

A mass balance over the lower half of the column gives

$$G_R (x - x_2) = G_E (y - y_2) \qquad 1$$

substituting $y = mx^* + y_o$

$$x^* = \frac{G_R}{mG_E} (x - x_2) + \frac{y_2 - y_o}{m} \qquad 2$$

$(N.T.U.)_{mR}$ is defined as

$$(N.T.U.)_{mR} = \int_{x_2}^{x_1} \frac{d_x}{x - x^*} \qquad 3$$

The extraction factor ε is defined as

$$\varepsilon = \frac{mG_E}{G_R} \qquad 4$$

Combination of 2 and 4 gives

$$(N.T.U.)_{mR} = \int_{x_2}^{x_1} \frac{dx}{x(1 - \frac{1}{\varepsilon}) + \frac{x_2}{\varepsilon} - \left(\frac{y_2 - y_o}{m}\right)} \qquad 5$$

For $\varepsilon \neq 1$, integration then leads to

$$(N.T.U.)_{mR} = \frac{1}{1 - \frac{1}{\varepsilon}} \ln \left[\frac{x_1 - \left(\frac{y_2 - y_o}{m}\right)}{x_2 - \left(\frac{y_2 - y_o}{m}\right)} \cdot (1 - \frac{1}{\varepsilon}) + \frac{1}{\varepsilon} \right] \qquad 6$$

Similarly, for $(N.T.U.)_{mE}$,

$$(N.T.U.)_{mE} = \frac{1}{1 - \varepsilon} \ln \left[\frac{y_2 - m(x_1 + x_o)}{y_1 - m(x_1 + x_o)} \cdot (1 - \varepsilon) + \varepsilon \right] \qquad 7$$

where $x^* = \frac{y}{m} + x_o$

For $\varepsilon = 1$, integration of equation 3 using the substitution

$$x^* = (x - x_2) + \frac{y_2 - y_o}{m} \qquad 8$$

gives $$(N.T.U.)_{mR} = \frac{x_1 - x_2}{x_2 - \frac{(y_2 - y_o)}{m}} \qquad 9$$

and $$(N.T.U.)_{mE} = \frac{y_2 - y_1}{y_1 - (x_1 + x_o)m} \qquad 10$$

Appendix 12

```
10  REM     "BCKMXNG B.T. "
20  INPUT N,G1,G2,X,E,N1
25  H1=1.22/N1
30  E1=(-.14+.136*N*(1-X)/(G1/10))*7.62*(G1/10)/(1-X)
35  PRINT E1
40  E2=N*25.81/(.393E-02*(3.84*N↑2)↑1.54*(7.41)↑4.18*(444.94*N↑2)↑.61)
45  PRINT E2
50  P1=100*G1*122/(E1*1000)
55  PRINT P1
60  P2=G2*122*100/(E2*865*X)
65  PRINT P2
70  F1=1-((1-EXP(-P1))/P1)
75  PRINT F1
78  IF P2>.1E06 THEN 82
80  F2=1-((1-EXP(-P2))/P2
82  F2=1
85  PRINT F2
90  F3=(1/F1)+E1*(1-E)/((G1/10)*H1)
95  PRINT F3
100  F4=(1/F2)-E2*(1-E)/((G2/8.65*X)*H1)
105  PRINT F4
106  H2=(1/F3)*(E1/(G1/10))+(1/F4)*(E2/(G2/(8.65*X)))
110  PRINT H2
120  PRINT H1-H2
130  PRINT 1.22/H2
```

Supporting Publication.

Paper presented at I.S.E.C. '74 Lyon, (1974).

DROPLET SIZE DISTRIBUTION AND INTERFACIAL AREA IN AGITATED CONTACTORS

D.R. Arnold, C.J. Mumford and G.V. Jeffreys
Department of Chemical Engineering, University of Aston in Birmingham, United Kingdom. December 1973.

ABSTRACT

The prediction of drop sizes and interfacial areas in rotary agitated contactors is discussed, together with the short comings of usual methods especially with regard to the extension of mathematical models for batch systems to continuous ones. An empirical design equation has been developed which enables the prediction of mean drop sizes at various points in the Oldshue-Rushton Contactor to be made from a knowledge of column geometry, system properties and operating parameters where non-mass transfer conditions approximate to the real situation. Experimental results are correlated by the equation

$$\left(\frac{d_{32}}{D}\right) = 2.44 \left(\frac{H}{H_T}\right)^{-0.06} \left(\frac{V_I^2 D \rho_m}{\sigma_i}\right)^{-0.63} \left(\frac{V_K}{V_I}\right)^{0.18}$$

for the system toluene-water in a six inch diameter 16 compartment pilot scale unit.

The changes in drop size distribution up the column have been recorded for a range of operating conditions, and the distribution is shown to be log-normal.

Flooding of the column was investigated for a wide range of operating conditions. It is concluded that phase inversion normally takes place before flooding in the Oldshue-Rushton Column.

INTRODUCTION

In liquid-liquid, or gas-liquid, contactors maximisation of the area offered by one phase to the other assists in the attainment of the greatest possible rate of mass transfer. Therefore in the design of liquid-liquid extraction equipment attention has generally been focussed on the creation of a large interfacial area, at the expense of throughput and back-mixing. Comprehensive reviews of equipment for liquid extraction have shown that many designs of varying geometric complexity have been proposed and used[1,2].

In rotary agitated contactors dispersion of one phase as droplets within the other (continuous) phase is achieved by the transmission of kinetic energy from the agitator to the continuous phase and thence by various means to the dispersed phase, causing droplet distortion and subsequent break-up.

For rotary agitated contactors operating at an impeller Reynolds' Number below 10^4, where the flow regime of the bulk of the continuous phase is predominantly laminar, energy mainly is transmitted from the continuous phase to the dispersed phase by viscous shear. At higher Reynolds' numbers, above the laminar - turbulent transition, transmission energy is by inertial forces, i.e. the impact of turbulent continuous phase eddies on the surface of the drop. Hinze[3] has illustrated how these different mechanisms of energy transfer may cause break-up.

The power input to the agitator is thus transferred into the kinetic, surface, potential and heat energy of the droplets. Designs of rotary agitated contactors may therefore be classified in terms of the rate of energy input per unit volume of continuous phase, measured by the familiar equation

$$E = K N^3 D^5 \rho_c$$

where E is the energy input per unit volume, N is the agitator speed, D is the agitator diameter, ρ_c the continuous phase density and K is a constant which depends only on system geometry, for $Re_I > 10^4$.

Thus the Rotating Disc Contactor is a low energy device with a value of K = 0.1, whereas the Oldshue-Rushton or Scheibel column has a K value = 4.4 and is consequently a high energy device. Therefore fundamental differences exist between the mechanisms of energy transfer to the dispersed phase in these units.

An attempt has been made[5] to derive equations for the prediction of drop sizes in the R.D.C., using Kolmogorov's theory of isotropic turbulence together with a mathematical model of flow patterns around a rotating disc derived by Cochran[6]. These predictions agreed well with experimental values despite deviation of the experimental conditions from the underlying assumption of Kolmogorov[7] concerning local isotropic turbulence.

The advances in design data and mathematical analysis since the publications of Reman[8] relating to the R.D.C. [4,47] have not been matched for the high energy contactors. Studies of the Oldshue-Rushton Column[9] have been limited to analyses of hydrodynamics based on the prediction of drop sizes as an extension of studies in stirred tanks[10], or the interpretation of mass transfer data in terms of H.T.U.'s or H.E.T.S., with the obvious attendant limitations of this approach[11]. Interstage or Axial mixing has also received some attention[9,12,13,14,15], albeit under non-mass transfer conditions. Therefore a detailed study has been made of the performance of this type of extraction column, including measurements of drop size distributions, volumetric hold up, and associated variables, over a wide range of operating conditions. This has covered non-mass transfer conditions and transfer in both directions[48]. The work under non-mass transfer conditions is described in this paper, including original observations of phase inversion phenomena in continuous flow.

The Oldshue Rushton Column

The energy required to break-up droplets in a mechanically agitated rotary extraction column is provided by the agitator. Since droplets are suspended in the continuous phase an analysis of energy distributions and flow patterns is necessary prior to the consideration of actual mechanisms of break-up.

The Oldshue-Rushton Contactor is neither a compartmental or truly continuously differential device, but has some properties of both. Compartments are separated by horizontal stator rings and the vertical component of velocity of any droplet within each stator opening determines whether or not it moves to the next compartment. Each compartment may be regarded as a stirred tank in its own right. The motion of droplets between compartments is therefore dependent upon droplet size, the physical properties of the phases, the phase flowrates and the agitator speed, for a gixed geometry system. The correlation of these variables therefore involves an examination of fluid flow patterns within each compartment, and between adjacent compartments[48].

The sizes of the droplets within each compartment depends upon similar variables, and, since the drop size distribution of the dispersion passing through the stator opening is determined by conditions within the previous compartment, it is droplet behaviour within the circulating flow of each compartment that determines column operating characteristics.

Droplet Sizes in Agitated Tanks

Droplet sizes in fully baffled, stirred tanks have been studied extensively. Theoretical analyses of droplet break-up have resulted in predictions of minimum, mean, and maximum droplet diameters at volumetric hold-up values ranging from zero to 30 per cent. The dependence of drop diameter on system properties in stirred vessels is summarised in Table 1.

TABLE 1

EXPONENTS FOR SINGLE TANKS

	Authors	N	D	Reference
*	Kolmogorov	-1.2	-2.0	16
*	Obukhov	-1.2	-2.0	17
+	Vermeulen et.al.	-1.2	-0.8	18
+	Rea et.al.	-1.0	-1.5	19
+	Kafarov and Babanov	-1.1	-0.7	20
+	Pavlushenko et.al.	-1.0	-1.65	21
+	Rodger et.al.	-0.72	-0.75	22
+	Yamoguchi et.al.	-1.5	-2.45	23
+	Pebalk and Mishev	-0.912	-1.624	24
+	Calderbank	-1.1	-0.7	25
	Shinnar	-1.2	-0.8	26
+	Shinnar and Church	-1.2	-0.3	27
+	Brown and Pitt	-1.2	-0.3	28
*	Hinze	-1.2	-2.0	3
*	Taylor	-1.5	-1.0	29
+	Mylneck and Resnick	-1.2	-0.3	30
+	Giles et.al.	-1.2		31
+	Giles et.al.	-1.0		31
+	Luhning and Sawistowski	-1.2		32

+ Experimental Data * theoretical

Significantly the exponent of the impeller speed N varies between -1.5 and -0.72, and the exponent of the impeller diameter D between -2.45 and -0.70. For experimental studies these large differences may be explained by the use of different systems which cannot be characterised solely in terms of density, viscosity and interfacial tension. It is not clear in some cases whether the systems were in thermodynamic equilibrium. Finally the expression of drop size in terms of a limited number of variables may be invalid.

A notable exception in the table is the correlation of Rodger et. al.[22] which gives $d \propto N^{-0.72}$. The dimensional analysis of their results contains a group to account for the degree of contamination of the drops by surfactants expressed as a ratio of the settling time of the dispersion to that of the pure liquid. However in addition to surfactant concentration, settling time must be dependent on drop size, due to the differing buoyancy of the drops, and therefore the precise dependence of d on N is difficult to determine from the correlation.

Detailed consideration of theoretical models for droplet sizes is beyond the scope of this paper. However, it is of interest to examine the relevance of Kolmogorov's Theory of isotropic turbulence to droplet analysis in stirred tanks, since all the models relate droplet sizes to both impeller speed and diameter, and hence to energy input to the system.

The two basic postulates of the theory concern the relationship between the mean square relative velocity $\overline{u^2(r)}$ between any two points a distance r apart and the energy per unit mass in the fluid.

Thus

$$\overline{u^2(r)} = C_1 E^{\frac{2}{3}} r^{\frac{2}{3}} \qquad \text{for} \quad L \gg r \gg z \qquad (1)$$

$$\overline{u^2(r)} = \frac{C_2 E r^2}{D} \qquad \text{for} \quad L \gg z \gg r \qquad (2)$$

where the symbols have their usual meanings.

The familiar development then leads to the two equations

$$r_{sd} = K_1 \left(\frac{\sigma_i}{\rho_c}\right)^{0.6} \left(\frac{1}{E}\right)^{0.4} \qquad (3)$$

and

$$r_{sd} = K_2 \left(\frac{\sigma_i \mu_c}{\rho_c^2}\right)^{1/3} \left(\frac{1}{E}\right)^{1/3} \qquad (4)$$

For fully turbulent flow the power number is constant and $E \propto N^3$. Hence,

$$r_{sd} \propto N^{-1.2} \qquad (5)$$

and

$$r_{sd} \propto N^{-1.0} \qquad (6)$$

These relationships were verified experimentally[31] for the nitration of toluene. For this system it was argued that which of equations (5) and (6) was applicable was dependent only on the value of the volumetric hold-up. No attempt was made to estimate the microscale of turbulence. Levins and Glastonbury[33] investigated mass transfer from solid particles in a stirred tank and determined the requirements for local isotropic turbulence. From a consideration of equations by which the size of the particles in a stirred tank may be compared with the size of the turbulent eddies present, the dependence of d on N was evaluated theoretically for specific cases of liquid-liquid systems at steady state, they concluded that equation (1) was of doubtful validity.

Microscales of turbulence in the Oldshue-Rushton column have been calculated[48] from Kolmogorov's definition

$$z = \left(\frac{\nu^3}{E}\right)^{\frac{1}{4}} \qquad (7)$$

together with

$$E = \frac{5.4\ N^3 D^5 \rho_c}{M} \qquad (8)$$

where M is the mass of continuous phase in the tank. Values of the microscale are for a standard fully baffled mixing vessel of identical geometry to a single compartment of the Oldshue-Rushton column containing water. These are given in Table 2. Cutter's [34] ratios of $E'/\bar{E}$ for the impeller region ($E'/\bar{E} = 7.7$) and for other lower energy regions ($E'/\bar{E} = 0.26$) were used to obtain the higher and lower limits. The magnitude of the calculated microscales is of the same order as the droplet diameters commonly encountered in mixer-settlers, the Oldshue-Rushton and similar high energy contactors, and therefore the use of equations (3) or (4) requires caution. Shinnar and Church[27] have derived an expression for mean drop size related to the Weber number and Brown & Pitt[28] have correlated drop size with hold-up by an equation of the form

$$\frac{d_{32}}{D} = k_1 (1 + k_2 x_d) We^{-0.6} \qquad (9)$$

for low hold-up values between 0.05 and 0.3

Bouyatiotis and Thornton found that for both batch and continuous operation with four different systems (including toluene-water) the measured distribution approximated to a normal one. Similar results for different systems have been reported by Chen and Middleman[42] and Brown and Pitt[28]. Pelbalk and Mishev[24], however, reported that for a variety of liquid-liquid systems, including kerosine-water as used by Brown & Pitt[28], the drop size distribution in a stirred tank was log-normal. Giles et al[51] reported a log-normal distribution during the nitration of toluene in a stirred tank.

Whether the drop size distribution is normal or log-normal is of practical significance in an extraction column. For a fixed volumetric throughput, a comparison of the two types of dispersion is illustrated in Table 3.

TABLE 2

Microscales of Turbulence for Water

N (r.p.m.)	$\bar{E}$ ($cm^2 s^{-3}$)	Z (mm) Impeller region	Circulation Zone
200	39.6	0.075	0.176
300	134	0.056	0.131
400	317	0.045	0.105
500	620	0.038	0.089
600	1070	0.033	0.077

TABLE 3

Property of dispersion	Normal	log-normal
Proportion of smaller droplets	Lower	Higher
mean m.t. coeffs.	Higher because more drops are circulating	Lower - more stagnant drops
Interfacial area	Lower	Higher
Settling rate	Higher	Lower
Tendency to flood column	Higher	Lower

From the point of view of predicting hydrodynamic and mass transfer performance the prefered distribution is a mono-dispersion with a consequent standard deviation of zero. Although this is impracticable in an extractor, a distribution where the mode is equal to the mean results in more drops being nearer the mean size than with a log-normal distribution. Droplet characteristics are thus more predictable in a normal distribution. Therefore it is desirable to obtain a normal distribution around a certain mean drop diameter rather than a log-normal one.

All models developed to date to predict drop sizes in stirred tanks are restricted to batch operations or continuous operations with either one or both of the phases flowing in a single tank. Fluids enter and leave the tank via many diverse geometric arrangements, which affect the hydrodynamics of operation. For example the geometry used by Thornton[10] resulted in the drop size being independent of flowrate, i.e. the mean residence time of the dispersed phase was large compared with the flowrate, and thus the dynamic equilibrium between droplet break-up and coalescence remained unaffected. Operation was therefore effectively batchwise.

In rotary agitated columns, entrance and exit mechanisms are very important. Larger drops have a greater vertical velocity than smaller ones and are less affected by small scale disturbances in other directions. Classification therefore occurs between compartments resulting in a tendency for the smaller drops to remain in a compartment and larger ones to pass to the next.

The positive skewness in the drop size distribution noted by Giles et. al.[31], is therefore less significant in the column, and a negative skewness would be expected. Oldshue-Rushton column designs based upon a mean drop size throughout the length of the column in which the drop size correlations are themselves based on data from single stirred tanks are therefore open to criticism.

The effect of hold-up on mean drop size in the column could be expected to follow the general form of Thornton's correlation,

$$d_{32} = d_o(1 + m\, x_d) \qquad (10)$$

This would only be expected to hold for any compartment at constant volumetric flowrate.

Phase Inversion

Phase inversion in liquid-liquid systems was first recorded by Ostwald[35]; the phase ratio at which it occurred was 3:1 and became known as "Ostwald's Ratio". Recently the phenomenon has received attention from Luhning and Sawistowski[32] for a single stirred tank operating batchwise, and Quinn and Sigloh[36]. The existence of an ambivalent range is well known, as is its dependence on agitator speed. The effect of mass transfer on the ambivalent region has been briefly studied[32].

Phase inversion will occur in a batch system only when the rate of coalescence of drops is greater than the rate of break-up. In a continuous system additional factors have to be taken into account. In a continuous single stirred tank both phases are in flow and as mentioned earlier the geometric arrangement for the entrance and exit of each phase will affect the dynamics of operation. The volumetric hold-up of dispersed phase reaches a steady state value in each compartment when the column is operating normally. This is achieved only when the input of each phase is equal to the output, and this is particularly important with reference to the dispersed phase.

A complex situation exists between consecutive compartments, because the droplets exist in a distribution of diameters, not as a monodipersion. Thus a polydispersion of droplets is flowing by buoyancy through the stator opening against the flow of continuous phase. Superimposed on the varying terminal velocities of the droplets in the dispersion is the turbulent flow mainly across the opening generated by the impellers at the centre of each compartment. When hold-up in the Oldshue-Rushton contactor is large, (about 0.6 - 0.8) phase inversion occurs and has the effect of relieving the imminent flooding situation. Phase inversion occurs in preference to flooding.

In any two phase counter current operation therefore there is a limit above which normal operation is not possible as either flowrate is increased incrementally. Under certain operating conditions flooding in the usual sense of the word takes place.

EXPERIMENTAL

Experimentation was performed in the sixteen-compartment, six inch diameter Oldshue-Rushton column. The glass column has stainless steel internals and the stators were machined to an exact fit inside the column. Sampling points in each compartment consisted of stainless-steel ports sealed by "teflon" "O" rings in holes drilled with an ultrasonic drill. The agitator and shaft were made of stainless steel, supported by a p.t.f.e. bearing at each end of the column. A brass bearing was installed in the centre of the column. The agitator shaft was driven by a $\frac{1}{4}$ h.p. electric motor controlled by a "Torovolt" variable voltage device, and its speed monitored by a directly coupled tachometer. Standard four blade disc turbines of identical dimensions to those used by Oldshue and Rushton were employed; the energy input of this geometric arrangement having been measured[11]. Fluid was transferred from the stainless steel 40 gallon storage tanks to the column by stainless steel centrifugal pumps with viton 'A' seals, controlled by a variable voltage device. All transfer lines were of 0.5 in. i.d. borosilicate glass or 5/8" dia. p.t.f.e. tubing. A variable height overflow leg was incorporated in the continuous phase outlet line to control the position of the interface. The unit was operated at ambient temperature, ($18 \pm 2^{\circ}C$).

The system toluene (commercial, redistilled grade) - distilled water was selected[38]. Toluene was the dispersed phase.

A photographic technique for recording the dispersions in the compartments was developed.

An Asahi-Pentax 35 mm still camera with a M^{0} 1 single extension tube was used to record the drop size distribution at the wall in several compartments on Kodak Plus X pan film. Enlargement of the negative and printing on Kodak grade 4 "Bromesko" paper gave sufficient magnification and contrast for the drops to be counted on a Carl Zeiss T.G. 3 particle size analyser and the distribution obtained. Figures 3 and 4 show typical photographs. Due to the high quality of the photographs produced, drop sizes as low as 0.12 mm could be recorded accurately. A Honeywell 316 digital computer was used to process the measurements to produce a comprehensive statistical analysis of the distribution. At least 300 drops were used for each distribution measurement obtained from three separate negatives for each compartment, giving a statistical accuracy better than 3%[41].

Hold up of the dispersed phase was measured by sampling of several compartments via the Simplifix toggle values. Accuracy of this technique was checked by comparison of the overall hold-up when the agitator was stopped and the column isolated. Three samples for each compartment were taken and these were generally consistent to within $\pm$ 5%. Both phases were mutually presaturated and the interfacial tension was checked by Wilhelmy's method prior to each run. The column was precleaned with a 2 per cent "Decon 90" solution and rinsed with distilled water.

RESULTS

Drop-size

The nature of the drop size distribution in various parts of the column was investigated.

Figure 5 (a) is a typical ogive for the toluene-water system, and as shown in Figure 5 (b) this conforms well with a log-normal distribution. At all impeller speeds (200 - 600 rpm) and at all points in the column the distribution of drop sizes was log-normal.

The interacting effects of drop size, volumetric hold-up, column height and agitator speed on dispersions of toluene in water under non-mass transfer conditions is demonstrated in Figures 6-11.

Figures 6 and 7 show the variation of d_{32} with position in the column at flowrates of 0.25 and 0.5 kg/sm^2. Although the mean drop size decreased up the column, a false picture would be gained from considering this in isolation. Figures 8 and 9 show the relationship of hold up to height up the column, and figure 10 depicts the typical variation of hold-up with agitator speed.

The variation of drop size with hold up in figure 11, is in agreement with the work of Thornton and Bouyatiosis[10], in as much as the mean drop size is a linear function of hold-up, for fixed agitator speed and column compartment. They found that m was a function of physical properties only,

i.e.

$$m = 1.18 \cdot \left(\frac{\sigma_i^2}{\mu_c^2 g}\right) \cdot \left(\frac{\Delta\rho \cdot \sigma_i^3}{\mu^4}\right)^{-0.62} \cdot \left(\frac{\Delta\rho}{\rho_c}\right)^{0.05} \qquad (10)$$

and

$$\left(\frac{d^0_{32}\,\rho_c^2 g}{\mu_c^2}\right) = 29.0 \left(\frac{\left(\frac{E}{M}\right)^3 g_c^3}{\rho_c^2 \mu_c g^4}\right)^{-0.32} \left(\frac{\rho_c^3 \sigma_i}{\mu_c^4 \cdot g}\right)^{0.14} \qquad (11)$$

The units of m are those of length, and for the toluene/water system the value of m from equation (10) is 2.62×10^{-4} m, compared with a mean of 2.49×10^{-3} m for the data figure 11 at 300 rpm. Further experimental data revealed that m is independent of impeller speed in the Oldshue Rushton Column as predicted by equation (10), but that values of d°_{32} extrapolated from the curves of figure [11] do not show d°_{32} to be proportional to $(E)^{1/3}$ as would be expected from equation (11).

A dimensional analysis was carried out to correlate all 15 dependent variables which may effect the drop size distribution and the mean drop size. These are listed in Table 4. A full dimensional analysis based on all these variables has not been completed, since those marked with an asterisk in the figure were maintained constant, and a "short" analysis results. Thus the drop size may be expressed as a function of height up the column, impeller speed, flowrates, physical properties and impeller diameter. Height up the column (i.e. compartment) is expressed as a fraction of the total height, as opposed to H/D as would be normally required in a formal analysis. The flowrates are expressed as a single quantity V_k, which is a common expression of characteristic velocity for two phase flow,

$$V_K = \frac{V_d \ (1 - x_d)}{x_d} + V_c \qquad (12)$$

TABLE 4

Variables Considered in the Dimensional Analysis

Quantity	Symbol		Dimensional Formula
Drop Size	d_{32}		L
Impeller Tip Speed	V_I		$L\ T^{-1}$
Column Height	H		L
Mean Viscosity	μ_m		$M\ L^{-1}T^{-1}$
Mean Density	ρ_m		$M\ L^{-3}$
Drop Characteristic velocity	V_K		$L\ T^{-1}$
Interfacial Tension	σ_i		$M\ T^{-2}$
Compartment Height	H	Combined as a geometric factor" Fg, dimensionless	
Column Diameter	D_T		
Baffle Width	B		-
Blade height	b_h		
Blade width	b_w		
Impeller diameter	D		L
Coalescence factor	C		-
Break-up factor	R		-
Buoyancy	$\Delta\rho/\rho$		-

Total number of variables = 16

Number of fundamentals = 3

$\therefore$ Number of dimensionless groups = 9

For a countercurrent system V_c is a negative quantity if V_d is regarded as positive. Mean densities are expressed by ρ_m,

$$\rho_m = (1-x_d)\rho_c + x_d\rho_c \qquad (13)$$

which has been shown in this form to be a realistic measure of mean density.[43]

Thus

$$\left(\frac{d_{32}}{D}\right) = C \left(\frac{H}{H_T}\right)^p \left(\frac{V_i^2 D \rho_m}{\sigma_i}\right)^r \left(\frac{V_K}{V_i}\right)^s \qquad (14)$$

for the range of variables considered under normal operation.

where $\frac{H}{H_T}$ is the fractional height up the column

$$V_I = \pi ND$$

$$V_K = V_d \cdot \frac{(1 - x_d)}{x_d} + V_c$$

$$\rho_m = (1 - x_d)\rho_c + x_d\rho_d$$

The exponents p, r & s and the constant C were evaluated experimentally, to yield

$$\left(\frac{d_{32}}{D}\right) = 2.44 \left(\frac{H}{H_T}\right)^{-0.06} \left(\frac{V_i^2 D \rho_m}{\sigma_i}\right)^{-0.63} \left(\frac{V_K}{V_i}\right)^{0.18} \qquad (15)$$

w

Phase Inversion

As the dispersed phase flowrate was increased at very low rotor speeds e.g. less than 250 rpm, droplets were rejected from the inlet end of the column, and a build-up of dispersed phase droplets occurred below the lowest stator ring. At high rotor speeds e.g. greater than 700 rpm and at high continuous phase flowrates, greater than 4.0 Kg/m^2s, droplets which entered from the distributor ruptured, due to the high level of turbulence in the first compartment and since the terminal velocity of the daughter droplets was lower than the downward velocity of the continuous phase and they were carried out of the contactor as a fine dispersion in the continuous phase, i.e. conventional 'flooding' occurred.

In between these two extremes, before flooding was reached, phase inversion was observed. No reference was found concerning inversion in liquid-liquid extraction columns, although during the course of this work Al-Hemiri[37] and Jillood[38] have observed a characteristic but disimilar effect in an R.D.C.

Compartments of the column have been observed to invert individually so that 'slugs' of coalesced dispersed phase progressed up the column. The compartment in which inversion first took place as flowrates were increased was reproducible, and may be predicted from experimental results. These results are recorded elsewhere[48].

Inversion points were determined precisely by allowing the column to attain hydrodynamic steady-state conditions at values of dispersed and continuous phase flowrates below those for inversion at a fixed impeller speed. The dispersed phase flowrate was then incrementally increased by between 2 - 5% and time allowed for steady-state to be obtained at the each new value. This usually required 10 - 20 minutes depending on the total flowrate. As soon as phase inversion began to occur on a cyclic basis, and a pseudo-steady-state was established with a steady frequency of the inversion, the dispersed phase flowrate was decreased by intervals of about 1% until the cycling ceased and phase inversion was eliminated.

At this point a slight increase in the dispersed phase flowrate caused the column to invert at one particular compartment, and this value was taken to be the characteristic flowrate for phase inversion. The particular compartment in which the inversion first occurred was recorded. Measurements of the volumetric hold-up of dispersed phase were made via the sampling point in the compartment immediately before and after phase inversion.

Inversion occurs when the input flowrate of either of the phases means that steady-state conditions are not able to cope with the flow. This situation is represented in figure 12 where flowrate of dispersed phase (G_d) is plotted against impeller speed (N) for various values of continuous phase flowrate (G_c). Characteristically these curves all tend towards a common asymptotic value of impeller speed between 200 and 250 rpm. The corresponding impeller Reynolds numbers with regard to continuous phase physical properties were between 0.858×10^4 and 1.075×10^4. Since the commonly accepted Reynolds' Number of transition from laminar to turbulent flow is 1.0×10^4, it appears that phase inversion is precluded by operation in the laminar region. The change in apparent fluid properties (such as density) corresponding to dispersed phase hold-up would result in lower Reynolds' Numbers[43,18,44,45] so that the transition from laminar to turbulent would occur at a slightly higher value of Reynolds Number. This is in agreement with the experimental results. Phase inversion could not be generated below an impeller speed of 225 rpm under any flowrate conditions, since at such low values of Re there was stratification of droplets in the compartment; when phase inversion occurred the coalesced dispersed phase therefore occupied only the upper half of the compartment.

Increasing flowrates at low impeller speeds, below 250 rpm, resulted in flooding in the generally accepted sense. Dispersed phase droplets were rejected from the first compartment and flowed out of the column via the continuous phase outlet.

According to Figure 13 phase inversion should be possible at negative values of G_d and G_c, especially at high impeller speeds e.g. 500 rpm. At zero flowrate of continuous phase, phase inversion could be obtained at impeller speeds of 350 rpm and greater. Extrapolation of these curves suggests that phase inver-

-sion could in theory occur during co-current operation.

Measurements of hold-up of dispersed phase immediately before and after phase inversion occurred were made in certain compartments for certain runs. The values of x_d for various flowrates, impeller speeds and positions in the column followed the general pattern up to the point of the limit of steady-state operation, after which the hold-up began to increase up to the phase inversion value. Figure 14 shows a typical phase inversion curve for the system toluene/water in the absence of mass transfer. As would be expected, the results show no variation of hold-up at phase inversion with changing flowrate of either phase. Each point on the figure is an arithmetic mean of the hold-up values obtained for each impeller speed, although the maximum deviation from the mean was only 5 per cent, the same order of magnitude as the experimental error of each reading.

In figure 14 the upper curve shows the hold-up immediately prior to inversion. The column was operated under conditions where inversion takes place periodically, and the hold up was measured in the compartment in which inversion was initiated. The hold-up value necessary for inversion to occur decreases with increasing rotor speed. This is in concert with the findings of Luhning & Sawistowski. The hold up of the residual phases after inversion, i.e. when the 'slug' of inverted fluids had passed to the next compartment, is shown as the lower curve.

CONCLUSIONS

Drop sizes in the Oldshue Rushton Column were related by equation (15) for the system toluene/water under non-mass transfer conditions. The dependence of d_{32} on $We^{-0.63}$ in equation (15) is in very good agreement with all prededing investigations in stirred tanks. The effects of column geometry are expressed in the other two terms in the equation, although there are more terms in the full analysis[48]. Some modification is necessary in the presence of mass transfer or varying interfacial tension but for dilute systems where major surfactant effects are absent, equation (15) serves as a guide to drop sizes for design purposes. Interfacial areas may be calculated directly from the familiar equation

$$a = \frac{6x_d}{d_{32}} \qquad (16)$$

for incremental column heights.

Phase inversion is an important feature of operation of the contactor which has to date received insufficient attention. Phase inversion can occur in any agitated contactor, and indeed operation under inverted conditions may improve mass transfer rates due to better mixing of the phases.

When phase inversion does not take place, equation (15) may be used to provide an estimate of drop size and mass transfer coefficients calculated[46,47]. Column performance is then evaluated bearing in mind the backmixing correlations.

The effects of mass transfer on the operating characteristics of the Oldshue-Rushton Column, and scale-up procedures are reported in detail elsewhere[48].

NOMENCLATURE

a	interfacial area
C_1, C_2	constants in equations (1) and (2)
D	impeller diameter
E	energy
d	drop diameter
G	mass velocity
g	gravitational constant
H	column height
K_1, K_2	constants in equations (3) and (4)
k_1, k_2	constants in equations (9)
L	Lagrangian macroscale of turbulence
M	mass
m	parameter in equation (10)
N	agitator speed
n	number of drops
r	radius of drop
$u^2(r)$	mean square velocity
V	Velocity
We	Weber Number
x	volumefraction
z	microscale of turbulence
μ	viscosity
ν	Kinematic viscosity = $\frac{\rho}{\mu}$
ρ	density
σ	interfacial tension

Subscripts

C	continuous phase
d	dispersed phase
I	Impeller
S.d	Stable drop
T	total
o	Zero hold-up
32	sauter mean

References

1. Mumford C.J. Brit. Chem. Eng. 1968 13 981.
2. Bailes P.J. and Winward A. Trans. Instn. Chem. Engrs. 1972 50 240.
3. Hinze J.O. A.I.Ch.E.Jnl 1955 1 289.
4. Misek T 'Rotating Disc Contactor' 1964 (Prague : Statni Nakadelotri Technicke Literatury).
5. Jeffreys G.V. and Mumford C.J. 1971 Proc. I.S.E.C. '71 S.C.I. The Hague (1971).
6. Cochran W.E. Proc. Camb. Phil. Soc. 1934 30 365.
7. Kolmogorov A.N. Dokl. Akad. Nauk. S.S.S.R. 1949 66 825.
8. Reman G.H. Proc. 3rd World Petr. Gongr. Hague 1951.
9. Bibaud R.E. and Treybal R.E. A.I.Ch.E.Jnl 1966 12 472.
10. Bouyatiotis B.A. and Thornton J.D. Ind. Chem. 1963 39 298.
11. Oldshue J.Y. and Rushton J.H. Chem. Eng. Progr. 1952 48 297.
12. Gutoff E.B. A.I.Ch.E.Jnl. 1965 11 712.
13. Ingham J. Ph.D. Thesis University of Bradford 1972 and Trans. Instn. Chem. Engrs. 1972 50 372.
14. Haug H.F. A.I. Ch.E . Jnl 1971 17 585.
15. Lelli, U. et al Chem. Engng. Science 1972 27 1109.
16. Kolmogorov A.N. Dokl. Acad. Nauk. S.S.S.R. 1941 32 19.
17. Obukhor A.M. ibid 1941 32 22.
18. Vermeulen T et. al. Chem. Engng Progr. 1955 51 85F.
19. Rea H.E. and Vermeulen UCRL - 2123 1953 cited in
20. Kafarov V.V. and Babanov D.M. Zh. Prikl. Khim. 1959 32 789.
21. Pavlushenko I.S. and Yanishevskii A.V. Zh. Prikl. Khim 1958 31 1348.

40. Mylneck Y. and Resnick W. Can. J. Chem. Engng. 1972 50 134.

41. B.S. 3406 Part 4 1963 p. 35.

42. Chen H.T. and Middleman S. A.I.Ch.E.Jnl 1967 13 989.

43. Laity D.S. and Treybal R.E. A.I.Ch.E.Jnl 1957 3 177.

44. Miller S.A. and Mann C.A. Trans. A.I.Ch.Engrs 1944 40 709.

45. Vanderkeen J.H. M.Sc. Thesis Univ. of California 1960. U.C.R.L. 8722.

46. Jeffreys G.V. Chem. Proc. Engng 1962 March p. 117.

47. Hanson C. (Editor) Recent Advances in Liquid-liquid Extraction Pergamon 1971.

48. Arnold D.R. Ph.D. thesis,University of Aston 1974.

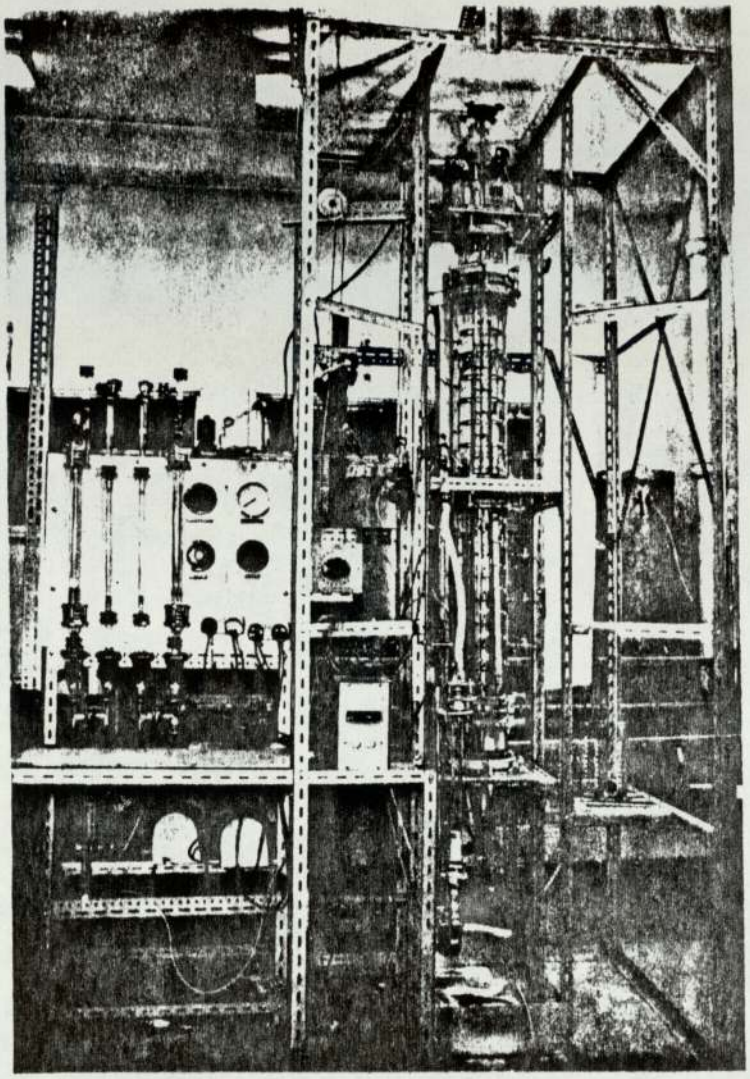

FIGURE 1

The Oldshue – Rushton Column

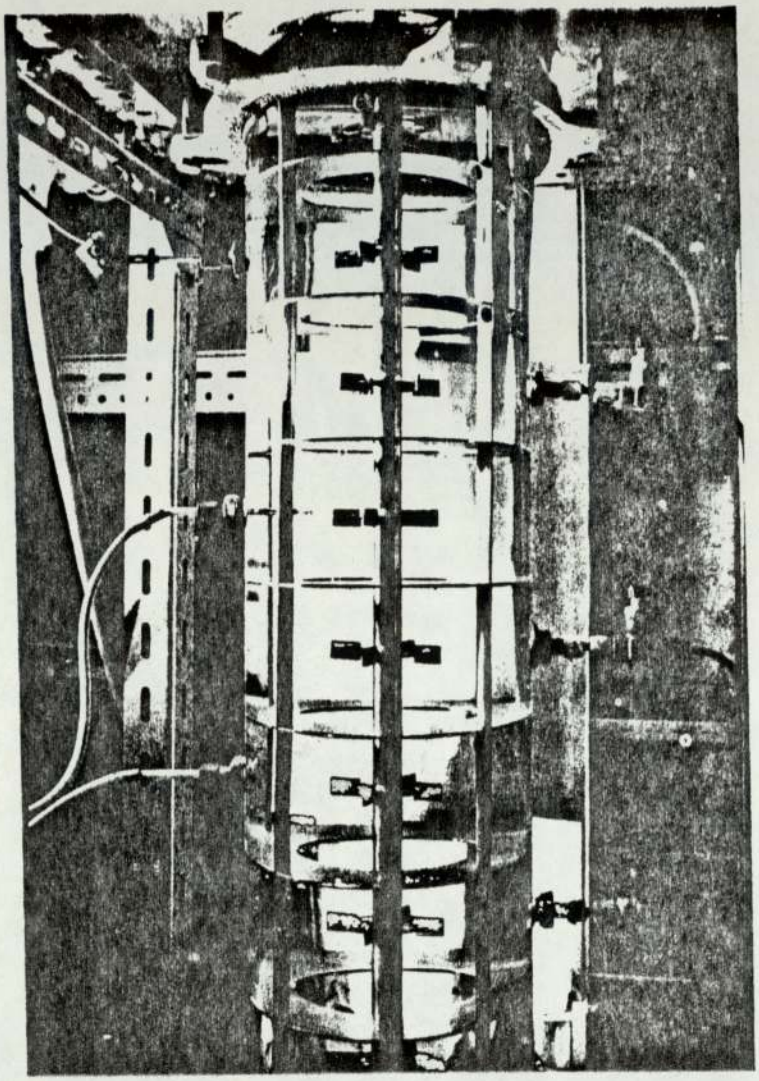

FIGURE 2

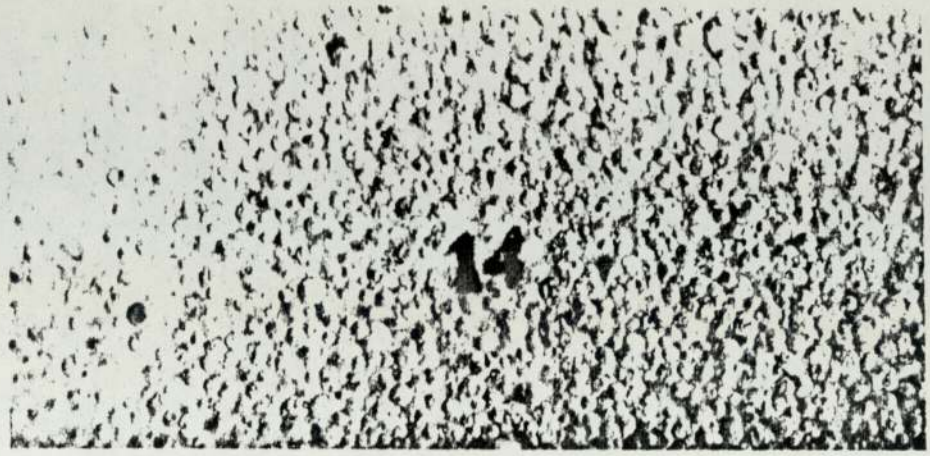

FIGURE 3

Dispersion in compartment 14 (near top)

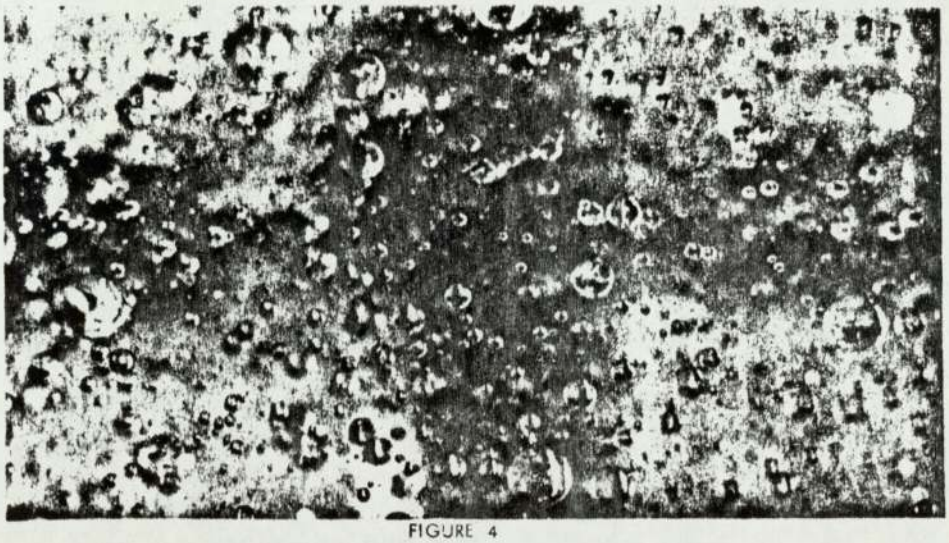

FIGURE 4

Dispersion in compartment 2 (bottom)

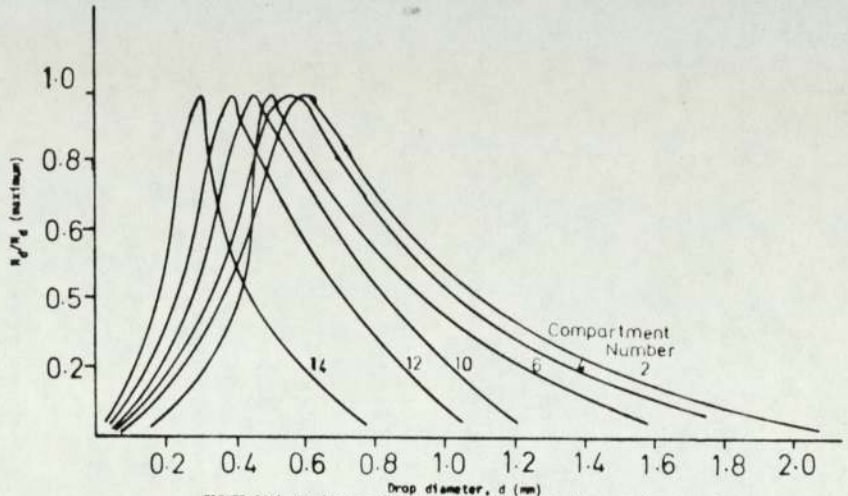

FIGURE 5(a) Variation of drop size distribution with compartment number
N = 400 r.p.m. $G_c = G_d = 0.5$ K_g/m^2s system: toluene/water

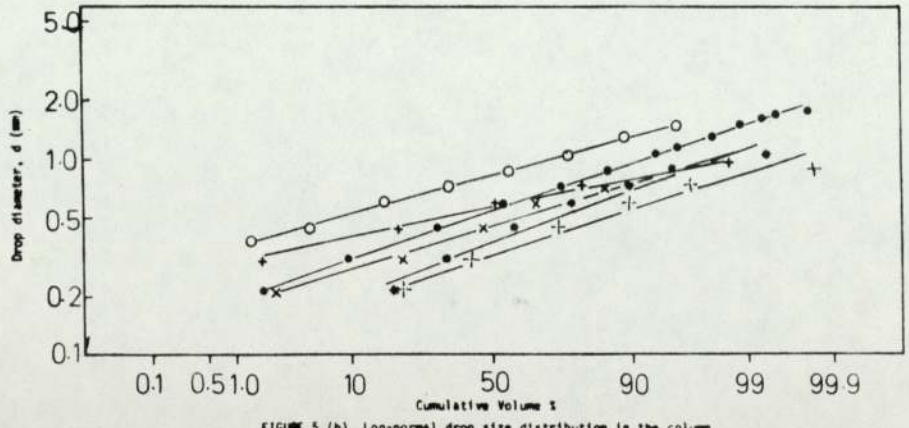

FIGURE 5 (b) Log-normal drop size distribution in the column
N=400 r.p.m. $G_c = G_d = 0.5$ K_g/m^2s system; toluene/water

FIGURE 6 and 7. Variation of mean drop size with height

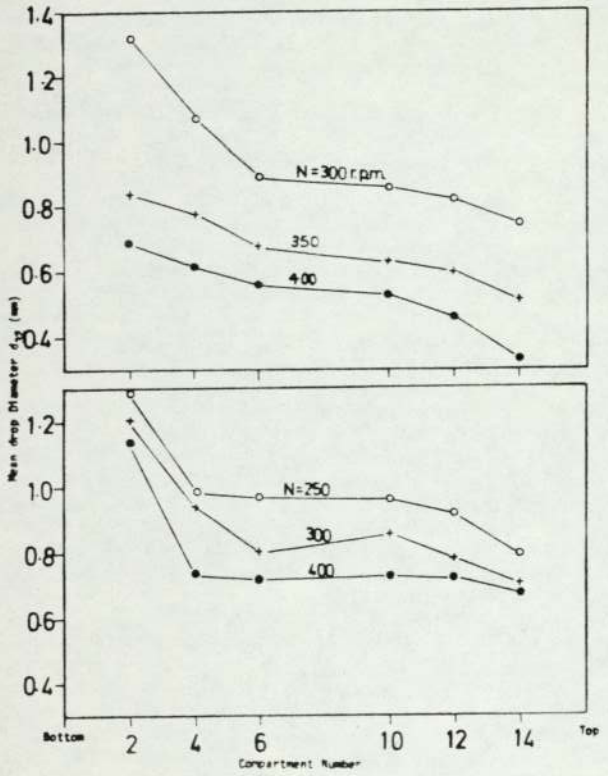

FIGURE 8 and 9 Variation of hold-up with height

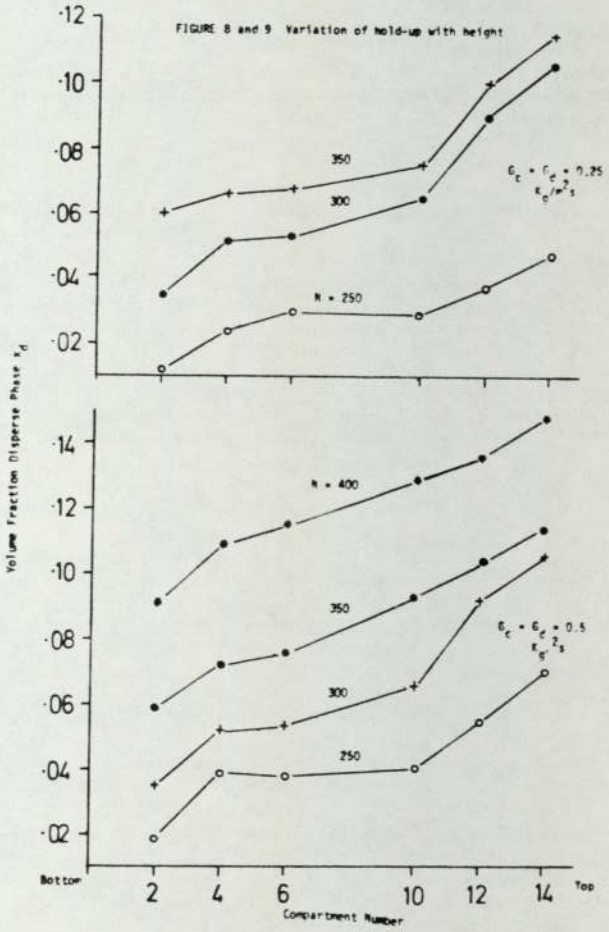

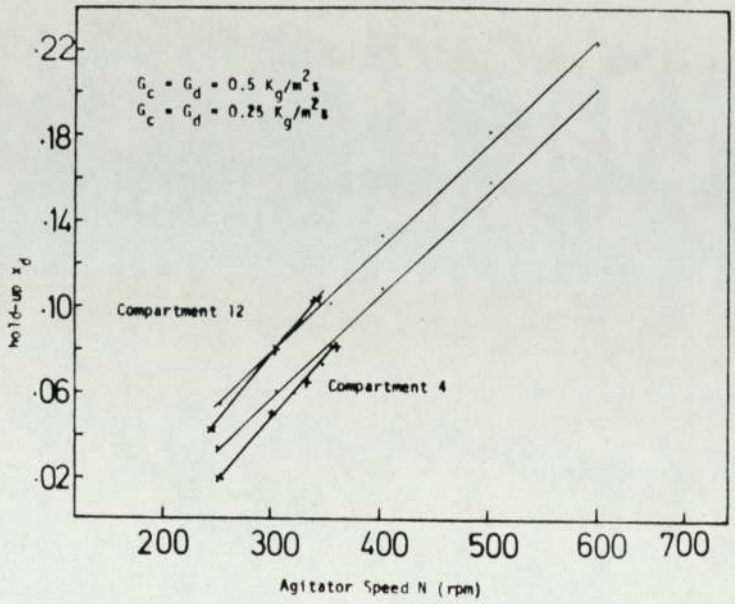

FIGURE 10 Variation of volume fraction dispersed phase with agitator speed

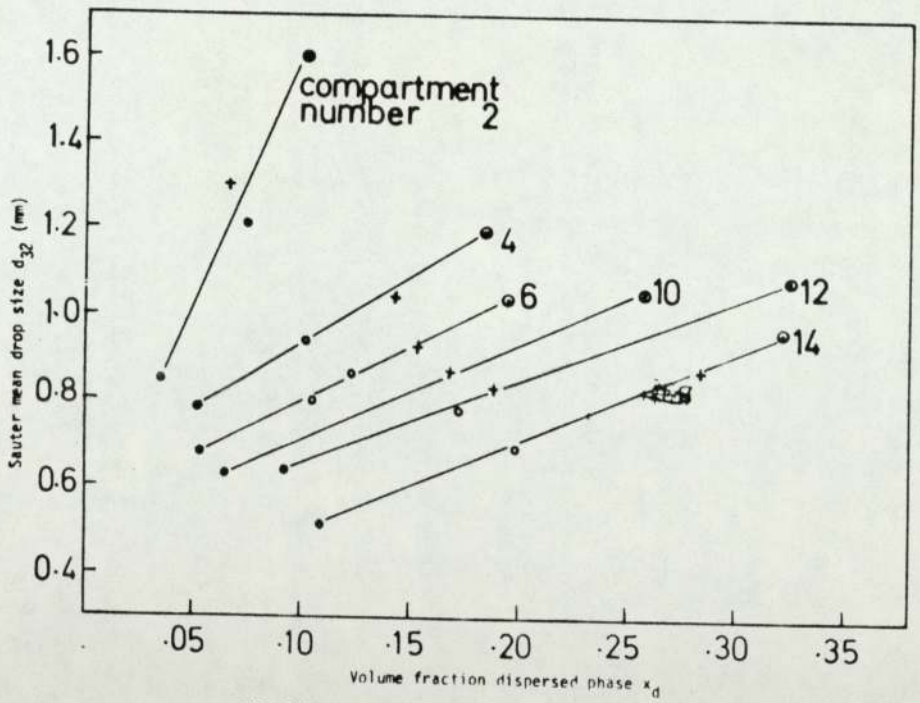

FIGURE 11. Mean drop size vs hold-up $G_c = G_d$ = 0.25 Kn/m^2s ●
0.50 " ○
0.75 " +
1.00 " ⊕
N = 300 rpm

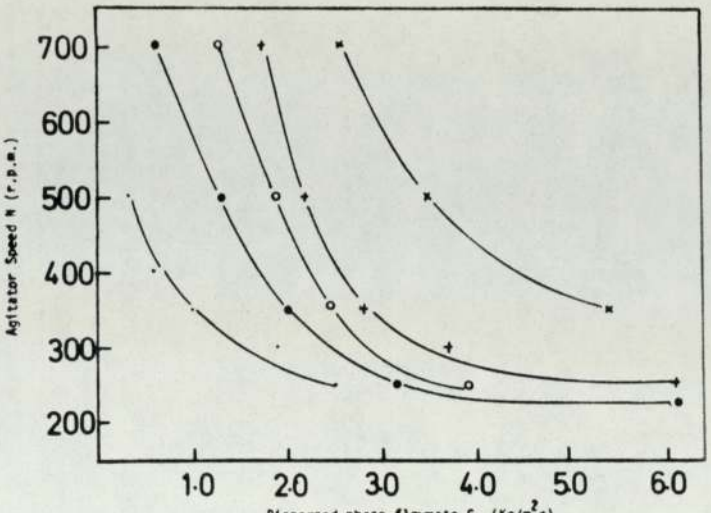

FIGURE 12 G_d vs N at phase inversion G_c = 0.00 Kg/m^{2}s ×
0.25 " +
0.50 " ○
0.75 " ●
1.00 " ·

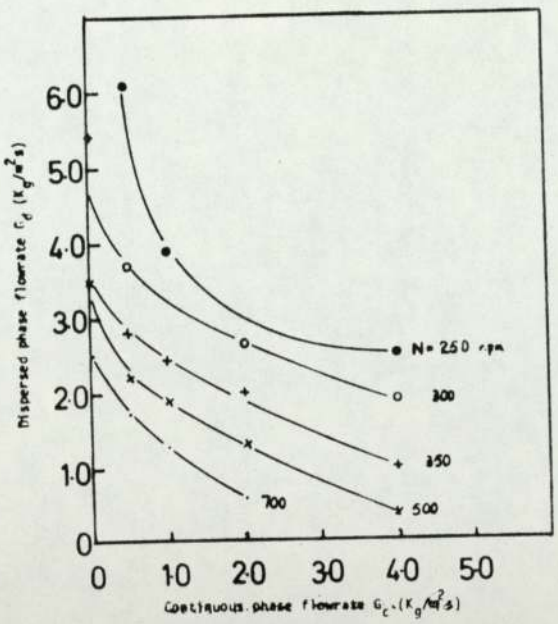

FIGURE 13 G_d vs G_c at phase inversion

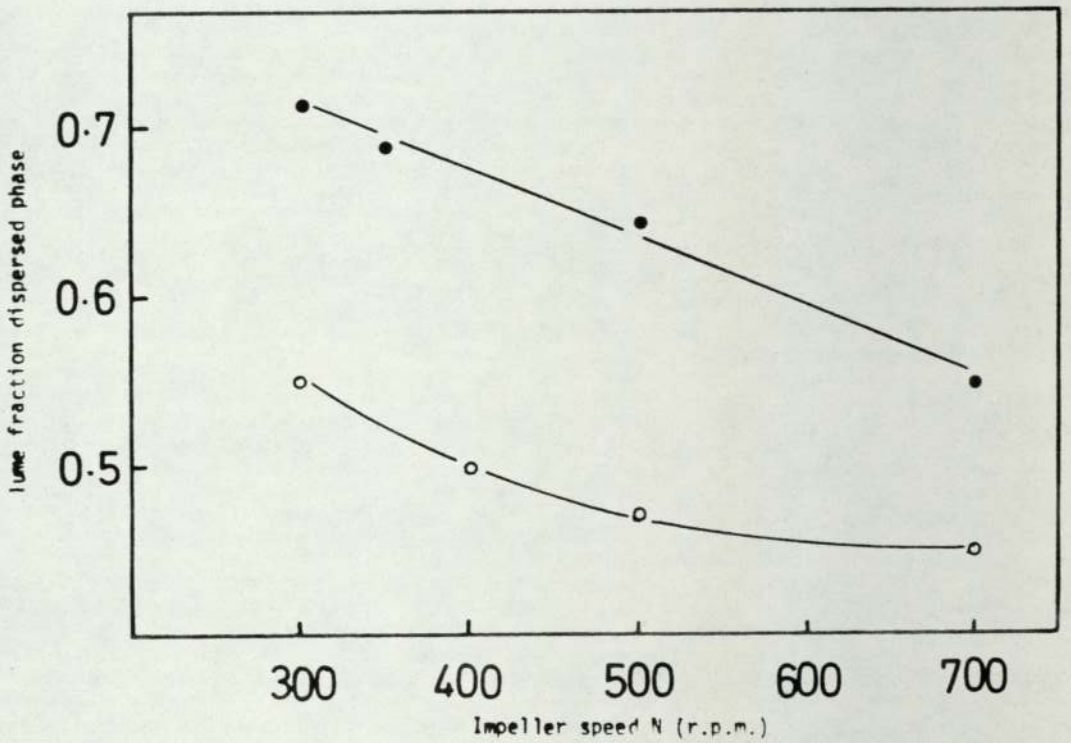

FIGURE 14 Phase inversion hold up vs impeller speed

Nomenclature.

A	Correlation coefficient in equation (94)
A_s	Stator gap diameter
a	Interfacial area
B_h	Blade height
B_w	Blade diameter
b	Baffle width
C	Concentration
$\mathfrak{D}$	Diffusivity
D	Agitator diameter
D_d	Disc diameter
d	Drop diameter
d_o	Drop size at zero hold-up
E_d	Kinetic energy supplied to drop
E'	Eddy diffusivity
e	Phase dispersion coefficient
Fr	Froude number V/gD
F_B	Superficial backmixing coefficient
f	Actual rate of interstage backflow
G	Mass flowrate per unit area
g	Gravitational constant, or intrastage flowrate
H	Compartment height
H_T	Column height
H.T.U.	Height of a transfer unit
h_m	Height of a theoretical stage
K	Mass transfer coefficient

k	Film mass transfer coefficient
k_s	Steady state mass transfer coefficient for solid particles
L	Lagrangian macroscale of turbulence
M	Mass of fluid in one compartment
m	Distribution coefficient
N	Impeller speed, number of moles transfered
N'	Rate of collision of drops
$(N.T.U)_a$	Apparent number of transfer units
$(N.T.U)_m$	Measured number of transfer units
$(N.T.U)_t$	True number of transfer units
Pe	Peclet number $H_T V_C/E_C$ or $H_T V_d/E_d(1-x_d)$
q	Net volumetric flowrate
Re_I	Agitator Reynolds number $D^2N\rho/\mu$
r	Drop radius
S	Compartment height in R.D.C.
Sh	Sherwood number
Sc	Schmidt number
T	Total number of drops
t	time
U	Superficial phase velocity
u	Velocity
V	Superficial velocity
V_K	Characteristic velocity of drops
V_S	Slip velocity
v	Velocity scale of turbulence
We	Weber number $ND^2\rho/\sigma$

w^*	Critical relative velocity along the line of centres between colliding drops
x	Solute concentration
x_d	Volumetric hold-up
Y	Probability density function
Z	Coalescence factor
η	Microscale of turbulence
α	Backflow coefficient
γ_1	Break-up coefficient
γ_2	Coalescence coefficient
ε	Extraction factor or energy per unit mass
θ	Time
θ_c	Time between coalescence and redispersion
λ_g	Taylor microscale of lateral turbulence
μ	Viscosity
ν	Kinematic viscosity (μ/ρ)
ξ	Dimensionless concentration $(x-x^*/x_o-x^*)$
ρ	Density
σ	Interfacial tension
τ	Shear stress
ψ	Collision frequency between drops
ω	Oscillation frequency

Subscripts

c	Continuous phase
col	Column
crit	Critical
d	Dispersed phase
E	Extract
i	Interfacial
m	Mean
max	Maximum
o	Overall or outlet
p	Particle
R	Raffinate
r	Relative
s.d.	Stable drop
w	In the vicinity of the column wall
*	Equilibrium value

Superscripts

'	Single drop
o	Zero hold-up

LITERATURE REFERENCES.

1. Newman, A.B., Trans. Am. Inst. Inst. Chem. Engrs., 27, 310 (1931).
2. Kronig, R., and Brink, J.C., Appl. Scient. Res., A2, 142 (1960).
3. Kintner, R.C., and Rose, P.M., A.I.Ch.E. Jnl., 12, 530 (1966).
4. Garner, F.H., and Tayeban, M., An. R. Soc. Esp. Fis. Quim., 56B, 491 (1960).
5. Jeffreys, G.V., Chem. Proc. Engng., March, p117 (1962).
6. Sawistowski, H., and Ying, W.E., Proc. I.S.E.C. '71 S.C.I. The Hague (1971).
7. Sawistowski, H., 'Interfacial Phenomena' in Hanson, C. (ed.) "Recent Advances in Liquid-Liquid Extraction" pp 293-366 (1970).
8. Thornton, J.D., Cited in (11).
9. Brown, D.E., and Pitt, K., Proc. Chemeca '70. Butterworth, (Australia) (1970).
10. Mumford, C.J., Brit. Chem. Engng., 13, (7) 981 (1968).
11. Bailes, P.J., and Winward, A., Trans. Instn. Chem. Engrs., 50, 240 (1972).
12. Logsdail, D.H., and Lowes, L., 'Industrial Contacting Equipment' in Hanson, C. (ed.) "Recent Advances in Liquid-Liquid Extraction" pp 139-168 (1970).
13. Reman, G.H., Proc. 3rd World Petr. Congr., The Hague, (1951).
14. Misek, T., 'Rotating Disc Contactor' (1964) (Prague, Statni Nakadelokri Technicke Literatury).
15. Hanson, C., (ed.) "Recent Advances in Liquid-Liquid Extraction" Pergamon (1971).

16. Oldshue, J.Y., and Rushton, J.H., Chem. Eng. Progr., 48, 297 (1952).

17. Bouyatiotis, B.A., and Thornton, J.D., Ind. Chem., 39, 298 (1963).

18. Bibaud, R.E., and Treybal, R.E., A.I.Ch.E. Jnl., 12, 472 (1966).

19. Reman, G.H., and Van der Vusse, J.G., Pet. Refiner, 34, (9) 129 (1955).

20. Mumford, C.J., Ph.D. Thesis, Univ. of Aston, (1970).

21. Al-Hemiri, A.A.A., Ph.D. Thesis, Univ. of Aston, (1973).

22. Jeffreys, G.V., Chemical Engineering Practice, Vol. 9, Ed. Cremer and Watkins, Butterworths, London (1965).

23. Gayler, R., Roberts, N.W., and Pratt, H.R.C., Trans. Instn. Chem. Engrs., 31, 57 (1953).

24. Thornton, J.D., Chem. Engng. Sci., 5, 201 (1956).

25. Logsdail, D.H., Thornton, J.D., and Pratt, H.R.C., Trans. Instn. Chem. Engrs., 35, 301 (1957).

26. Thornton, J.D., and Pratt, H.R.C., Trans. Instn. Chem. Engrs. 31, 289 (1953).

27. Thornton, J.D., Trans. Instn. Chem. Engrs., 35, 316 (1957).

28. Bouyatiotis, B.A., and Thornton, J.D., Instn. Chem. Engrs. Symp. Series, No. 26 (1967).

29. King, E.Y., and Beckman, R.B., A.I.Ch. E. Journal, 7, 319 (1961).

30. Misek, T., Coll. Czech. Chem. Comm., 28, 1631 (1963).

31. Misek, T., Coll. Czech. Chem. Comm., 29, 2086 (1964).

32. Vermeulen, T., et. al. Chem. Eng. Progr., 51, 85F (1955).

33. Brown, D.E., and Pitt, K., Proc. Chemeca '70, Butterworth, Australia (1970).

34. Resnick, W., Paper presented to 3rd Int. Congr. on Chem Eng., Marianske Lanze, (1969).

35. Cutter, L.A., A.I.Ch.E. Jnl., 12, 35 (1966).

36. Reman, G.H., and Olney, R.B., Chem. Eng. Progr., 51, 545 (1955).

37. Reman, G.H. Symposium on Scale-up of Chemical Plant and Processes, I.Chem. E. 56 (1957).

38. Reman, G.H., Pet. Ref., 36, 269 (1967).

39. Jeffreys, G.V., and Mumford, C.J., Proc. I.S.E.C. '71 S.C.I. The Hague (1971).

40. Strand, C.P., and Olney, R.B., and Ackerman, G.H., A.I.Ch.E. Jnl., 8, 252 (1962).

41. Stemerding, S., et. al., Chemie Ingr. Tech., 35, 844 (1963).

42. Westerterp, K.R., and Landsman, P., Chem. Eng. Sci., 17, 363 (1962).

43. Stainthorpe, F.P., and Sudall, N., Trans. Instn. Chem. Engrs., 42, 198 (1964).

44. Misek, T., and Rozkos, B., Int. Chem. Eng., 6, 130 (1966).

45. Miyauchi,T., et. al., A.I.Ch.E. Jnl., 12, 508 (1966).

46. Vermijs, H.J.A., and Kramers, H., Chem. Eng. Sci., 3, 55 (1954).

47. Bruin, ., et. al., Paper 100, I.S.E.C. '74, Lyon (1974).

48. Borrel, ., et. al., Paper 140, I.S.E.C. '74, Lyon (1974).

49. Misek, T., Chem. Eng., 68, 58 (1961).

50. Marek, J., Misek, T., and Widmer, F., Soc. Chem. Ind. Symp. Univ. of Bradford,(U.K.) 31st Oct. (1967).

51. Marek, J., and Misek, T., Soc. Chem. Ind. Conf. on Solvent Extraction, London, 27th March (1969).

52. Misek, T., and Marek, J., Brit. Chem. Eng., Feb. (1970).

53. Reman, G.H., Dutch Pat. 70,866.

54. Krishnajah, N.M., et.al., Brit. Chem. Eng., 12, 719 (1967).

55. Gouroji, I.C., Narula, A.S., and Pai, M.U., Brit. Chem. Eng., 5, 67 (1971).

56. Nakamura, A., and Hiratsuka, S., Kagaku Kogaku, 30, 1003 (1966).

57. Sokov, Y.F., and Putilova, Z.D., Tr. Vses. Nouchn. Tekn., 2nd Ed., Leningrad, p228 (1966).

58. Bailes, P.J., and Winward, A., Trans. Inst. Chem. Engrs., 50,240(1972)

59. Simonis, H., Proc. Eng., p110 Nov. (1972).

60. Scheibel, E.G., U.S. Pat. 2,493,265 (1950).

61. Karr, A.E., and Scheibel, E.G., Chem. Eng. Progr. Symp. Ser. No. 10, 50, 73 (1954).

62. Honecamp, J.R., and Burkhart, L.E., Ind. Chem. Eng. Proc. Des. and Dev., 1 (3), 177 (1962).

63. Scheibel, E.G., A.I.Ch.E. Jnl., 2, 74 (1956).

64. Tudose, R., Int. Chem. Eng., 3, 205 (1965).

65. Leisibach, J., Chem. Eng. Tech., 3, 205 (1965).

66. Kuhni, A.G., CH-4123 Auschwil-Basel, Switzerland.

67. Mogli, A., Chem. Eng. Tech., 37, 210 (1965).

68. Lightnin' Mixers Ltd., Poynton, Stockport, Cheshire (U.K.) Sales Literature.

69. Dykstra, J., Thompson, B.H., and Clouse, R.J., Ind. Eng. Chem., 50, 161 (1958).

70. Gutison, R.A., et.al., Chem. Eng. Prog. Symp. Ser. No.39, 58, (9) 8 (1959).

71. Levins, D.M., and Glastonbury, J.R., Trans. Inst. Chem. Engrs., 50, 132 (1972) and Chem. Eng. Sci.,27, 537 (1972).

72. Hinze, J.O., A.I.Ch.E. Jnl., 1, 289 (1955).

73. Kolmogorov, A.N., Doklady Acad. Nauk. S.S.S.R., 30, 301 (1941); 31, 538 (1941); 32, 16 (1941); 66, 825 (1949).

74. Stuart, R.W. and Tounsend, A.A., Trans, Phil. Roy. Soc., 243A, 359(1951

75. Taylor, G.I., Proc. Roy. Soc., 151A, 421 (1935).

76. Jandrell, T., Chem. Eng. Lab. Report, University of Aston (1972).

77. Kuboi, R., et. al., J. Chem. Eng. Japan, 5, 349 (1972).

78. Giles, J.G., Hanson, C., and Marsland, J ., Proc. I.S.E.C. '74 The Hague (1971).

79. Shinnar, R.and Church, J.M., Ind. Eng. Chem., 52, 253 (1960).

80. Rodger, W.A., Trice, V.G., Jnr, and Rushton, J.H., Chem. Eng. Prog., 52, 515 (1956).

81. Misek, T., Coll. Czech. Chem. Comm., 28, 426 (1963).

82. Thomas, R.J., and Mumford, C.J., Paper presented to I.S.E.C.'71 S.C.I., The Hague (1971).

83. Wilkinson, D., Ph.d. Thesis, University of Aston in Birmingham, (U.K.) (1974)

84. Lawson, G.B., Ph.d. Thesis, University of Manchester, (U.K.) (1968)

85. Howarth, W.J., Chem. Eng. Sci., 19, 33 (1964).

86. Shinnar, R., J. Fluid Mech., 31, 365 (1961).

87. Levich, V.G., "Physicochemical Hydrodynamics", Prentice-Hall N.J., (U.S.A.) (1962).

88. Misek, T., Coll. Czech. Comm., 28, 570 (1963).

89. Clay, C.H., Proc. Roy. Acad. Sci. (Amsterdam), 43, 852 and 979 (1940).

90. Linton, M. and Sutherland, K.L., J. Colloid Sci., 11, 391 (1956).

91. Hittit, A., Ph. D. Thesis, University of Aston in Birmingham (U.K.) (1972).

92. Obhukov, A.M., Dokl. Acad. Nauk. S.S.S.R., 32, 22 (1941).

93. Rea, H.E. and Vermeulen, T., U.C.R.L. - 2123.

94. Kafarov, V.V. and Babanov, D.M., Zh. Prikl. Khim., 32, 789 (1959).

95. Pavlushenko, I.S. and Yanishevskii, A.V., Zh. Prikl. Khim., 31, 1348 (1958).

96. Yamoguchi, I., Yabuta, S. and Nagata, S., Chem. Engng. (Japan) 27, 476 (1963).

97. Pebalk, V.L. and Mishev, V.M., Teor. Osnovy. Khim. Tekhnol., 3, 418 (1969).

98. Calderbank, P.H., Trans. Inst. Chem. Engrs., 36, 443 (1958).

99. Mylneck, Y. and Resnick, W., A.I.Ch.E.Jnl., 18, 122 (1972).

100. Luhning, R.W. and Sawistowski, H., Proc. I.S.E.C. '71, S.C.I., The Hague (1971).

101. Chen, H.T. and Middleman, S., A.I.Ch.E.Jnl., 13, 989 (1967).

102. Sprow, F.B., Chem. Eng. Sci., 22, 435 (1967).

103. Ostwald, W., Kolloid Z., 6, 103 (1910).

104. Quinn, J.A. and Sigloh, D.B., Can. J. Chem. Eng., 41, 15 (1963).

105. Selker, A.H. and Schleicher,C.A., Jnr. Can. J. Chem. Eng., 17, 298 (1965).

106. Schleicher, C.A., A.I.Ch.E.Jnl., 5, 145 (1959).

107. Angelo, J.B., Lightfoot, E.N. and Howard, D.W., A.I.Ch.E.Jnl., 12, 751 (1966).

108. Newman, J., Chem. Eng. Sci., 22, 83 (1967).

109. Marangoni, C., Annln. Phys., 143, 337 (1871).

110. Heertjes, P.M. and de Nie, L.H., 'Mass Transfer to Drops' in Hanson, C. (ed), "Recent Advances in Liquid-Liquid Extraction". Pergamon, (1971).

111. Cavers, et. al., Paper presented to I.S.E.C. '74 S.C.I., Lyon (1974).

112. Linton, M. and Sutherland, K.L., Chem. Eng. Sci., 12, 214 (1960).

113. Rowe, P.N., et. al., Trans. Inst. Chem. Engrs., 43, 14 (1965).

114. Kinard, G.E., Manning, F.S. and Manning, W.P., Brit. Chem. Eng., 8, 326 (1963).

115. Boussinesq. cited in 110.

116. Highmark, G.A., Ind. Eng. Chem. Fund., 6, 408 (1967).

117. Thorsen, G., et. al., Chem. Eng. Sci., 23, 413 (1968).

118. Mok, Y.I. and Treybal, R.E., A.I.Ch.E.Jnl., 17, 916 (1971).

119. Harriot, P., Can. J. Chem. Eng., 40, 60 (1962).

120. Ingham, J., Trans. Instn. Chem. Engrs., 50, 372 (1972).

121. Rod, V., C.Sc. Thesis, Prague Technical University, Czech. (1966).

122. Misek, T., Chapter in "Recent Advances in Liquid-Liquid Extraction" Hanson, C. (ed.) Pergamon, (1971).

123. Young, E.F., Chem. Eng., 64, 241 (1957).

124. Miyauchi, T. and Vermeulen, T., Ind. Eng. Chem. Fund., 2, 304 (1957).

125. Kerkhof, P.J.A.M. and Thijssen, H.A.C., Chem. Engng. Sci., 29, 1427 (1974).

126. Miyauchi, T. and Vermeulen, T., Ind. Eng. Chem. Fund., 2, 304 (1963).

127. Hartland, S. and Mecklenburgh, J.C., Chem. Engng. Sci., 21, 1209 (1966).

128. Landau, J. and Prochazka, J., Chem. Proc. Eng., 48, 51 (1967).

129. Landau, J. and Prochazka, J., Colln. Czech. Chem. Comm., 28, 1927 (1963) and 31, 1685 (1966).

130. Schleicher, C.A., A.I.Ch.E.Jnl., 6, 529 (1960).

131. Vermeulen, T. and Miyauchi, T., Chem. Engng. Prog., 62, 95 (1966).

132. Tolic, A. and Miyauchi, T., J. Chem. Eng. Japan, 6, 241 (1973).

133. Danckwerts, P.V., Chem. Engng., 2, 1 (1953).

134. Eguchi, W. and Nagata, S., Chem. Engng., Tokyo, 22, 2181 (1958).

135. Eguchi, W. and Nagata, S., Mem. Fac. Eng. Kyoto Univ., 21, 70 (1959).

136. Miyauchi, T. and Vermeulen, T., Ind. Engng. Chem. Fund., 2, 113(1963).

137. McMullen, A.K., Miyauchi, T. and Vermeulen, T., cited in 112.

138. Wilburn, N.P., Ind. Engng. Chem. Fund., 3, 189 (1964).

139. Beek, W.J., Chem. Weekblad., 58, 327 (1962).

140. Rod, V., Colln, Czech. Chem. Comm., 34, 387 (1969).

141. Hartland, S. and Mecklenburg, J.C., Chem. Symp. Ser. No. 26, 115(1967).

142. Stemerding, S. and Zuigerweg, F.J., Chem. Engr., CE156 (1963).

143. Misek, T. and Rod, V., Paper presented to C.H.I.S.A. Marienbad, Czechoslovakia, (1965).

144. Olney, R.B., A.I.Ch.E.Jnl., 10, 827 (1964).

145. Gutoff, E.B., A.I.Ch.E.Jnl., 11, 712 (1965).

146. Miyauchi, T., Mitsutake, H. and Harase, I., A.I.Ch.E.Jnl., 12, 508 (1966).

147. Stemerding, S., Lumb, E.C. and Lips, J., Chemie - Ingr. - Tech. 35, 844 (1963).

148. Westerterp, K.R. and Landsman, P., Chem. Engng. Sci., 17, 363(1962)

149. Haug, H.F., A.I.Ch.E.Jnl., 17, 585 (1971).

150. Lelli, U., Magelli, F. and Sama, C., Chem. Eng. Sci., 27, 1109(1972)

151. Treybal, R.E., "Liquid Extraction", 2nd edition McGraw - Hill, New York, (1963).

152. Doulah, M.S. and Thornton, J.D., Inst. Chem. Engrs. Symp. on Extraction, April (1967).

153. Resnick, W., Paper presented to Third Int. Congr. on Chem. Eng. Marianske Lazne, September (1969).

154. Piper, H.B., M.Sc. Thesis, University of Manchester (U.K.)(1966).

155. Smith, T.N., Chem. Eng. Sci., 29, 538 (1974).

156. B.S. 3406 Part 4 p.35 (1963).

157. Doyle, K.G., Ph. d. Thesis, University of Aston in Birmingham (U.K.)(1974).

158. Jillood, A., M.Sc. project report, University of Aston in Birmingham (U.K.)(1973).

159. Laity, D.S. and Treybal, R.E., A.I.Ch.E.Jnl., 3, 177 (1957).

160. Ward, A.F.H. and Brooks, L.H., Trans. Farad. Soc., 48, 1124 (1952)

161. Oldshue, J.Y., Personal Communication, (1974).